PRODRUGS OF ANTIVIRAL PHOSPHONATES

ANTONY GRAHAM MITCHELL

Doctor of Philosophy

UNIVERSITY OF ASTON IN BIRMINGHAM

November 1991

The University of Aston in Birmingham

PRODRUGS OF ANTIVIRAL PHOSPHONATES

by

ANTONY GRAHAM MITCHELL

A thesis submitted for the degree of Doctor of Philosophy

1991

SUMMARY

Phosphonoformate and phosphonoacetate are effective antiviral agents, however they are charged at physiological pH and as such penetration into cells and diffusion across the blood-brain barrier is limited. In an attempt to increase the lipophilicity and improve the transport properties of these molecules, prodrugs were synthesised and their stabilities and reconversion to the parent compound subsequently investigated by the techniques of ^{31}P nuclear magnetic resonance spectroscopy and high performance liquid chromatography.

A series of 4-substituted dibenzyl (methoxycarbonyl)phosphonates were prepared and found to be hydrolytically unstable giving predominantly the diesters, benzyl (methoxycarbonyl)phosphonates. This instability arose from the electron-withdrawing effect of the carbonyl group promoting nucleophilic attack at phosphorus. It was possible to influence the mechanism and, to some extent, the rate of hydrolysis of the phosphonoformate triesters to the diesters by varying the electronic nature of the substituent in the 4-position of the aromatic ring. Strongly electron-withdrawing groups increased the sensitivity of phosphorus to nucleophilic attack, thus promoting P-O bond cleavage and rapid hydrolysis. Conversely, weakly electron-withdrawing substituents encouraged C-O bond fission, presumably through resonance stabilisation of the benzyl carbonium ion. The loss of the protecting group on phosphorus was in competition with nucleophilic attack at the carbonyl group, resulting in P-C bond cleavage with dibenzyl phosphite formation. The high instability and P-C bond fission make triesters unsuitable prodrug forms of phosphonoformate.

A range of chemically stable triesters of phosphonoacetate were synthesised and their bioactivation investigated. Di(benzoyloxymethyl) (methoxycarbonylmethyl)phosphonates degraded to the relevant benzoyloxymethyl (methoxycarbonylmethyl)phosphonate in the presence of esterase. The enzymatic activation was restricted to the removal of only one protecting group from phosphorus, most likely due to the close proximity of the benzoyloxy ester function to the anionic charge on the diester. However, in similar systems di(4-alkanoyloxybenzyl) (methoxycarbonylmethyl)phosphonates degraded in the presence of esterase with the loss of both protecting groups on phosphorus to give the monoester, (methoxycarbonylmethyl)phosphonate, *via* the intermediacy of the unstable 4-hydroxybenzyl esters. The methoxycarbonyl function remained intact. The rate of enzymatic hydrolysis and subsequent removal of the protecting groups on phosphorus was dependent on the nature of the alkanoyl group and was most rapid for the 4-n-butanoyloxybenzyl and 4-iso-butanoyloxybenzyl esters of phosphonoacetate. This provides a strategy for the design of a prodrug with sufficient stability in plasma to reach the central nervous system in high concentration, wherein rapid metabolism to the active drug by brain-associated enzymes occurs.

Key words: Phosphonoformate, Phosphonoacetate, Prodrug, Synthesis, Bioactivation.

DEDICATION

To mum, dad and Alison
with love

Acknowledgements

I would like to thank my supervisor, Dr Sally Freeman, for her continual guidance, encouragement, inexhaustible enthusiasm and valued friendship throughout the period of this research. It has been an honour and a pleasure to be associated with Sally.

I would also like to thank my advisor, Dr William Irwin, and Dr Dave Nicholls for invaluable discussions, advice and practical assistance in all aspects of this project. Thanks also to Dr Brian Denny for his assistance in the molecular modelling studies and to Graham Smith for his superb artwork. I am grateful to all members of the department, past and present, for their help and friendship.

I acknowledge and appreciate the financial support of the Science and Engineering Research Council.

Finally, I would like to thank my family and Alison for their continual encouragement, inspiration and, above all, love. Without you this would not have been possible.

CONTENTS

ABBREVIATIONS AND SYMBOLS

AIDS	Acquired immune deficiency syndrome
Ar	Aryl
BBB	Blood-brain barrier
br	Broad
°C	Degrees celsius
$CDCl_3$	Deuterated chloroform
CD_3CN	Deuterated acetonitrile
CI	Chemical ionisation (mass spectrometry)
cm	Centimetres
CMV	Cytomegalovirus
^{13}C NMR	Carbon nuclear magnetic resonance spectroscopy
CNS	Central nervous system
conc	Concentration
CSF	Cerebrospinal fluid
d	Doublet
DNA	Deoxyribonucleic acid
D_2O	Deuterated water
EC_{50}	Concentration of drug which reduces extent of infection by 50% in infected cell cultures

EI	Electron impact (mass spectrometry)
Eqn	Equation
Es	Taft steric parameter
eV	Electron volts
FAB	Fast atom bombardment (mass spectrometry)
Fig	Figure
g	Grammes
GABA	γ-Aminobutyric acid
h	Hours
HIV	Human immunodeficiency virus
^{1}H NMR	Proton nuclear magnetic resonance spectroscopy
HPLC	High performance liquid chromatography
HSV	Herpes simplex virus
Hz	Hertz
I	Inductive
IR	Infra-red
J	Coupling constant
k	Rate constant
K	Ionisation constant

kg	Kilogrammes
Li^+	Lithium cation
Log P	Logarithm of partition coefficient
m	Multiplet
M	Mesomeric
M	Molar
$M^{+\cdot}$	Molecular ion
max	Maximum
mg	Milligramme
MHz	Megahertz
min	Minutes
ml	Millilitre
mM	Millimolar
mmHg	Measurement of pressure in millimetres of mercury
mp	Melting point
m/z	Mass divided by charge
Na^+	Sodium cation
nm	Nanometres
NMR	Nuclear magnetic resonance spectroscopy

P	Partition coefficient
PAA	Phosphonoacetate
PBS	Phosphate-buffered saline
pen	Pentet
PFA	Phosphonoformate
PMEA	9-(2-Phosphonylmethoxyethyl)adenine
PMEG	9-(2-Phosphonylmethoxyethyl)guanine
^{31}P NMR	Phosphorus nuclear magnetic resonance spectroscopy
ppm	Parts per million
q	Quartet
r	Correlation coefficient
Rf	Retention factor
RNA	Ribonucleic acid
Rt	Retention time
s	Singlet
SD	Standard Deviation
sept	Septet
t	Triplet
TC_{50}	Concentration of drug which reduces cell growth by 50%

$t_{1/2}$	Half-life
TLC	Thin layer chromatography
UV	Ultra-violet
v/v	Volume/volume
Å	Angstrom
δ	Chemical shift measured in parts per million
µl	Microlitres
µM	Micromolar
π	Lipophilicity
σ	Hammett constant
~	Approximately
>	Greater than

LIST OF FIGURES

LIST OF TABLES

INTRODUCTION

CHAPTER 1 - INTRODUCTION

1.1. Viruses

Many life-threatening diseases such as rabies, acquired immune deficiency syndrome (AIDS), hepatitis, influenza, gastroenteritis and herpes are all viral infections. Viruses are obligate intracellular parasites sharing many of the nutritional requirements and synthetic pathways with the host cells they infect.[1, 2] Unlike microorganisms, they contain only a single species of nucleic acid as their genetic material, which may be either deoxyribonucleic acid (DNA, eg. herpesviruses) or ribonucleic acid (RNA, eg. retroviruses), but not both. In different families of viruses the nucleic acid is single- (eg. retroviruses) or double-stranded (eg. poxviruses), a single nucleotide strand or several, and if a single strand, either linear (eg. poxviruses) or cyclic (eg. papoviruses). The molecular weights of the DNAs of different animal viruses vary from 1.5 (hepadnaviruses) to 185 million (poxviruses); the range of molecular weights of viral RNAs is much less, from just over 2.5 (picornaviruses) to 15 million (reoviruses). The genomes of all DNA viruses consist of a single strand of nucleic acid, but the genomes of many RNA viruses consist of several different strands.

Viruses again differ from cellular microorganisms in that they exist in two or sometimes three physically and functionally different states. Firstly, they exist as viral particles, or virions, which are the inert form that carries the viral genome from one host cell to another. The second functional state is 'vegetative virus', in which the viral genome undergoes replication, directs the formation of polypeptides, and controls the assembly and often the release of progeny virions. In this state the virus is part of the host cell that it infects. Finally, with a few families of viruses, including retroviruses, the viral genome is at times integrated into the host cell DNA as a 'provirus'. In the case of retroviruses the provirus is a DNA copy of the RNA genome of the virion.

The major constituent of the virion is protein, whose primary role is to provide the viral nucleic acid with a protective coat known as a capsid (**Fig 1.1**). The morphological units that form part of a capsid are called capsomers. It may be naked or enclosed within a lipoprotein envelope (peplos) which is derived from cellular membranes as the virus matures by budding. Units projecting from the envelope are called peplomers. Where the capsids directly enclose the viral nucleic acid, as is usual with tubular capsids (eg. filoviruses) but less common with isometric capsids (eg. herpesviruses), the complex is called the nucleocapsid.

Fig 1.1 – Schematic diagram of the structure of a simple non-enveloped(naked) virion with an icosahedral capsid (**A**, eg. retroviruses) and an enveloped virion with a tubular nucleocapsid with helical symmetry (**B**, eg. paramyxoviruses)

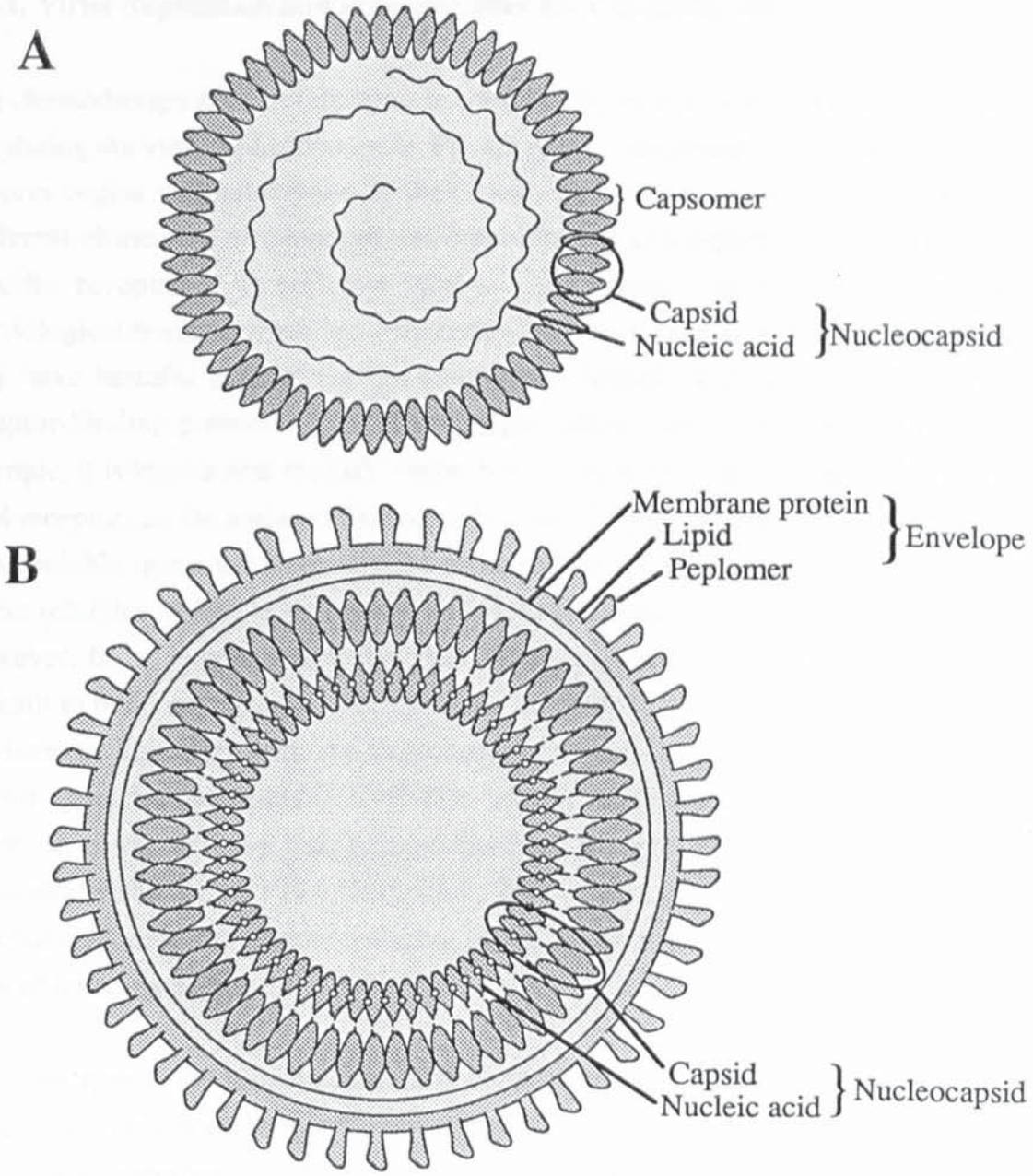

Apart from a few viruses, such as the arenaviridae family responsible for Lassa fever, virions do not contain organelles and as such rely on the host cell to provide the systems for synthesising the components that they themselves do not possess. This is the underlying reason for its obligate intracellular parasitism and inability to multiply in any other situation

1.1.1. Virus Replication and Potential Sites for Chemotherapy

The chemotherapy of viral infections is complicated by the close involvement of the host cell during the virus replication cycle. **Fig 1.2** gives a simplified version of this cycle. The process begins with adsorption of the virion, via receptors, onto the host cell surface. Different viruses use different cell surface molecules as receptors, hence the term, virus-specific receptors.[3] These virus receptors are normal cellular components with a physiological function, therefore destruction, or even blocking of cellular virus receptors may have harmful effects. On the other hand, ligands with specific affinity for the receptor-binding proteins of the virion might inhibit virus replication efficiently. For example, it is known that the HIV virion binds via an envelope glycoprotein, gp 120, to CD4 receptors on the surface of susceptible cells (T4 lymphocytes and macrophages) [4, 5, 6] A soluble truncated form of CD4 produced by recombinant DNA technology is a potent inhibitor of HIV-1 replication and HIV-1 induced cell fusion *in vitro* .[7, 8, 9, 10, 11] However, because of the short half-life of the truncated CD4 in blood it has proved difficult to build up adequate concentrations in the body. One approach to overcome this has been to link CD4 with the immunoglobulin IgG, to form a class of compounds known as immunoadhesins.[12, 13, 14] This has the advantage of having a half-life of the order of days, and by using a portion of the immunoglobulin molecule, the immunoadhesins can act like antibodies. When these molecules bind to free virus or infected cells they can initiate the same set of reactions as normal antibodies to rid the body of invading pathogens.

After adsorption, the virus penetrates the cell, either by endocytosis of the virus into a cytoplasmic vesicle or, for certain enveloped viruses, fusion of the viral membrane with the cellular membrane and subsequent release of the virus nucleocapsid into the cytoplasm.[15] These are normal cellular events and as such it is difficult to attack the virus specifically at this stage, although some monoclonal neutralizing antibodies have been developed.[16] Fusion of the virus with the cellular membrane via specific envelope glycoproteins appears to be an essential early step in the replication of all enveloped

Fig 1.2 – Life cycle of a virus and targets for antiviral chemotherapy

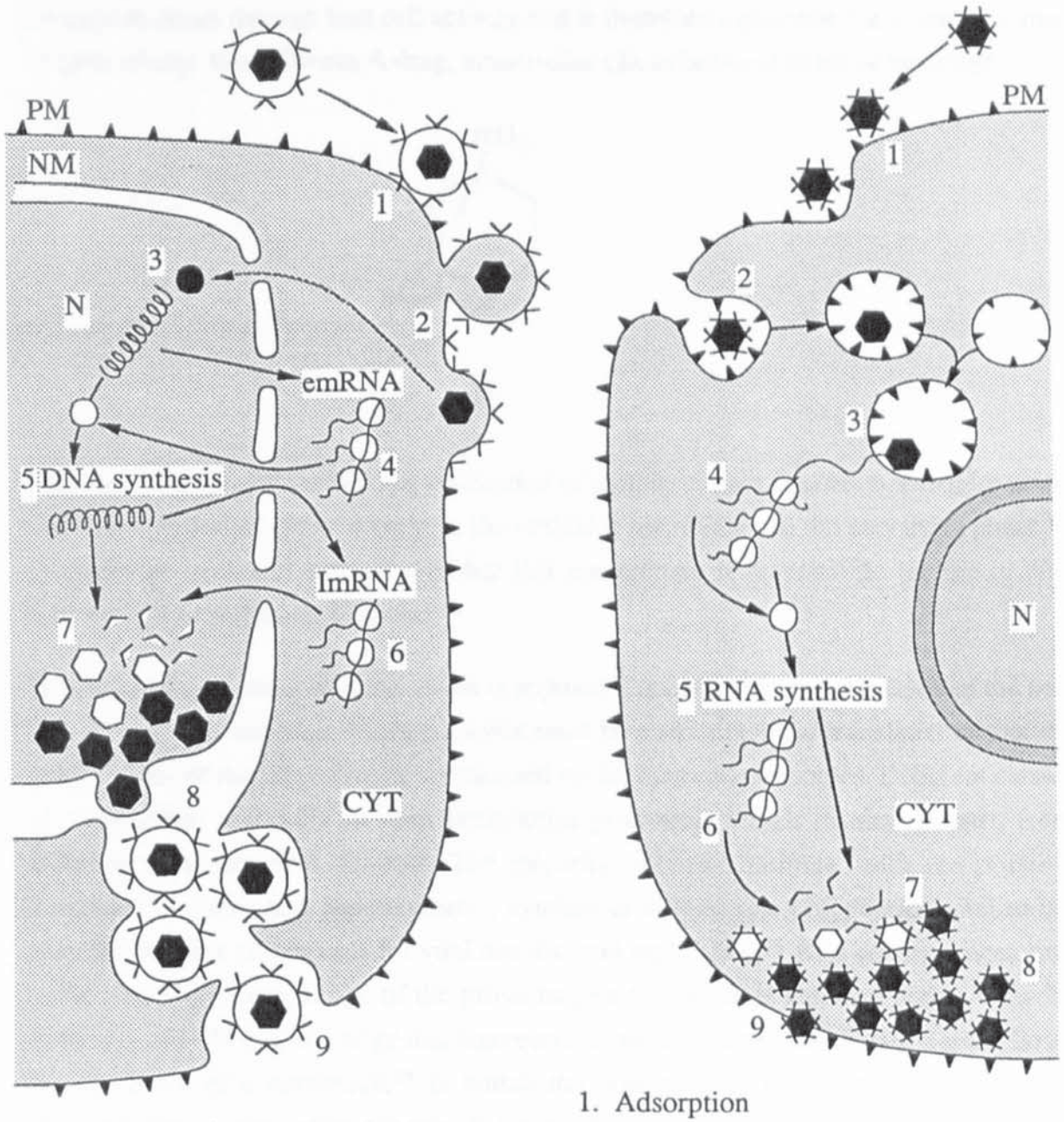

PM = Plasma membrane
NM = Nuclear membrane
N = Nucleus
CYT = Cytoplasm

1. Adsorption
2. Penetration
3. Uncoating
4. Early protein synthesis
5 Nucleic acid replication
6. Late protein synthesis
7. Nucleocapsid assembly
8. Virion maturation
9. Release of virions

viruses. By inhibiting the post-translational modification of these envelope proteins, it is possible to interfere with the penetration step indirectly.[17]

Following penetration, the virus uncoats to reveal the virus genome available for virus-specific synthetic processes (transcription and translation).[15] The uncoating process is thought to occur through host cell activity and is therefore a poor site for antiviral action. In spite of this, the influenza A drug, amantadine **(1)**, is believed to act at this stage.

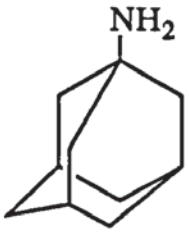

(1)

This basic compound inhibits the replication of certain viruses *in vitro* that require acid-dependent fusion of virion protein to the vesicular membranes in the uncoating phase.[18, 19] However, it is still unclear whether this mechanism is responsible for the *in vivo* activity against influenza A in man.[20]

When the genetic material of the virion is exposed it is integrated into the DNA of the host cell. The genetic message which it carries must be transcribed and translated so that the polypeptides of the virus may be synthesised on the host cell ribosomes. Different classes of virus differ markedly in their replication processes, which results, in part, from differences in the viral genome. The majority of virus families, with the possible exception of parvo and papovaviruses, synthesise at least one polypeptide vital to the enzyme complex responsible for viral nucleic acid replication.[21] As a consequence, viral nucleic acid synthesis is one of the prime targets for selective antiviral action.[22] In the treatment of HIV it is this stage that has received the most attention to date. HIV follows the life cycle of a retrovirus,[23] in which the normal flow of genetic information is reversed. That is, the genome is encoded in RNA, which must be reverse transcribed into DNA before replication can take place. First, DNA polymerase makes a single strand DNA copy of the viral RNA, then a second enzyme, ribonuclease, destroys the original RNA, and the polymerase makes a second DNA copy using the first as a template. The polymerase and ribonuclease together are often referred to as reverse transcriptase. A considerable number of anti-HIV agents under current investigation, such as

azidothymidine[24] (AZT), 9-[2-(phosphonylmethoxy)ethyl] adenine[24] (PMEA) and phosphonoformate[25] (PFA) are reverse transcriptase inhibitors.

Once the viral nucleic acid has been integrated into the nucleus of the host cell, viral RNA strands are generated by transcription, which act as messenger RNA for the translation and synthesis of virus proteins using the host cell ribosomes. Synthetic antiviral agents acting at this phase are not known, although interferons do appear to inhibit viral protein synthesis in some systems.[26] Alternatively, post-translational modification of viral proteins may be a more promising target for antiviral action, as many proteins are synthesised initially as large polypeptide precursors which are subsequently cleaved by viral or host cell proteolytic enzymes.[27, 28] For example, the HIV protease is responsible for the hydrolysis of several very specific peptide bonds in the *gag* and *gag-pol* polyproteins to produce the mature *gag* and *pol* encoded proteins.[29] It is this activity that causes the transition to the mature infectious form of the virus, hence the synthesis of highly active and specific inhibitors of HIV protease is now a major research area in AIDS chemotherapy.

Virus assembly is not known to require any virus specific enzymatic activity, however there are substances which can be incorporated into maturing viruses which make them non-infectious[17] or susceptible to attack by particular agents.

The final stage, budding of virions from cellular membranes, may also be a potential target for antiviral action. Indeed, it has been found that neuraminidases present in certain enveloped viruses[21] have a role in the budding process, therefore specific neuraminidase inhibitors may halt viral replication.

1.2. Phosphonates as Antiviral Agents

Phosphonates are compounds containing a phosphorus-carbon bond.[30] They have been found in a variety of organisms in nature and several metabolic processes involving phosphonates have been elucidated. Naturally occurring phosphonates were first discovered in 1959 when 2-aminoethylphosphonic acid **(2)** was isolated from the anemone.

$H_2NCH_2CH_2P(O)(OH)_2$

(2)

Since that date other phosphonates, phosphonolipids and phosphonopeptides have been detected in living species. For example, 2-methylaminoethylphosphonic acid (**3**), 2-amino-3-phosphonopropionic acid (**4**) and the antibiotic, phosphonomycin (**5**) have all been isolated.

$MeNHCH_2CH_2P(O)(OH)_2$ (**3**)

$H_2NCH(COOH)CH_2P(O)(OH)_2$ (**4**)

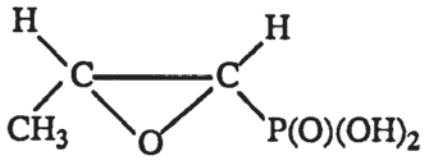

(**5**)

A wide range of phosphonates have been found to possess antibacterial, antifungal and antiviral activity. Their mode of action has been attributed to the chemically and biologically inert nature of the P-C bond and to its stuctural similarity to the P-O bond of phosphate esters. Consequently, there is much current interest in this topic and many synthetic phosphonate analogues of biological phosphates are being prepared and investigated for their possible biochemical activity. For example, Dixon and Sparkes[31] have synthesised analogues of dihydroxyacetone phosphate and 3-phosphoglycerate in which the phosphate group, $-O-PO_3H_2$ was replaced by the phosphonomethyl group, $-CH_2-PO_3H_2$, to give 4-hydroxy-3-oxobutylphosphonic acid (**6**) and 2-hydroxy-4-phosphonobutyric acid (**7**) respectively. These isosteres act as substrates for glycolytic enzymes.

$H_2O_3P-CH_2-CH_2-CO-CH_2OH$ (**6**)

$H_2O_3P-CH_2-CH_2-CH(OH)CO_2H$ (**7**)

A given phosphonate should be more stable towards hydrolysis than its phosphate analogue and should also be less acidic, hence the degree of dissociation under physiological conditions will be different. In addition the phosphonate will have slightly different dimensions and possess a different overall configuration than its phosphate analogue. Two important antiviral phosphonates are phosphonoacetate (PAA, **8**) and phosphonoformate (PFA, **9**), which are both analogues of inorganic pyrophosphate (**10**).

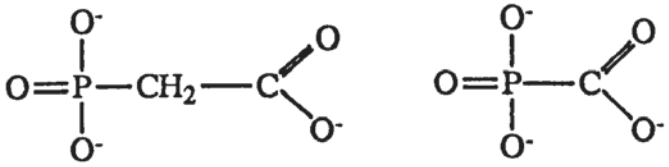

(8)

(9)

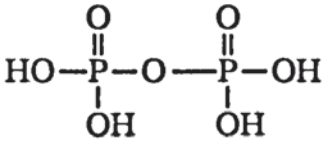

(10)

1.2.1. Phosphonoacetate (8)

Phosphonoacetate (PAA, 8) inhibits the replication of herpes viruses,[32] including herpes simplex virus,[33] cytomegalovirus,[34] Epstein-Barr virus, pseudorabies virus, equine abortion virus, Marek's disease virus[35] and human herpesvirus-6,[36] by inhibiting virus-induced DNA polymerase activity. It is also effective against varicella zoster virus[37] and it has been used in the treatment of warts.[38] Other DNA viruses, such as simian virus-40 and human adenovirus-12, and RNA viruses, such as polio, rhinovirus or measles, were not inhibited.[39] Likewise, PAA does not inhibit the reverse transcriptase activities of HIV.[25]

PAA is partially triionic at physiological pH with pKa's of 2.30 (P-OH), 5.40 (COOH) and 8.60 (P-OH),[32] and therefore cellular penetration is restricted. For example, Bopp *et al*[40] showed that only 14% of a 10 mg kg^{-1} orally administered dose of PAA was absorbed by the rat ($t_{1/2}$ 5.8 h) and only 8% of a 20 mg kg^{-1} dose absorbed by the monkey ($t_{1/2}$ 13.9 h). PAA does not appear to be metabolised to other compounds in either herpes virus-infected cell cultures, in uninfected cell cultures, or in animals.[32, 40] Most of the PAA that is administered orally to a rat is rapidly excreted in both urine and faeces in unchanged form.[32]

At concentrations up to 200 μg ml^{-1} of the disodium salt, PAA was neither cytotoxic nor mutagenic to uninfected cells in culture, but it effectively blocked herpes virus replication. Treatment of viruses or cells with PAA before infection had no effect on herpes simplex virus replication.[41] When given subcutaneously to mice, PAA has an LD_{50} of 1500 mg kg^{-1}.[42] A deposition in bone has been reported for PAA.[32] Toxic reactions to PAA have been reported for rabbits given 300 mg kg^{-1} day^{-1} intravenously[43] and monkeys given 500 - 1000 mg kg^{-1} day^{-1}.[42] PAA caused severe dermal degeneration in guinea pigs[44]

and was irritating when applied liberally in a 2-5% cream to herpetic skin lesions on the genitalia of cebus monkeys.[45] This local irritancy, dermal toxicity and also the existence of PAA-resistant mutants[46] has suspended the clinical development of PAA.

PAA does not inhibit the adsorption, penetration or release of the virus, nor the synthesis of RNA and early viral proteins,[47] but it does affect the synthesis of DNA and the late viral proteins.[48] PAA selectively binds to and inhibits the herpes virus-induced DNA polymerase[39] at concentrations of 1-2 μM, which does not significantly reduce cellular DNA synthesis. PAA inhibition of herpes virus-induced DNA polymerase is believed to occur by competitive inhibition at the pyrophosphate binding site on the polymerase enzyme.[49] PAA forms a stable six-membered chelate ring with an essential zinc ion **(11)** in DNA polymerase thereby blocking the site that should accept inorganic pyrophosphate, thus preventing further chain elongation of DNA.[50] Inactivation of RNA transcriptases occur through the same mechanism.

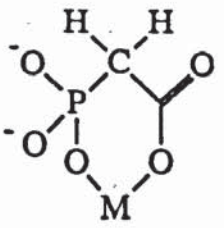

(11)

The anti-herpes activity of pyrophosphate analogues have highly specific structural requirements.[51] Neither the carboxylic nor the phosphono groups of PAA could be replaced, by for example a sulpho group, and the distance between these two groups is important. Increase of this distance by the addition of methylene groups caused complete loss of activity. Indeed, phosphonopropionic acid **(12)** is limited to the formation of energetically unfavourable seven-membered chelate rings and was found to be inactive.[51]

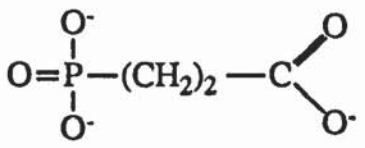

(12)

Addition of some substituents on the methylene carbon of PAA resulted in a reduction, but not loss, of activity. Replacement of the two hydrogen atoms on the methylene group

of PAA by two chlorine atoms caused a complete loss of activity. In contrast, a decrease in the length of the carbon chain to phosphonoformate (9) retained anti-herpes activity.

1.2.2. Phosphonoformate (9)

The antiviral activity of phosphonoformate (PFA, 9) was discovered by screening analogues of PAA against herpes simplex virus DNA polymerase. PFA was found to be as effective as PAA in selectively inhibiting the DNA polymerase .[52, 53, 54] PFA is also active against the hepatitis B[55] and vesicular stomatitis viruses.[56] Influenza-virus RNA polymerase is inhibited by PFA[53] to a greater extent than by PAA.[57] This activity was enhanced in the presence of magnesium (II) or manganese (II) ions. In cell culture, PFA is active against herpes virus type 1 and 2, pseudorabies virus[53] and herpes virus sylvilagus.[58] PFA is also effective against cutaneous herpes virus infections in the guinea pig, but unlike PAA, it is not irritating to the skin.[44, 59] A 2% PFA topical cream showed marked therapeutic activity when applied to herpes-infected human skin.[60] PFA inhibited HIV reverse transcriptase enzyme by 50% at a concentration of 0.1 μM and totally inactivated the enzyme at 5 μM.[61, 62, 25] PFA has recently become licenced for the treatment of cytomegalovirus (CMV) infection in AIDS patients.[63]

Like PAA, PFA is triionic at physiological pH with pKa's of 0.49 (P-OH), 3.41 (COOH) and 7.27 (P-OH) resulting in limited cellular penetration[64, 65] and as such high dose infusions are required to achieve therapeutic effects.[66] Sjovall *et al* [67] found that oral administration of 4g of PFA in solution every 6 h for 3 days to humans resulted in low plasma levels of the drug, the extent of absorption ranging from 12 to 22%. PFA was found to have three half-lives of 0.45, 3.3 and 18h and a mean plasma clearance of 0.1 to 3.1 ml kg^{-1} min^{-1}.[67] PFA is mainly eliminated unchanged by the kidneys[64] and dosing has to be adjusted in patients with impaired renal function. Using a 3% (w/w) PFA cream containing ^{14}C-labeled PFA, percutaneous absorption has been studied in guinea pigs.[64] The absorption of PFA through intact skin was measured at 2-4% and through stripped skin at 60-75%. Some PFA (7-10%) remains in the skin 48h after administration.

Extensive toxicity, fertility and teratogenicity studies have been performed on PFA[52] showing a good safety margin [LD_{50} 600 mg kg^{-1} (intravenous); > 4000 mg kg^{-1} (oral)] and permitting human studies. However, intravenous infusion of PFA (200 mg kg^{-1} day^{-1}) has been shown to cause reversible renal dysfunction, thrombophlebitis at the infusion site, headaches, anaemia and genital ulceration.[68, 69, 63] Like PAA, 10-28% of a

cumulative intravenous dose of PFA was found to bind tightly, but reversibly, to the inorganic matrix of bone with no apparent adverse effects.[67]

PAA-resistant DNA polymerase is also resistant to PFA,[54] suggesting that PAA and PFA have the same mode of action,[70] blocking the inorganic pyrophosphate binding site. PFA binds to a metal ion (probably zinc) in a similar manner to PAA but forming a five-membered chelate ring.[71]

1.2.3. Phosphonylmethoxyalkyl Purine and Pyrimidine Analogues

Recently a new class of acyclic nucleotide analogues **(13)** and **(14)** have been identified as potent and selective inhibitors of HIV.[24, 72]

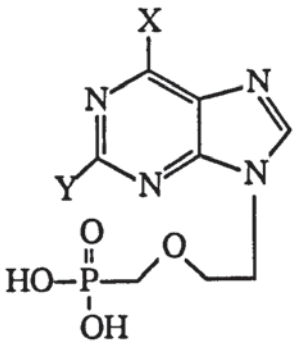

(13)

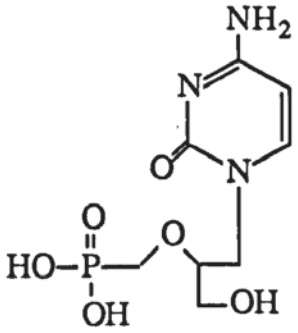

(14)

(13, X=NH_2, Y=H): 9-(2-phosphonylmethoxyethyl)adenine (PMEA)
(13, X=OH, Y=NH_2): 9-(2-phosphonylmethoxyethyl)guanine (PMEG)
(14) (S)-1-(3-hydroxy-2-phosphonylmethoxypropyl)cytosine (HPMPC)

These compounds have a broad range of antiviral activity encompassing not only HIV, but also many herpes viruses, including herpes simplex virus, varicella-zoster viruses and cytomegalovirus.[24, 72]

Existing licensed antiviral nucleoside analogues, such as acyclovir **(15)** and azidothymidine (AZT, **16**) require three phosphorylation steps involving viral and cellular kinases to convert them into their active triphosphate forms, whereas only two phosphorylation steps are needed for the phosphonylmethoxyalkyl derivatives **(13)** and **(14)**

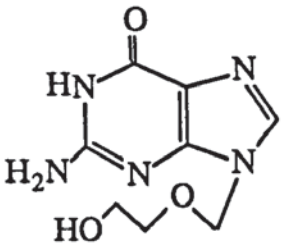

(15)

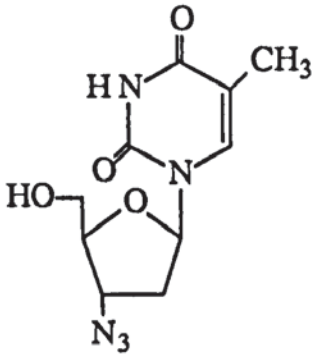

(16)

The bisphosphate of PMEA has been shown to prevent viral DNA synthesis by the inhibition of DNA polymerase,[73] ribonucleotide reductase[74] and reverse transcriptase.[75] The fact that PMEA is effective against both herpes and retrovirus infections in the same animal model[76] make it particularly attractive for the therapy of AIDS, since it could be used in the treatment of opportunistic herpes virus infections as well as the underlying retroviral disease.

An additional advantage of these phosphonylmethoxyalkyl derivatives **(13)** and **(14)** over existing antiviral nucleosides such as AZT **(16)** is that their actions are prolonged: HPMPC **(14)** is active against cytomegalovirus infection and PMEA **(13)** is active against retrovirus infection for several days following a single dose.[72] This prolonged action would allow perhaps weekly doses to be given - a practical option for cytomegalovirus and HIV infections, which require long term treatment. This marked stability probably arises through attachment of phosphorus directly to carbon, thereby imparting resistance to enzymatic as well as chemical degradation.

In common with PAA and PFA, one of the major problems associated with PMEA, and the nucleoside analogues in general, is their polar nature and hence their limited absorption from the gastro-intestinal tract following oral administration.

1.3. The Blood-Brain Barrier

Highly charged compounds, such as PFA, PAA and PMEA, have only limited cellular penetration and large intravenous doses of the drug are often required to achieve therapeutic efficacy.[66] An area where drug transport is a major problem is in the treatment of viral infections of the brain and central nervous system (CNS) where entry of ionic molecules by passive diffusion is prevented by the blood-brain barrier (BBB). Following oral delivery PFA can utilise the inorganic phosphate active transport system to pass

through the stomach wall,[77] however autoradiography studies show that PFA barely traverses the BBB and entry into the brain is minimal.[52]

There are two barrier sytems which a drug must cross to get into the brain, the BBB and the blood-cerebrospinal fluid (CSF) barrier. The BBB resides largely in microvessel endothelial cells and has a surface area that is 5000-fold greater than that of the blood-CSF barrier and therefore the BBB is the principal diffusion barrier separating the brain interstitial space and blood.[78] The two morphological characteristics of the brain capillaries which make up the BBB are the epithelial-like high resistance tight junctions which cement all endothelia of brain capillaries together, and the scanty pinocytosis or transendothelial channels, which are abundant in endothelia of peripheral organs.[79]

In general, hydrophilic drugs, for example phosphonates, which gain access to other tissues are barred from entry into the brain because they are unable to traverse the BBB. Substances circulating in the blood may gain access to brain interstitial space only via one of four mechanisms:-

I) lipid-mediation (passive diffusion), which allows for the free-diffusion of lipid-soluble substances such as the steroid hormones through the BBB;[80]

II) carrier-mediation (active transport), which allows for the transport of circulating water-soluble nutrients (eg. D-glucose, L-lactate, L-arginine, adenine) through the BBB via the action of nutrient-specific carrier systems (eg. monosaccharides, monocarboxylic acids and amino acids) localized in the lumenal and antilumenal membranes of brain capillaries;[81]

III) pore-mediation, which allows for the transport of water through water-specific pores in the BBB;[82] and

IV) receptor-mediated transcytosis of circulating peptides (eg. insulin) via peptide-specific receptor systems, localized on both the lumenal and antilumenal membranes of brain capillaries.[82]

Viruses can spread from the blood to the brain cells by two primary routes.[83, 84] Firstly, hematogenous spread: Growth through the endothelium of small cerebral vessels has been demonstrated in several systems, and there is evidence that virions may sometimes be passively transferred across the vascular endothelium. The production of meningitis rather than encephalitis by enteroviruses, and the ease with which these agents are

recovered from the CSF, can be explained by postulating that the virus in the blood either grows or passes through the choroid plexus. The second general mechanism of CNS viral infection is neural spread: Diffusion from the periphery to the CNS is possible without generalisation of viruses through the bloodstream, for the peripheral nerves and the nerve fibres of the olfactory bulb offer potential direct pathways. The route of spread along peripheral nerves is usually by growth within the endoneural cells. Apart from rabies and herpes B virus infections of man after monkey bites, no examples of neural spread have been established in natural human infections. However, transmission in the reverse direction from the dorsal root ganglia down the corresponding peripheral nerves, appears to be the most likely mode of spread of virus in herpes zoster and recurrent herpes simplex.

Serious viral infections of the CNS which could be controlled by phosphonates include herpes simplex virus, in particular herpes encephalitis,[85] human cytomegalovirus brain infection[86] and HIV-1. A common and important cause of morbidity in patients with advanced stages of infection with HIV-1 is the AIDS dementia complex, a complicating neurological syndrome characterised by abnormalities in cognition, motor performance and behaviour[87]. It is unclear whether HIV-1 enters the brain as free virus, within infected monocytes and macrophages, or through primary infection of the choroid plexus or meningeal cells. There is evidence that AIDS dementia complex is caused by direct brain infection with HIV-1,[87, 88] however, it has also been suggested that the mechanism of brain damage by HIV-1 could be indirect (eg. interference with neuroleukin).[89] The instrument of that damage may therefore be either a viral or host encoded gene product released from infected macrophages causing impairment of neuronal function rather than neuronal death. The virus frequently invades the CNS early in the course of systemic infection, even in asymptomatic individuals.[90] Invasion of the CNS by HIV-1, coupled with the possibility that it could create a reservoir of persistent infection even if peripheral clearance were realized[91] has led to the general agreement that an ideal chemotherapeutic agent for HIV-1 should penetrate the BBB and be highly active in the CNS.[90]

1.4. Drug Delivery and Prodrug Design

A powerful pharmacological-based approach for drug delivery to the brain is via the design of prodrugs. A prodrug is an inactive derivative of the parent drug molecule that has improved delivery properties over the parent drug. The prodrug needs to undergo a chemical or enzymatic transformation, within the target organ, to release the active drug.[92] For passive diffusion, prodrug design involves the conversion of an active

hydrophilic drug into an inactive lipophilic molecule, thus promoting transport through the membrane (BBB). The process for a bipartite prodrug consisting of a carrier moiety attached to the parent drug is represented diagramatically in **Fig 1.3.**

In designing an effective prodrug[93, 94, 95] at least four criteria must be satisfied:-

I) The prodrug must be able to cross the BBB.

II) The prodrug derivative must undergo reconversion to the drug *in vivo*.

III) The active drug must be generated at such a rate that the target organ receives an effective concentration of the drug before systemic metabolism of the prodrug occurs.

IV) The prodrug, together with the generated carrier moiety must be both non-toxic and inactive, or certainly less active, than the parent drug.

Bipartite prodrugs are susceptible to delivery problems. For example, an inherent instability of the drug-carrier bond, resulting in degradation before the site of action has been reached, or conversely, inhibition of enzymatic hydrolysis due to the steric or electronic properties of the drug. Carl et al[96] proposed a tripartite prodrug in which the carrier and drug are linked together by a special connector group **(Fig 1.4)**. Here enzymatic activation now proceeds through hydrolysis of the carrier-link bond rather than the carrier-drug bond. To be successful the link should be designed in such a way that, following enzymatic or chemical activation, the link-drug bond spontaneously cleaves to release the active drug.

Fig 1.3 – Bipartite prodrug system

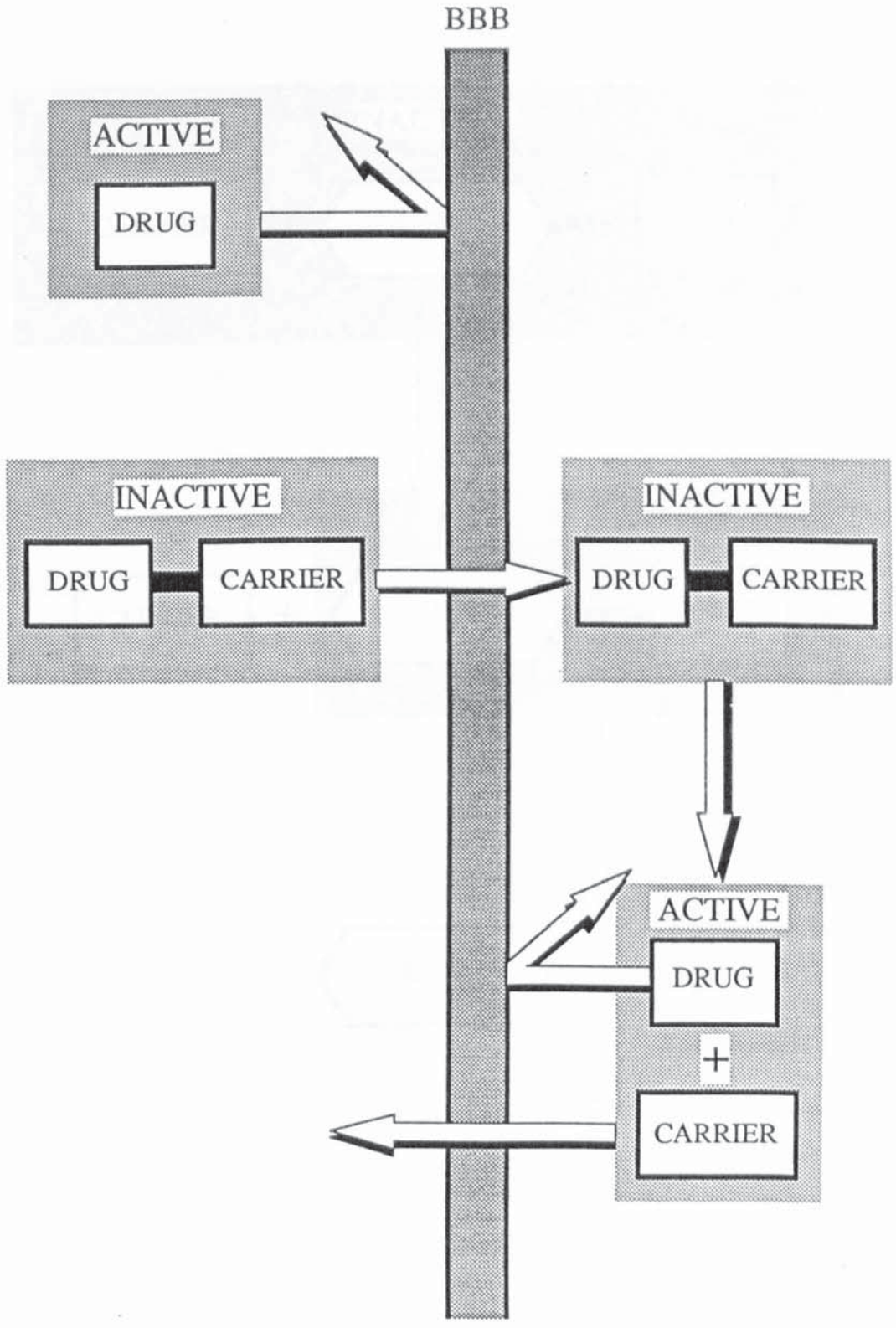

Fig 1.4 – Tripartite prodrug system

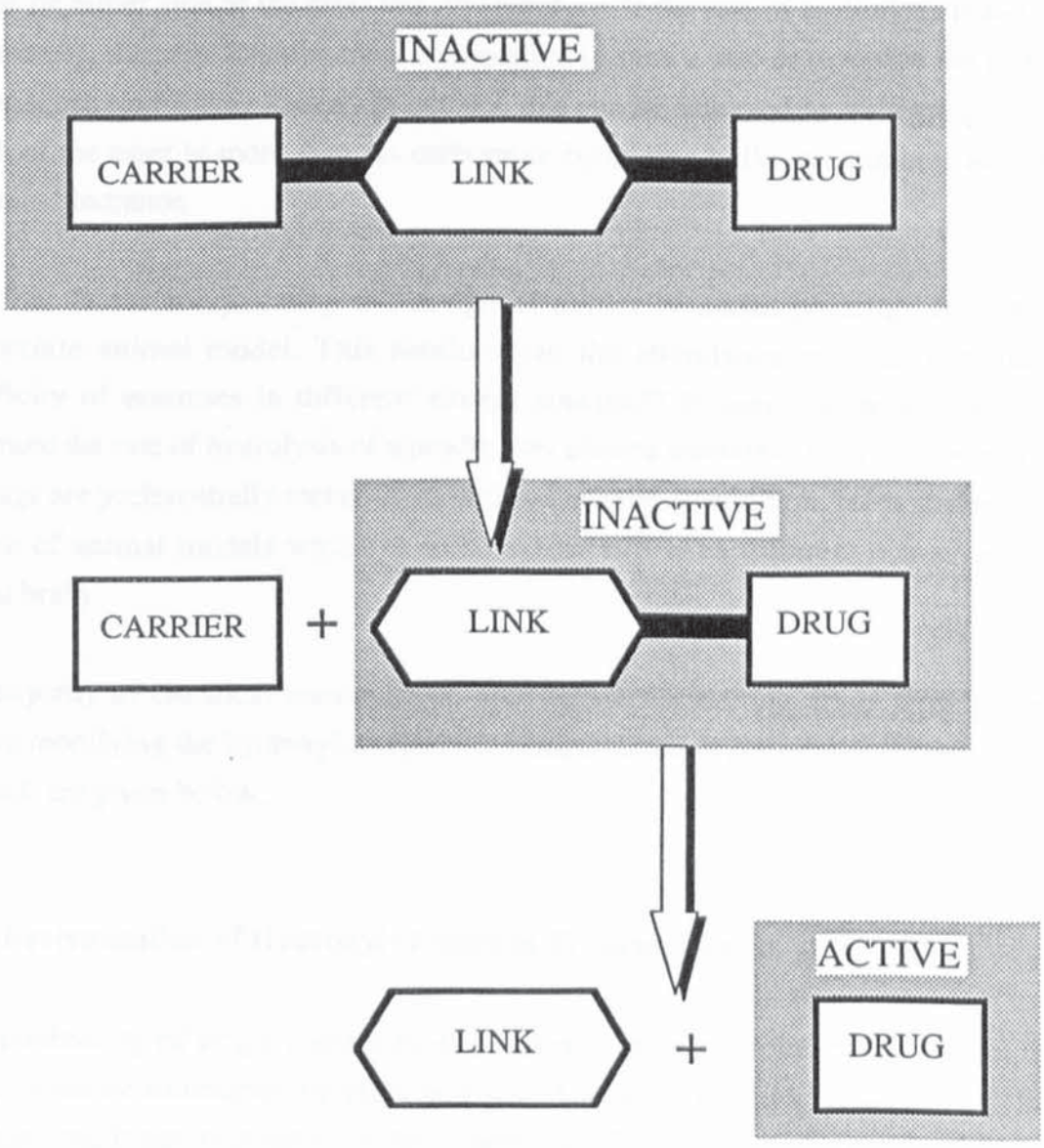

Before a brain-directed prodrug can reach its target it must be transported via the blood and through the liver, both sites of high enzyme activity. Researchers have generally relied on designing lipophilic ester prodrugs that are sufficiently stable in plasma and in the liver to allow a therapeutic dose to reach the brain, wherein the prodrug should be hydrolysed enzymatically or chemically and cleaved to give the parent drug. The substrate specificity of esterases for prodrugs is dependent on the length and steric properties of the groups on either side of the ester link.[97] Therefore, if the rate of hydrolysis is too rapid, for example, the ester function must be modified in such a way as to render the prodrug a poorer substrate for the esterase. In general, this can be achieved by increasing the chain length of the ester to more than six carbons or by adding bulky substituents to increase the steric hindrance.

A further factor complicating the design of clinically useful prodrugs is finding an appropriate animal model. This results from the abundance and varying substrate specificity of esterases in different animal species.[97] Human plasma can be used to determine the rate of hydrolysis of a prodrug by plasma esterases *in vitro* , however some prodrugs are preferentially metabolised within the liver. In addition, brain studies require the use of animal models which to some extent will have different characteristics to human brain.

The majority of chemical manipulation approaches for making drugs more lipophilic involve modifying the hydroxyl, carboxylic acid, amino and phosphate groups, examples of which are given below.

1.4.1. Derivatisation of Hydroxyl Groups in Prodrug Design

The lipophilicity of drugs containing the hydroxyl group can be increased simply by esterification or sometimes by etherification. A striking example of a hydroxy-linked brain-directed bipartite prodrug is the conversion of the highly polar drug, morphine, to diacetylmorphine (heroin), which has greater lipophilicity than the parent compound and consequently diffuses through the BBB 100-fold faster.Once inside the brain it is rapidly hydrolysed by the action of esterases to monoacetylmorphine and morphine, which are responsible for its pharmacologic actions.[98]

1.4.2. Derivatisation of Carboxylic Acid Groups in Prodrug Design

The development of carboxyl-linked prodrugs for brain delivery is a rapidly expanding area of research. The lipophilicity of drugs containing carboxyl groups can be greatly increased by their conversion to carboxylic esters. An example of this involves the penicillin β - lactam antibiotics **(17)** which contain a thiazolidine carboxylic acid group and are therefore ionised at both physiological and intestinal pH.

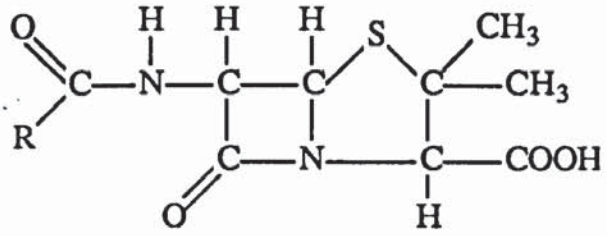

(17)

R=alkyl, aryl

In an attempt to increase the lipophilicity and oral absorption of penicillin, bipartite prodrugs in the form of simple alkyl and aryl esters of the carboxylate group have been synthesised. Although they are rapidly hydrolysed to the free penicillin acid in animals, they proved far too stable in man to have any therapeutic potential.[99] This problem was resolved by the synthesis of a series of double esters of penicillin (tripartite prodrugs), incorporating an acyloxymethyl group into the molecule **(18)**.[100]

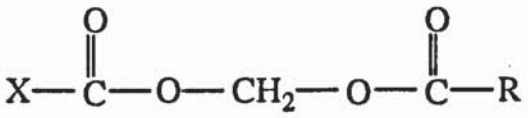

(18)

X = Remainder of drug

These acyloxymethyl esters **(18)** are rapidly hydrolysed in the blood and tissues of humans to regenerate the active penicillin. The first step in the hydrolysis of the acyloxymethyl esters is enzymatic cleavage of the terminal ester bond to give an unstable hydroxymethyl ester **(19)** which rapidly dissociates to the parent penicillin and formaldehyde **(Fig 1.5)**.

Fig 1.5 - Hydrolysis of acyloxymethyl esters

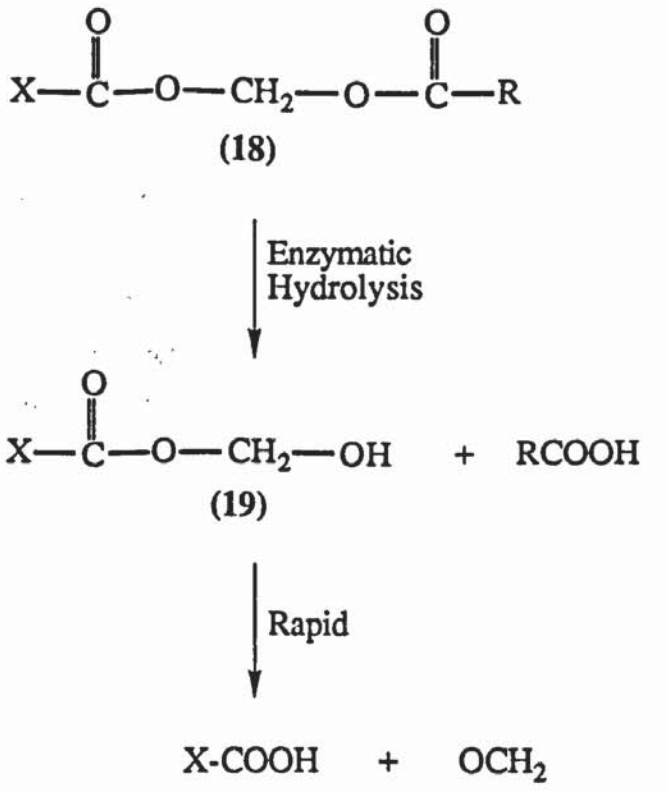

This tripartite prodrug principle has been used successfully to improve oral bioavailability of a number of penicillins.[101, 102, 103]

In the area of cancer chemotherapy much effort has focused on the development of brain-directed anticancer prodrugs for the treatment of tumours of the CNS. Methotrexate **(20, R=H)**, is restricted from entering the brain by the presence of two amino and two carboxylate residues, which are charged at physiological pH.

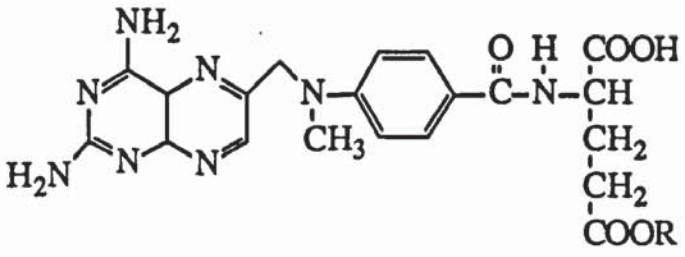

(20)

Attempts have been made to increase the lipohilicity of this drug by masking its carboxylate functions.[104] One study to assess the brain uptake of the lipophilic γ - monobutyl ester **(20, R=C_4H_9)** of methotrexate in the rhesus monkey revealed that 99%

of the compound became protein bound following intravenous administration. As a consequence, the combined CSF levels of the ester and methotrexate were very similar to those following an intravenous administration of equimolar methotrexate.

1.4.3. Derivatisation of the Amino Group in Prodrug Design

Many amine drugs are protonated at physiological pH and as such are not sufficiently lipophilic to passively diffuse across the BBB. Considerable effort has been focused on the synthesis of prodrugs of the central inhibitory neurotransmitter, γ-aminobutyric acid (GABA) (21).

(21)

GABA is zwitterionic at physiological pH and as such penetration of the BBB is minimal. Acylation of the amino group[105, 106] does improve brain delivery quite considerably, however, enzymatic cleavage of such amides has proved difficult in humans.

One of the most novel approaches to site-specific and sustained release of amine drugs to the brain, involving N-acylation, has been developed by Bodor and coworkers.[107, 108, 109] By linking such drugs to a lipophilic dihydropyridine carrier through an amide linkage, the dihydro derivative obtained (22) is distributed quickly throughout the body, including the brain, following its administration. The dihydro form (22) is then rapidly oxidised enzymatically to the quaternary salt (23), which because of its ionic character is trapped within the brain. The slow enzymatic cleavage of the amide linkage of the ammonium salt (23) then results in a sustained delivery of the active amino drug (24) to the brain.

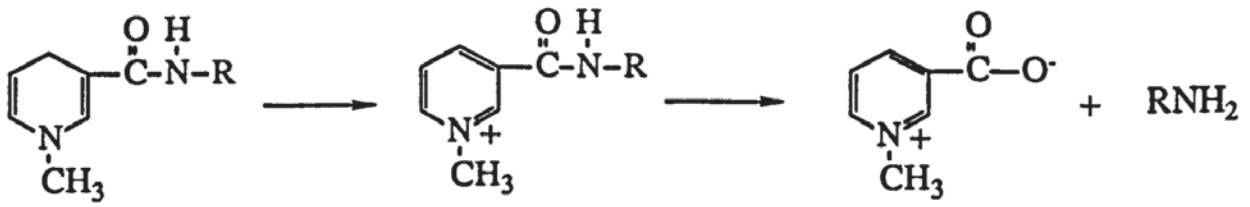

(22) (23) (24)

This technique has been applied to the brain - directed delivery of phenethylamine and dopamine[107] for the treatment of Parkinson's disease and also to 2', 3' dideoxynucleosides[110] in an attempt to treat AIDS dementia.

Another study by Carl and coworkers[96] involved the synthesis of benzyl esters of carbamates (**25**) as tripartite prodrugs for compounds containing the amino group. These model prodrugs underwent rapid hydrolysis in the presence of trypsin to release the model drug, 4-nitroaniline (**28**) (**Fig 1.6**). They proposed that enzymatic activation resulted in conversion of the weakly electron-donating acyl-amido group of (**25**) to the strongly electron-donating amino group of (**26**). The lone pair of electrons on the amino group results in the 'cascade effect' whereby additional electron density is released into the π system, thus stabilising the development of the positive charge on the benzylic carbon atom of (**27**). The benzyl carbonium ion (**27**) reacts with water to give 4-aminobenzyl alcohol, whereas the carbamate product loses carbon dioxide to give the model drug (**28**).

Fig 1.6 - Enzymatic hydrolysis of benzyl carbamate prodrugs

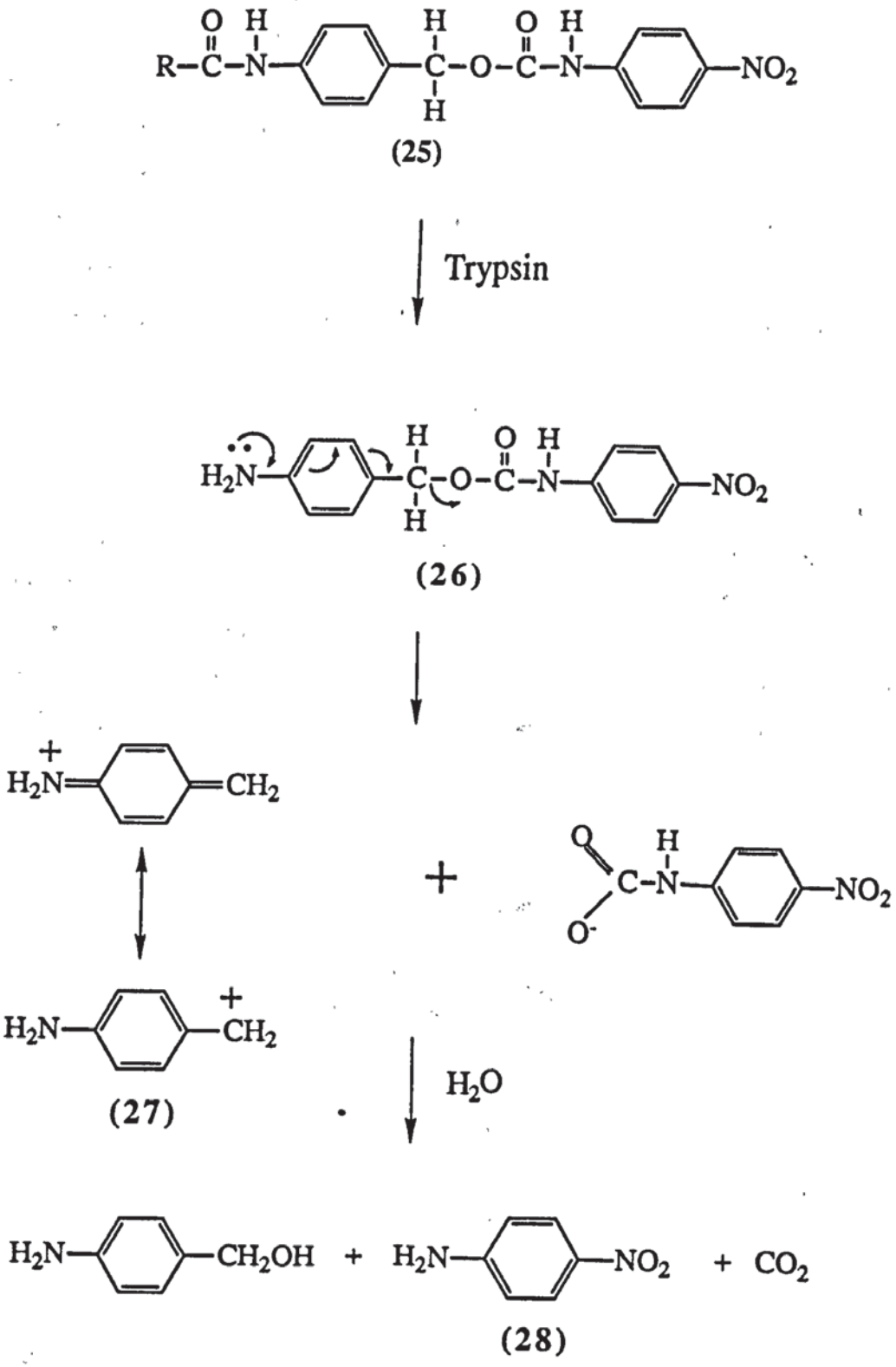

1.4.4. Derivatisation of Phosphates in Prodrug Design

A vital step in the mode of action of purine and pyrimidine nucleosides against viral diseases is their conversion into their 5'-mono, di or triphosphates (nucleotides) by cellular or virus-induced kinases. The nucleoside form is most often administered because of the ease with which it penetrates cells, however the necessary phosphorylation to the active nucleotide form does not always follow. In addition, the nucleotides are not directly applicable as chemotherapeutic agents because of their poor penetration of cell membranes and rapid enzymatic dephosphorylation to the parent nucleosides. Since masking of the ionised and hydrophilic phosphate group might be expected to increase the penetrability of the nucleoside phosphates, the development of suitable biologically reversible phosphate protective groups constitutes an important task.

A number of bipartite and tripartite prodrug derivatives for the phosphate group of nucleotides have been investigated. For example, the ionic phosphate moiety can be converted to an ester function to obtain less ionic character and better cellular penetrability. Once inside the cell, enzymatic hydrolysis to the active nucleotide would be expected to occur. A series of lipophilic 5'-alkyl phosphate esters of Ara-C (29) have been synthesised,[91] however these proved too unstable in plasma to be of any therapeutic potential.

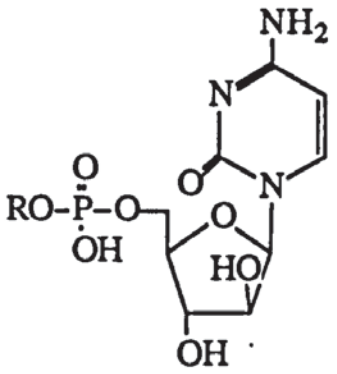

(29)

R=alkyl

A more successful approach has been to synthesise cyclic 3',5'-phosphates of Ara-C (30) which exhibited a higher degree of stability in the host circulation.

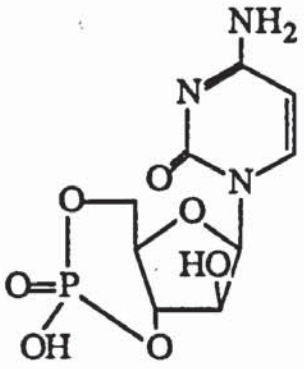

(30)

A series of cyclic phosphotriester derivatives of 2'-deoxy-5-fluorouridine (31) have been prepared in an attempt to increase the lipophilicity and membrane permeability of the nucleotide.[92] Variations in the degree of stability was again a feature of these compounds.

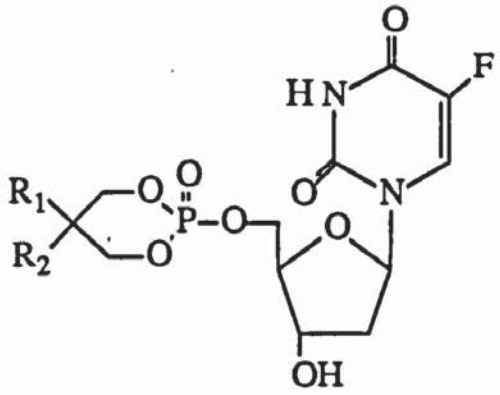

(31)

R=alkyl

A tripartite prodrug system applicable to phosphates is the acyloxyalkyl group, analogous to the acyloxyalkyl esters of carboxylic acid in **section 1.4.2.** Farquhar and co-workers[111, 112] have prepared a number of lipophilic di(alkanoyloxymethyl) esters of phosphoric acid and model benzyl and phenyl phosphates (32) and studied their degradation in aqueous buffer solutions, mice plasma and in the presence of hog liver esterase. The rate of enzymatic hydrolysis of the various derivatives was dependent on the nature of the acyl group, the more sterically hindered groups undergoing only slow hydrolysis. The mechanism of chemical and enzymatic hydrolysis is shown in **Fig 1.7.** The hydroxymethyl derivatives (33) formed have only transitory existence and spontaneously eliminate formaldehyde via a cascade process, initiated by electron donation from the hydroxyl function.

Fig 1.7 - Hydrolysis of di(alkanoyloxybenzyl) phosphates

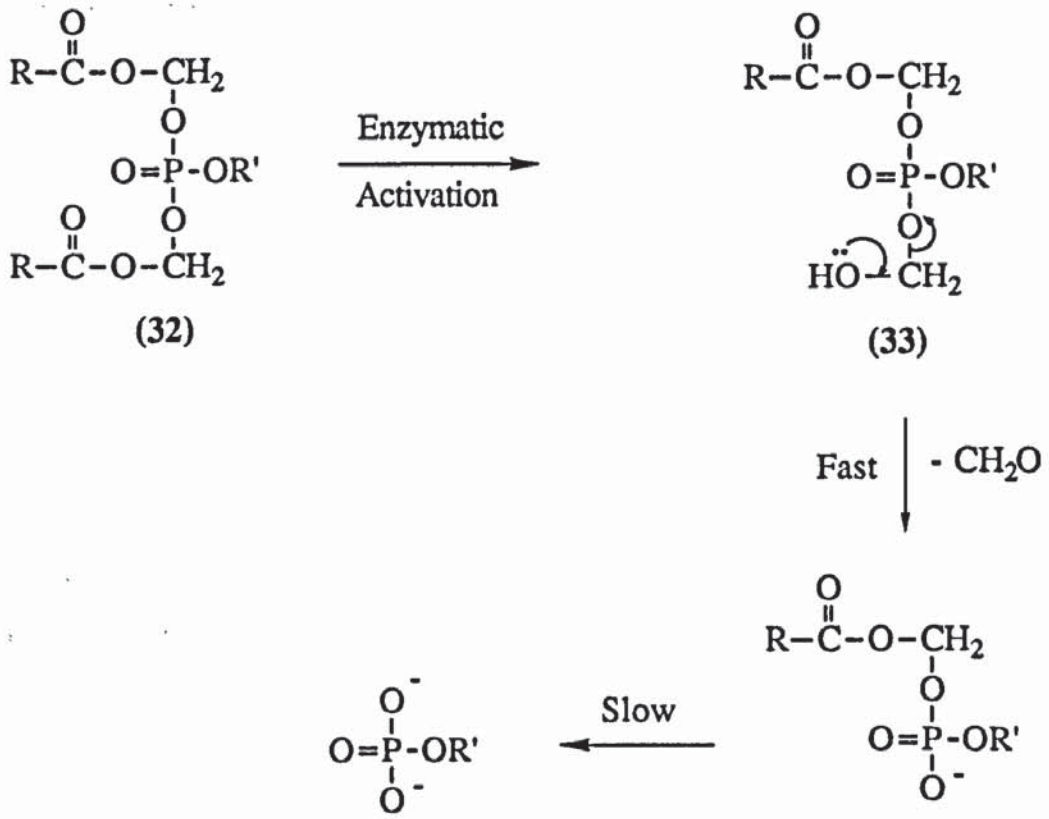

1.4.5. Derivatisation of Phosphonates in Prodrug Design

Simple alkyl and aryl esters of PFA have been prepared[113] in an attempt to increase lipophilicity and improve cell penetration of the drug. All three acidic groups of PFA need to be free for antiviral activity, however, only certain *P,P*-aryl esters of PFA can be biotransformed to PFA within cells.

The synthesis and evaluation of PFA and PAA linked to nucleosides has also received considerable attention. Such compounds could act as combined prodrugs in which the lipophilicity of each component is enhanced, thereby improving cellular penetration. Metabolic activation might then generate the nucleoside and the pyrophosphate analogue, which could exert their antiviral effects in a synergistic manner. Vaghefi *et al*[114] prepared a series of PFA derivatives which were attached through the phosphonate group to the 5'-hydroxyl of a nucleoside, in the hope of providing the required specificity of an inhibitor of reverse transcriptase which would not inhibit normal cellular RNA or DNA polymerase.[115] The 2'-deoxyadenosine 5'-(hydroxycarbonyl) phosphonate analogue **(34)** was the most active, possessing a similar ED_{50} value to PFA itself. It is unclear whether

whether this compound exerts its antiviral effect directly or via intracellular biotransformation to PFA.

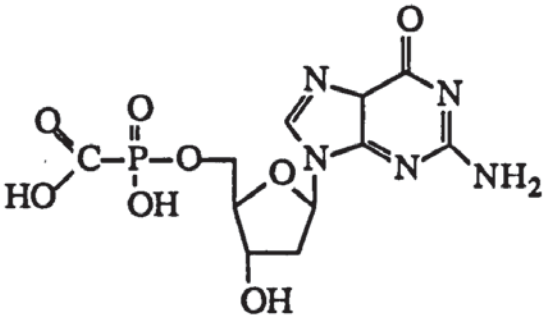

(34)

In another study PFA and PAA derivatives of 5'-substituted 2'-deoxyuridines (35) have been synthesised and their antiherpes activity evaluated.[116]

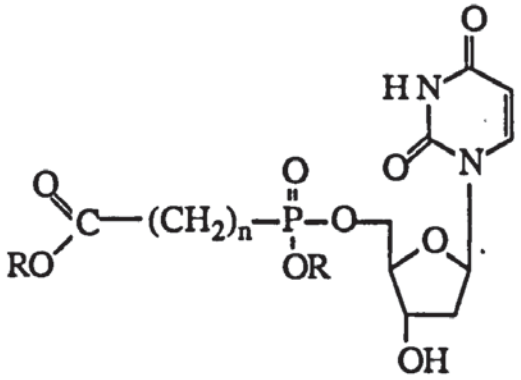

(35)

R=H, alkyl, aryl

The activity of these molecules was related to the ease with which they were hydrolysed and the parent compound released. It was found however, that the activities of the parent compounds were greater than those of the prodrugs, and no synergistic effect was demonstrated. The lack of synergism was surprising as this effect had previously been demonstrated against HSV-1 when PFA was combined with acyclovir *in vitro* [117] and *in vivo* .[118]

A similar study involved the synthesis and antiherpes evaluation of PAA and PFA esters of 5-bromo-2'-deoxyuridine and related pyrimidine nucleosides and acyclonucleosides.[119] Of these compounds only phosphonate esters in the 2'-deoxyuridine series showed significant activity against HSV-2, with the PFA **(36, n=0)**

and PAA (**36, n=1**) derivatives found to be more active than the parent nucleoside against HSV-2.

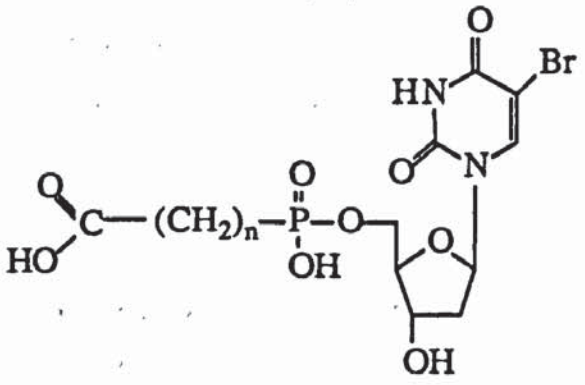

(36)

The active compounds may exert their effects by extracellular or intracellular hydrolysis to the corresponding antiviral agents, although an intrinsic component of antiviral activity may also be involved.

In an attempt to provide an effective inhibitor of HIV-1 reverse transcriptase, PFA has recently been coupled with AZT to form an AZT-PFA conjugate (**37**).[120]

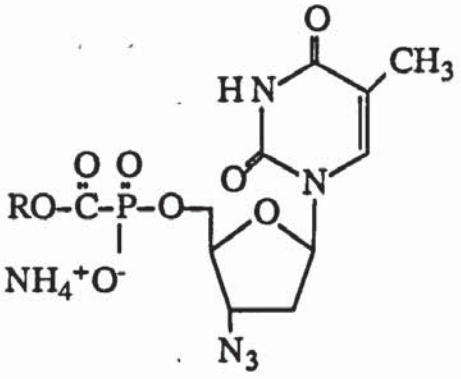

(37)

A synergistic effect has been reported when AZT and excess PFA were given in combination to intact cells,[121] however the ammonium salt of the combined prodrug, 3'-azido-5'-(ethoxycarbonylphosphinyl)-3'-deoxythymidine (**37, R=CH_3CH_2**) was found to inhibit HIV-1 reverse transcriptase activity to a lesser extent than AZT. The lower potency of the conjugate may be due to a slower uptake of the molecule than the parent nucleoside, as well as slow metabolism to the active components. Although it possessed lower anti-HIV activity than AZT, the conjugate was also less cytotoxic

1.5. Aims of Research

The aim of this project is to design prodrugs of antiviral phosphonates with sufficient lipophilicity to permit passive diffusion through the BBB into the brain and CNS, wherein metabolic reconversion to the hydrophilic parent drug can occur. The ideas developed could also be extended to the delivery of nucleotides and bisphosphonates used in the treatment of bone cancer.[122]

Based on the tripartite prodrug cascade approach developed by Carl *et al*[96] the present studies will investigate the synthesis and metabolic activation of a series of di(4-substituted-benzyl) esters of phosphonoformate (**38**) and phosphonoacetate (**39**). The substituent in the 4-position of the benzene ring (**X**) should be electron-withdrawing but also able to undergo metabolic conversion to an electron-donating substituent (**Y**). For example, in the presence of esterases, an alkanoyloxy group (**X**) may be hydrolysed to give the hydroxy group (**Y**), or alternatively an azide substituent (**X**) could be converted to an electron rich amino group (**Y**) by reduction. These triesters (**38, 39**) may be sufficiently lipophilic to passively diffuse into the brain, where the electron-deficient **X** group could be metabolically converted to an electron-donating function **Y** (**40**), thus promoting decomposition of the molecule *via* the cascade effect to form the benzyl diester (**41**) and a resonance stabilised benzyl carbonium ion (**42**) (**Fig 1.8**). This process should be repeated with the loss of the second benzyl group to form the monoester (**43**) which itself could undergo enzymatic hydrolysis to the active drug.

The synthesis and metabolic activation of benzoyloxymethyl triesters of PAA (**44**) will also be investigated. This series of compounds is based on the alkanoyloxymethyl phosphate esters developed by Srivastva and Farquhar.[111, 112] In common with the di(4-substituted-benzyl) phosphonate esters (**38, 39**) it is hoped that these molecules will be able to traverse the BBB. Once inside the CNS, esterase action may hydrolyse the benzoyl group and the resulting hydroxymethyl intermediate (**45**) could degrade to PAA (**8**) with the loss of formaldehyde (**Fig 1.9**)

Fig 1.8 - Proposed metabolic activation of dibenzyl triesters

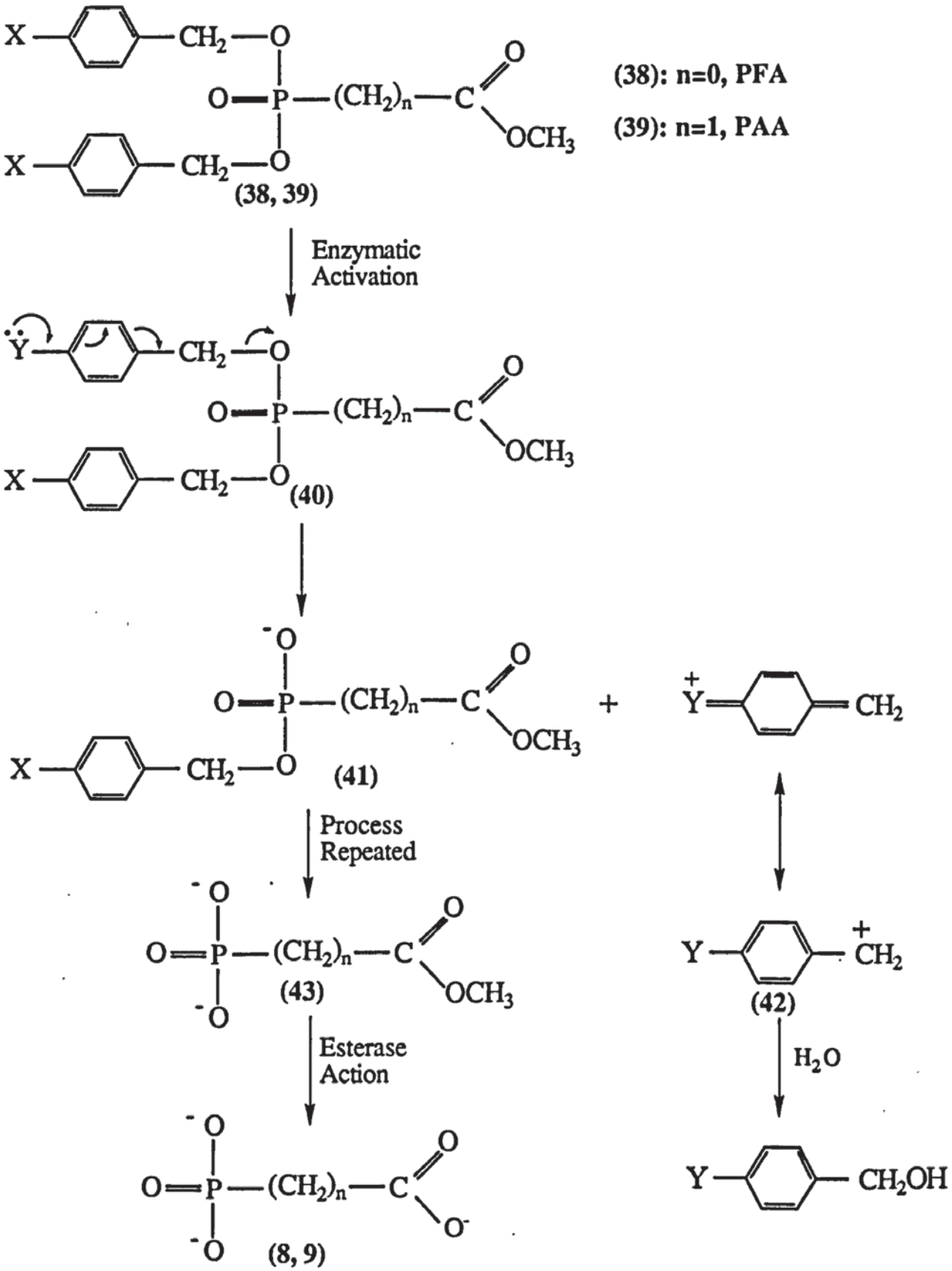

Fig 1.9 - Proposed metabolic degradation of di(benzoyloxymethyl) triesters

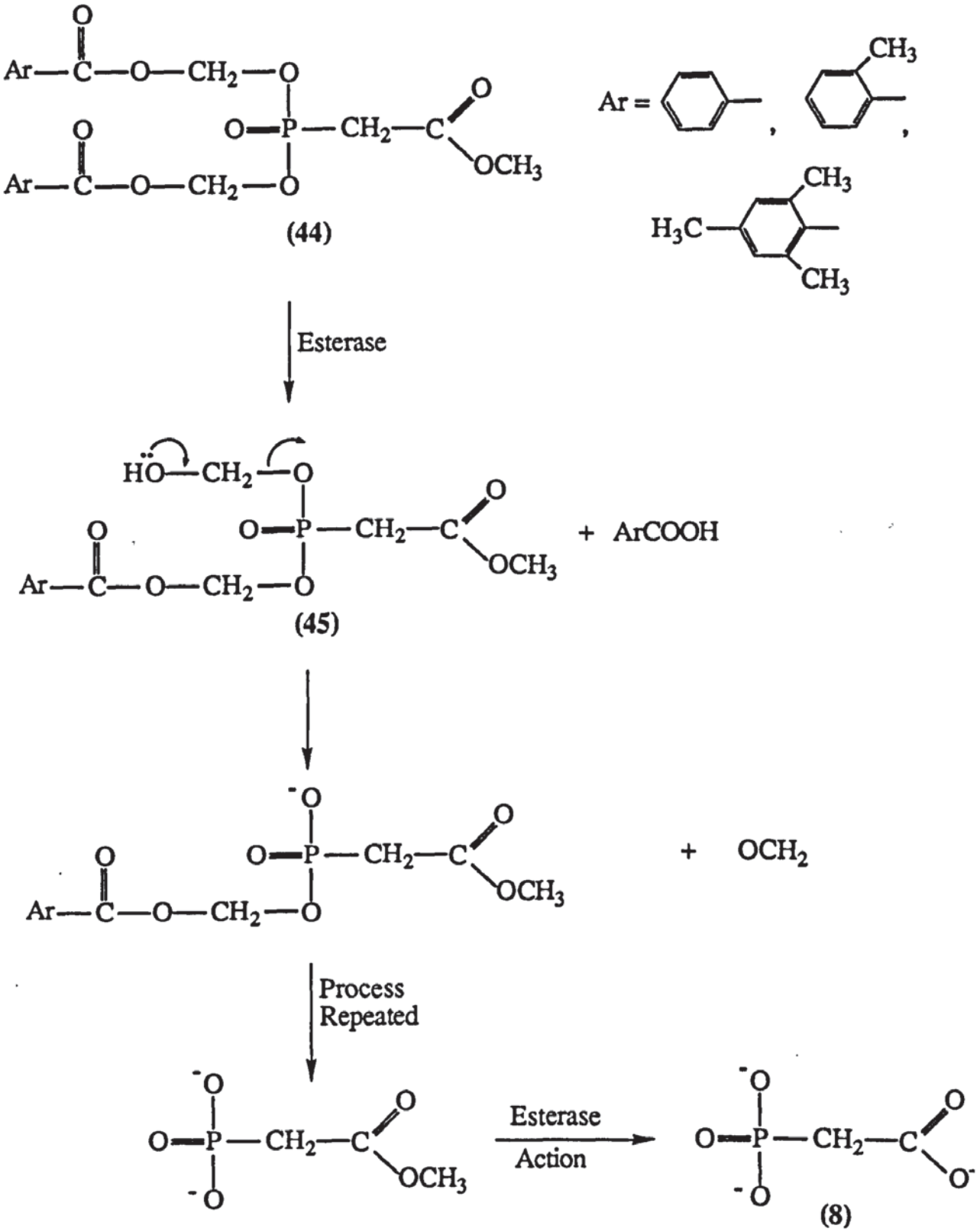

RESULTS AND DISCUSSION

CHAPTER 2 - ESTERS OF PHOSPHONOFORMATE

2.1. Synthesis of Dibenzyl (Methoxycarbonyl)phosphonates (38)

Two methods were used to prepare the dibenzyl triesters of PFA (38). The first method is outlined in **Fig 2.1** and involves the synthesis of (methoxycarbonyl)phosphonic dichloride (50). Reaction of two equivalents of the appropriate benzyl alcohol (51) with (50) in the presence of two equivalents of triethylamine to remove the hydrochloric acid released, yielded a series of 4 - substituted dibenzyl triesters of phosphonoformate (38, **X=H, N_3, CH_3, CH_3COO, $(CH_3)_3CCOO$, Cl, CF_3**).

Fig 2.1 - First method for the synthesis of dibenzyl (methoxycarbonyl)phosphonates(38)

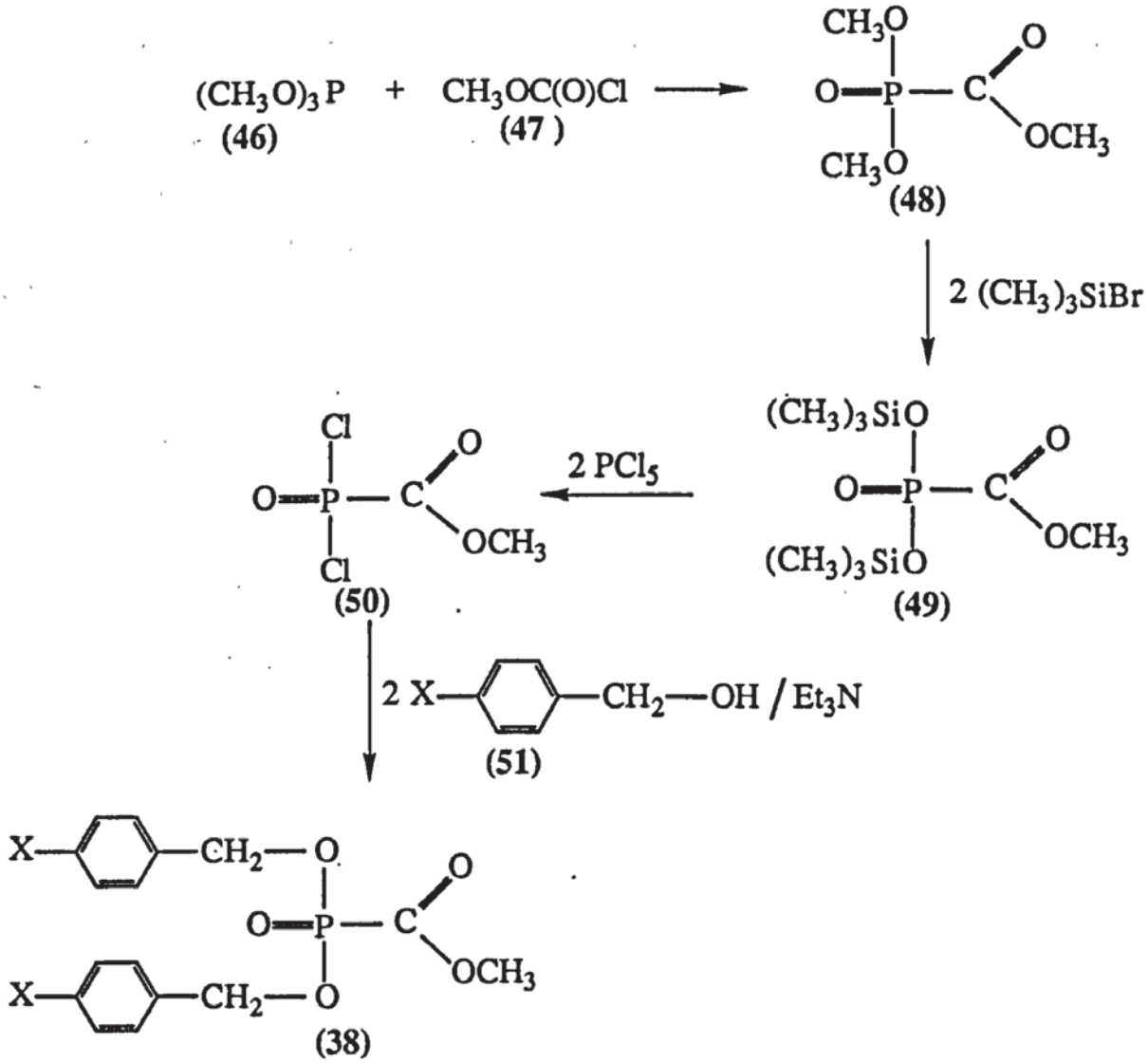

Initially the (methoxycarbonyl)phosphonic dichloride (50) proved difficult to prepare. The key step in the first attempted route involved an Arbusov reaction[123, 124, 30] to form a

P-C bond between methyl chloroformate and tris(trimethylsilyl) phosphite to form di(trimethylsilyl) (methoxycarbonyl)phosphonate (**49**).[125] The reaction gave a very low yield of (**49**), perhaps as a result of the extremely moisture sensitive nature of the silylated substrate and product. The more successful approach to the synthesis of the dichloride (**50**) (**Fig 2.1**) involved first the preparation of dimethyl (methoxycarbonyl)phosphonate (**48**). This route also required an Arbusov reaction[123, 124, 30] to form the phosphonate (**48**), but here the substrate, trimethyl phosphite (**46**), was less moisture sensitive than tris(trimethylsilyl) phosphite. The reaction was straightforward and gave an 80% yield of dimethyl (methoxycarbonyl)phosphonate (**48**). This compound is also commercially available. Based on the method of McKenna and coworkers[127] for the dealkylation of phosphonic acid dialkyl esters with bromotrimethylsilane, dimethyl (methoxycarbonyl)phosphonate (**48**) was reacted with 2.5 molar equivalents of bromotrimethylsilane at room temperature to give di(trimethylsilyl) (methoxycarbonyl)phosphonate (**49**) in 60% yield. This reaction probably occurs *via* attack on silicon by the phosphoryl oxygen of dimethyl (methoxycarbonyl)phosphonate (**48**) to give the intermediate (**52**), followed by substitution of the displaced halide ion to give the methyl trimethylsilyl (methoxycarbonyl)phosphonate (**53**). A second cycle of the same reaction sequence would give di(trimethylsilyl) (methoxycarbonyl)phosphonate (**49**) (**Fig 2.2**).[128] The phosphonate (**49**) was then reacted with PCl_5 to give a 72% yield of (methoxycarbonyl)phosphonic dichloride (**50**).[129]

Fig 2.2 - Mechanism for the formation of di(trimethylsilyl) (methoxycarbonyl)-phosphonate (**49**)

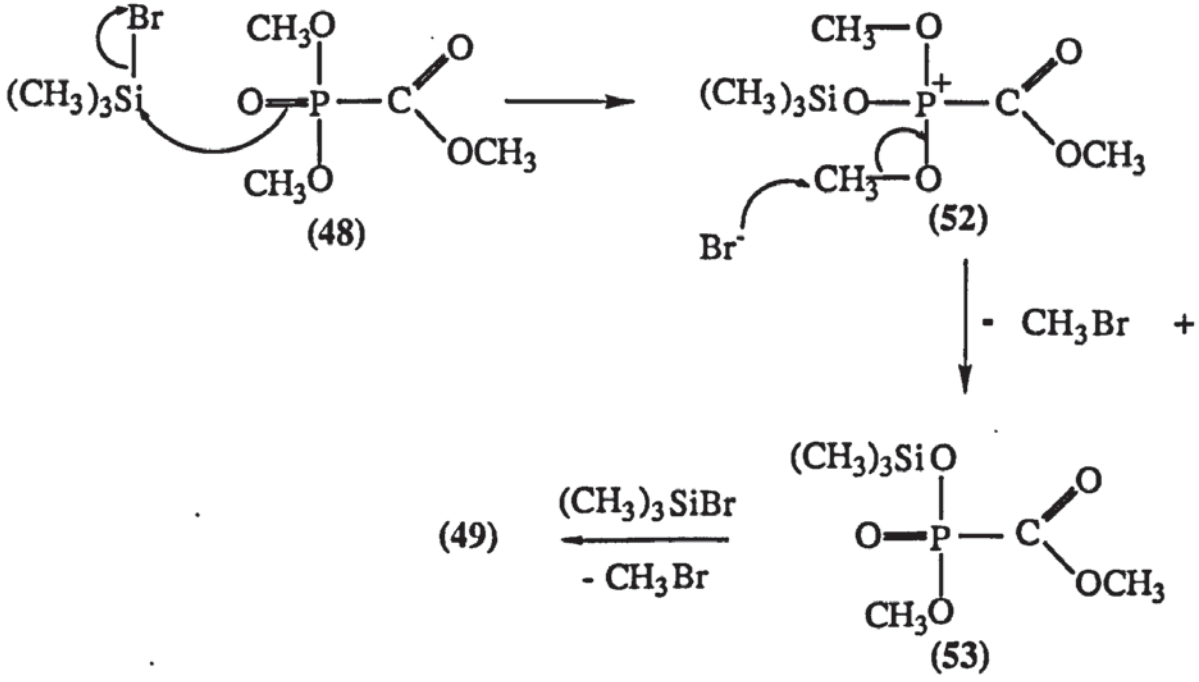

The benzyl alcohols required for coupling with the phosphonic dichloride (**50**) were either commercially available or readily prepared. 4-Azidobenzyl alcohol (**51, X=N_3**) was prepared by the diazotisation of 4-aminobenzyl alcohol and subsequent nucleophilic substitution with sodium azide.[130] The alkanoyloxybenzyl alcohols (**51, X=CH_3COO, $(CH_3)_3CCOO$**) were prepared by the reaction between 4-hydroxybenzyl alcohol and the appropriate anhydride.[131]

The second method for the synthesis of dibenzyl (methoxycarbonyl)phosphonates (**38**) is given in **Fig 2.3.** This route involves the passage of di(trimethylsilyl) (methoxycarbonyl)phosphonate (**49**) down an ion-exchange column to give disodium (methoxycarbonyl)phosphonate (**54**), which is converted to the corresponding disilver salt (**55**) by reaction with silver nitrate. A nucleophilic substitution reaction between disilver (methoxycarbonyl)phosphonate (**55**) and the appropriate benzyl iodide (**56**) gave the desired phosphonate triester (**38**).[113]

Fig 2.3 - Second method for the synthesis of dibenzyl (methoxycarbonyl)phosphonates

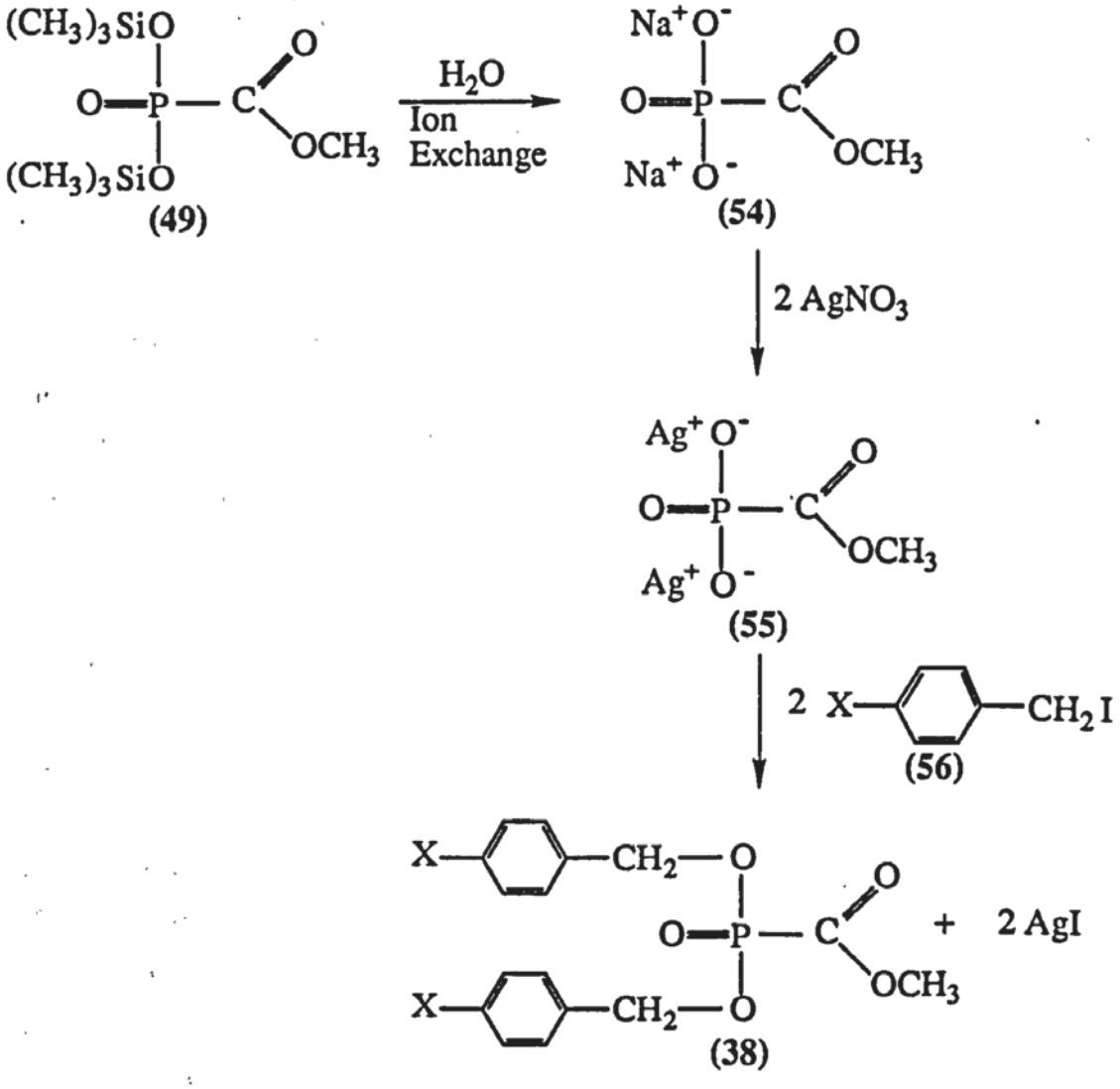

This method was only used for the synthesis of bis(4-nitrobenzyl) (methoxycarbonyl)phosphonate (**38, X=NO_2**), but is likely to be applicable to all analogues. 4-Nitrobenzyl iodide (**56, X=NO_2**) was obtained from the reaction of 4-nitrobenzyl chloride with potassium iodide.[132]

The triesters (**38, X=H, NO_2, CH_3, CH_3COO, $(CH_3)_3CCOO$, Cl**) were purified by flash column chromatography.[133] The 4-azido analogue (**38, X=N_3**), however, was found to be unstable on silica and was used without further purification. The 4-nitro analogue (**38, X=NO_2**) was a colourless solid at room temperature (mp 58 - 62°C) and was further purified by recrystallisation from toluene/petroleum ether. 4-trifluoromethylbenzyl alcohol (**51, X=CF_3**) was removed from di(4-trifluoromethylbenzyl) (methoxycarbonyl)phosphonate (**38, X=CF_3**) by Kugel distillation rather than flash column chromatography due to very poor chromatographic separation between the triester (**38, X=CF_3**) and the alcohol.

All of the triesters were fully characterised by elemental analysis, high resolution fast atom bombardment (FAB) or chemical ionisation (CI) mass spectrometry, high resolution ^1H, ^{31}P and ^{13}C nuclear magnetic resonance (NMR) spectroscopy and infra-red spectroscopy. The mass spectra of most triesters showed the most abundant peak with an *m/z* corresponding to the appropriate 4-substituted benzyl fragments. The exception was the nitrobenzyl triester (**38, X=NO_2**) which showed the most abundant peak at m/z 428 corresponding to the molecular ion plus an NH_4^+ cation. The ^1H NMR spectra ($CDCl_3$) of all triesters (**38**) showed a characteristic doublet (J_{PH} ~8 Hz) in the region of δ_H 5 ppm, which integrated for 4 H, confirming that the benzyloxy groups were attached to phosphorus. The ^{31}P (^1H coupled) NMR spectra were characterised by a pentet of quartets (J_{PH} ~8, 1 Hz) in the region of δ_P -5 ppm, arising from coupling of the 4 benzylic protons with phosphorus, together with long range interaction between the methoxycarbonyl function and phosphorus. **Fig 2.4** gives the ^1H and ^{31}P (^1H coupled) NMR spectra for a typical phosphonoformate triester, dibenzyl (methoxycarbonyl)phosphonate (**38, X=H**).

The synthesis of di(4-methoxybenzyl) (methoxycarbonyl)phosphonate (**38, X=CH_3O**) was attempted *via* both routes shown in **Figs 2.1** and **2.3**, but was unsuccessful. The only compound recovered from each reaction mixture was di(4-methoxybenzyl) ether (**57**). This result supports the present rationale for prodrug design outlined in **section 1.5**, suggesting that the triester (**38, X=CH_3O**), or an intermediate towards its synthesis, is unstable owing to the electron-donating mesomeric effect of the methoxy group causing degradation via a cascade effect (**Fig 2.5**). The highly electrophilic 4-methoxybenzyl

Fig 2.4 – ^{1}H and ^{31}P NMR spectra for dibenzyl (methoxycarbonyl)phosphonate

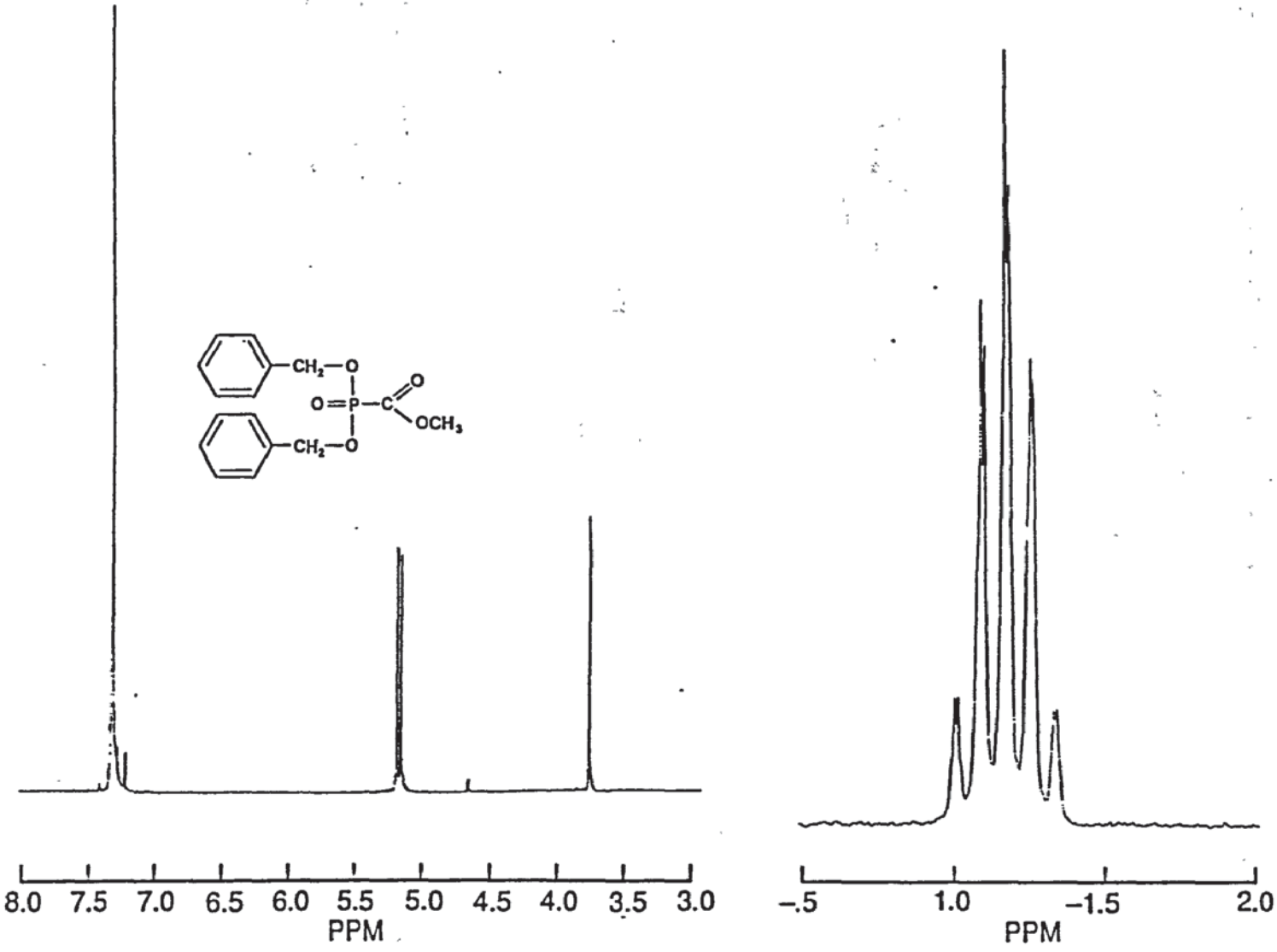

carbonium ion (**58**) generated from this breakdown probably reacts with the 4-methoxybenzyl alcohol in the reaction mixture to form the ether (**57**). The highly reactive nature of the 4-methoxybenzyl carbonium ion (**58**) has been observed in a seperate study by Amyes and Richard.[134]

Fig 2.5 - General scheme for the degradation of methoxybenzyl phosphonates

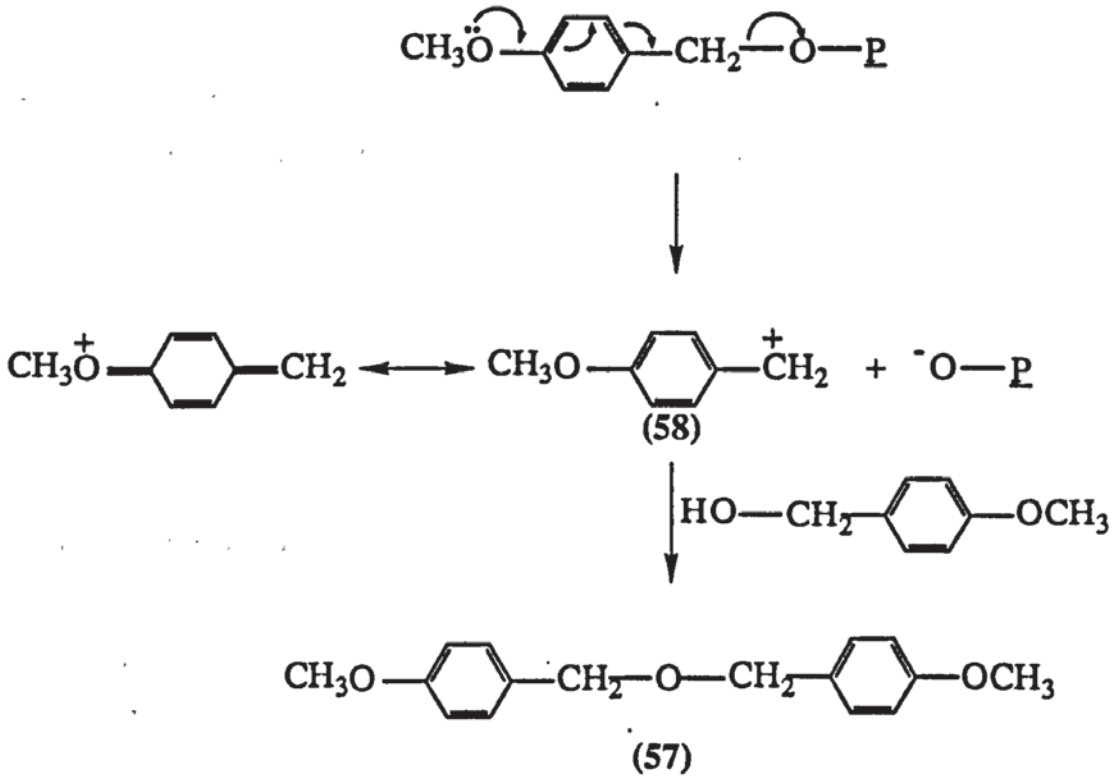

It was, however, possible to synthesise the 3-substituted derivative, di(3-methoxybenzyl) (methoxycarbonyl)phosphonate (**59**) in good yield from the reaction of 3-methoxybenzyl alcohol with (methoxycarbonyl)phosphonic dichloride (**50**).

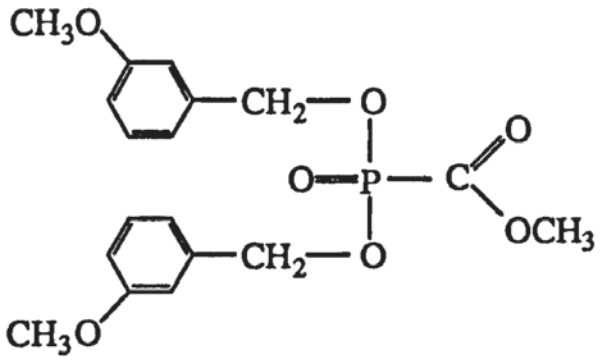

(**59**)

As anticipated this suggests that the cascade effect only operates for electron-donating substituents in the 4-position of the benzene ring. A similar effect has been observed by Higuchi and Schroeter[135] who studied the abnormally high reactivity of drugs containing the 2- or 4-hydroxybenzyl structure. In a survey of reactions of several drugs (eg. epinephrine) with bisulphites, a 2- or 4-hydroxyl or amino group was essential for reaction and subsequent formation of substituted benzyl sulphonic acids. 3-substituted isomers were unreactive with sulphite under the experimental conditions. This suggests the formation of a quinone methide **(60)** by reversible dehydration, followed by a rapid reaction with bisulphite to form the sulphonate product. In another study, Bogardus and Higuchi[136] proposed the involvement of a quinone methide intermediate in the hydrolysis of quaternary ammonium derivatives of tertiary amines.

(60)

2.2. Synthesis of Sodium Benzyl (Methoxycarbonyl)phosphonates (61)

It was anticipated that hydrolysis of the triesters **(38)** would give the corresponding benzyl (methoxycarbonyl) phosphonate diesters **(61)**. Hence, the sodium salts of the diesters were prepared by the reaction of sodium iodide with the appropriate dibenzyl phosphonate triester **(38)** in dry acetone, either heating under reflux or at room temperature **(Fig 2.6)**.[137]

Fig 2.6 - Synthesis of sodium benzyl (methoxycarbonyl)phosphonates **(61)**

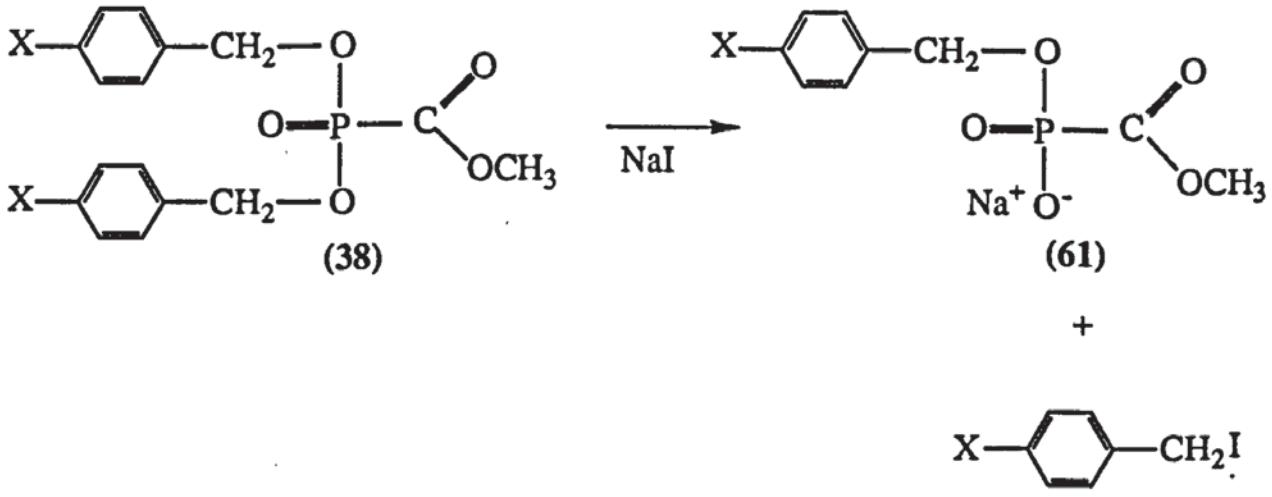

In this reaction the strongly nucleophilic character of the iodide ion[138] was used to selectively remove one phosphonate-bound benzyl group to give the diesters **(61)**, which were precipitated as colourless solids. The precipitates are usually almost pure and repeated washing with acetone ensured complete removal of the benzyl iodide generated in the reaction. The salts were further purified by precipitation following the addition of acetone to an aqueous solution of the diester. Yields varied from 17% **(61, X=H)** to 91% **(61, X=Cl)** and could be increased by minimising the volume of solvent used, indicating a degree of solubility of the sodium salts in acetone.

The diester salts were fully characterised by elemental analysis, high resolution FAB mass spectrometry, high resolution ^{1}H, ^{31}P and ^{13}C NMR spectroscopy and infra-red spectroscopy. The FAB mass spectra of all diesters revealed the most abundant peak with an *m/z* corresponding to the molecular ion plus a sodium cation. The ^{1}H NMR spectra (D_2O) of these salts showed a characteristic doublet (J_{PH} ~8 Hz) in the region of δ_H 5 ppm, which integrated for 2 H, confirming that one benzyloxy group was attached to phosphorus. The ^{31}P (^{1}H coupled) NMR spectra (D_2O) showed a triplet of quartets (J_{PH} ~8, 1 Hz) at approximately δ_P -3 ppm arising through coupling of the 2 benzylic protons with phosphorus and long range interaction with the methoxycarbonyl function.

2.3. Antiviral Properties

The protective activity and toxicity of potential anti-HIV compounds is measured in one experiment using a colorimetric assay (MTT method) which determines the ability of viable cells to reduce a tetrazolium compound to a blue formazan product which can be measured at 540 nm. Formazan results are confirmed by examining syncytia formation and measuring antigen p24 by Elisa. The phosphonoformates tested for anti-HIV activity by Dr Derek Kinchington of St Mary's Hospital (London) were:

Di(4-azidobenzyl) (methoxycarbonyl)phosphonate **(38, X=N_3)**

Di(4-nitrobenzyl) (methoxycarbonyl)phosphonate **(38, X=NO_2)**

Sodium 4-azidobenzyl(methoxycarbonyl)phosphonate **(61, X=N_3)**

Disodium (methoxycarbonyl)phosphonate **(54)**

Trisodium phosphonoformate **(9)**

The compounds were compared with AZT and **Table 2.1** gives the results of anti-HIV testing expressed as the concentration of drug which reduces the antigen p24 by 50% in infected cell cultures (EC_{50}).

Table 2.1 - Concentration of drug which reduces the antigen p24 by 50% in infected cell cultures (EC_{50})

Compound	$EC_{50}(\mu M)$
38, $X=N_3$	inactive
38, $X=NO_2$	inactive
61, $X=N_3$	inactive
54	200
9	20
AZT	0.016

The assay indicates that the triesters (**38**, $X=N_3$, NO_2) and diester (**61**, $X=N_3$) were inactive at the highest concentration tested (200 μM). Disodium (methoxycarbonyl)phosphonate (**54**) was found to be active at 200 μM, with trisodium phosphonoformate (**9**) being the most active with an EC_{50} of ~20 μM.

The inactivity of the triesters, diesters and monoesters of phosphonoformate in an *in vitro* assay was not altogether unexpected. The molecules were designed as prodrugs and as such are inactive until metabolism to the parent drug has taken place. The cell line used has little metabolising capacity, hence the only true test of their anti-HIV activity is either an *in vivo* study or incubation in the presence of metabolising enzymes which will assess their ability to degrade to the active drug, phosphonoformate (**9**).

2.4. Hydrolysis Studies of Dibenzyl (Methoxycarbonyl)phosphonate (38, X=H)*

2.4.1. Rate of Hydrolysis by HPLC

The triester (**38**) (100 or 400 μg ml^{-1}) was subjected to hydrolysis in a phosphate buffer (pH 7.4, 0.1 M) - acetonitrile mixture (1:1, v/v) at 37°C and the reaction was monitored

by ion-pair reversed-phase high performance liquid chromatography (HPLC). Samples were injected directly onto a C-18 endcapped column and eluted for 20 min with a linear or convex gradient of acetonitrile - 10 mM tetrabutylammonium chloride in water, initial conditions, 35:65 (v/v); final conditions, 90:10 (v/v) at a flow rate of 1 ml min^{-1}. An ion-pairing agent was used to ensure that the charged hydrolysis products did not elute with the solvent front. As a consequence, the disappearance of the highly lipophilic triester (**38**, retention time = 15.2 min) as well as the appearance of any charged species could be followed simultaneously throughout the hydrolysis. The reaction was observed to follow first order kinetics and the half-life ($t_{1/2}$) was calculated as 24.9 min (standard deviation 2.9) from **Eqn 2.1.**

$$t_{1/2} = \ln 2 / k \qquad \textbf{Eqn 2.1}$$

where k is the rate constant for the disappearance of triester.

The high degree of chemical instability was surprising especially when compared to the much greater stabilities of a range of phosphate diesters and triesters.[139] For example, the half-life for the hydrolysis of dimethyl phosphate at pH 7.4 is too slow to be measured, even at high temperatures. Further to this Hudson and Harper[140] measured a half-life of 11 min for dibenzyl methylphosphonate (**62**) at 100°C. However, very recent observations by Iyer and coworkers[141] on the synthesis and stability of P,P-di(alkanoyloxymethyl) esters of phosphonoformate (PFA), together with studies by Krol *et al* [142] on the hydrolysis of a series of alkyl and aryl PFA esters also suggest a high rate of degradation associated with triesters of PFA. In an attempt to understand the reason for the high reactivity of dibenzyl (methoxycarbonyl)phosphonate (**38**) the mechanism of hydrolysis for the triester was investigated in detail.

2.4.2. Identification of Products

It was anticipated that the hydrolysis of the triester (**38**) would be straightforward, the only expected products being the diester, benzyl (methoxycarbonyl)phosphonate (**61**), and benzyl alcohol (**Fig 2.7**).

* In section 2.4 structures (**38**) and (**61**) possess X=H in **Fig 2.6.**

Fig 2.7 - Expected hydrolysis of dibenzyl (methoxycarbonyl)phosphonate (38)

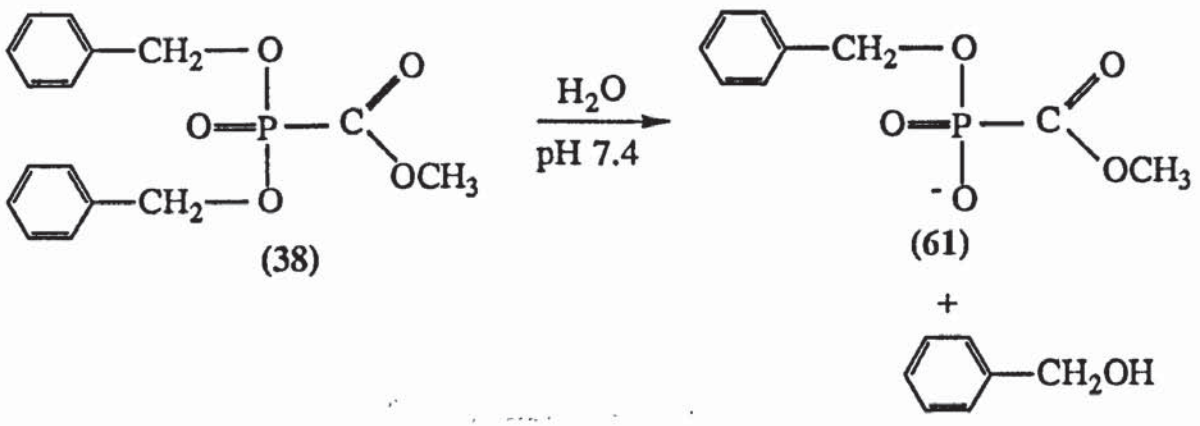

A typical HPLC chromatogram (**Fig 2.8**) revealed that benzyl alcohol and the diester (**61**) were indeed the major products eluting at 4.6 and 5.4 min respectively, however there were also four unexpected products (**63**), (**64**), (**65**) and (**66**) having retention times of 14.1, 4.3, 11.8 and 10.1 min respectively.

In an attempt to characterise these four degradation products the hydrolysis experiment was repeated and monitored by ^{31}P NMR spectroscopy. After 90 min there were 3 main phosphorus containing compounds present, the triester (**38**, δ_P -3.70 ppm), the diester (**61**, δ_P -4.71 ppm) and an unknown peak at δ_P 10.82 ppm. When the ^{31}P NMR spectrum was recorded again with ^{1}H coupling, the unknown peak at δ_P 10.82 ppm gave rise to a doublet of pentets with coupling constants of 719 and 9.6 Hz. The very large coupling to phosphorus, which is consistent only with a P-H group, together with the pentet pattern suggested the formation of dibenzyl phosphite (**63**). This was supported by the work of Noren and coworkers[113] who observed some phosphite formation following the hydrolysis of trialkyl esters of phosphonoformate. For example, the di-iso-propyl (methoxycarbonyl)- and di-n-butyl (methoxycarbonyl)phosphonates were observed to hydrolyse to their corresponding phosphites under slightly alkaline conditions. Further evidence for phosphite formation can be derived from the study by Warren and Williams[143] on the acid catalysed decarboxylation of PFA to give phosphorous acid (**Fig 2.9**).

Fig 2.8 – HPLC chromatogram for the hydrolysis of dibenzyl (methoxycarbonyl)phosphonate

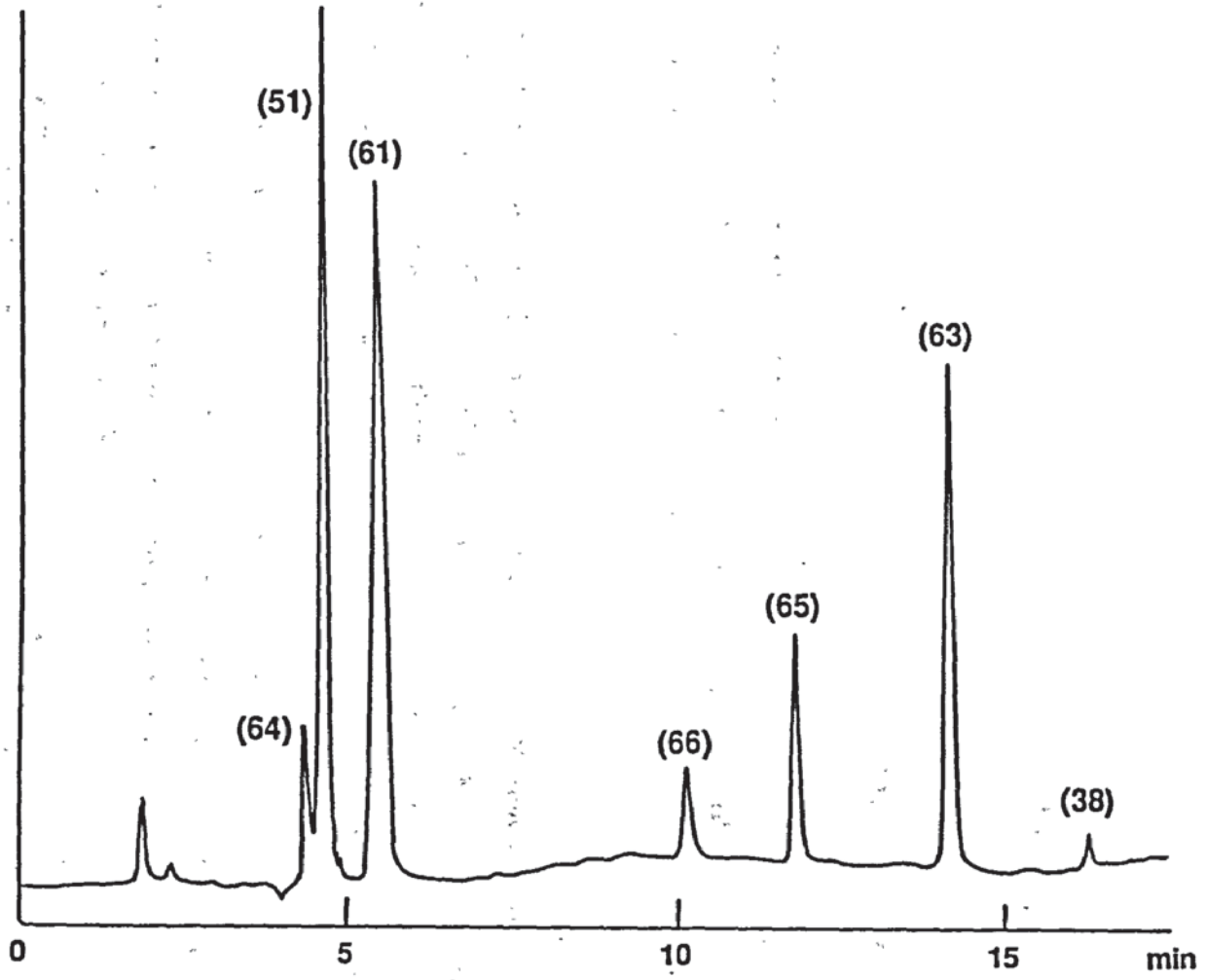

Fig 2.9 - The acid-catalysed decarboxylation of phosphonoformate

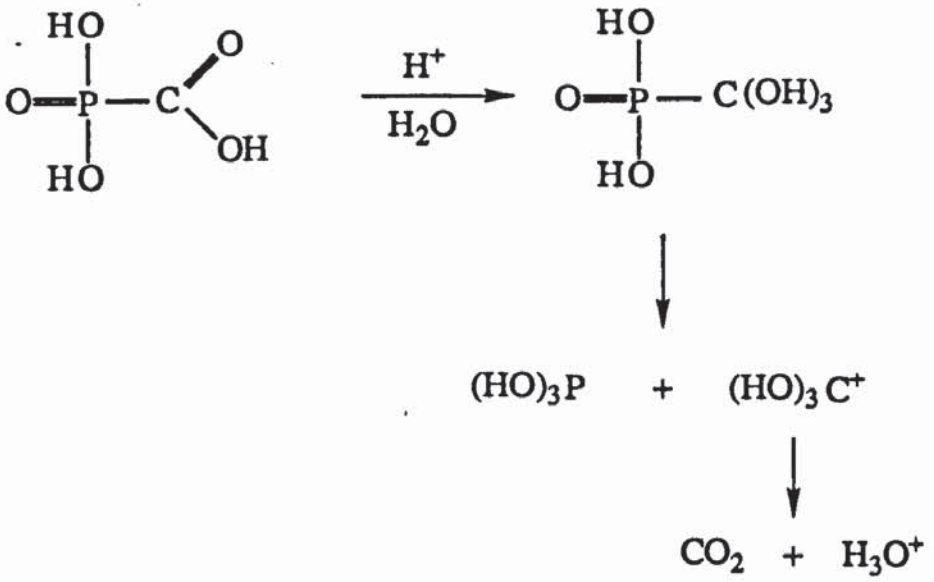

The formation of dibenzyl phosphite **(63)** from the triester **(38)** was confirmed following isolation of the compound on a solid phase extraction column, and subsequent spectroscopic and chromatographic comparison with an authentic sample of the phosphite **(63)**.

The ^{31}P NMR spectrum of the hydrolysis of the triester **(38)** was recorded again after a further 2 weeks at 37°C **(Fig 2.10A)** and both the triester **(38)** and dibenzyl phosphite **(63)** had completely degraded, with the generation of a new peak at δ_P 5.90 ppm. When the ^{31}P NMR spectrum was recorded with ^{1}H coupling **(Fig 2.10B)** this peak was split into a doublet of triplets, with coupling constants of 625 and 8.3 Hz. From the large coupling constant, together with the triplet pattern, this peak was assigned as monobenzyl phosphite **(64)**. Its identity was confirmed by spectroscopic and chromatographic comparison with an authentic sample of the phosphite prepared by the reaction of dibenzyl phosphite with sodium iodide.

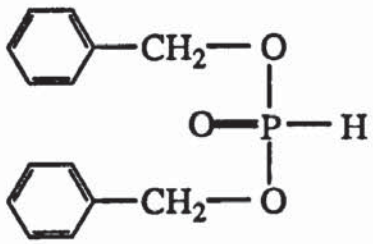

(63)

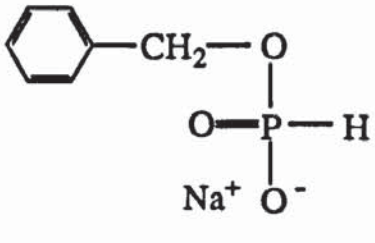

(64)

Characterisation of the minor products **(65)** and **(66)** was not so straightforward. The first question to be answered was whether these compounds were charged species. To establish this, the HPLC analysis was repeated in the absence of ion-pairing agent

Fig 2.10 – ^{31}P NMR (^{1}H decoupled and coupled) spectra for the hydrolysis of dibenzyl (methoxycarbonyl)phosphonate

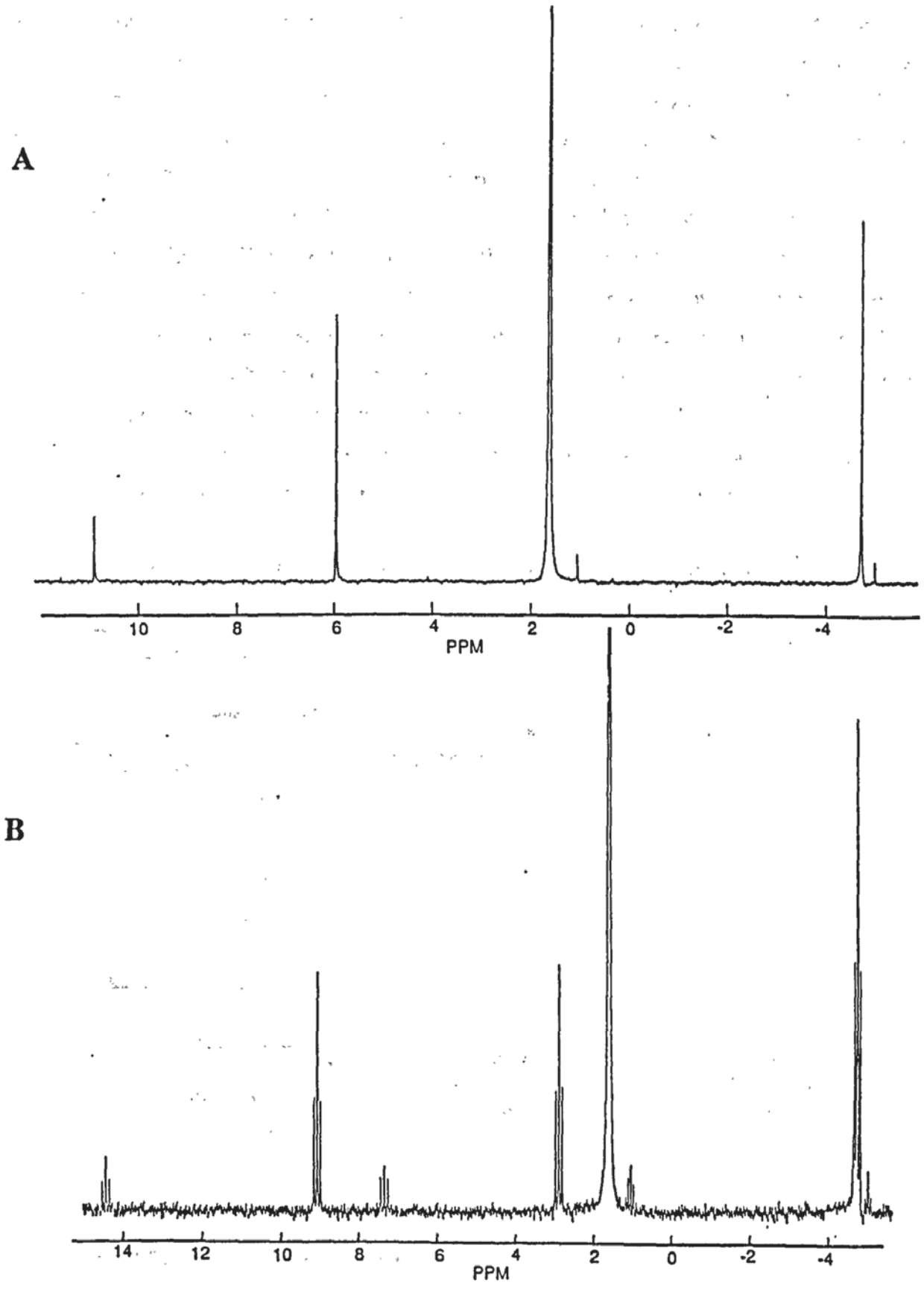

causing the elution of any charged species at the solvent front. The triester (**38**), dibenzyl phosphite (**63**) and benzyl alcohol eluted at their usual retention times, whereas the diester (**61**) and benzyl phosphite (**64**), together with the unknown compounds (**65**) and (**66**) now eluted with the solvent front. This implied that the unknown compounds were indeed charged species, and were probably monoanionic as they possessed relatively long retention times in the presence of ion-pairing reagent. The ^{31}P NMR (^{1}H decoupled) spectrum (**Fig 2.10A**) also revealed the formation of two minor phosphorus-containing compounds with shifts of δ_P -4.97 ppm and 1.07 ppm. When the spectrum was run with ^{1}H coupling (**Fig 2.10B**), the peak at δ_P -4.97 ppm gave rise to a triplet (J_{PH} 6.7 Hz), suggesting the attachment of one benzyloxy group to phosphorus, whereas the other unknown gave a pentet (J_{PH} 6.7 Hz), indicative of 2 benzyloxy groups attatched to phosphorus. The possibility of transesterification with benzyl alcohol was considered, therefore a sample of sodium benzyl (benzyloxycarbonyl)phosphonate (**65**) was prepared by the reaction of dibenzyl (benzyloxycarbonyl)phosphonate (**67**) with NaI (**Fig 2.11**) and found to elute at the same retention time (11.75 min) as unknown (**65**).

Fig 2.11 - Synthesis of sodium benzyl (benzyloxycarbonyl)phosphonate (**65**)

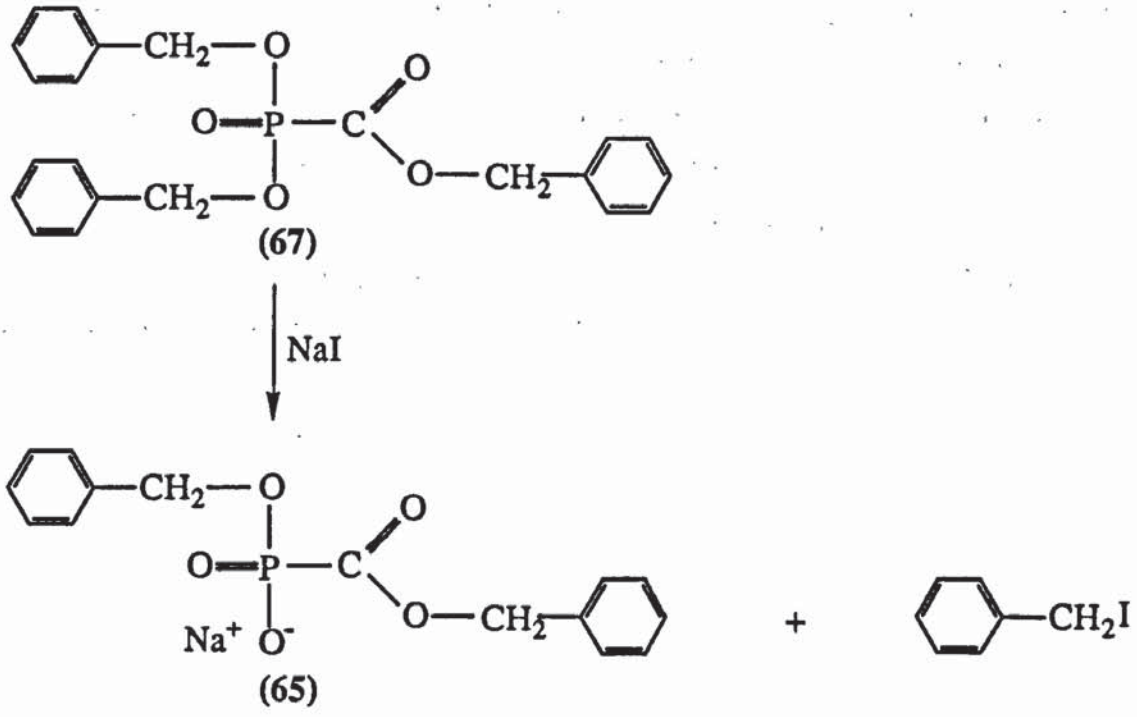

Isolation of (**65**) from the hydrolysis mixture by solid phase extraction, followed by ^{1}H coupled ^{31}P NMR spectroscopy gave rise to a triplet at -4.79 ppm (J_{PH} 7.3 Hz), the size of which was enhanced by the addition of an authentic sample of sodium benzyl (benzyloxycarbonyl)phosphonate (**65**). The chemical shift and coupling constant were

slightly different from those observed in the original hydrolysis experiment, probably because of a variation in solvent composition or pH.

The unknown compound (**66**) was found to coelute with dibenzyl phosphate, which was also isolated by solid phase extraction. ^{31}P (^{1}H coupled) NMR spectroscopy gave rise to a pentet at 1.06 ppm (J_{PH} 7.2 Hz) which was enhanced by the addition of an authentic sample of dibenzyl phosphate (**66**).

2.4.3. Kinetic Profile by ^{31}P NMR Spectroscopy

Once the identity of all the products had been established, the reaction was monitored over 6 h by ^{31}P (^{1}H decoupled) NMR spectroscopy. A control experiment was performed to evaluate the ^{31}P NMR response of each component type. Known quantities (~ 10 μmol) of the hydrolytically stable diester (**61**), monobenzyl phosphite (**64**) and dibenzyl phosphate (**66**) were dissolved in CD_3CN - D_2O phosphate buffer (pH 7.4, 0.1 M) (1:1, v/v). The assumption was made that monobenzyl phosphite (**64**) and dibenzyl phosphite (**63**) have identical responses, as do the triester (**38**) and the diesters (**61, 65**). ^{1}H NMR spectroscopy confirmed the ratios from the weights, however, under identical spectrometer conditions to the kinetics experiment, the ^{31}P NMR spectrum showed that monobenzyl phosphite (**64**) had an area response 1.55 times greater than the diester (**61**), and dibenzyl phosphate (**66**) had an area response 1.1 times greater than the diester (**61**). This probably results from differences in the rates of relaxation of nuclei. These factors were applied to the data and the time course for the disappearance of the triester and appearance of the products is given by **Fig 2.12.**

Fig 2.12 – Time-concentration profile for the hydrolysis of dibenzyl (methoxycarbonyl)phosphonate

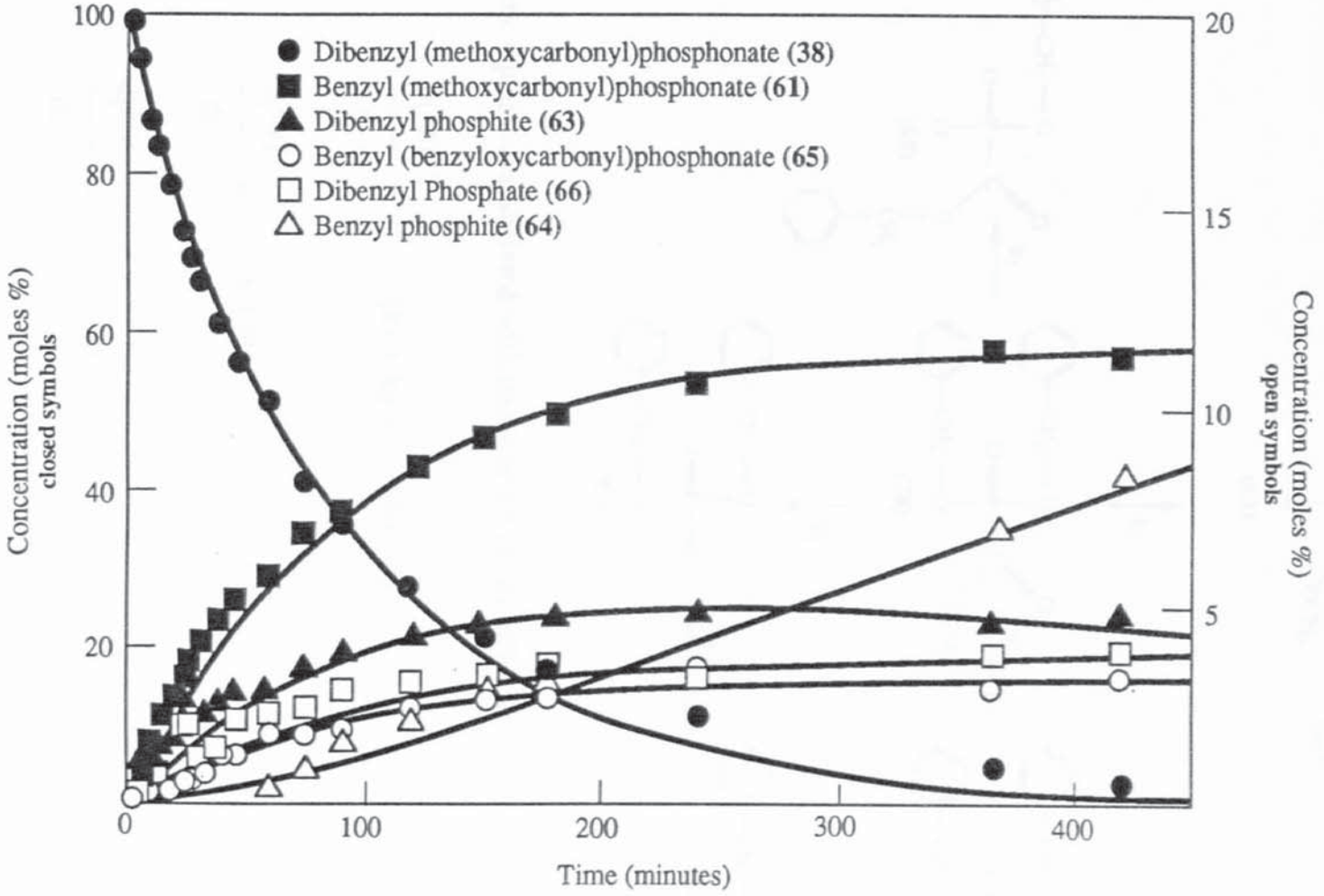

The hydrolysis of dibenzyl (methoxycarbonyl)phosphonate (38) is represented by **Fig 2.13** where k_1-k_5 are first order rate constants for each reaction.

Fig 2.13 - Hydrolysis of dibenzyl (methoxycarbonyl)phosphonate (38)

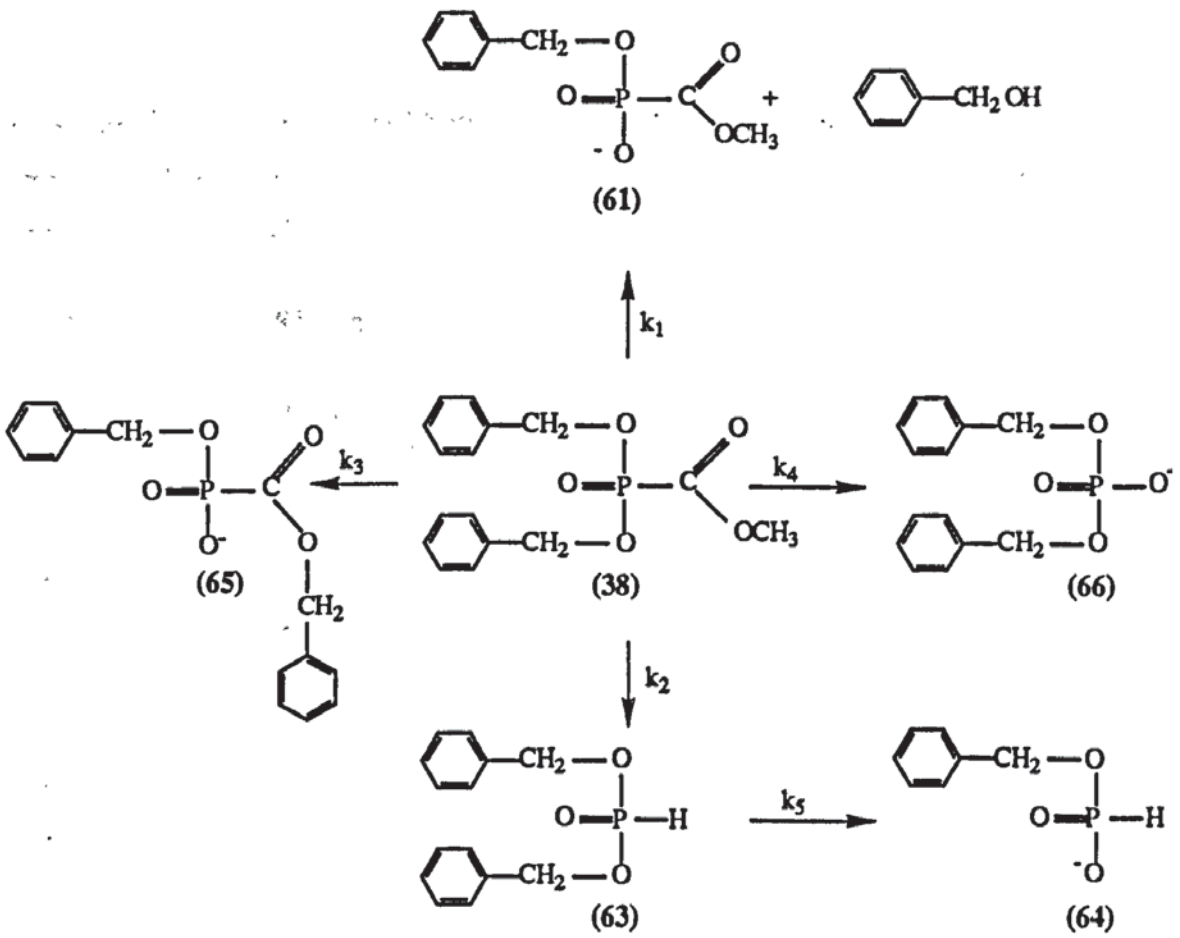

The kinetic equations associated with this scheme are as follows:-

$$\frac{d[38]}{dt} = -(k_1 + k_2 + k_3 + k_4)\,[38]$$

$$\frac{d[61]}{dt} = k_1[38]$$

$$\frac{d[63]}{dt} = k_2[38] - k_5[63]$$

$$\frac{d[64]}{dt} = k_5[63]$$

$$\frac{d[65]}{dt} = k_3[38]$$

$$\frac{d[66]}{dt} = k_4[38]$$

If these expressions are integrated between initial (t=0) and current (t=t) time limits the concentration, [ ], of the individual species at any time (t) can be calculated from the following equations (2.2-2.7):

$$[38]_t = [38]_0 \,.\, \exp(-k.t) \qquad \text{Eqn. 2.2}$$

$$[61]_t = \frac{[38]_0.k_1}{k}.\,[1 - \exp(-k.t)] \qquad \text{Eqn. 2.3}$$

$$[63]_t = \frac{[38]_0 \,.\, k_2}{k-k_5} \,.\, [\exp(-k_5.t) - \exp(-k.t)] \qquad \text{Eqn. 2.4}$$

$$[64]_t = [38]_0 \,.\, k_2 \,.\, k_5 \left(\frac{1}{k_5.k} - \frac{\exp(-k_5.t)}{k_5.(k-k_5)} - \frac{\exp(-k.t)}{k.(k_5-k)} \right) \qquad \text{Eqn. 2.5}$$

$$[65]_t = \frac{[38]_0 \,.\, k_3}{k} \cdot [1 - \exp(-k.t)] \qquad \text{Eqn. 2.6}$$

$$[66]_t = \frac{[38]_0 \,.\, k_4}{k} \cdot [1 - \exp(-k.t)] \qquad \text{Eqn. 2.7}$$

where $k = k_1 + k_2 + k_3 + k_4$

The time-concentration data were fitted to **equations 2.2 - 2.7** by means of non-linear least squares regression using program NONREG[144] which was extended to deal with the 6 simultaneous functions required in this analysis. The rate constants obtained with

their standard deviations (SD) are given in **Table 2.2**, and the fit of these theoretical rate constants to the data points is shown by the solid lines in **Fig 2.12.**

Table 2.2 - Rate constants for the hydrolysis of dibenzyl (methoxycarbonyl)phosphonate **(38)**

k	Rate constant (min^{-1})	SD
k_1	6.56×10^{-3}	0.07×10^{-3}
k_2	3.55×10^{-3}	0.06×10^{-3}
k_3	3.59×10^{-4}	0.45×10^{-4}
k_4	4.24×10^{-4}	0.45×10^{-4}
k_5	9.04×10^{-4}	0.29×10^{-4}

The reliability of the rate constants is indicated by the close agreement between the experimental half-life ($t_{1/2}$) of 60 min for the triester **(38)** with the value of 64 min calculated from **Eqn. 2.8**

$$t_{1/2} = \frac{0.6932}{(k_1 + k_2 + k_3 + k_4)} \qquad \textbf{Eqn. 2.8}$$

These half-lives from ^{31}P NMR spectroscopy differ from the value obtained from HPLC studies ($t_{1/2}$ = 24.9 min) and are probably more reliable. Inaccuracies associated with the HPLC analysis may arise from the inability to quench the hydrolysis reaction on injection onto the HPLC column, therefore degradation of the triester **(38)** continues during passage through the instrument. The reasonable degree of correspondance between experimental NMR data from peak area measurements and theoretical profiles calculated from these rate constants using equations **2.2 - 2.7** are shown in **fig 2.12.** The correlation coefficients (r) for the fit are as shown in **Table 2.3.**

Table 2.3 - Correlation coefficients for the hydrolysis of dibenzyl (methoxycarbonyl)phosphonate (38)

Component	r
Triester (38)	0.9974
Diester (61)	0.9966
Dibenzyl phosphite (63)	0.9948
Monobenzyl phosphite (64)	0.9907
Diester (65)	0.9445[a]
Dibenzyl phosphate (66)	0.9743[a]

a) The values for (65) and (66) are somewhat poor due to the low levels of these compounds and the consequently higher errors involved in measuring concentrations.

These rate constants confirm that the major hydrolysis pathway involves the formation of benzyl (methoxycarbonyl)phosphonate (**61**, k_1) and dibenzyl phosphite (**63**, k_2), which degrades to monobenzyl phosphite (**64**, k_5) at about one fifth of the rate of its formation. The competing rearrangements to benzyl (benzyloxycarbonyl)phosphonate (**65**, k_3) and dibenzyl phosphate (**66**, k_4) are approximately 10-fold slower.

The triester (**38**), with a half-life of 60 min at 37°C, was considerably less stable to hydrolysis than expected, especially when under identical reaction conditions dibenzyl (methoxycarbonylmethyl)phosphonate (**39, X=H**) and dibenzyl methylphosphonate (**62**) were found to be completely stable over 48 h. Reports in the literature also support the stability of benzyl esters of the phospho group, for example dibenzyl methylphosphonate (**62**) was found to have a half-life of 11 min in water at 100°C[140] and tetrabenzyl pyrophosphate (**68**) has a half-life of 4.1 h in propan-1-ol at 50°C.[145]

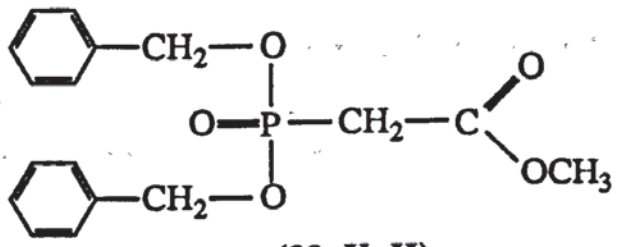

(39, X=H)

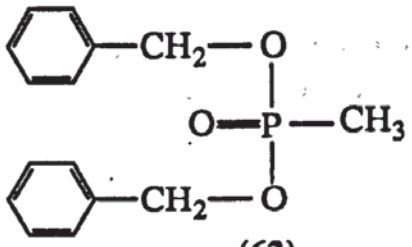

(62)

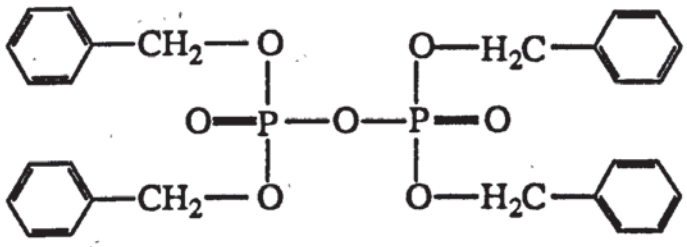

(68)

2.4.4. Mechanism of Hydrolysis to give Benzyl (methoxycarbonyl)phosphonate (61) and Benzyl (Benzyloxycarbonyl)phosphonate (65)

There are two mechanisms by which the triester (38) can degrade to the diester (61). The first route involves the loss of a benzyl group by C-O bond fission to generate the benzyl carbonium ion and the diester (61). This C-O bond cleavage mechanism has been observed previously for the hydrolysis of dibenzyl methylphosphonate (62).[140] Alternatively, the triester (38) could undergo direct nucleophilic attack by water to displace the benzyl group by P-O bond cleavage. This type of mechanism has been observed for the alkaline hydrolysis of alkyl and aryl phosphate triesters.[139] In an attempt to establish the mechanisms of hydrolysis of the triester (38) the ^{31}P NMR experiment was repeated in an 80% enriched ^{18}O-labelled water-acetonitrile mixture (1:1, v/v) at pH 7.4. If the triester degrades by C-O bond fission (Fig 2.14, A), then the $^{18}0$ label will be incorporated into the benzyl alcohol and not the diester. Conversely , P-O bond fission (Fig 2.14, B) would result in incorporation of the ^{18}O label in to the diester and not the benzyl alcohol.

Fig 2.14 - Two possible mechanisms of hydrolysis of dibenzyl (methoxycarbonyl)-phosphonate (**A** - C-O bond fission; **B** - P-O bond fission) to form benzyl (methoxycarbonyl)phosphonate

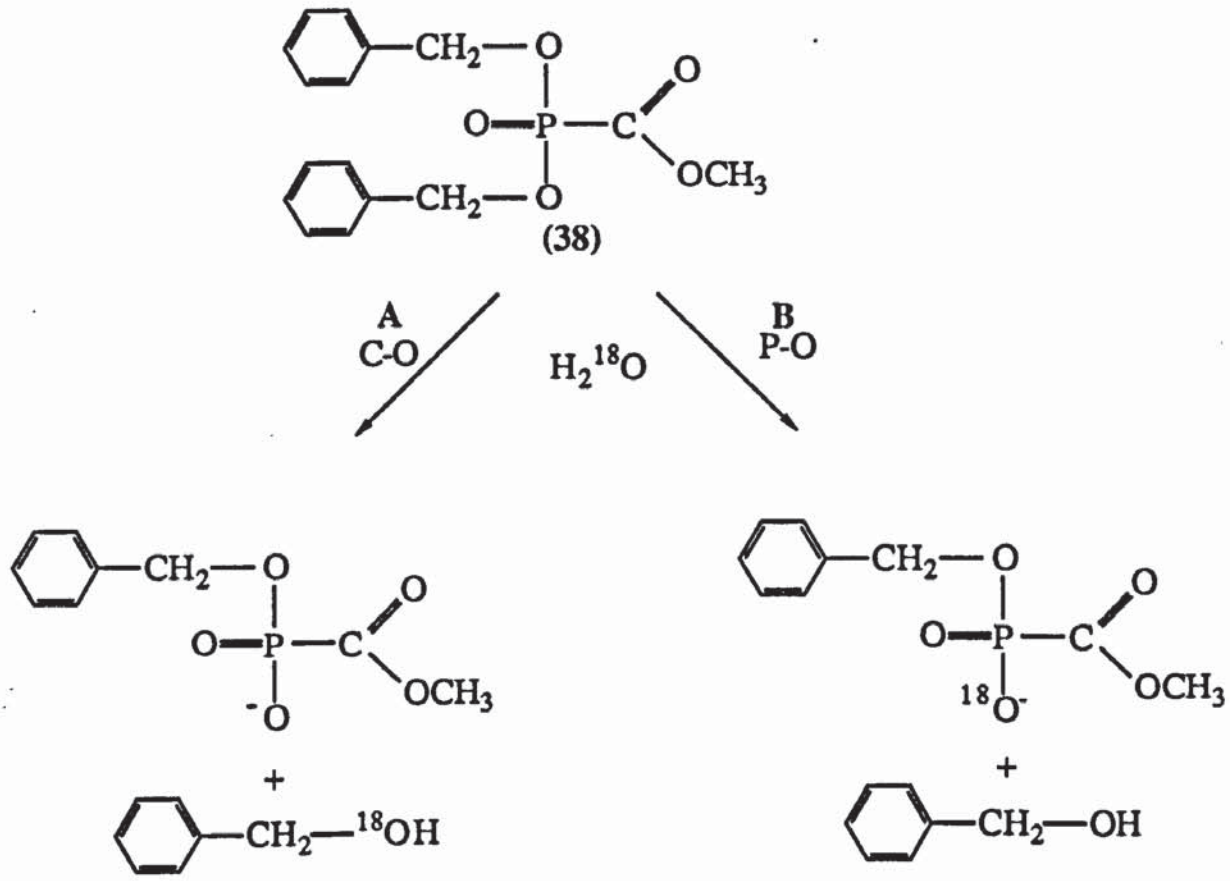

After 24 h the reaction mixture was analysed by ^{31}P (^{1}H decoupled) NMR spectroscopy (**Fig 2.15**). This technique relies on a small upfield shift in resonance when an ^{18}O atom, rather than ^{16}O, is attached directly to phosphorus.[146] As can be seen, the diester (**61**) gave 2 peaks at -4.635 (^{16}O, 27.5%) and -4.668 (^{18}O, 72.5%) ppm showing that an ^{18}O label was attached directly to phosphorus in this molecule. The reaction mixture was also analysed by ^{13}C NMR spectroscopy as an ^{18}O atom exerts a similar effect in carbon resonance.[147] The presence of a singlet at 64.4 ppm suggested that the methylene group of benzyl alcohol did not contain an ^{18}O label. In a similar experiment, the reaction mixture was extracted with dichloromethane and concentration of the aqueous layer gave a mixture of the diesters (**61**) and (**65**). This mixture was subsequently analysed for ^{18}O incorporation by fast atom bombardment (FAB) mass spectrometry. There were peaks at *m/z* 275 (^{16}O, 30%) and 277 (^{18}O, 70%) corresponding to sodium benzyl (methoxycarbonyl)phosphonate (**61**) plus a sodium cation. However, there was no evidence for the incorporation of two ^{18}O labels into the molecule which rules out exchange into the carbonyl group.

Fig 2.15 – ^{31}P NMR spectrum of the products from the hydrolysis of dibenzyl (methoxycarbonyl)phosphonate with $H_2{}^{18}O$

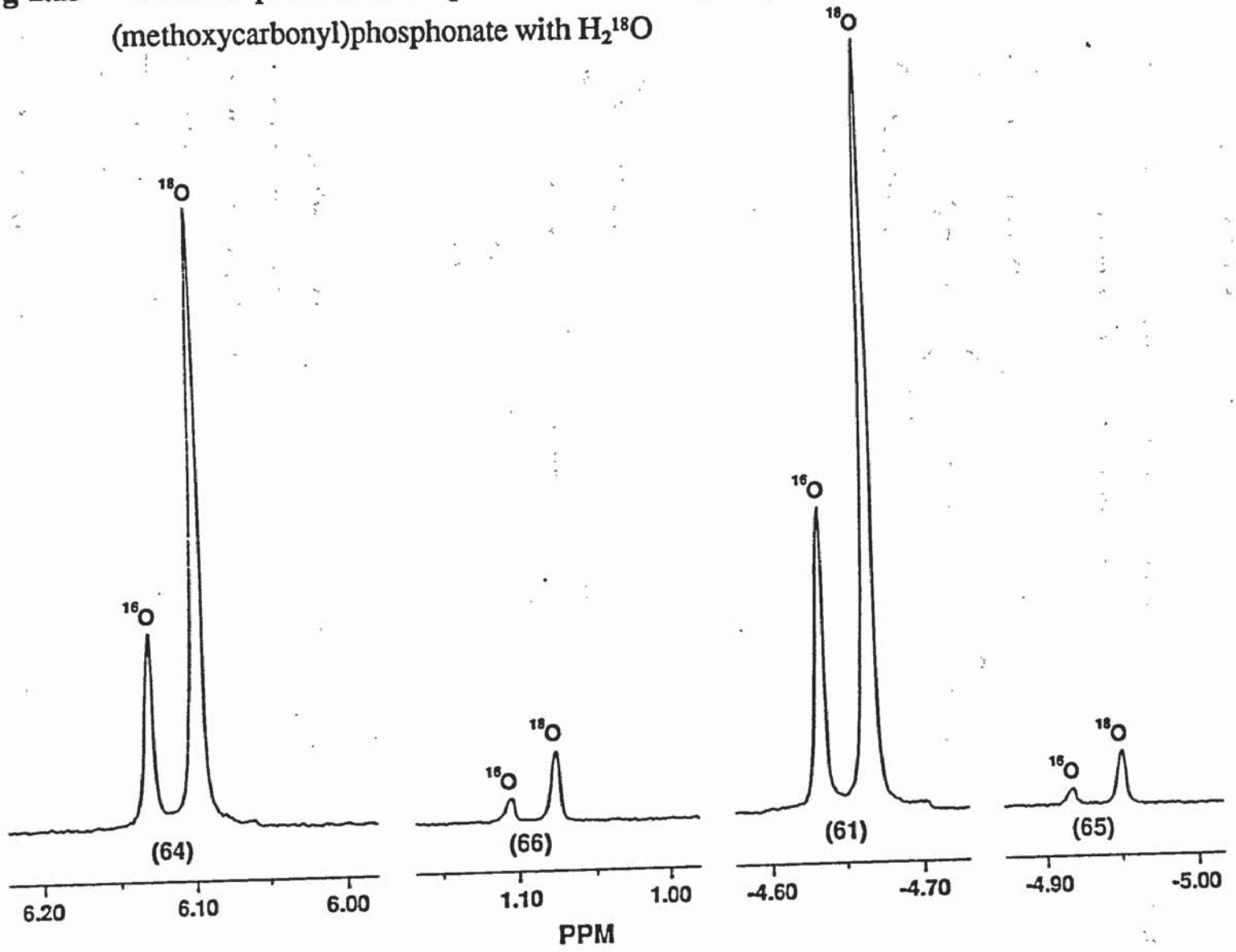

These results are consistent with the hydrolysis of the triester (38) to the diester (61) proceeding by nucleophilic attack of water at phosphorus resulting in P-O bond cleavage, probably via the pentacoordinate intermediate (69) (Fig 2.16)

Fig 2.16 - Mechanism of formation of benzyl (methoxycarbonyl)phosphonate (61) from the hydrolysis of dibenzyl (methoxycarbonyl)phosphonate (38)

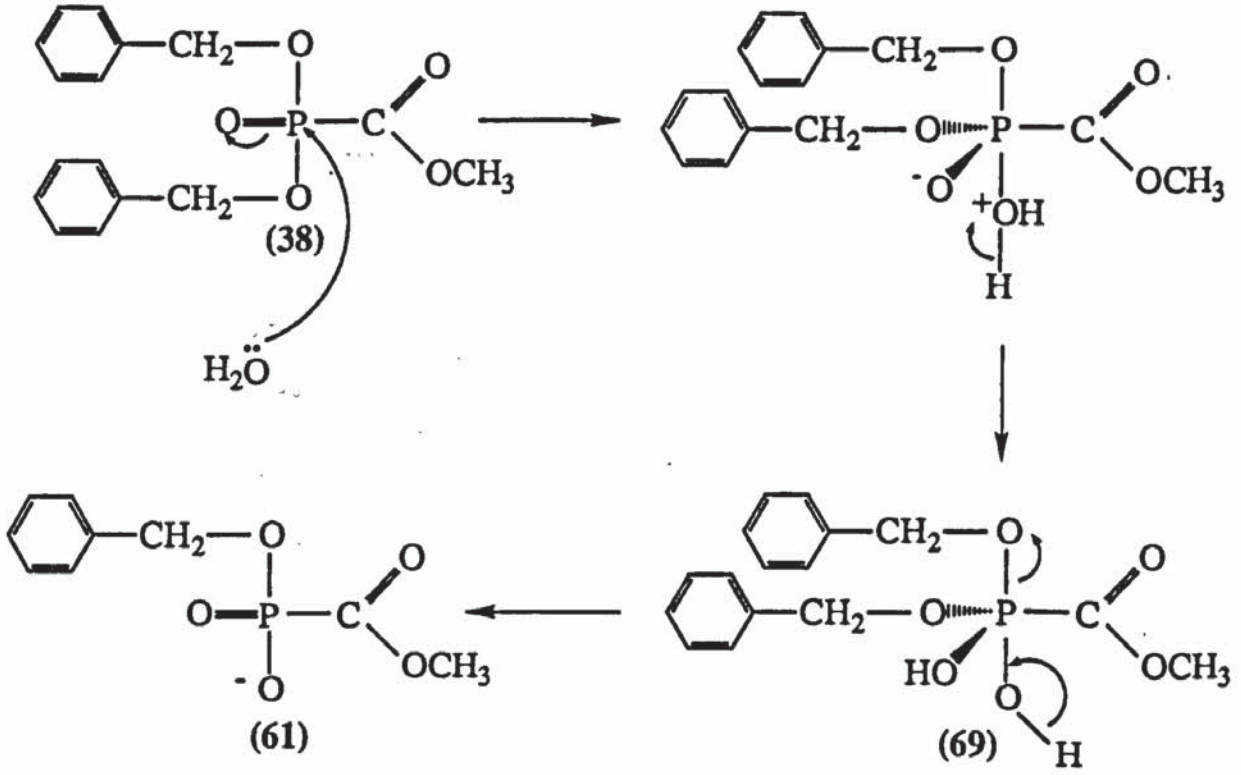

Hydrolysis of the triester (38) with P-O bond cleavage was surprising as both dibenzyl methylphosphonate (62)[140] and tetrabenzyl pyrophosphate (68)[145] have been shown to lose a benzyl group *via* C-O bond cleavage. The high reactivity and change in mechanism of hydrolysis for the phosphonoformate triester (38) must therefore be attributed to the electron-withdrawing effect of the methoxycarbonyl group increasing the susceptibility of phosphorus towards nucleophilic attack.

The ^{31}P NMR spectrum from the ^{18}O experiment (**Fig 2.15**) shows that benzyl (benzyloxycarbonyl)phosphonate (65) also contains an ^{18}O label attatched directly to phosphorus. This was supported by FAB mass spectrometry with peaks at *m/z* 350 (^{16}O, 30%) and 352 (^{18}O, 70%) corresponding to sodium benzyl (benzyloxycarbonyl)phosphonate (65) plus a sodium cation. The mechanism of formation of this diester was initially thought to arise from the hydrolysis of the triester, dibenzyl

(benzyloxycarbonyl)phosphonate (67), which could be formed from the transesterification of the triester (38) with benzyl alcohol (Fig 2.17).

Fig 2.17 - The transesterification of the triester (38) to form the diester (65)

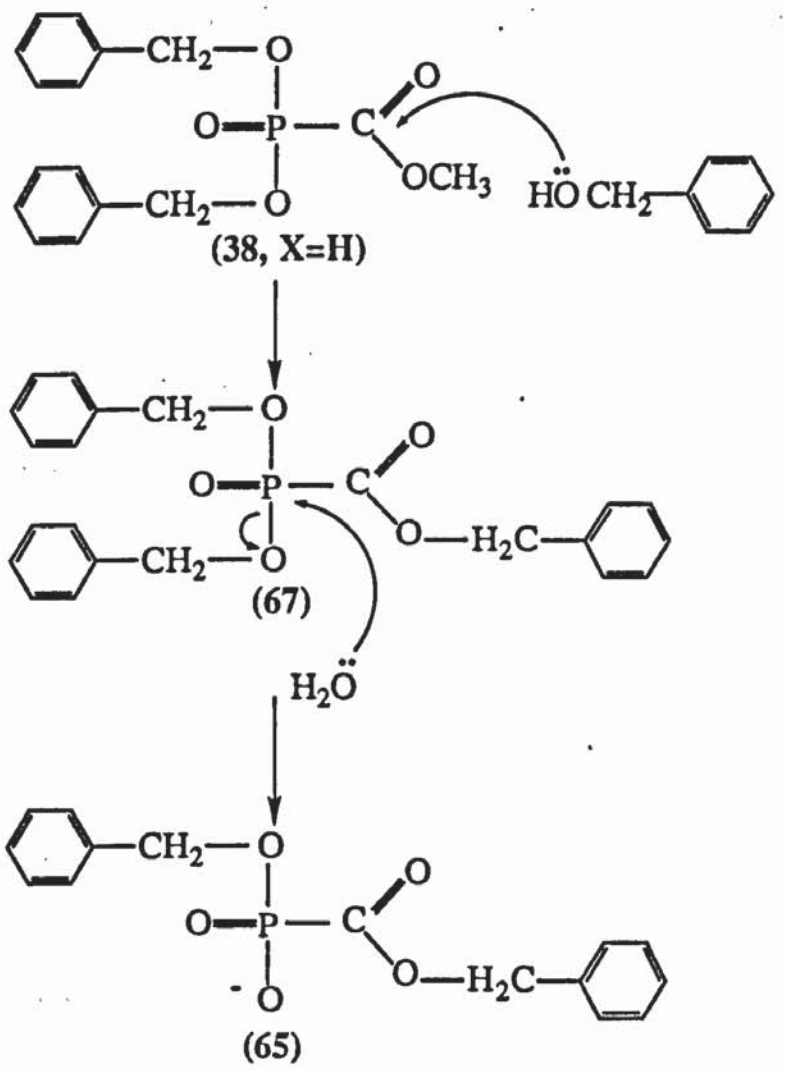

This was shown to be the incorrect mechanism as the triester (67) was not detected at all by HPLC throughout the course of the reaction (standard elutes at 16.7 min using convex gradient 5, with which triester (38) elutes at 13.6 min), even when a 10-fold molar excess of benzyl alcohol was added to the reaction mixture. Furthermore, the ratio of the diesters (61):(65) was constant at 17 +/- 2 during the course of the reaction, confirming that benzyl alcohol does not contribute to the formation of diester (65). A possible mechanism again involves the pentacoordinate intermediate (69), which instead of losing benzyl alcohol to give the diester (61), could undergo a 1,2-shift of the benzyloxy group from phosphorus to carbon to give (71), proceeding *via* the intermediate (70) (Fig 2.18). The diester (65) is then formed by loss of methanol from (71).

Fig 2.18 - Mechanism of formation of diester **(65)** from the hydrolysis of dibenzyl (methoxycarbonyl)phosphonate **(38)**

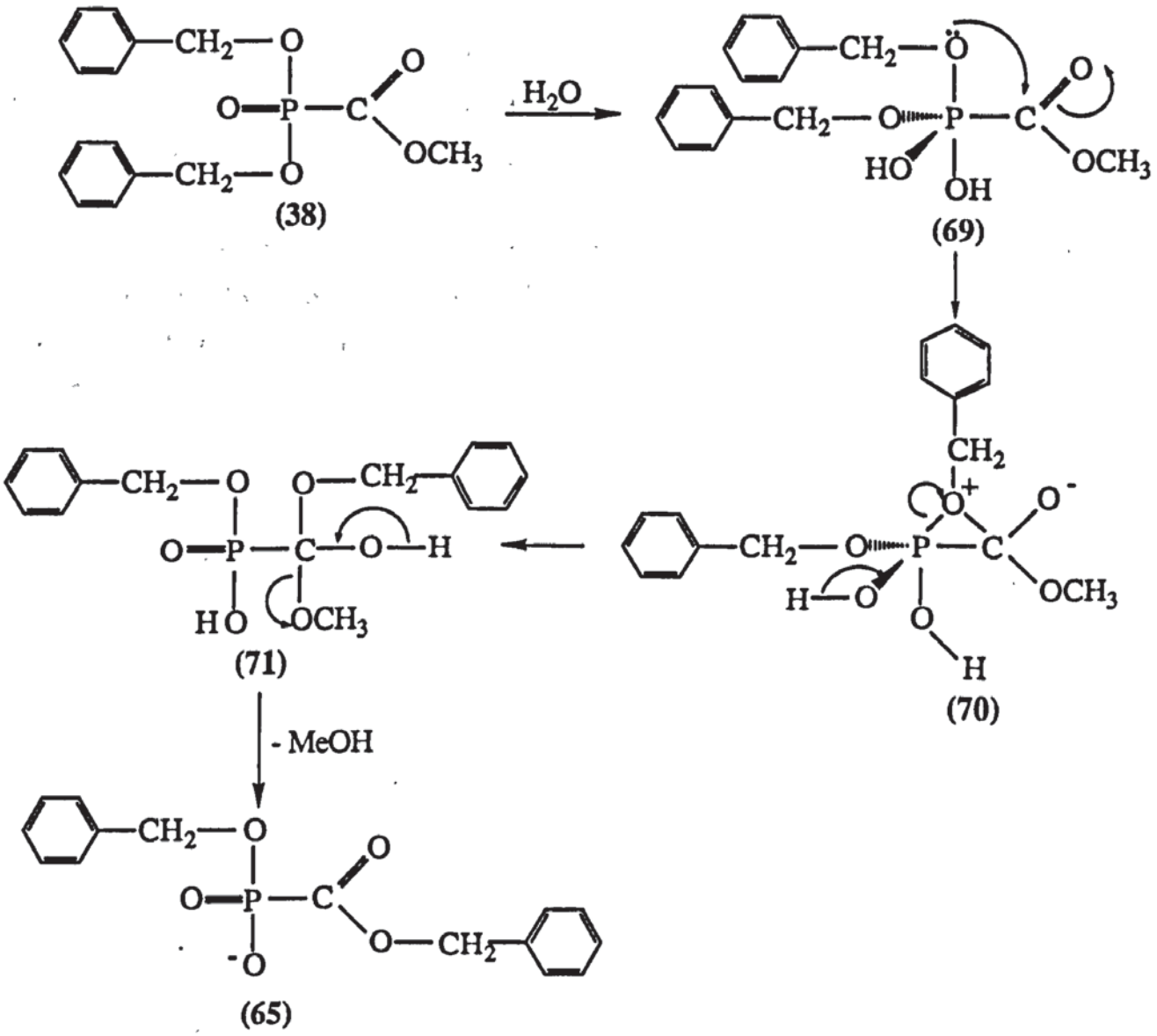

The above mechanism may also contribute to the formation of the diester **(38)** if the intermediate **(71)** were to lose benzyl alcohol rather than methanol.

2.4.5. Mechanism of Hydrolysis to give Dibenzyl Phosphite (63) and Monobenzyl Phosphite (64)

Kluger and coworkers[148] found that dimethyl acetylphosphonate (**72**) was rapidly cleaved in water (pH 7) to form acetate (**73**) and dimethyl phosphite (**74**). The rapid hydrolysis of the phosphonate (**72**) was believed to result from the energetically favourable formation of the carbonyl hydrate (**75**) due to the electronic effect of the phosphonate diester.[149] Carbonyl groups next to phosphoryl groups are very electrophilic. For example, α-ketophosphine oxides are virtually impossible to prepare since nucleophiles add so easily to the carbonyl group.[150] This effect also promotes ionisation of the hydrate[151] resulting in P-C bond cleavage to achieve the overall rapid hydrolysis (**Fig 2.19**). The reaction was first order with respect to hydroxide ion and substrate concentration.

Fig 2.19 - Mechanism of hydrolysis of dimethyl acetylphosphonate (**72**)

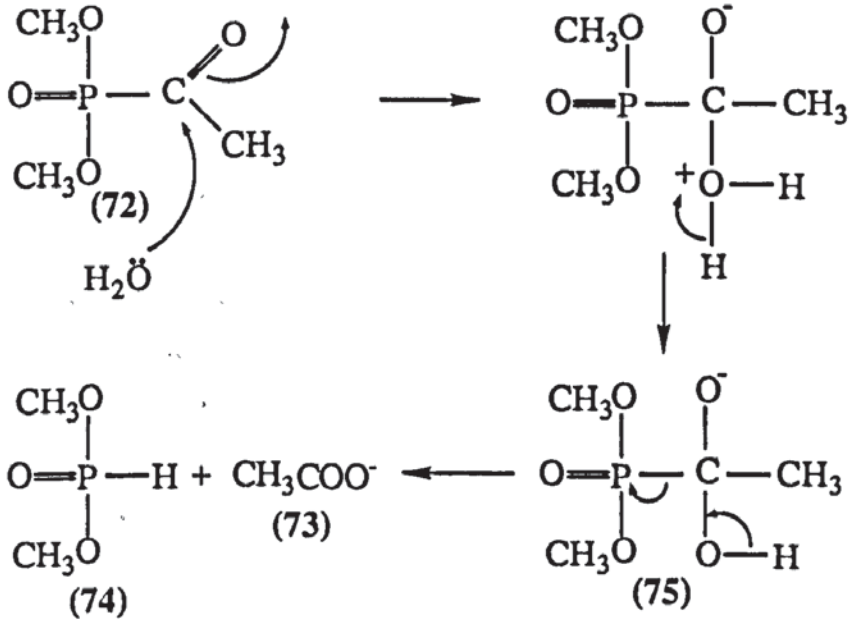

On the basis of the above mechanism (**Fig 2.19**) the formation of dibenzyl phosphite (**63**) is likely to proceed via a carbonyl hydrate (**76**), which is most likely formed by nucleophilic attack at the carbonyl function (**Fig 2.20**, pathway A) or possibly by a hydroxy group migration from the pentacoordinate intermediate (**69**) proceeding via the epoxide (**77**) (**Fig 2.20**, pathway B).

Fig 2.20 - Formation of carbonyl hydrate (**76**) from the hydrolysis of dibenzyl (methoxycarbonyl)phosphonate (**38**)

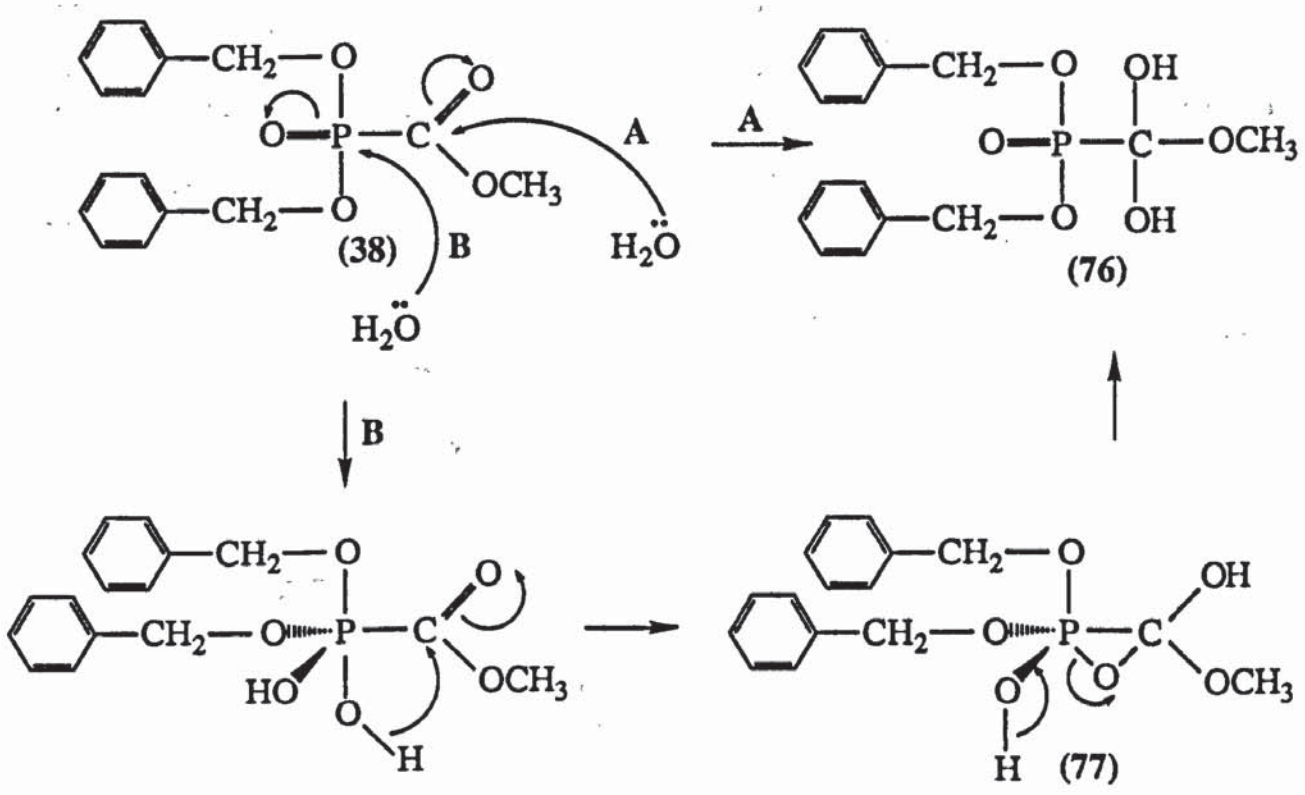

Surprisingly, the mass spectra revealed a lack of incorporation of ^{18}O-label from $H_2{}^{18}O$ into the carbonyls of the diesters (**61**) and (**65**), suggesting that the formation of the hydrate (**76**) is not reversible. In common with the formation of other carbonyl hydrates[148] the formation of (**76**) should be base-catalysed. In support of this, the hydrolysis of the triester (**38**) was found to be very rapid at pH 9.0, with complete reaction after 35 min, whereas at pH 4, the triester (**38**) was considerably more stable with a half-life of approximately 90 h at 37°C. The carbonyl hydrate (**76**) could give dibenzyl phosphite (**63**) by two mechanisms. Either, the P-C bond of the carbonyl hydrate (**76**) could cleave to give dibenzyl phosphite (**63**) and methyl carbonate (**78**), which could undergo decarboxylation to form methanol and carbon dioxide (**Fig 2.21**, pathway **A**). Alternatively, methanol could be lost from the hydrate (**76**) to give the carboxylic acid (**79**), which, by an intramolecular 5-membered ring proton transfer, can decarboxylate to give dibenzyl phosphite (**63**) (**Fig 2.21**, pathway **B**). A similar intramolecular 5-membered ring proton transfer has been suggested by Narayanan and co-workers[152] for the hydrolysis of diethyl benzoylphosphonate.

Fig 2.21 - Mechanism of formation of dibenzyl phosphite **(63)** from the carbonyl hydrate **(76)**

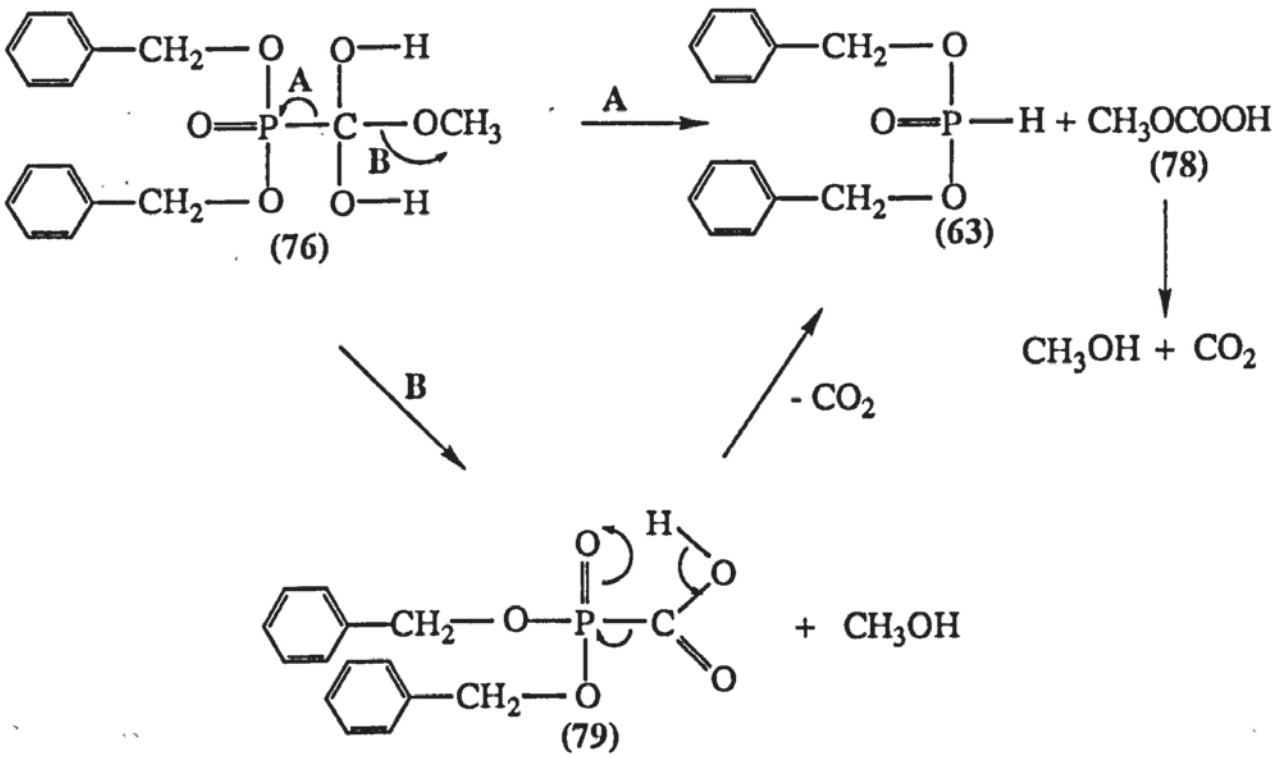

In an attempt to distinguish between mechanisms **A** and **B** in **Fig 2.21**, the triester **(38)** was incubated with porcine liver carboxylesterase at pH 5.0 and 37°C. HPLC analysis revealed that after 10 min the triester had completely degraded to give only dibenzyl phosphite **(63)**. Although this result could be consistent with either pathway, catalysis of P-C bond cleavage by an esterase has never been reported and, thus, initial formation of the carboxylic acid **(79)** is expected under these conditions. Recently, Walker of our laboratory has examined the hydrolysis of dimethyl (phenoxycarbonyl)phosphonate **(80)**[113] (pH 7.4, 37°C) by ^{31}P NMR spectroscopy. The triester **(80)**, with a better carboxyl leaving group than dibenzyl (methoxycarbonyl)phosphonate **(38)**, was found to hydrolyse instantly to give dimethyl phosphite **(81)** [δ_P (^1H coupled) 14.6 ppm, d sept, J_{PH} 718, 12 Hz]. This reaction probably proceeds through the carboxylic acid **(82)** formed spontaneously due to the presence of the good carboxyl leaving group **(Fig 2.22)**.

Fig 2.22 - Hydrolysis of dimethyl (phenoxycarbonyl)phosphonate (80)

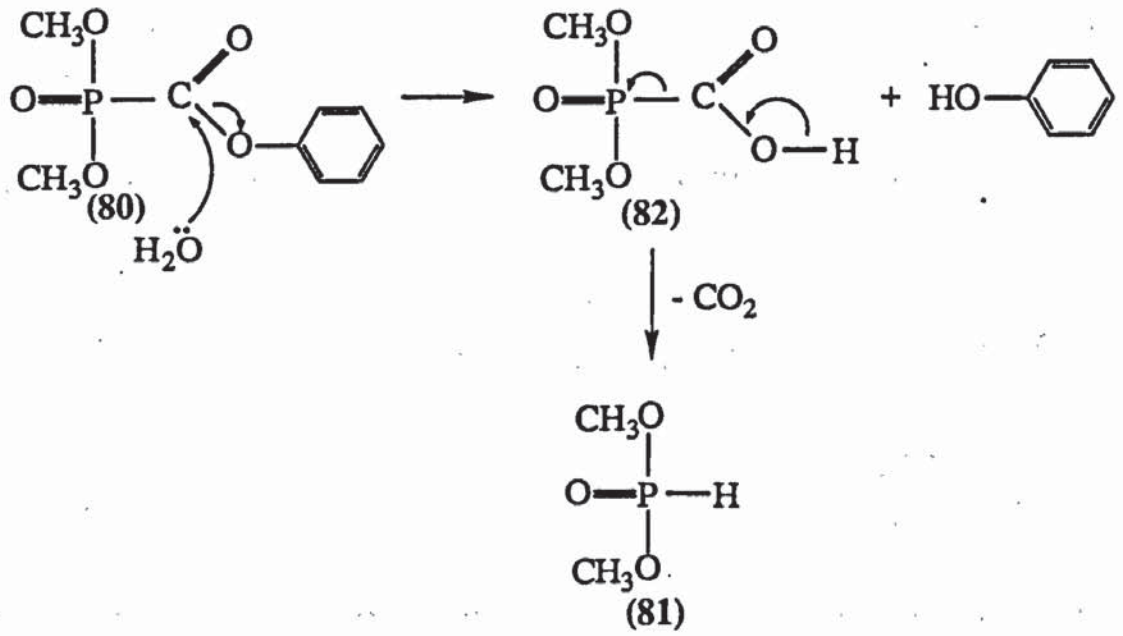

Thus formation of dibenzyl phosphite (63) probably occurs through P-C bond cleavage of the carboxylic acid (79) proceeding *via* the carbonyl hydrate (76) (**Fig 2.21**, pathway **B**). Further studies have supported this mechanism: Krol and co-workers[142] observed a reactive carboxylic acid intermediate (83) during the hydrolysis of diethyl (*p*-nitrophenoxycarbonyl)phosphonate (84) which decarboxylated to give diethyl phosphite (85) (**Fig 2.23**).

Fig 2.23 - Hydrolysis of diethyl (p-nitrophenoxycarbonyl)phosphonate (84)

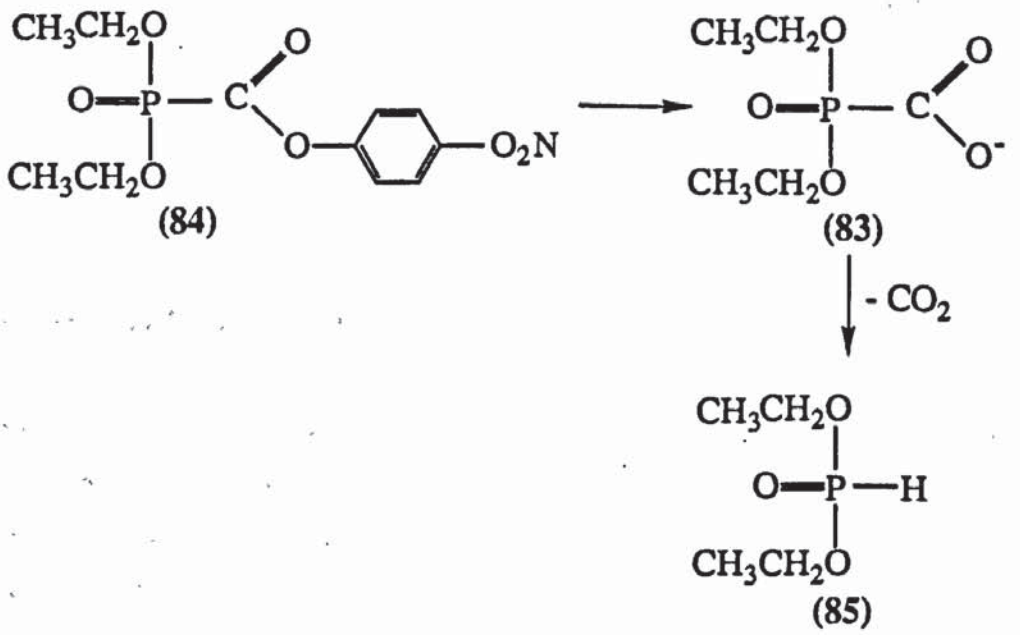

In addition Warren and co-workers[153] have shown that carbon dioxide can act as a leaving group when phosphinoyl formate esters (**86**) are dealkylated by iodide ions (**Fig 2.24**). In this reaction, the carboxylic acid is generated without the intermediacy of the carbonyl hydrate supporting further the formation of the carboxylic acid (**79**) from the hydrolysis of the triester (**38**).

Fig 2.24 - Dealkylation of phosphinoyl formate esters (**86**) by iodide ions

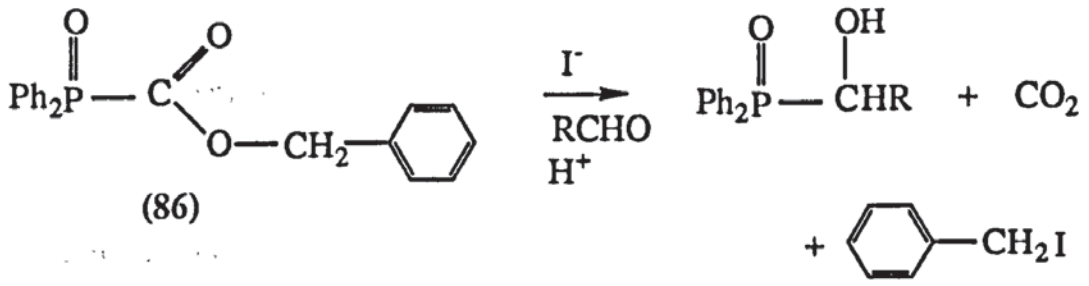

Benzyl phosphite (**64**) was formed from the hydrolysis of dibenzyl phosphite (**63**). The reaction in $H_2{}^{18}O$ showed that benzyl phosphite (**64**) contained an ^{18}O label attached directly to phosphorus (^{18}O, 76.5%, **Fig 2.15**), therefore the reaction must proceed *via* nucleophilic attack at phosphorus followed by P-O bond cleavage (**Fig 2.25**). This mechanism is consistent with that observed for dimethyl phosphite (**81**).[154]

Fig 2.25 - Mechanism of formation of monobenzyl phosphite (**64**)

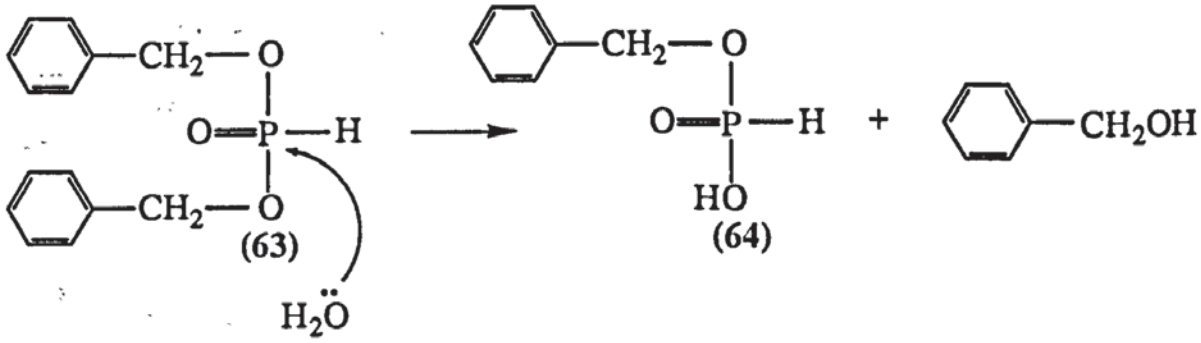

2.4.6. Mechanism of Hydrolysis to give Dibenzyl Phosphate (66)

Initially it was thought that dibenzyl phosphate (**66**) could be formed by the oxidation of dibenzyl phosphite (**63**), however three observations showed that this did not occur. First, from the time course (**Fig 2.12**), the formation of the phosphate (**66**) did not increase with the degradation of the phosphite (**63**). Second, a control experiment was performed in which the phosphite (**63**) was incubated under the reaction conditions for 24

h and monitored by ^{31}P NMR spectroscopy: Dibenzyl phosphate (66) was not detected. Third, when the triester (38) was incubated in 80% ^{18}O enriched water dibenzyl phosphate (66) contained an ^{18}O label attached directly to phosphorus (^{18}O, 75%, Fig 2.15). This suggested that the phosphate (66) is a primary product, and its formation must involve nucleophilic attack of water directly at phosphorus. A probable mechanism again involves rearrangement of the pentacoordinate intermediate (69) to form an epoxide (77). This then undergoes P-C bond cleavage to form intermediate (87) which degrades by C-O bond cleavage to dibenzyl phosphate (66) (Fig 2.26).

Fig 2.26 - Mechanism of formation of dibenzyl phosphate (66) from the hydrolysis of dibenzyl (methoxycarbonyl)phosphonate (38)

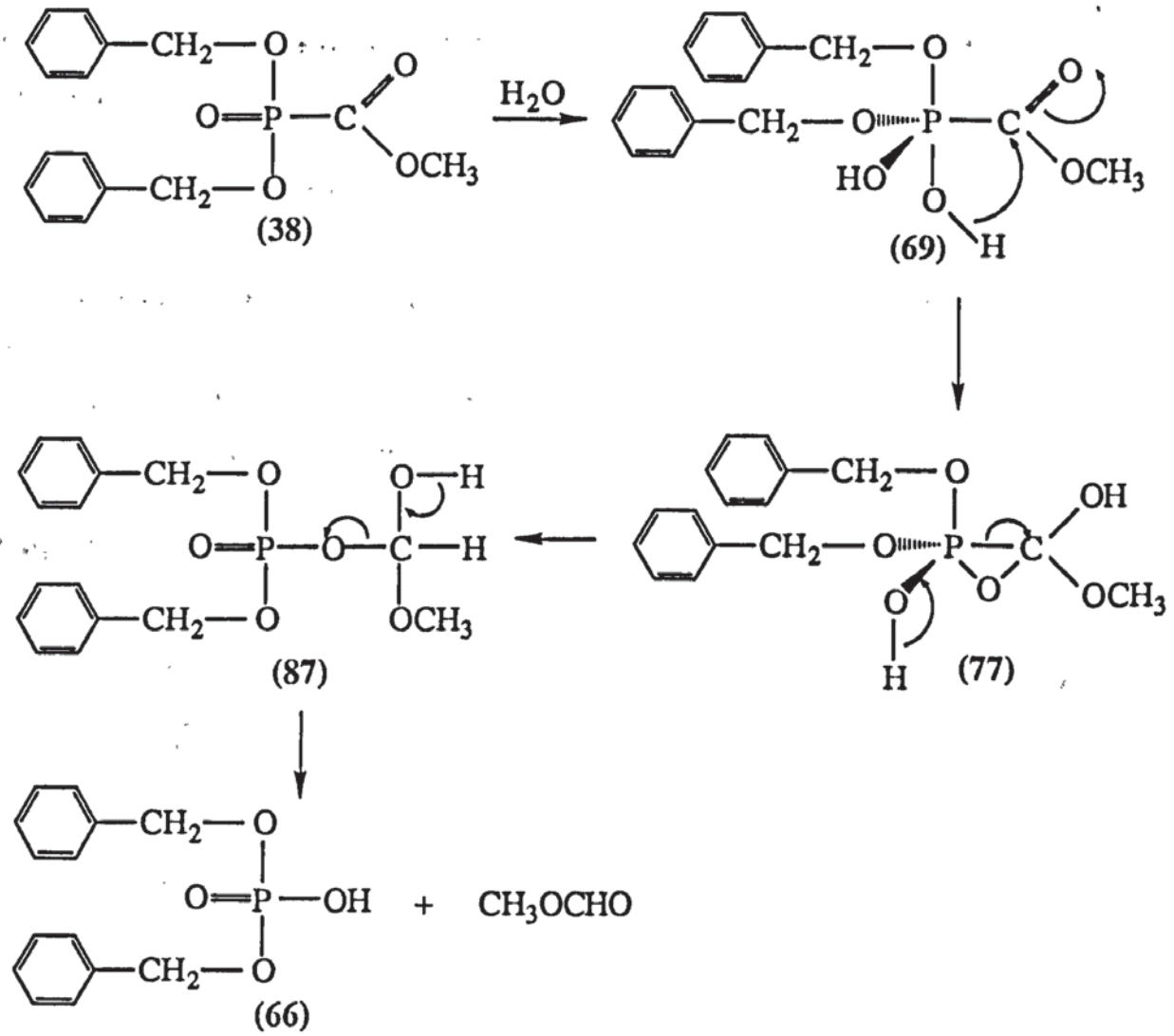

2.4.7. Summary

The hydrolysis of dibenzyl (methoxycarbonyl)phosphonate (38) was more rapid and considerably more complicated than expected. The high degree of instability of this

compound is attributed to the electron-withdrawing effect on phosphorus of the methoxycarbonyl group, which is absent in the more hydrolytically stable phosphonates, such as dibenzyl methylphosphonate (**62**). The complexity of the reaction results from competition between initial nucleophilic substitution at phosphorus and at the carbonyl carbon. In support of the present study, Krol and co-workers[142] have also recently reported the rapid hydrolysis of phosphonoformate triesters to mixtures of hydrogen phosphonate, phosphonoformate esters and free acids. It was considered that both the reactivity and the product distribution of the dibenzyl (methoxycarbonyl)phosphonates could be altered by the incorporation of 4-substituents into the P-benzyl groups.

2.5. Hydrolysis Studies of Di(4-substituted-benzyl) (Methoxycarbonyl)-phosphonates (38, X=N_3, NO_2, CH_3, CH_3COO, $(CH_3)_3CCOO$, Cl, CF_3)

2.5.1. Half-lives by HPLC

The triesters were subjected to hydrolysis in an identical manner to dibenzyl (methoxycarbonyl)phosphonate (**38, X=H**) and monitored by HPLC using the same conditions (**section 2.4.1.**). All triesters were observed to degrade rapidly and their hydrolysis half-lives ($t_{1/2}$) are given in **Table 2.4.**

Table 2.4 - HPLC hydrolysis half-lives for phosphonoformate triesters (**38**)

X	Retention Time(min)	Half-life(min)[a]
H	16.2	24.9 +/- 2.9
N_3	15.2	<3[b]
NO_2	16.2	<3[b]
CH_3	15.4	18.5 +/- 0.3
CH_3COO	15.0	15.6 +/- 3.7[c]
$(CH_3)_3CCOO$	17.3	17.3 +/- 0.8
Cl	16.7	9.9 +/- 0.8
CF_3	17.3	4.5 +/- 0.2

a) mean +/- SD, n=3 unless otherwise stated

b) hydrolysis too rapid to allow accurate determination of half-life

c) mean +/- SD, n=5.

Careful inspection of the chromatograms revealed that all the triesters appeared to degrade in a similar manner to the hydrolysis of dibenzyl (methoxycarbonyl)phosphonate (**38, X=H**). This can be represented by the general scheme shown in **Fig 2.27**, where k_1 - k_5 are the first order rate constants.

Fig 2.27 - Hydrolysis of phosphonoformate triesters (38)

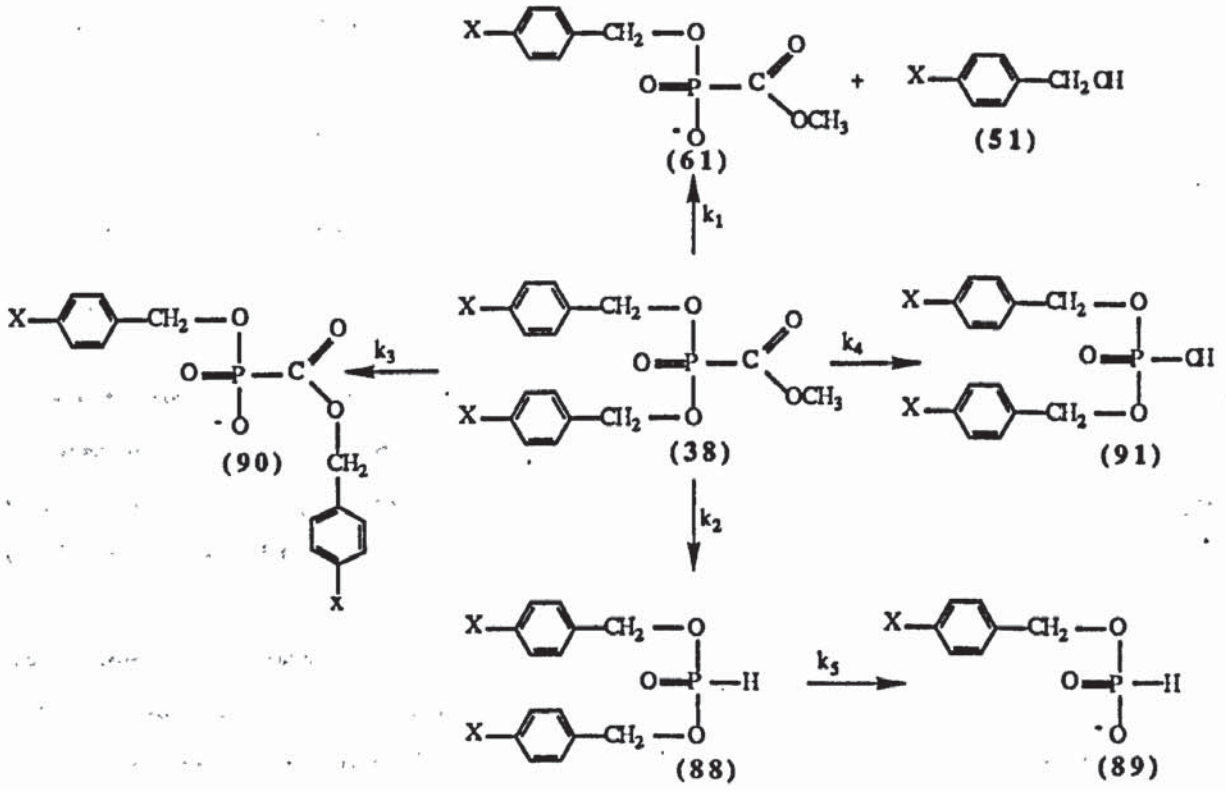

2.5.2. Product and Kinetic Profile and Mechanisms of Hydrolysis by ^{31}P NMR Spectroscopy

In an attempt to determine the influence of the **X** substituent on the rates and mechanisms of individual product formation, the hydrolyses of 3 triesters (**38, X=N_3, NO_2, CF_3**) were followed by ^{31}P NMR spectroscopy at 37°C and pH 7.4. In common with the hydrolysis of the triester (**38, X=H**) the peak areas were corrected to account for the different ^{31}P NMR responses of the individual components and the same mathematical treatment applied to the results.[144] The rate constants (k / min^{-1}) for individual product

formation from the hydrolyses of the four triesters (38, X=H, N_3, NO_2, CF_3) together with their NMR hydrolysis half-lives ($t_{1/2}$) are given in Table 2.5.

Table 2.5 - Rate constants (min^{-1}) and half-lives by ^{31}P NMR for the hydrolysis of triesters (38, X=H, N_3, NO_2, CF_3)

X	k_1 min^{-1}	k_2 min^{-1}	k_3 min^{-1}	k_4 min^{-1}	k_5 min^{-1}	$t_{1/2}$ min
H	$6.56x10^{-3}$	$3.55x10^{-3}$	$3.59x10^{-4}$	$4.24x10^{-4}$	$9.04x10^{-4}$	64
N_3	0.27	$3.14x10^{-3}$	$3.21x10^{-3}$	$3.49x10^{-3}$	$1.00x10^{-3}$	2.5
NO_2	0.10	$1.44x10^{-2}$	$4.85x10^{-3}$	$1.33x10^{-3}$	$1.53x10^{-2}$	5.6
CF_3	$3.38x10^{-2}$	$8.74x10^{-3}$	$2.64x10^{-3}$	$1.33x10^{-3}$	$5.66x10^{-3}$	15.0

The results for the azidobenzyl (38, X=N_3) and nitrobenzyl (38, X=NO_2) triesters must be treated with caution owing to their very rapid hydrolyses and consequently limited number of time points, however it can be seen that k_1 is the most sensitive parameter towards the nature of the 4-substituent (X).

4-Azidobenzyl (methoxycarbonyl)phosphonate [61, X=N_3, δ_P -4.78 ppm (t q, J_{PH} 7.3, 0.9 Hz, ^1H coupled), k_1=0.27 min^{-1}] was the major product detected from the hydrolysis of the azidobenzyl triester [38, X=N_3, δ_P -3.70 ppm (pent q, J_{PH} 8.7, 1.1 Hz, ^1H coupled)] . This pathway was so fast, the triester having a half-life of 2.5 min, that competitive nucleophilic attack at the carbonyl group was minimal and thus P-C bond cleavage only occurred to a small extent to form di(4-azidobenzyl) phosphite [88, X=N_3, δ_P 10.94 ppm (d pent, J_{PH} 730, 10.1 Hz, ^1H coupled), $k_2=3.14x10^{-3}$ min^{-1}] and 4-azidobenzyl phosphite [89, X=N_3, δ_P 5.85 ppm (d t, J_{PH} 620, 8.4 Hz, ^1H coupled), $k_5=1.00x10^{-3}$ min^{-1}]. Other very minor products of hydrolysis were 4-azidobenzyl (4-azidobenzyloxycarbonyl)phosphonate [90, X=N_3, δ_P -5.09 ppm, $k_3=3.21x10^{-3}$ min^{-1}] and di(4-azidobenzyl) phosphate [91, X=N_3, δ_P 2.23 ppm (pent, J_{PH} 5.1 Hz, ^1H coupled), $k_4=3.49x10^{-3}$ min^{-1}].

The increased rate of formation of the diester (**61**, X=N_3) from triester (**38**, X=N_3), when compared to the unsubstituted analogue (**38**, X=H), suggested that the azidobenzyl triester (**38**, X=N_3) may react by a different pathway, therefore its mechanism of hydrolysis was investigated further using ^{18}O labelled water. In this experiment the triester was incubated at 37°C, pH 7.4 in an 80% enriched $H_2{}^{18}O$ sodium phosphate-buffered water - acetonitrile mixture (1:1, v/v). The sodium salt of the diester (**61**, X=N_3) was isolated from the reaction mixture and analysed by FAB mass spectrometry to reveal peaks at *m/z* 294 (^{16}O, 94%) and 296 (^{18}O, 6%) indicating that there was minimal incorporation of ^{18}O label into the salt, as an authentic sample of the diester also shows a 4% peak at 294. In contrast, mass spectrometry (EI) of the 4-azidobenzyl alcohol (**51**, X=N_3) from the reaction mixture revealed peaks at *m/z* 149 (^{16}O, 26%) and 151 (^{18}O, 74%) confirming incorporation of an ^{18}O label into the molecule. These results were contrary to those observed for the dibenzyl triester (**38**, X=H) suggesting that the azidobenzyl group must be lost by C-O bond cleavage (**Fig 2.28**).

Fig 2.28 - Mechanism of formation of 4-azidobenzyl diester (**61**) from the hydrolysis of di(4-azidobenzyl) (methoxycarbonyl)phosphonate (**38**, X=N_3)

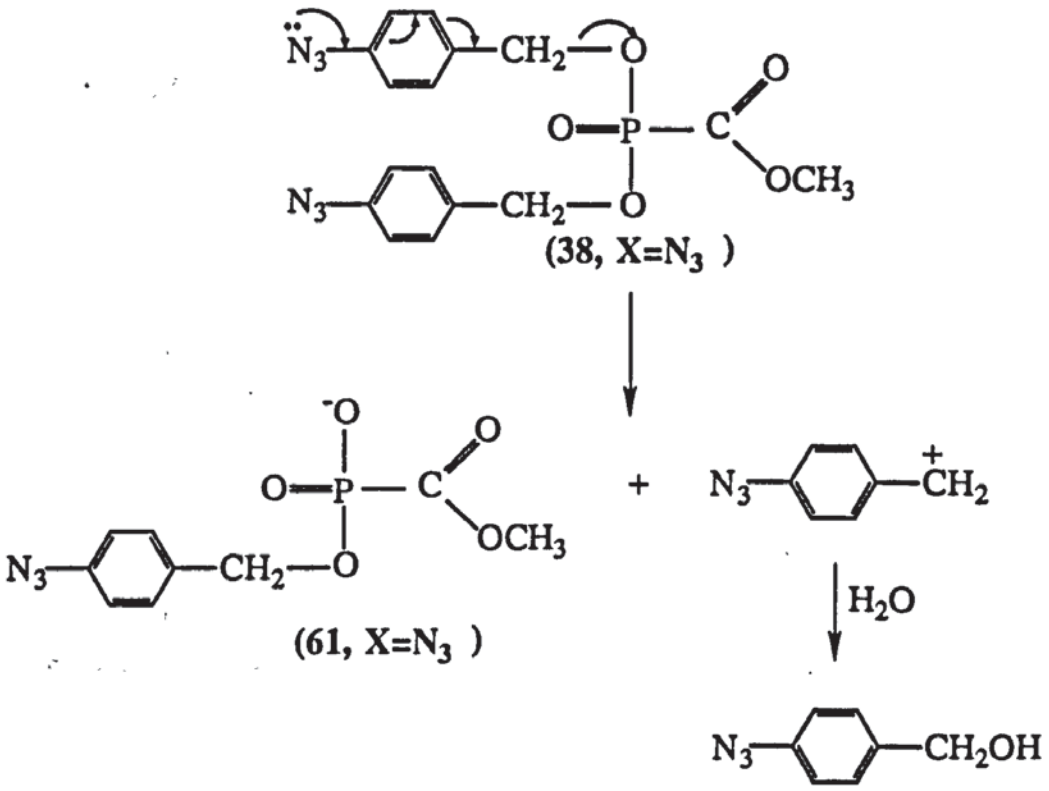

The electronic nature of the azido group may account for the observed change in mechanism. The electronic properties (σ) of a substituent can be derived from the Hammet equation,[155]

$$\sigma = \log K_x - \log K_H \qquad \textbf{Eqn. 2.9}$$

where K_H is the ionisation constant for benzoic acid in water at 25°C and K_x is the ionisation constant for a *meta* or *para* derivative under the same experimental conditions. Positive values of σ represent electron-withdrawal from the aromatic ring by the substitutent; negative σ values indicate electron-release to the ring. In effect, the Hammet equation states that the electronic effect of substituents on the ionisation of benzoic acids can be used as a model for the effect of substituents on other reaction centres attached to aromatic systems. Sigma constants are position-dependent; that is, σ for a given substituent in the *meta* position (σ_m) is different from that in the *para* position (σ_p). After the definition of the Hammet equation, it was soon observed that certain groups require the use of special sigma values which include the effect of direct resonance interaction between the substituent and the site of reaction. An example of this effect is the stabilisation of the phenolate ion by the *para*-nitro group **(Fig 2.29)**.

Fig 2.29 - Resonance stabilisation of the 4-nitrophenolate ion

Therefore different sets of sigma values are used when there is direct resonance interaction between the substituent and the reaction centre. For reactions in which a positive centre is generated adjacent to the ring, σ_p^+ values are used for *para*-substituents, such as $-OCH_3$, which can donate electrons to the positive site by direct resonance interaction. Conversely, for reactions in which a negative centre is generated σ_p^- values are used for resonance electron-withdrawing substituents, such as NO_2. **Table 2.6** gives the sigma constants (σ) of the benzyl substituents involved in the phosphonoformate triester **(38)** series.

Table 2.6 - Hammet substituent constants (σ) of some common functional groups[156]

Substituent	σ_m	σ_p	σ_p^+
Hydrogen	0.00	0.00	0.00
Nitro	0.71	0.78	0.79
Trifluoromethyl	0.43	0.54	0.61
Acetoxy	0.38	0.50	0.57
Chloro	0.37	0.23	0.11
Azido	0.37	0.08	-0.54
Methoxy	0.12	-0.27	-0.78
Hydroxy	0.12	-0.37	-1.00
Methyl	-0.07	-0.17	-0.31
Amino	-0.16	-0.66	-1.30

The electron-withdrawing effect (σ_m) of the azido substituent in the *meta* position is similar to that of the halogens. The small positive value calculated for σ_p indicates that the azido group is inductively electron-withdrawing (-I) but at the same time mesomerically electron-releasing (+M, σ_p^+) in the *para* position. The electron-donating mesomeric effect of the azido group outweighs the electron-withdrawing inductive effect (+M > -I), consequently, this resonance effect will serve to stabilise the 4-azidobenzyl carbonium ion **(92)** **(Fig 2.30)** favouring degradation of the triester **(38, X=N_3)** via C-O bond cleavage.

Fig 2.30 - Resonance stabilisation of the 4-azidobenzyl carbonium ion **(92)**

(92)

This resonance stabilisation effect is further supported by the work of Hoz and co-workers[157] who calculated that the azido group has the ability to stabilise an α-carbonium ion (**Fig 2.31**), the value between that of an OH and an NH_2 substituent.

Fig 2.31 - Resonance stabilisation of an azido α-carbonium ion

Electron-donating substituents in the 4-position of the aromatic ring serve to destabilise the dibenzyl phosphonoformate triesters (**38**). In an attempt to find more stable dibenzyl phosphonoformate triesters, analogues with strongly electron-withdrawing groups in the 4-position were considered. From **Table 2.6** the nitro group certainly fits this criteria, however it has already been shown that bis(4-nitrobenzyl) (methoxycarbonyl)phosphonate [**38**, **X=NO_2**, δ_P -3.54 ppm (pent q, J_{PH} 8.6, 1.1 Hz, ^1H coupled)] is also hydrolysed rapidly ($t_{1/2}$ 5.4 min). Although 4-nitrobenzyl (methoxycarbonyl)phosphonate [**61**, **X=NO_2**, δ_P -4.75 ppm (t q, J_{PH} 7.3, 0.9 Hz, ^1H coupled), k_1=0.10 min^{-1}] was again the major product of hydrolysis, the reaction was slower than the azidobenzyl triester (**38**, **X=N_3**) and competing nucleophilic attack by water at the carbonyl group was more significant, to give di(4-nitrobenzyl) phosphite [**88**, **X=NO_2**, δ_P 11.53 ppm (d pent, J_{PH} 733, 10.0 Hz, ^1H coupled), k_2=1.44x10^{-2} min^{-1}] and 4-nitrobenzyl phosphite [**89**, **X=NO_2**, δ_P 5.94 ppm (d t, J_{PH} 629, 8.4 Hz, ^1H coupled), k_5=1.53x10^{-2} min^{-1}]. The other minor hydrolysis products were 4-nitrobenzyl (4-nitrobenzyloxycarbonyl)phosphonate [**90**, **X=NO_2**, δ_P -5.27 ppm (t, J_{PH} 7.9 Hz, ^1H coupled), k_3=4.85x10^{-3} min^{-1}) and di(4-nitrobenzyl) phosphate [**91**, **X=NO_2**, δ_P 0.82 ppm, k_4=1.33x10^{-3}].

The mechanism of hydrolysis of the triester (**38**, **X=NO_2**) was investigated using 80% ^{18}O enriched water. The sodium salt of the diester (**61**, **X=NO_2**) was isolated from the reaction mixture and analysed by FAB mass spectrometry. By comparison with the unlabelled material, the mass spectrum showed peaks at *m/z* 298 (^{16}O, 30%) and 300 (^{18}O, 70%) indicating the incorporation of an ^{18}O label into the molecule. This was confirmed from the ^{31}P NMR spectrum of the diester (**61**, **X=NO_2**) which gave peaks at -2.79 (^{16}O, 20%) and -2.93 (^{18}O, 80%) ppm showing that the molecule contained an ^{18}O label attached directly to phosphorus. In addition the CI mass spectrum of 4-nitrobenzyl alcohol (**51**, **X=NO_2**) recovered from the reaction mixture showed a molecular ion at *m/z* 171 (^{16}O + NH_4^+) consistent with the absence of an ^{18}O label in this molecule. Therefore, contrary to the hydrolysis of the 4-azidobenzyl triester (**38**, **X=N_3**), but

consistent with that observed for the benzyl triester (38, X=H), bis(4-nitrobenzyl) (methoxycarbonyl)phosphonate (38, $X=NO_2$) undergoes hydrolysis with the loss of 4-nitrobenzyl alcohol (51, $X=NO_2$) *via* P-O cleavage, presumably by a mechanism similar to that outlined for (38, X=H) (Fig 2.16, section 2.4.4.). The marked hydrolytic instability of the 4-nitrobenzyl triester (38, $X=NO_2$) must be due to the very strong electron-withdrawing properties of the nitro group (σ_p 0.78) increasing the susceptibility of phosphorus to attack by nucleophiles.

The 4-trifluoromethylbenzyl triester (38, $X=CF_3$) was found to have a half-life in water of 15 min by ^{31}P NMR spectroscopy. The rate of hydrolysis was therefore slower than either the azidobenzyl (38, $X=N_3$) or the nitrobenzyl (38, $X=NO_2$) triesters and as a result the degree of competitive nucleophilic attack by water at the carboxyl carbon was greater. Hence, although the diester, 4-trifluoromethylbenzyl (methoxycarbonyl)phosphonate [61, $X=CF_3$, δ_P 4.78 ppm (t q, J_{PH} 7.2, 0.9 Hz, ^1H coupled), $k_1=3.38\times10^{-2}$ min^{-1}] was still the major product, more di(4-trifluoromethylbenzyl) phosphite [88, $X=CF_3$, δ_P 11.37 ppm (d pent, J_{PH} 728, 9.9 Hz, ^1H coupled), $k_2=8.74\times10^{-3}$ min^{-1}] and 4-trifluoromethylbenzyl phosphite [89, $X=CF_3$, δ_P 5.93 ppm (d t, J_{PH} 627, 8.2 Hz, ^1H coupled), $k_5=5.66\times10^{-3}$ min^{-1}] was formed, together with the minor products 4-trifluoromethylbenzyl (4-trifluoromethylbenzyloxycarbonyl)phosphonate [90, $X=CF_3$, δ_P -5.22 ppm (t, J_{PH} 7.0 Hz, ^1H coupled), $k_3=2.64\times10^{-3}$ min^{-1}] and di(4-trifluoromethylbenzyl) phosphate [91, $X=CF_3$, δ_P 0.96 ppm (pent, J_{PH} 7.7 Hz, ^1H coupled), $k_4=1.33\times10^{-3}$ min^{-1}]. This is demonstrated by comparison of the ^{31}P (^1H coupled) NMR spectra (Figs 2.32, 2.33, 2.34) for the hydrolysis of the three triesters (38, $X=N_3$, NO_2, CF_3).

The mechanism of hydrolysis of the 4-trifluoromethylbenzyl triester (38, $X=CF_3$) was not investigated further. However, based on the σ_p value (0.54), the trifluoromethyl group is moderately electron-withdrawing and as such may promote hydrolysis *via* P-O bond cleavage proceeding by a mechanism similar to that described for the benzyl (38, X=H) and 4-nitrobenzyl (38, $X=NO_2$) triesters.

Fig 2.32 – ^{31}P NMR (^{1}H coupled) spectrum for the hydrolysis of di(4-azidobenzyl) (methoxycarbonyl)phosphonate (t = infinity)

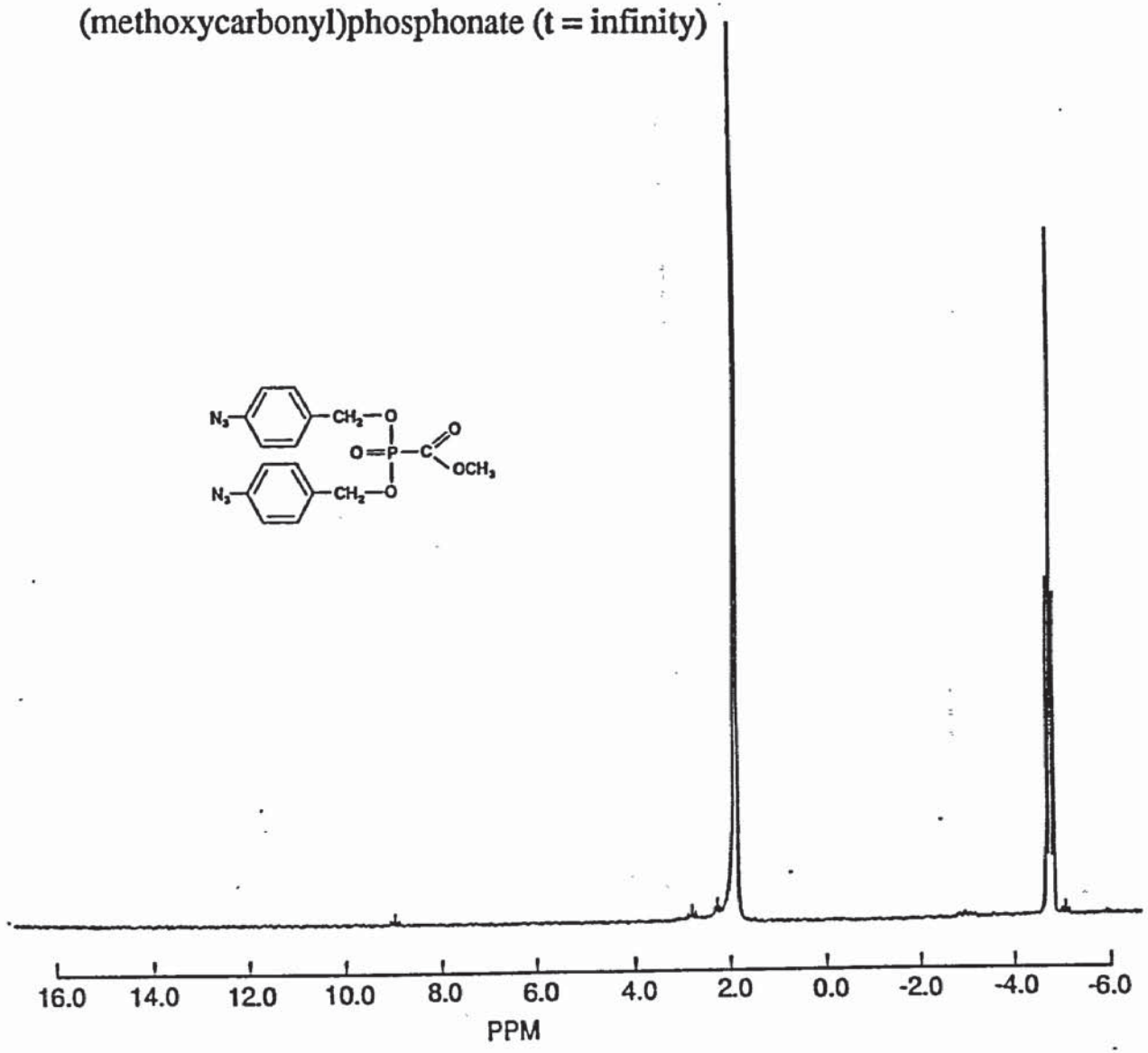

Fig 2.33 – ^{31}P NMR (^{1}H coupled) spectrum for the hydrolysis of di(4-nitrobenzyl) (methoxycarbonyl)phosphonate (t = infinity)

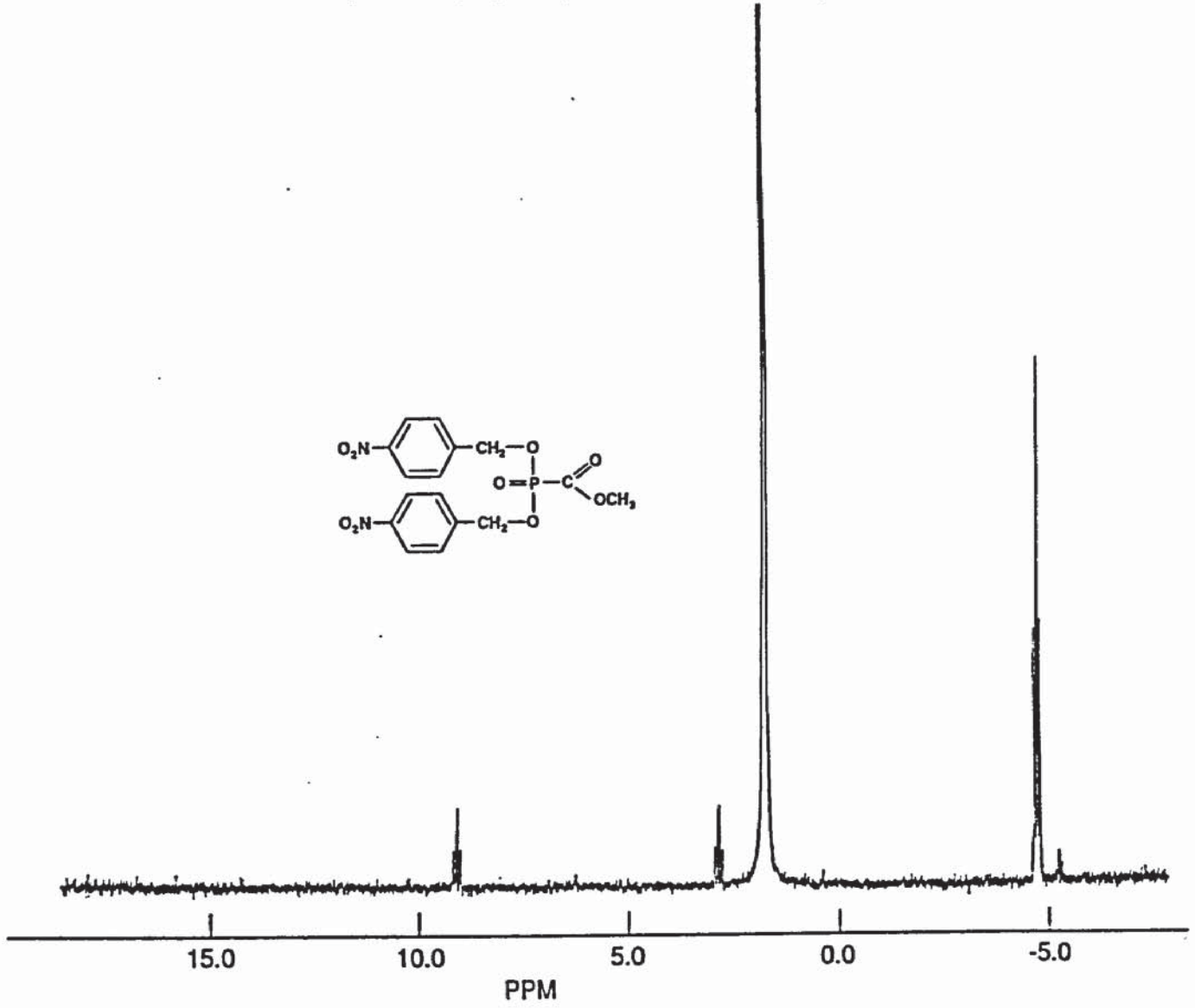

Fig 2.34 – ^{31}P NMR (^{1}H coupled) spectrum for the hydrolysis of di(4-trifluoro-methylbenzyl) (methoxycarbonyl)phosphonate (t = infinty)

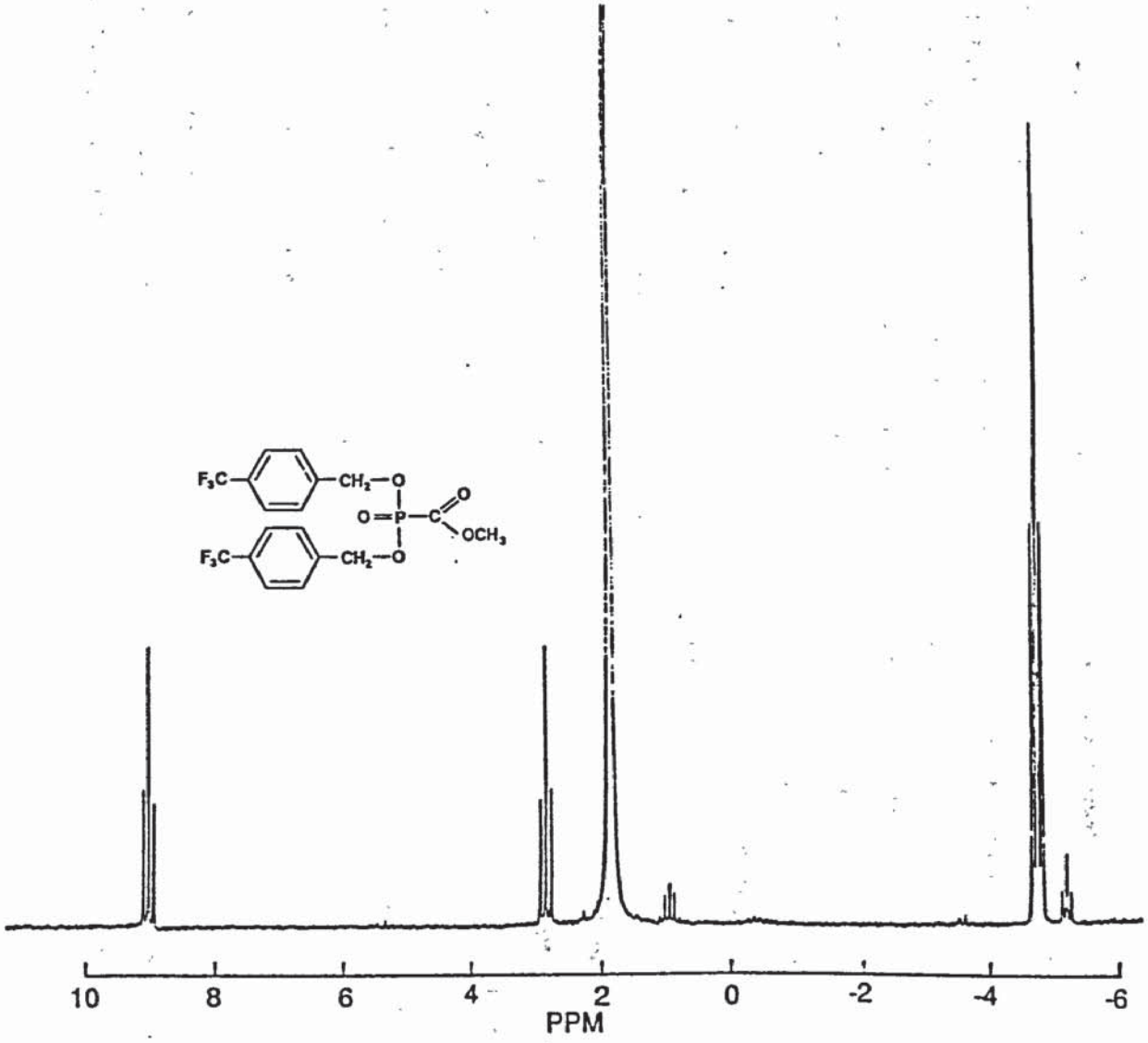

2.5.3. Molecular Orbital Calculations on the Triesters (38)

To further explore the reasons for different mechanisms and rates of hydrolysis of the *para*-substituted dibenzyl (methoxycarbonyl)phosphonates (38), semi-empirical molecular orbital calculations were performed in an attempt to investigate the influence of the *para* substituent on the electron density at phosphorus, and hence its sensitivity to nucleophilic attack.

The co-ordinates of the crystal structure of trisodium phosphonoformate hexahydrate obtained from the Cambridge Crystallographic Database[158] were used as the basis for building the *para*-substituted dibenzyl triesters of phosphonoformate (38). This basic structure was modified using the Chem X molecular modelling package[159] and the resulting structures were optimised using the semi-empirical molecular orbital program, MOPAC, running on a VAX 8650 computer. The optimisation was achieved within this program using the Self-Consistent Field (SCF) method, Modified Neglect of Differential Overlap (MNDO). An SCF calculation involves an iterative procedure in which the energy of the molecule is minimised and the difference between consecutive electron density matrices should approach zero. The SCF is produced by considering electron-electron repulsion from the interaction between a given electron and the mean field of other electrons in the molecule. The simplest SCF method is CNDO (Complete Neglect of Differential Overlap), which assumes the atomic orbitals to be spherically symmetrical and not overlapping when evaluating electron repulsion integrals. MNDO, parameterised for s and p orbitals only, accounts for a certain amount of orbital overlap and considers the directionality of the atomic orbitals in calculating the repulsion integrals. A comprehensive review of semi-empirical molecular orbital methods is available[160].

Table 2.7 gives the atomic charges at phosphorus (charge on the electron) and the carbon of the benzylic methylene group from MNDO calculations together with the ^{31}P NMR shifts for a series of 4-substituted dibenzyl (methoxycarbonyl)phosphonates (38).

Table 2.7 - Atomic charges at P and CH_2 (mean) and ^{31}P NMR chemical shifts for triesters (38)

para substituent (X)	Charge on P	Charge on CH_2	δ_P
H	1.253	0.268	-3.75
NO_2	1.234	0.254	-3.90
NH_2	1.253	0.273	-
N_3	1.253	0.269	-4.78
Cl	1.263	0.271	-4.80
CH_3	1.255	0.260	-5.02
CH_3COO	1.253	0.269	-4.92

From these results the nature of the substituent in the 4-position of the benzene ring does not appear to influence the atomic charges at either P or CH_2. For example, the charge on the electron at phosphorus for the hypothetical 4-aminobenzyl triester (**38, X=NH_2**) (1.253) is identical to that calculated for the unsubstituted triester (**38, X=H**), suggesting that both molecules should exhibit comparable stabilities. However, it has already been shown that strongly electron-donating substituents, such as NH_2 (σ_p -0.66) or CH_3O (σ_p -0.27), in the 4-position of the benzene ring greatly destabilise the molecule and, triesters (**38, X=NH_2, CH_3O**) cannot be synthesised. By contrast, the unsubstituted triester (**38, X=H**), although susceptible to hydrolysis ($t_{1/2}$ = 60 min), can be synthesised with comparative ease. In addition, the atomic charges on both P and CH_2 for the 4-nitrobenzyl triester (**38, X=NO_2**) were calculated to be slightly lower than those for the unsubstituted analogue, suggesting that the highly electron-withdrawing nitro group (σ_p 0.78) has actually donated negative charge to the system. This is not consistent with the ^{31}P NMR data in which the nitrobenzyl triester (**38, X=NO_2**) has a higher chemical shift (δ_p -3.90 ppm), and thus lower electron density at phosphorus, than the methyl analogue (**38, X=CH_3**, δ_p -5.03), the only triester synthesised with an electron-donating substituent attached to the aromatic ring (σ_p -0.17). Therefore the results obtained from the molecular orbital calculations must be considered as unreliable. This is exemplified by a complete lack of correlation between the calculated charges at P (**Table 2.7**) and their corresponding substituent Hammett values (σ_p, **Table 2.6**) (**Fig 2.35**).

Fig 2.35 - Plot of the MNDO calculated charges on phosphorus for the dibenzyl (methoxycarbonyl)phosphonates against their corresponding substituent Hammett values

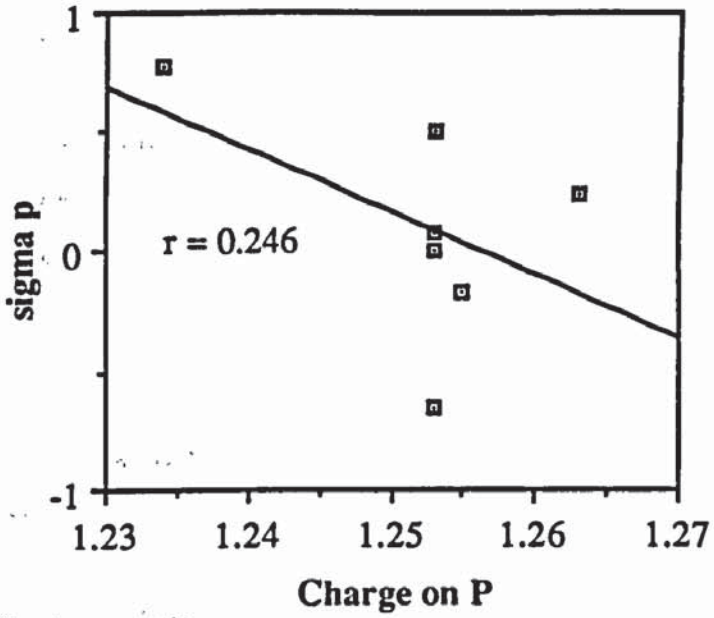

The dibenzyl (methoxycarbonyl)phosphonates (38) are not suitable for MNDO calculations. This may be due to MNDO using only s and p orbitals, hence hypervalent molecules, for example phosphonates, are likely to generate unreliable results. This problem could be overcome by using the PM3[161] method (Parametric Method) rather than MNDO. PM3 is a relatively new semi-empirical technique which has been parameterised more thoroughly than MNDO and can effectively handle phosphorus. Indeed, preliminary work by Dr B. Denny of the Pharmaceutical Sciences Institute, Aston University, concerning the application of PM3 calculations to the dibenzyl (methoxycarbonyl)phosphonates (38) has established a good correlation between the charge at P, the Hammett values for a range of substituents and the ^{31}P NMR data, thus providing a basis for any future modelling studies involving these and similar molecules.

2.5.4. Summary

The phosphonoformate triesters (38, X=H, N_3, NO_2, CH_3, CH_3COO, $(CH_3)_3CCOO$, Cl, CF_3) are inherently unstable due to the electron-withdrawing effect of the carboxyl group promoting nucleophilic attack at phosphorus. Despite this instability it is still possible to influence the mechanism and to some extent the rate of hydrolysis of these triesters by varying the electronic nature of the substituent in the 4-position of the aromatic ring. Strongly electron-withdrawing substituents, such as the nitro group (σ_p 0.78) and, to a lesser extent, the ethanoyloxy group (σ_p 0.50), are likely

to increase the susceptibility of phosphorus to nucleophilic attack, thus promoting P-O bond cleavage and rapid hydrolysis. On the other hand, weakly electron-withdrawing groups, such as the azido group (σ_p 0.08, σ_p^+ -0.54) and perhaps the chloro group (σ_p 0.23, σ_p^+ 0.11), may in fact mesomerically donate electrons to the ring promoting rapid hydrolysis through stabilisation of the benzyl carbonium ion and subsequent C-O bond cleavage. This may explain why dibenzyl (methoxycarbonyl)phosphonate (**38, X=H**), which contains a neutral H atom in the 4-position, is the most stable triester of the series. The high degree of P-C bond cleavage and phosphite formation in the hydrolysis of the dibenzyl triesters (**38**), together with their low chemical stability, makes them unsuitable as prodrug forms of phosphonoformate.

2.6. The Chemical Activation of Sodium 4-Azidobenzyl (Methoxycarbonyl)phosphonate (61, X=N_3)

The inherent instability of the dibenzyl triesters of phosphonoformate (**38**) towards chemical hydrolysis meant that it was impossible to examine the activation of these molecules. Instead the chemical activation of the hydrolytically stable diester, sodium 4-azidobenzyl (methoxycarbonyl)phosphonate (**61, X=N_3**) was studied in an attempt to observe the 'cascade' effect and thus further justify the present rationale for prodrug design.

The azido substituent has been likened to the chloro group with respect to both lipophilicity and electronic characteristics[162] and it has been shown that aryl azides may be reduced, enzymatically or *via* circulating thiols, to the corresponding aryl amines.[163] Thiols, such as dithiothreitol (DTT) and the endogenous substance, glutathione, reduce aryl azides at physiological pH and temperature.[164, 165, 166] The DTT reduction is thought to proceed *via* nucleophilic attack of the dithiol on either the α or γ nitrogen atom of the azide group followed by intramolecular cyclisation and liberation of nitrogen to produce the cyclic disulphide and aryl amine[167] (**Fig 2.36**).

Fig 2.36 - DTT reduction of aryl azides

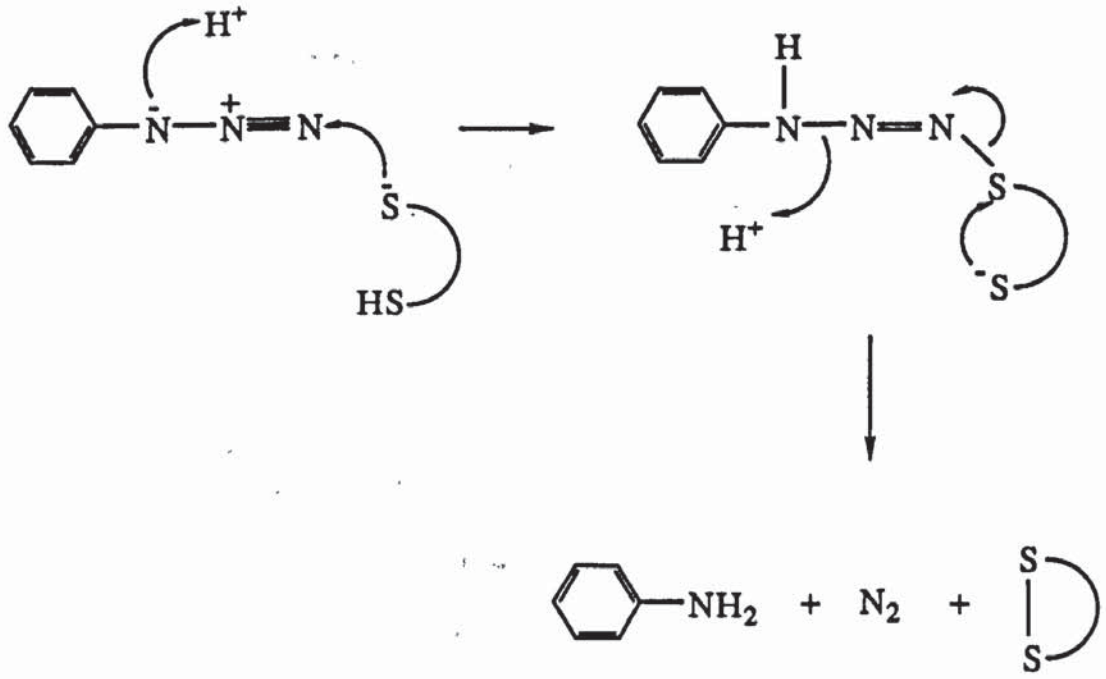

In the activation experiment, sodium 4-azidobenzyl (methoxycarbonyl)phosphonate (**61,** $X=N_3$) was incubated with a 10 molar excess of DTT at 37°C, pH 7.4 and the reaction was monitored by ^{31}P NMR spectroscopy. The diester [**61,** $X=N_3$, δ_P -4.56 ppm (t q, J_{PH} 7.5, 1.1 Hz, ^1H coupled)] degraded quickly ($t_{1/2}$=13.5 min) to give a peak at -2.59 ppm, which on ^1H coupling gave a quartet with a coupling constant of 0.9 Hz, consistent with the formation of (methoxycarbonyl)phosphonate (**54**). Although the amino intermediate (**61,** $X=NH_2$) was not detected the reaction almost certainly proceeds via reduction of the azido group to give the diester (**61,** $X=NH_2$), which then cascades *via* C-O bond cleavage to form the monoester (**54**), owing to the ability of the electron-rich amino group (σ_p -0.66) to stabilise the 4-aminobenzyl carbonium ion (**Fig 2.37**).

This experiment clearly demonstrates the effectiveness of the benzylic cascade approach to prodrug design. The next stage must be to explore this rationale with other phosphonate triesters which are both stable towards chemical hydrolysis and sufficiently lipophilic to promote membrane permeation.

Fig 2.37 - Degradation of sodium 4-azidobenzyl (methoxycarbonyl)phosphonate (**61,** $X=N_3$) in the presence of DTT

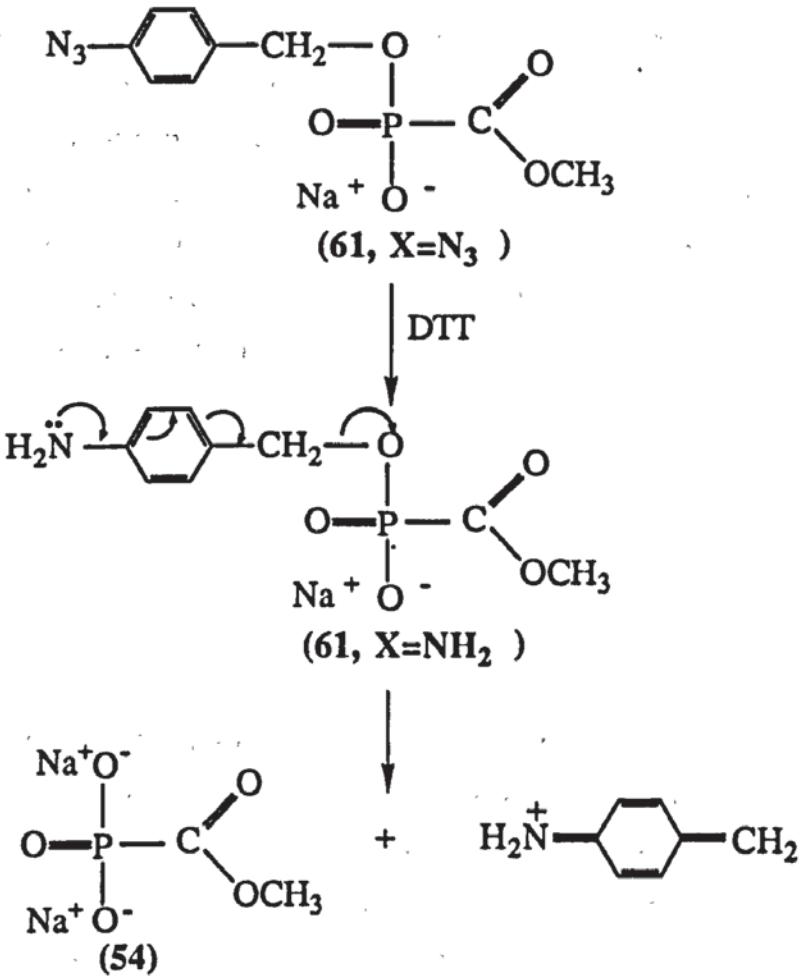

CHAPTER 3 - ESTERS OF PHOSPHONOACETATE

The instability of the triesters of phosphonoformate (38) towards chemical hydrolysis requires that prodrugs of other antiviral phosphonates should be evaluated. The instability of the phosphonoformate triesters (38) was thought to arise from the electron-withdrawing effect on phosphorus of the adjacent methoxycarbonyl group. Therefore, it was considered that distancing this group further away from phosphorus would stabilise the molecule. The compound chosen for investigation was the antiviral drug, phosphonoacetate (PAA) (8), in which the phosphorus atom and the carboxyl function are separated by a methylene group.

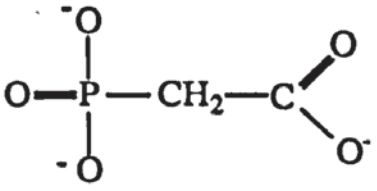

(8)

A series of di(benzoyloxymethyl) triesters (44), dibenzyl triesters (39) and di(alkanoyloxybenzyl) triesters (93) of PAA were synthesised and their chemical and enzymatic hydrolyses investigated. The electron density on phosphorus for the triesters of PAA (44, 39, 93) is increased relative to the triesters of PFA (38), hence the PAA triesters should be less sensitive towards nucleophilic attack at phosphorus than the corresponding PFA analogues.

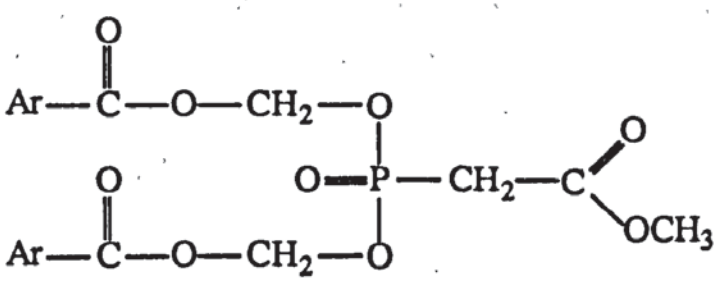

(44)

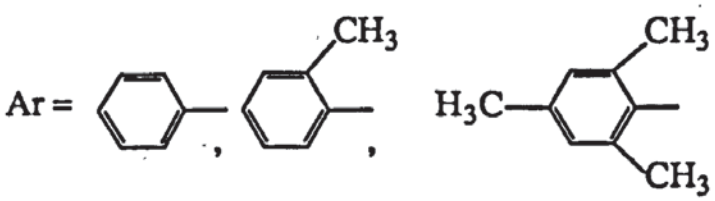

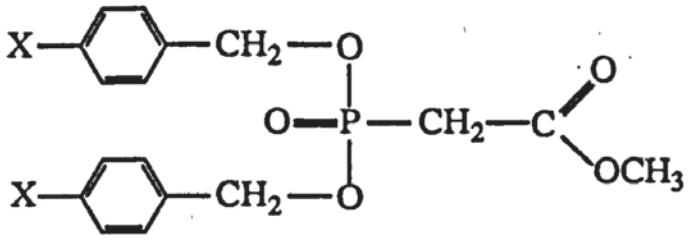

(39)

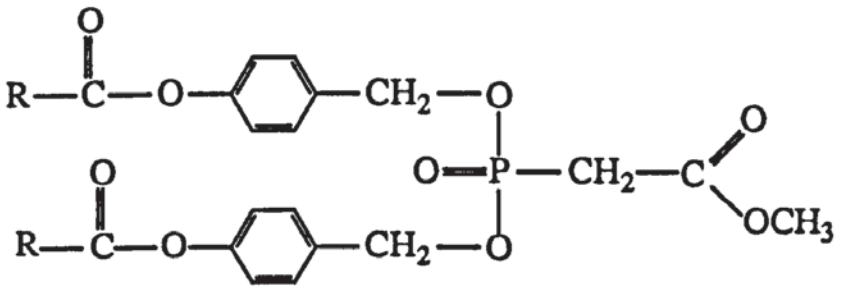

(93)

R = alkyl

3.1. Synthesis of Di(benzoyloxymethyl) (Methoxycarbonylmethyl)phosphonates (44)

Using a method similar to that described by Srivastva[112] for the synthesis of alkanoyloxymethyl phosphate esters, the di(benzoyloxymethyl) triesters (44) were synthesised by the reaction of the appropriate iodomethyl benzoate (98) with disilver (methoxycarbonyl)phosphonate (97). The disilver salt was obtained from the reaction of disodium (methoxycarbonylmethyl)phosphonate (96) with silver nitrate (Fig 3.1). Three di(benzoyloxymethyl) triesters were prepared, 44, Ar=C_6H_5; 44, Ar=2-$CH_3C_6H_4$; 44, Ar=2,4,6-$(CH_3)_3C_6H_2$. All 3 triesters were purified by flash column chromatography in approximately 40% yields.

The iodomethyl benzoates (98) were prepared from the reaction of the appropriate benzoyl chloride (99) with paraformaldehyde at 90°C in the presence of a catalytic amount of zinc chloride[168] (Fig 3.2). Treatment of the product, chloromethyl benzoate (100) with sodium iodide, followed by purification by flash column chromatography gave an approximate 70% yield of the iodomethyl benzoates (98).[169]

Fig 3.1 - Synthesis of di(benzoyloxymethyl) (methoxycarbonylmethyl)phosphonates (44)

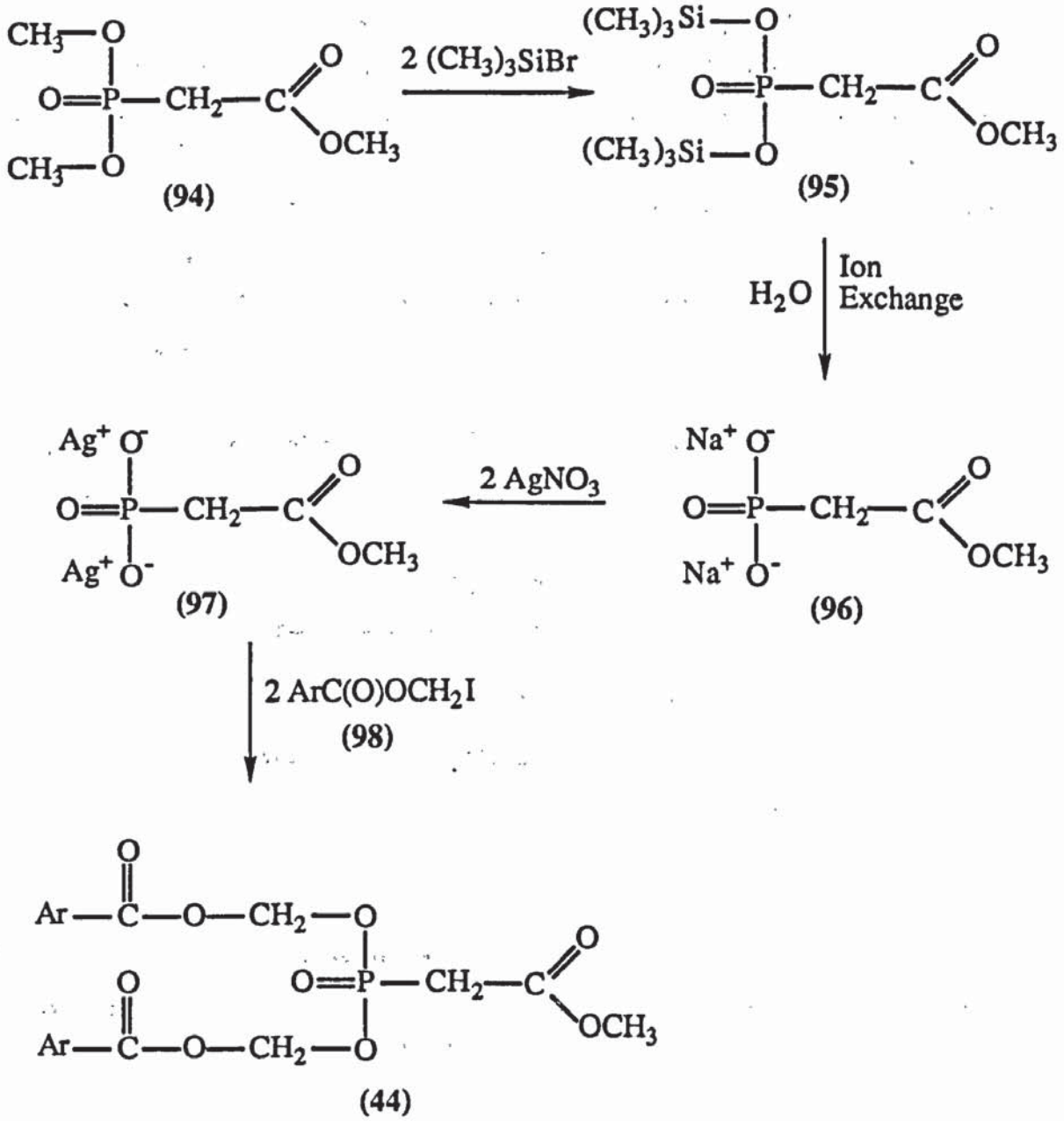

Fig 3.2 - Synthesis of iodomethyl benzoates (98)

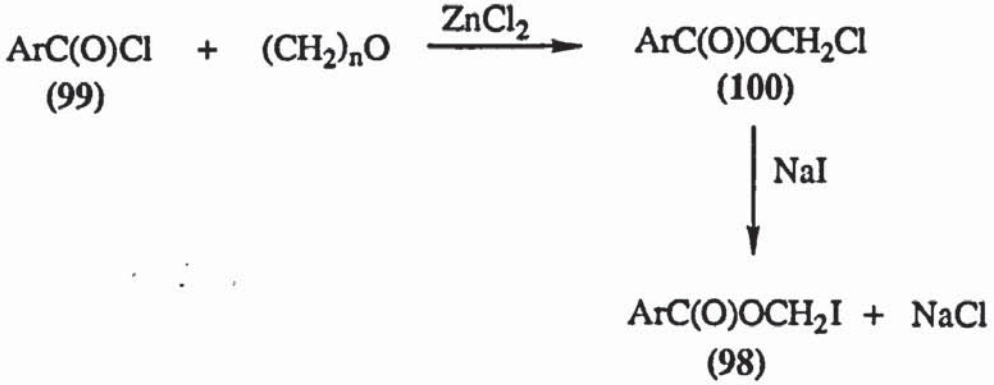

The triesters (44) were characterised by high resolution FAB mass spectrometry, high resolution ^{1}H, ^{31}P and ^{13}C NMR spectroscopy and infra-red spectroscopy. The ^{1}H NMR spectra includes a doublet (J_{PH} ~21 Hz) at approximately 3 ppm resulting from coupling between the P-methylene group and phosphorus. When using $CDCl_3$ as solvent, the ^{1}H and ^{31}P NMR spectra revealed the O-CH_2-O protons to be non-equivalent (Fig 3.3). The ^{1}H NMR spectra showed 2 sets of doublets of doublets at approximately 5 ppm (J_{gem} ~12 Hz, J_{PH} ~8 Hz), each proton being split by the geminal proton and the phosphorus atom. The ^{31}P (^{1}H coupled) NMR spectra showed a very complicated 27 line pattern at ~20 ppm consistent with a triplet of triplets of triplets from coupling of phosphorus with H_A, H_B and H_C. Overlapping signals prevented the measurement of any coupling constants.

Fig 3.3 - The non-equivalence of the O-CH_2-O protons in the di(benzoyloxymethyl) triesters (44)

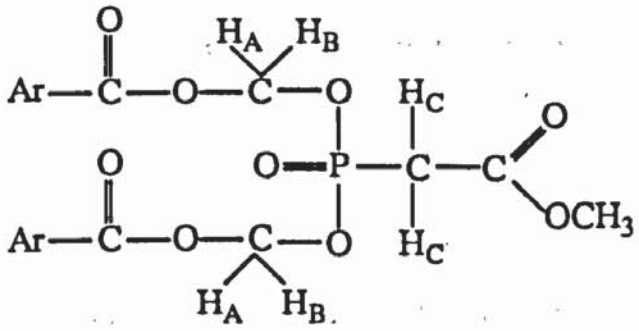

The synthesis of the benzoyloxymethyl diesters (101) was attempted from the triester (44) and sodium iodide. The reaction was unsuccessful and only starting material was isolated, suggesting that the O-CH_2-O group is not susceptible to nucleophilic attack by iodide.

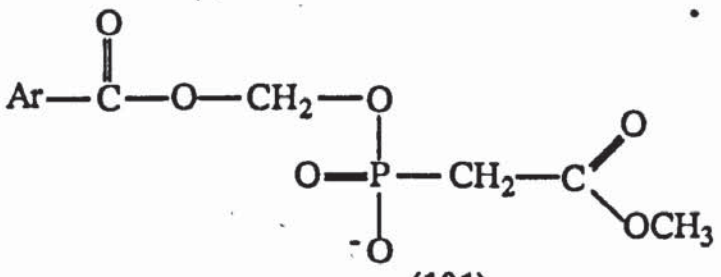

(101)

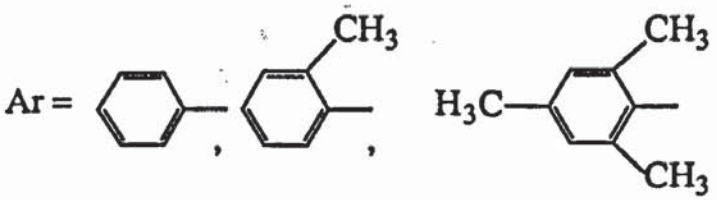

3.2. Synthesis of Dibenzyl (Methoxycarbonylmethyl)phosphonates (39) and Di(4-Alkanoyloxybenzyl) (Methoxycarbonylmethyl)phosphonates (93)

Triesters (39) and (93) were prepared in a similar manner to the PFA triesters (38) (Fig 2.1) from the reaction between the appropriate benzyl alcohol (51) and (methoxycarbonylmethyl)phosphonic dichloride (103) (Fig 3.4). Rather than proceeding through the bis(trimethylsilyl) derivative, required for the preparation of (methoxycarbonyl)phosphonic dichloride (50), (methoxycarbonylmethyl)phosphonic dichloride (103) was prepared in 79% yield from the direct reaction between dimethyl (methoxycarbonylmethyl)phosphonate (102) and phosphorus pentachloride at 70°C for 3 h.[170] Dimethyl (methoxycarbonylmethyl)phosphonate (102) is commercially available, however it can be prepared from the reaction of dimethyl phosphite and chloroacetic acid in methanol, in the presence of sodium methoxide.[171] The 4-alkanoyloxybenzyl alcohols were prepared as previously described (Section 2.1.)

Fig 3.4 - Synthesis of Dibenzyl (Methoxycarbonylmethyl)phosphonates (39) and Di(4-alkanoyloxybenzyl) (Methoxycarbonylmethyl)phosphonates (93)

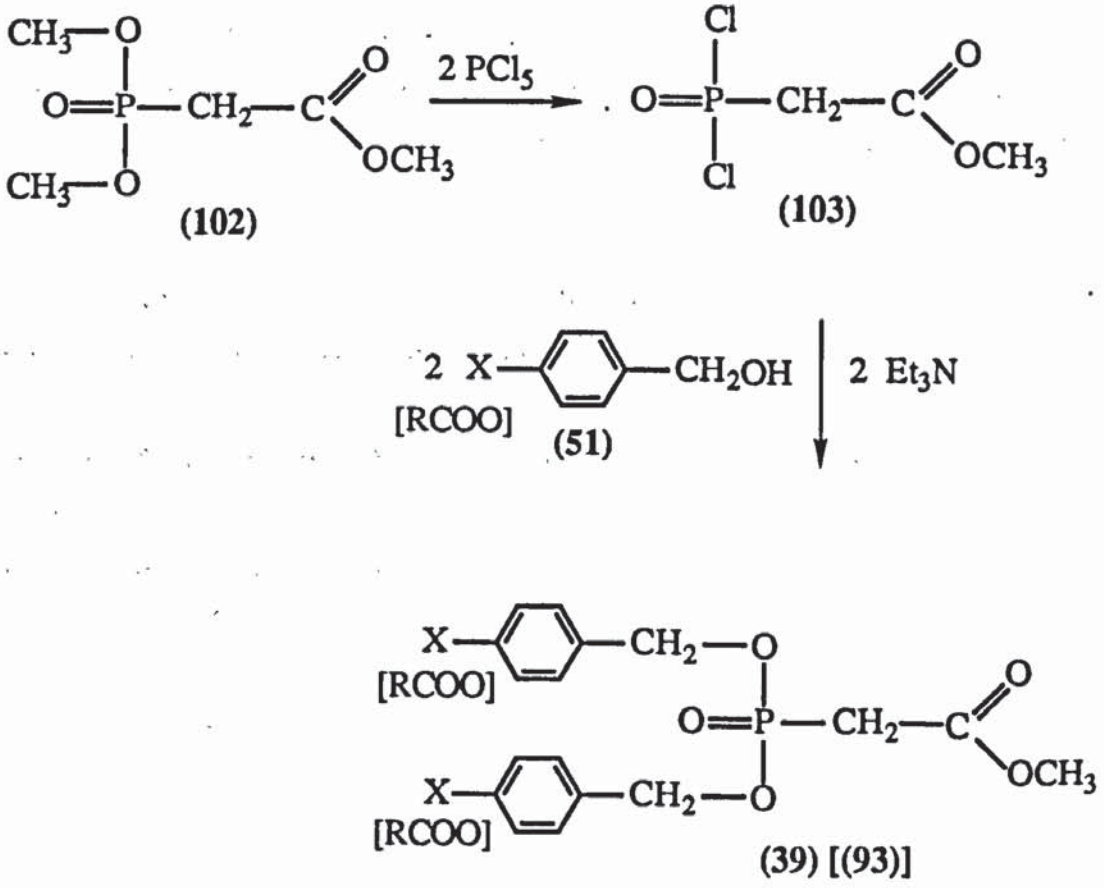

A series of 4-substituted benzyl triesters (39, X=H, NO_2) and di(alkanoyloxybenzyl) triesters (93, R=CH_3, CH_3CH_2, $CH_3(CH_2)_2$, $CH_3(CH_2)_3$, $CH_3(CH_2)_4$, $(CH_3)_2CH$, $(CH_3)_3C$) were prepared in this manner. All triesters were purified by flash column chromatography in yields ranging from 5 to 34%.

The triesters (39, 93) were fully characterised by elemental analysis, high resolution FAB mass spectrometry, high resolution ^1H, ^{31}P and ^{13}C NMR spectroscopy and infra-red spectroscopy. In common with the di(benzoyloxymethyl) triesters (44), ^1H and ^{31}P NMR spectra revealed prochirality of the benzylic protons. As can be seen in **Fig 3.5** The ^1H NMR spectra showed 2 sets of doublets of doublets (J_{gem} ~12 Hz, J_{PH} ~9 Hz) at ~5 ppm and the ^{31}P (^1H coupled) NMR spectra showed a multiplet consistent with a triplet of triplets of triplets (27 lines) at ~20 ppm. The ^1H NMR spectra also showed a doublet (J_{PH} ~21 Hz) at ~3 ppm characteristic of a methylene group attached directly to phosphorus. Interestingly when the spectra were recorded using D_2O as solvent, the benzylic protons appeared equivalent. In this case the ^{31}P (^1H coupled) NMR spectra revealed a triplet of pentets (J_{PH} ~21, 9 Hz) and the ^1H NMR spectra revealed a doublet (J_{PH} ~8 Hz) at ~5 ppm.

The synthesis of di(4-methoxybenzyl) (methoxycarbonylmethyl)phosphonate (39, X=CH_3O) attempted *via* the route shown in **Fig 3.4** was unsuccessful. Similar to the attempted synthesis of the corresponding triester of PFA (38, X=CH_3O), the only compound recovered from the reaction mixture was di(4-methoxybenzyl) ether (57).

3.3. Synthesis of Lithium 4-Alkanoyloxybenzyl (Methoxycarbonylmethyl)phosphonates (104)

Lithium salts of the diesters (104) were prepared by the action of lithium iodide on the appropriate di(4-alkanoyloxybenzyl) triester (93) in the minimum volume of a mixture of dry diethyl ether and acetone (6:4) at room temperature (**Fig 3.6**). Yields were in the range of 35 - 81%. The syntheses were initially attempted using sodium iodide, however yields were very low, possibly due to the greater solubility of sodium salts over the corresponding lithium phospho salts.

Fig 3.5 – ^{1}H NMR spectrum of di(4-ethanoyloxybenzyl) (methoxycarbonylmethyl)-phosphonate

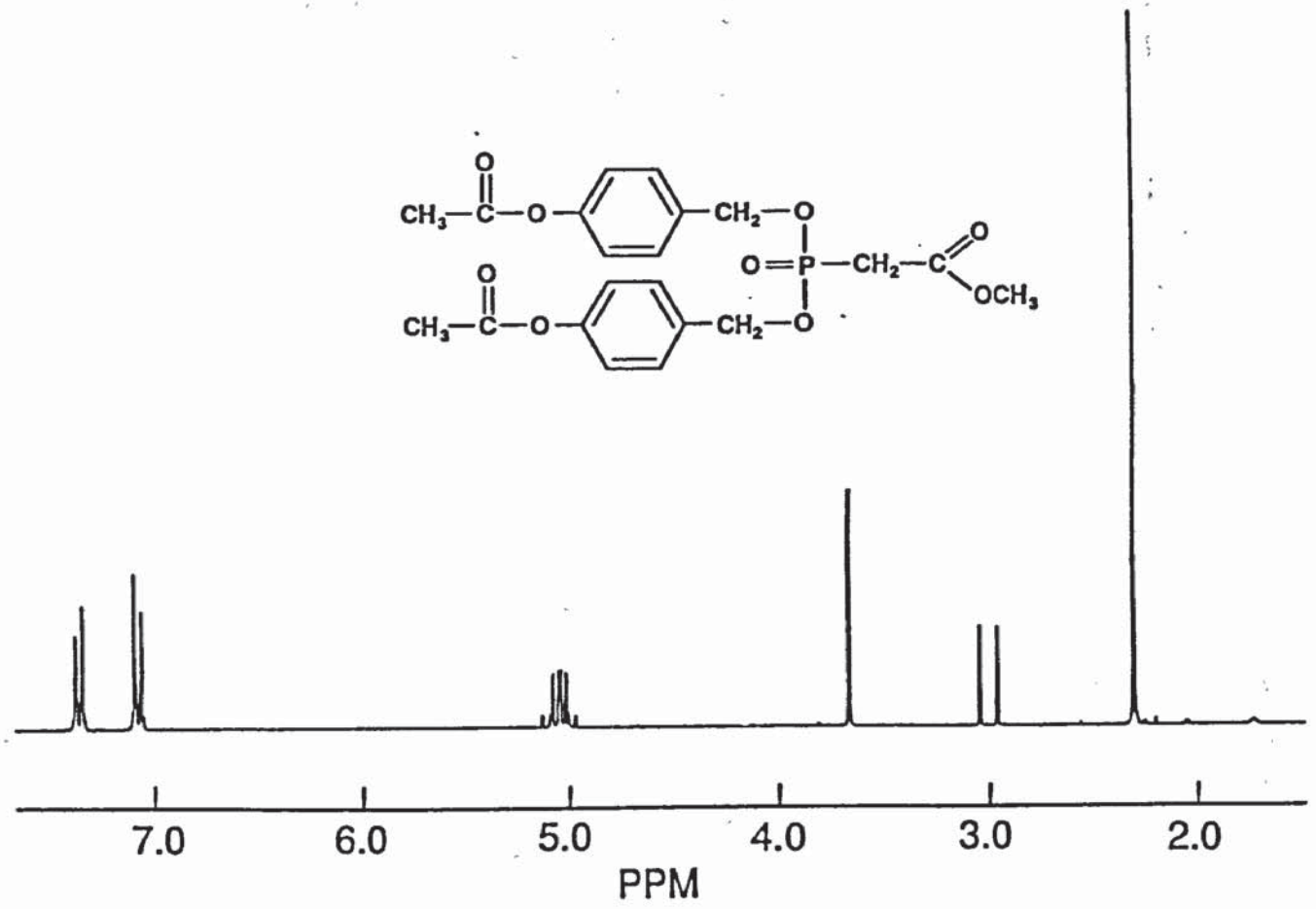

Fig 3.6 - Synthesis of Lithium 4-Alkanoyloxybenzyl (Methoxycarbonylmethyl)-phosphonates **(104)**

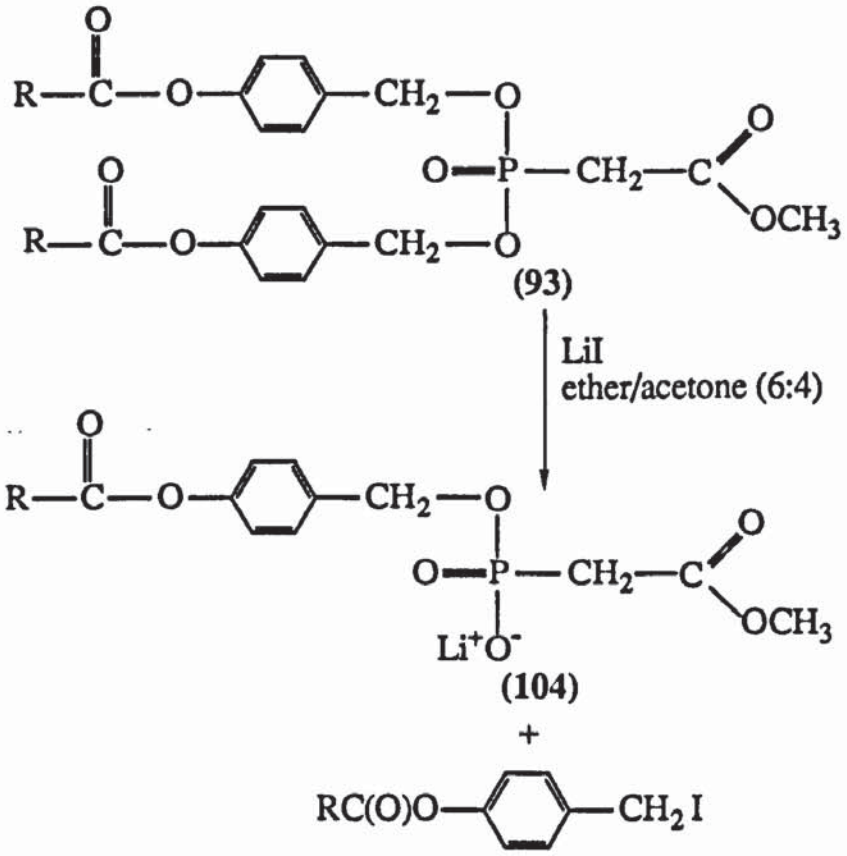

The diesters **(104)** were characterised by high resolution FAB mass spectrometry, high resolution ^{1}H, ^{13}C and ^{31}P NMR spectroscopy and infra-red spectroscopy. By ^{1}H and ^{31}P NMR spectroscopy the benzylic protons appeared equivalent. The ^{1}H NMR (D_2O) spectrum **(Fig 3.7)** were characterised by two doublets, one at ~3 ppm (J_{PH} ~21 Hz) for the PCH_2 group, and the other at ~5 ppm (J_{PH} ~8 Hz) for the equivalent benzylic protons. The ^{31}P (^{1}H coupled) NMR spectra confirmed this equivalence, revealing a triplet of triplets (J_{PH} ~21, 8 Hz) at ~15 ppm. It was difficult to obtain good elemental analysis data, probably resulting from hydration of the salt or incomplete removal of lithium iodide from the samples.

Fig 3.7 – ^{1}H NMR spectrum of lithium 4-ethanoyloxybenzyl(methoxycarbonylmethyl)-phosphonate

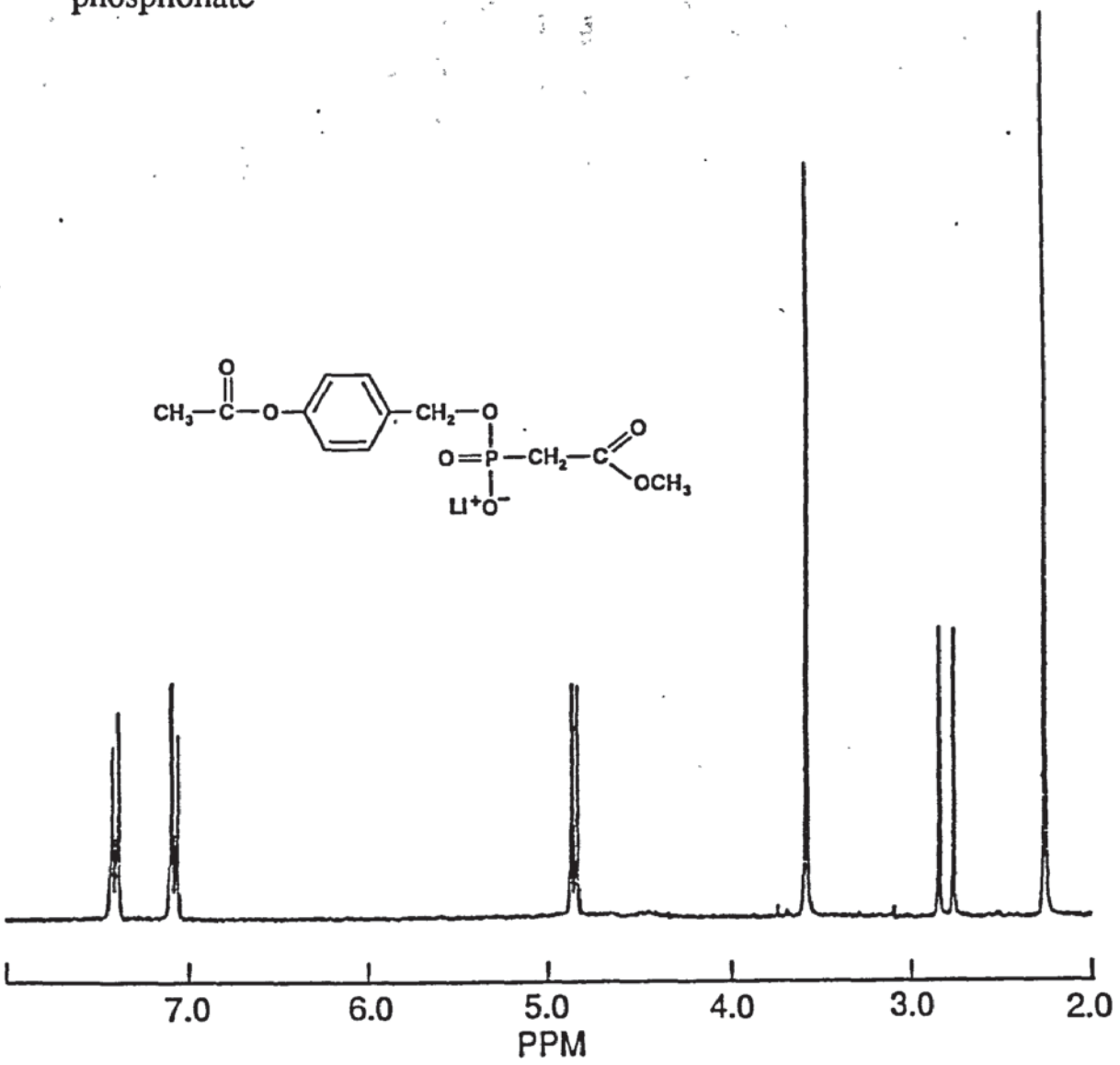

3.4. Antiviral Properties

Two di(alkanoyloxybenzyl) triesters (**93**, R=CH_3, $(CH_3)_3C$) were tested by Dr Naheed Mahmood and Dr Alan Hay at the Medical Research Council Laboratories (London). The compounds were incubated with HIV-1 infected C8166 cells at 37°C and their activities and toxicities measured by MTT and p24 antigen assays. The results are given in **Table 3.1.**

Table 3.1 - Anti-HIV activities and cytotoxicities of alkanoyloxybenzyl triesters (**93**)

R	max conc(μM)	EC_{50}	TC_{50}
CH_3	0.08	inactive	0.008
$(CH_3)_3C$	1	inactive	0.4

EC_{50} represents the concentration of drug which reduces the antigen p24 by 50% in infected cell cultures.
TC_{50} represents the concentration of drug which reduces cell growth by 50%.

Both compounds were found to be inactive and also highly toxic to cells. These results were confirmed by Dr Abraham Karpas at the MRC centre, Cambridge University. The fact that phosphonoacetate is known to be only a weak inhibitor of HIV reverse transcriptase and considering the lack of metabolising enzymes under the test conditions, the inactivity was not too surprising.

3.5. Hydrolysis Studies of Triesters (44) and (39)

The triesters (**44**, **39**, 400 μg ml^{-1}) were subjected to hydrolysis in a phosphate buffer (pH 7.4, 0.1 M)-acetonitrile mixture (1:1, v/v) at 37°C and the reactions monitored by ion-pair reversed-phase HPLC. The samples were injected directly onto a C-18 endcapped column and eluted for 20 min with a convex gradient of acetonitrile-10 mM tetrabutylammonium hydroxide in water, initial conditions, 35:65 (v/v); final conditions, 90:10 (v/v) at a flow rate of 1 ml min^{-1}. Each reaction was performed in duplicate and the triesters were found to be hydrolytically stable over 24 h. The individual retention times are given in **Table 3.2.**

Table 3.2 - Retention times of di(benzoyloxymethyl) **(44)** and dibenzyl (methoxycarbonylmethyl)phosphonates **(39)**

Compound	Retention Time (min)
44, Ar=C_6H_5	13.18
44, Ar=2-$CH_3C_6H_4$	15.07
44, Ar=2,4,6-$(CH_3)_3C_6H_2$	19.17
39, X=H	14.45
39, X=NO_2	11.37

The chemical stability of both the di(benzoyloxymethyl) (methoxycarbonylmethyl)-phosphonates **(44: R=C_6H_4, R=2-$CH_3C_6H_4$, R=2,4,6-$(CH_3)_3C_6H_2$)** and dibenzyl (methoxycarbonylmethyl)phosphonates **(39, X=H, NO_2)** confirm that the instability of the PFA triesters **(38)** was due to the electron-withdrawing effect of the methoxycarbonyl group. Perhaps more importantly a chemically stable system had been developed with which the cascade process at the triester level could be investigated.

3.6. Hydrolysis Studies of Triesters (93) and Diesters (104)

The triesters **(93,** 1μmol ml^{-1}) and diesters **(104,** 5 μmol ml^{-1}) were subjected to hydrolysis in a D_2O phosphate buffer (pD 8.0, 0.1 M)-acetonitrile mixture (9:1, v/v) at 37°C and the reactions monitored by ^1H NMR spectroscopy. A lower concentration of the triester was used due to its poor solubility and for the same reason, the half-lives of the triesters must be treated with a certain amount of caution. **Tables 3.3** and **3.4** give the appropriate chemical shifts and the half-lives of hydrolysis for the triesters **(93)** and diesters **(104)** respectively.

Table 3.3 - Chemical shifts of triesters and products (diester or carboxylic acid[a]) and half-lives ($t_{1/2}$) for the chemical hydrolysis of di(4-alkanoyloxybenzyl) triesters **(93)**

R	δ_H (triester)	δ_H (product)[a]	$t_{1/2}$(h)
CH_3	5.00 (d, J_{PH} 9.8 Hz, 2 x CH_2OP)	4.87 (d, J_{PH} 6.9 Hz, CH_2OP)	23
CH_3CH_2	5.00 (d, J_{PH} 9.8 Hz, 2 x CH_2OP)	4.86 (d, J_{PH} 7.7 Hz, CH_2OP)	25
$CH_3(CH_2)_2$	4.99 (d, J_{PH} 9.5 Hz, 2 x CH_2OP)	4.87 (d, J_{PH} 7.5 Hz, CH_2OP)	29
$(CH_3)_2CH$	4.99 (d, J_{PH} 10.9 Hz 2 x CH_2OP)	4.86 (d, J_{PH} 7.3 Hz, CH_2OP)	45
$(CH_3)_3C$[a]	1.01 (s, 2 x $(CH_3)_3$)	1.27 (s, $(CH_3)_3C$)	85

a) when **R=$(CH_3)_3C$** the CH_2OP signal for the diester product is obscured by the HOD peak, hence the intensities of the $(CH_3)_3C$ peaks for the triester and generated carboxylic acid were used to calculate the half-lives.

Table 3.4 - Chemical shifts of diester and generated carboxylic acid[a] and half-lives ($t_{1/2}$) for hydrolysis of lithium 4-alkanoyloxybenzyl diesters **(104)**

R	δ_H (triester)	δ_H (product)	$t_{1/2}$ (h)
CH_3	1.94 (s, CH_3)	1.81 (s, CH_3COOH)	105
CH_3CH_2	1.11 (t, J_{HH} 7.5 Hz, CH_3)	0.95 (t, J_{HH} 7.7 Hz, CH_3)	200
$CH_3(CH_2)_2$	0.92 (t, J_{HH} 7.5 Hz, CH_3)	0.80 (t, J_{HH} 7.4 Hz, CH_3)	230
$(CH_3)_2CH$	1.22 (d, J_{HH} 7.0 Hz, $(CH_3)_2$)	0.98 (d, J_{HH} 7.0 Hz, $(CH_3)_2$)	449
$(CH_3)_3C$	1.28 (s, $(CH_3)_3$)	1.02 (s, $(CH_3)_3$)	~2000

a) the generated carboxylic acid peaks were used to calculate half-lives rather than the respective PCH_2 intensities as slow deuterium exchange into the acidic methylene protons of the monoester occurred throughout the hydrolyses.

It is apparent from **Tables 3.3** and **3.4** that both the triesters **(93)** and diesters **(104)** undergo slow hydrolysis to the appropriate alkanoyloxybenzyl diester **(104)** and monoester [**(105)**, δ_H 2.59 (2 H, d, J_{PH} 19.6 Hz, PCH_2), and 3.58 ppm (3 H, s, OCH_3); δ_P 11.70 ppm (s), (t, J_{PH} 18.5 Hz, ^1H coupled)] respectively. The triesters are approximately ten times more reactive than the diesters, thus if the triester hydrolyses had been monitored for a sufficient length of time degradation to the monoester **(105)** would also have been observed. Together with the 4-alkanoyloxybenzyl diesters **(104)** and monoester **(105)**, 4-hydroxybenzyl alcohol was also formed [δ_H 7.19 (2 H, d, J_{HH} 8.5 Hz, Ar), 6.79 (2 H, d, J_{HH} 8.6 Hz, Ar) and 4.44 ppm (2 H, s, CH_2)]. 4-Alkanoyloxybenzyl alcohols were not formed suggesting that the reactions proceed by hydrolysis of the alkanoyloxybenzyl group to give the 4-hydroxybenzyl intermediates **(106)** and **(107)**, which were not detected. As a result of the electron-donating ability of the hydroxyl group (σ_p -0.37) these intermediates have only transitory existence and are rapidly degraded to the diester **(104)** and monoester **(105)** via C-O bond cleavage. The highly reactive benzyl carbonium ion reacts with water to give 4-hydroxybenzyl alcohol **(Fig 3.8)**.

Fig 3.8 - Mechanism of hydrolysis of 4-alkanoyloxybenzyl triesters **(93)** and diesters **(104)**

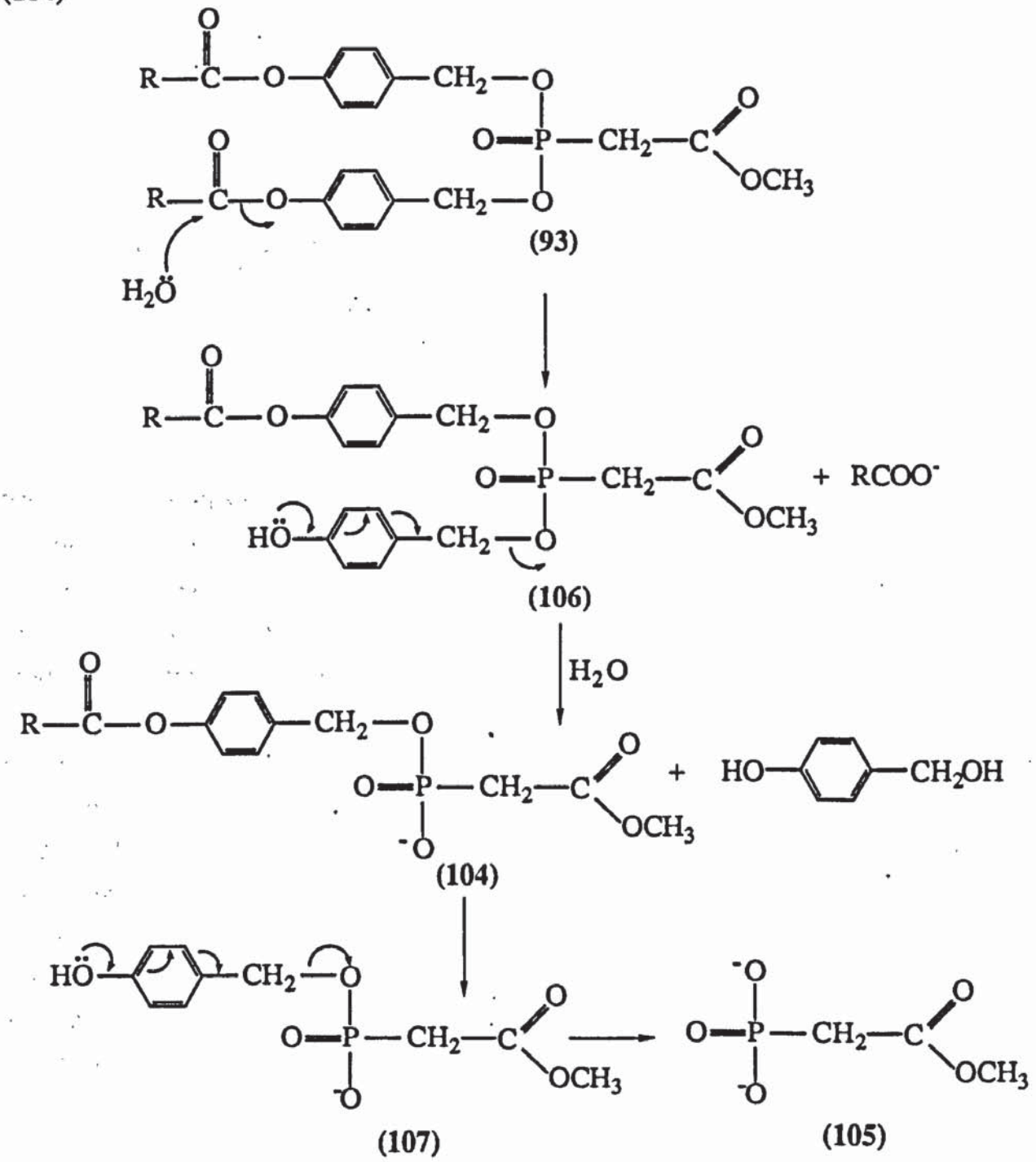

The presence of a doublet at 4.76 ppm (J_{PH} 8.9 Hz) integrating for 2 H, together with unassigned peaks at 7.32 (2 H, d, J_{HH} 8.5 Hz) and 6.85 ppm (2 H, d, J_{HH} 8.4 Hz) suggest that some of the 4-hydroxybenzyl carbonium ion is also trapped by inorganic phosphate to give 4-hydroxybenzyl phosphate **(108)** **(Fig 3.9)**. This will be considered in more detail in **section 3.8.**

Fig 3.9 - Fate of the 4-hydroxybenzyl carbonium ion

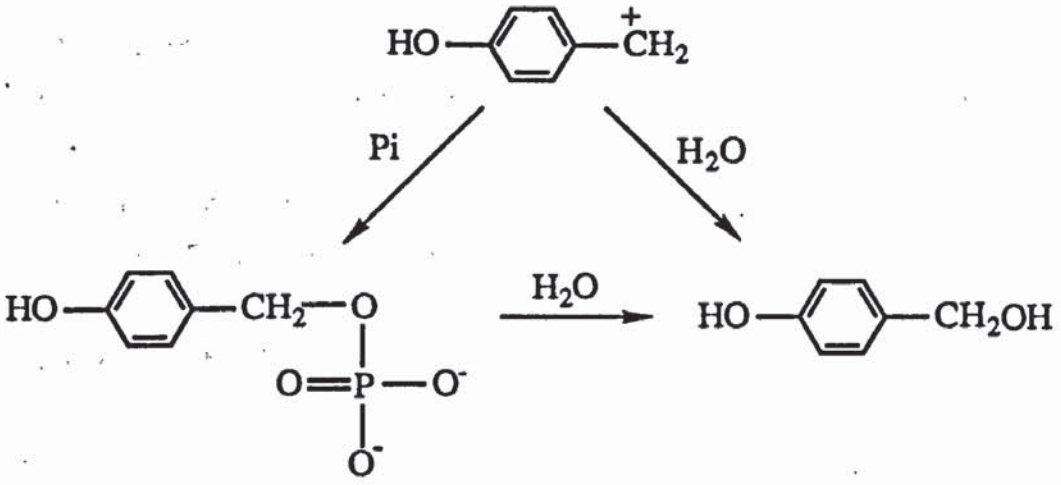

(108)

The rates of hydrolysis are an order of magnitude slower for the alkanoyloxybenzyl diesters **(104)** than the corresponding triesters **(93)**. This is presumably due to the negative charge on the diester reducing the molecules susceptibility to nucleophilic attack by water. This relatively small difference in the rates of hydrolysis provides additional evidence for reaction occuring at C=O rather than at phosphorus. The difference in the rates of hydrolysis of phosphorus triesters and diesters *via* nucleophilic attack at phosphorus is normally very high, for example the rate constants (k) for the hydrolyses of dimethyl phosphate and trimethyl phosphate have been measured as 0.3 s^{-1} (25°C) and 36.5 x 10^6 s^{-1} (100°C) respectively. From **Tables 3.3** and **3.4** the reactivity trend is the same throughout each series. That is, an increase in both the length of the alkyl chain and methyl substitution of the α-carbon results in a more stable molecule. This effect is clearly demonstrated by the diester **(104)** series **(Table 3.4)** in which the half-life of hydrolysis increased from 105 h **(104, R=CH_3)** to approximately 2000 h **(104, R=$(CH_3)_3$)**.

The relationship between steric size and reaction rates can be investigated further by correlating triester **(93)** and diester **(104)** hydrolysis half-lives with the Taft steric parameters (Es)[172, 173] calculated for the corresponding R groups. Taft derived the first generally successful numerical definition of steric effects in organic reactions, the steric constant, Es as

$$Es = \log(k_R/k_O)_A$$

where k_R and k_O refer to the rate constants for acid hydrolysis (denoted by A) of the substituted and standard esters, RCOOR', respectively. The size of both R and R' will affect attainment of the transition state of ester hydrolysis. This definition assumes that

the electronic effects of R can be neglected on attainment of the transition state, therefore when **R=CH_3**, Es=0. Consequently, bulkier R groups than CH_3 will have Es<0, retarding the hydrolysis reaction. Taft Es values cannot be measured for many substituents because of the nature of the model reaction upon which it is based. As a way around this problem Charton[174] and Kutler and Hansch[175] suggested that for spherically symmetrical groups one may use the radius as a measure of steric bulk. The good correlation between Es and radius confirm the reliability of Es. The Taft Es values[172, 173] for the alkyl groups employed in the 4-alkanoyloxybenzyl triester (93) and diester (104) series are given in **Table 3.5.**

Table 3.5 - Taft Es values for alkyl groups

R	Es
CH_3	0
CH_3CH_2	-0.07
$CH_3(CH_2)_2$	-0.36
$CH_3(CH_2)_3$	-0.39
$CH_3(CH_2)_4$	-0.40
$(CH_3)_2CH$	-0.47
$(CH_3)_3C$	-1.54

Figs 3.10 and **3.11** show the triester (93) and diester (104) hydrolysis half-lives ($t_{1/2}$) plotted against the Es values for the R groups.

Fig 3.10 - Plot of half-lives of hydrolysis of di(alkanoyloxybenzyl) triesters **(93)** **(Table 3.3)** against R group Es values **(Table 3.5)**

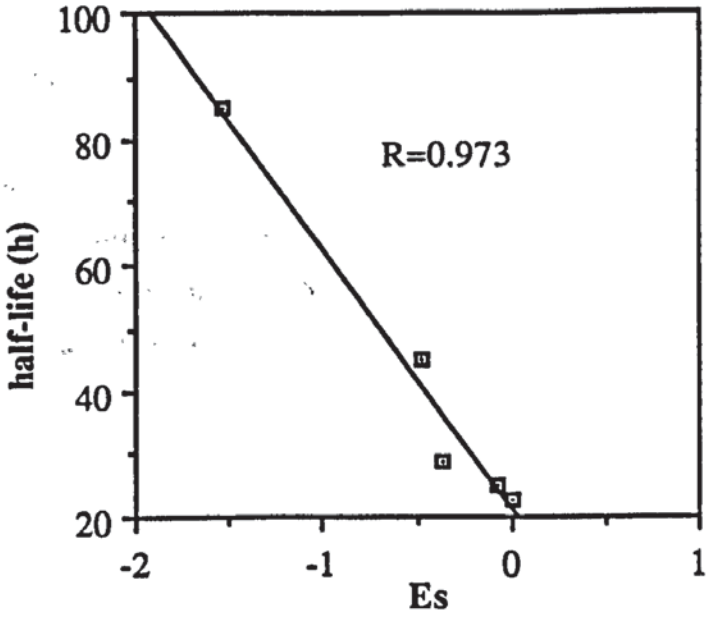

Fig 3.11 - Plot of half-lives of hydrolysis of alkanoyloxybenzyl diesters **(104)** **(Table 3.4)** against R group Es values **(Table 3.5)**

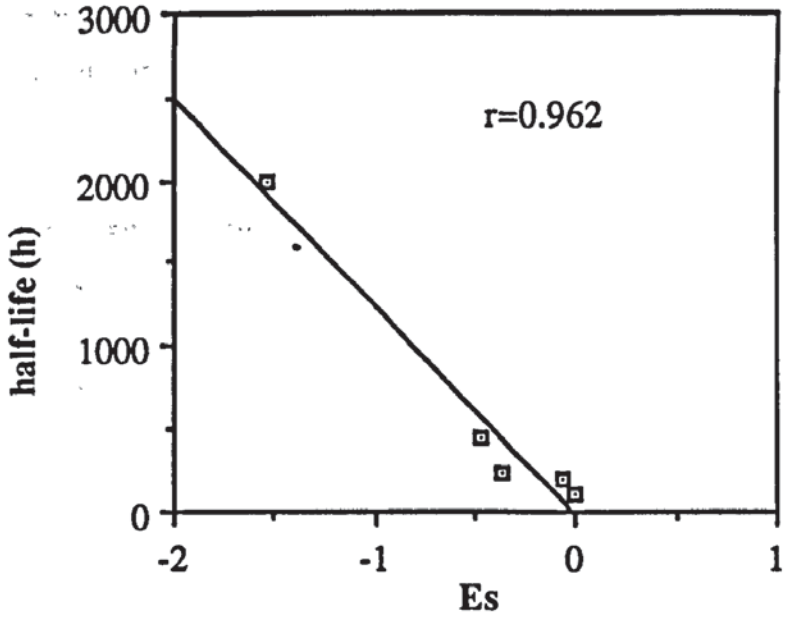

From **Figs 3.10** and **3.11** the experimental observations agree with Taft's theoretical hypothesis: The rate of hydrolyses of both the alkanoyloxybenzyl triesters **(93)** and diesters **(104)** decrease as the Taft Es values decrease. As expected increasing the size of the alkanoyloxy group decreases the rate of nucleophilic attack by water at the carboxyl function, thus slowing the rate of hydrolysis of the esters. This suggests that the rate-limiting step for the hydrolysis of the triesters **(93)** and diesters **(104)** is the formation of the 4-hydroxybenzyl intermediates **(106, 107)**. A similar steric effect was observed by Srivastva and Farquhar[112] for the hydrolysis of a series of di(alkanoyloxymethyl) phenyl phosphates **(108)**. Their study concluded that steric crowding adjacent to the carbonyl carbon was directly related to the stability of the phosphotriesters **(108)**; the larger the alkyl group, the slower the rate of hydrolysis.

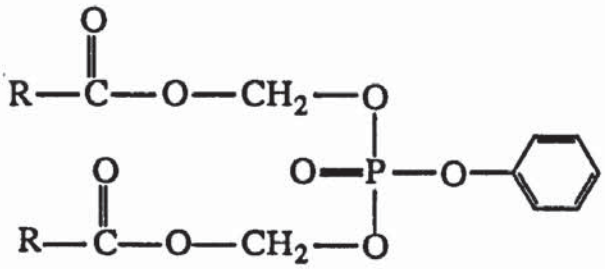

(108)

$R = CH_3, (CH_3)_2CH, (CH_3)_3C$

When compared with the triesters of PFA **(38)**, the triesters of PAA **(44, 93)** are considerably more stable towards chemical hydrolysis, therefore investigation into the enzymatic bioactivation of these compounds is possible.

3.7. Activation Studies of Di(benzoyloxymethyl) (Methoxycarbonylmethyl)-phosphonates (44)

In a study on the enzymatic activation of di(alkanoyloxymethyl) phenyl phosphates **(108)**, Srivastva and Farquhar[112] found that incubation of these compounds with hog liver esterase and mouse plasma resulted in hydrolysis at the alkanoyl group to give the hydroxymethyl intermediate **(109)**, which readily loses formaldehyde to give the diester **(110)**. By a similar pathway, diester **(110)** then degrades to phenyl phosphate **(111)** **(Fig 3.12)**.

Fig 3.12 - Enzymatic activation of di(alkanoyloxymethyl) phenyl phosphates **(108)**

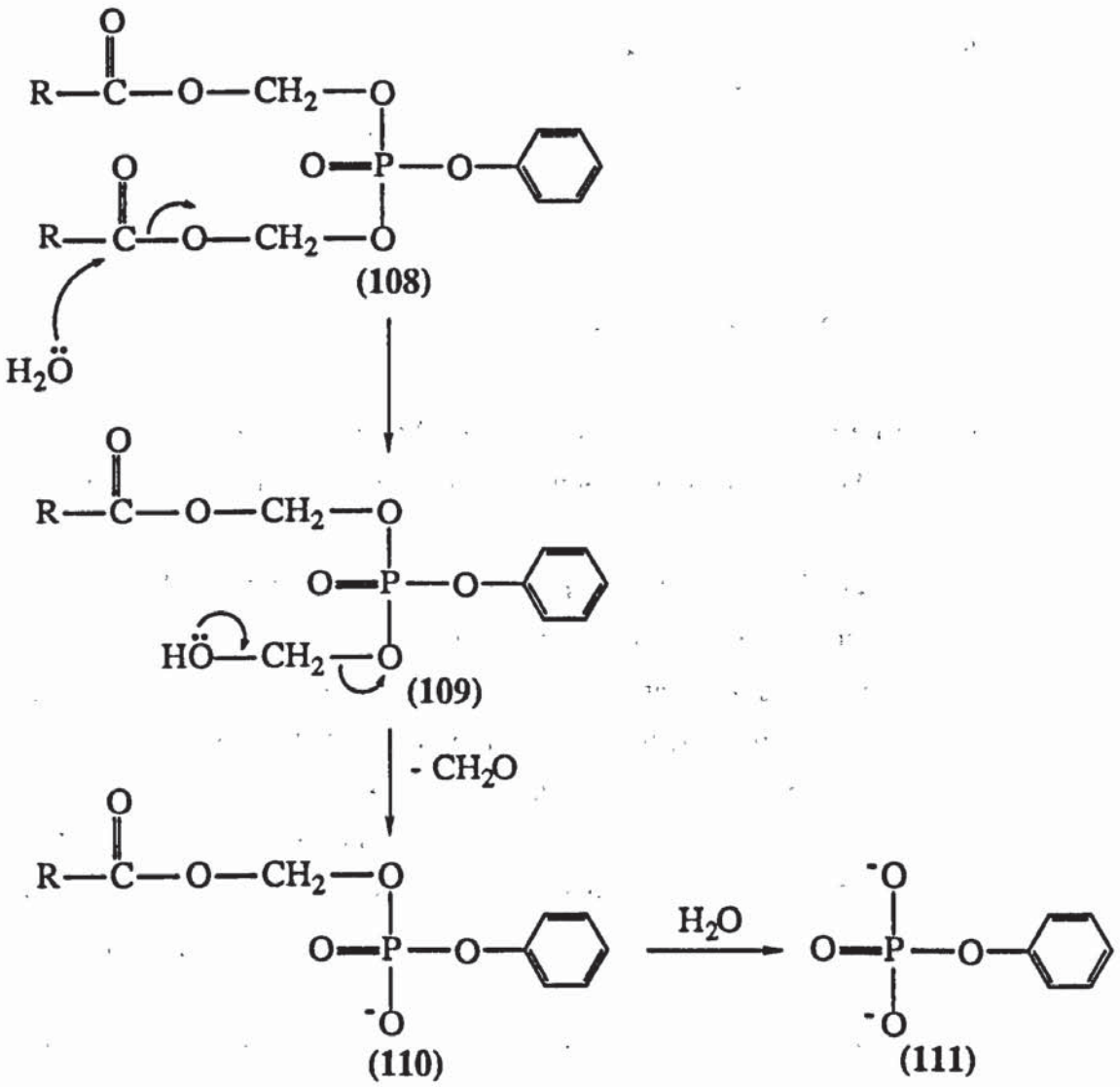

The main limitation with the use of the alkanoyloxymethyl group is the hydrolytic instability of these compounds in the absence of esterase. For example, the ethanoyloxymethyl analogue **(108, R=CH_3)** has a half-life of 193 min at pH 7.4, 37°C. In the light of this it is important to investigate the bioactivation of the considerably more stable benzoyloxymethyl triesters **(44)** and alkanoyloxybenzyl triesters **(93)** and diesters **(104)** with carboxylesterases and plasma.

3.7.1. Bioactivation of Triesters (44) with Carboxylesterase

Carboxylesterases catalyse the hydrolysis of a large number of uncharged carboxylic esters, usually restricted to short chain fatty acid esters. Carboxylesterases function *via* the nucleophilic attack of a serine residue at the active site of the enzyme on the carbonyl group of the substrate to form the enzyme-acetyl intermediate **(112)**. Hydrolysis of **(112)** gives the carboxylic acid and the free enzyme **(Fig 3.13)**:[176]

Fig 3.13 - Carboxylesterase-mediated hydrolysis of carboxylic esters

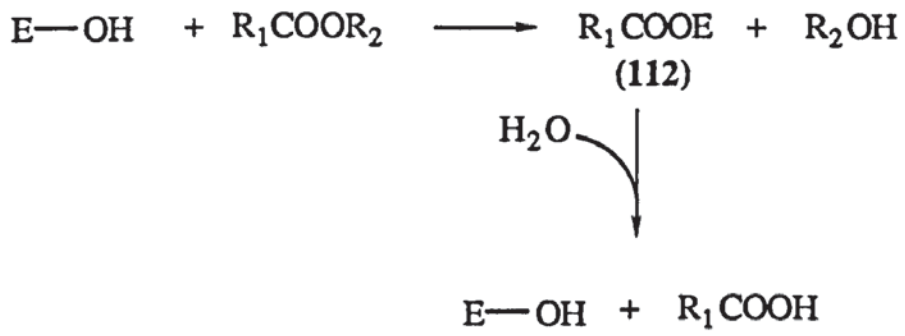

Esterases are widely distributed in tissues and blood serum of vertebrates.[177] In mammals the highest activities are found in the liver, kidney, duodenum and brain.[178]

The triesters (**44**, **Ar=C_6H_5**, **2-$CH_3C_6H_4$**, **2,4,6-$(CH_3)_3C_6H_2$**, 200 μg ml^{-1}) were incubated with porcine and rabbit liver carboxylesterases (37 units*) and the reactions analysed by ion-pair reversed-phase HPLC using the same conditions as described for the chemical hydrolyses of these compounds. Unfortunately, the low solubility of these triesters, together with the lack of standards (the corresponding diesters were not prepared) meant that accurate rate data were not obtained. However, analysis of the chromatograms produced by the different triesters (**Figs 3.14, 3.15**) indicates a change in product distribution on increasing the methyl substitution on the phenyl ring.

* One unit of porcine liver carboxylesterase will hydrolyse 1μmol of ethyl butyrate to butyric acid and ethanol per min at pH 8.0 at 25°C.

* One unit of rabbit liver carboxylesterase will hydrolyse 1 μmol of o-nitrophenyl butyrate to butyric acid and o-nitrophenol per min at pH 7.5 at 25°C.

Fig 3.14 – Chromatograms obtained from the incubation of di(benzoyloxymethyl) triesters of phosphonoacetate with porcine liver carboxylesterase

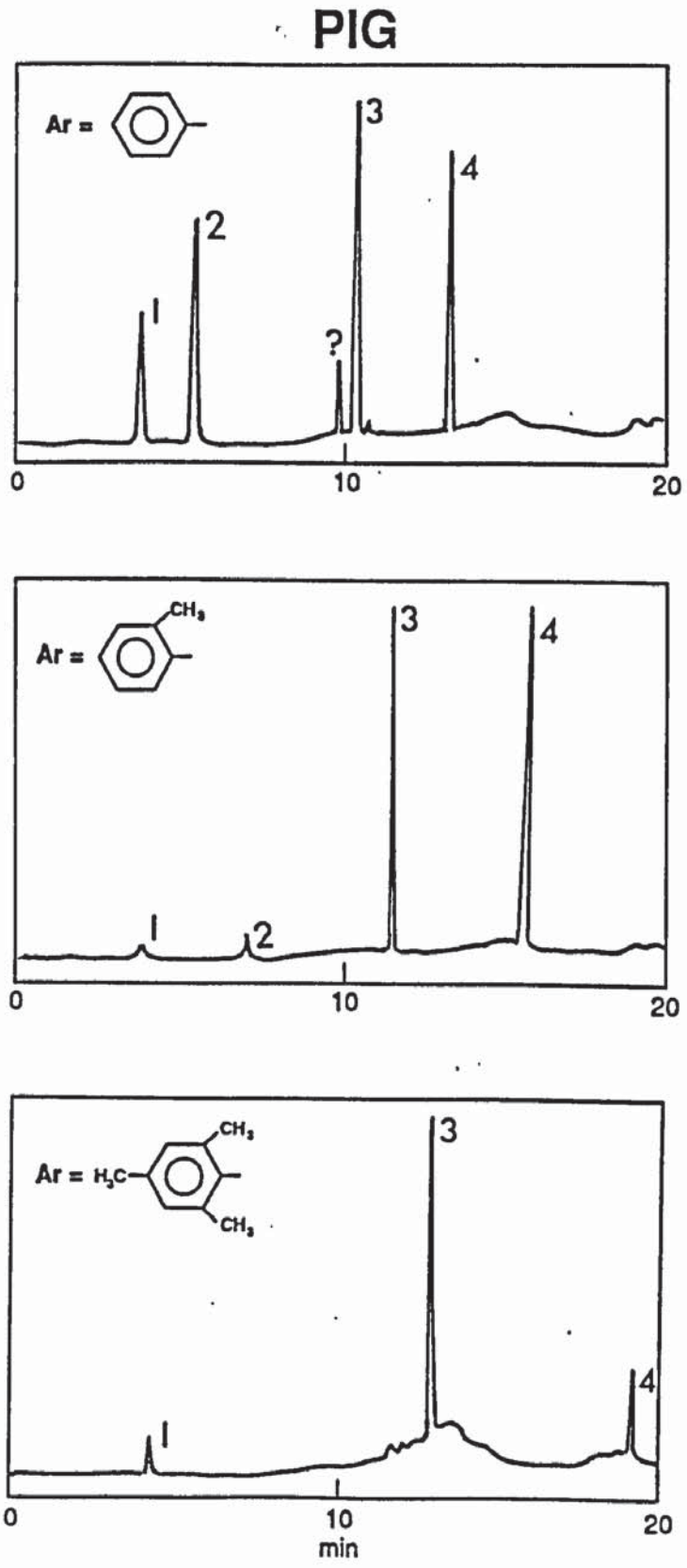

Fig 3.15 – Chromatograms obtained from the incubation of di(benzoyloxymethyl) triesters of phosphonoacetate with rabbit liver carboxylesterase

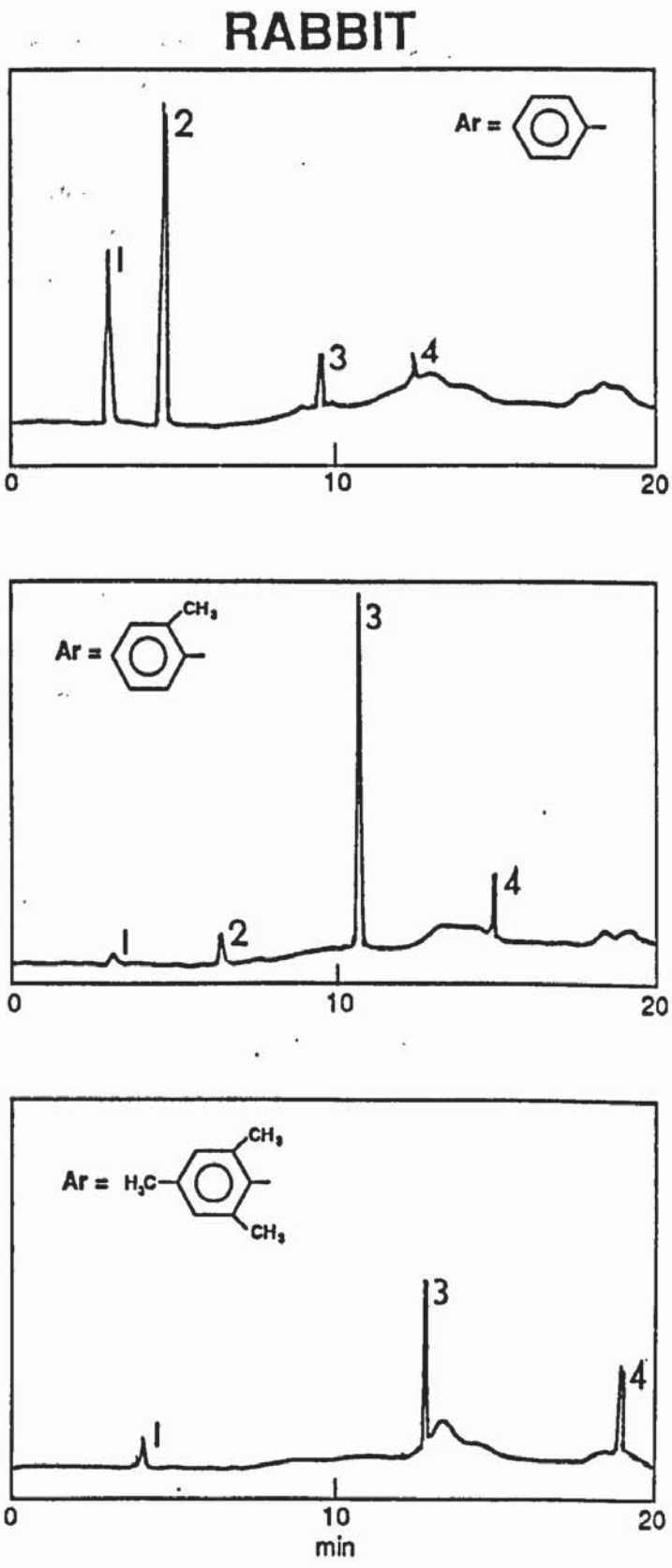

It is apparent from **Figs 3.14** and **3.15** that the parent triesters (peak 4) degraded to several products in the presence of carboxylesterase. The retention times (min) for the substrates and hydrolysis products for di(benzoyloxymethyl) triesters **(44)** are given in **Table 3.6.**

Table 3.6 - Retention times for substrates and enzymatic hydrolysis products for the di(benzoyloxymethyl) triesters **(44)**

Ar	Peak 1 (min)	Peak 2 (min)	Peak 3 (min)	Peak 4 (min)
C_6H_5	4	6	10	13
2-$CH_3C_6H_4$	4	7	11	15
2,4,6-$(CH_3)_3C_6H_2$	5	-	13	19

Peak 1 was assigned as the appropriate benzoic acid, $RCOO^-$, confirmed by comparison of the retention times on HPLC with authentic samples. Based on chromatographic properties peak 2 was assigned as the monoanionic benzoyloxymethyl diester **(101)** and peak 3 was thought to be the monoanionic di(benzoyloxymethyl) diester **(113).**

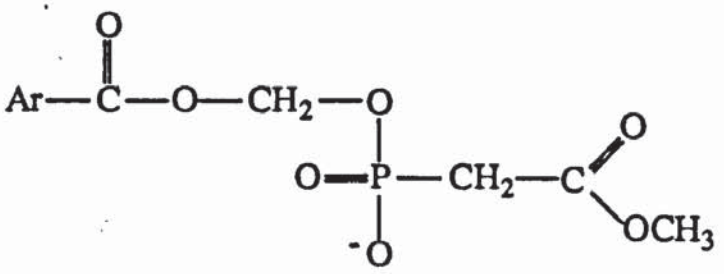

(101)

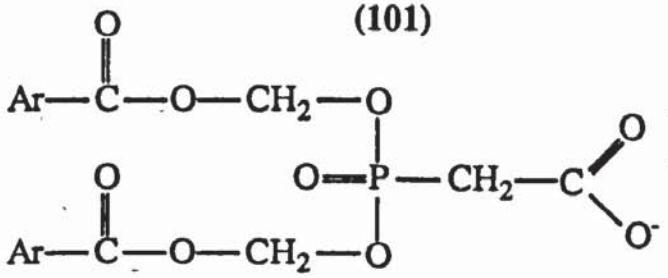

(113)

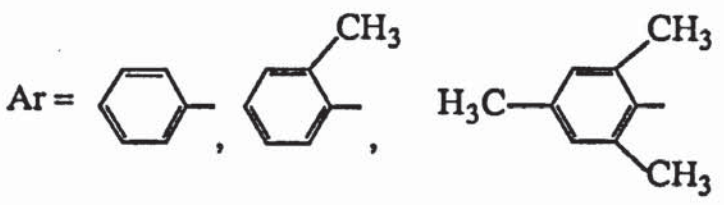

The assignment of structure **(113)** was supported by treatment of the enzyme incubation mixture of the di(2,4,6-trimethylbenzoyloxymethyl) triester **(44, Ar=2,4,6-$(CH_3)_3C_6H_2$)** with the methylating agent, diazomethane. A simultaneous reduction in the size of peak 3 together with a proportionate increase in the size of peak 4 strongly suggested methylation of the free carboxyl group of **(113)** had taken place to regenerate the parent triester **(Fig 3.16).**

Fig 3.16 - The methylation of di(2,4,6-trimethylbenzoyloxymethyl) diester **(113)** by diazomethane

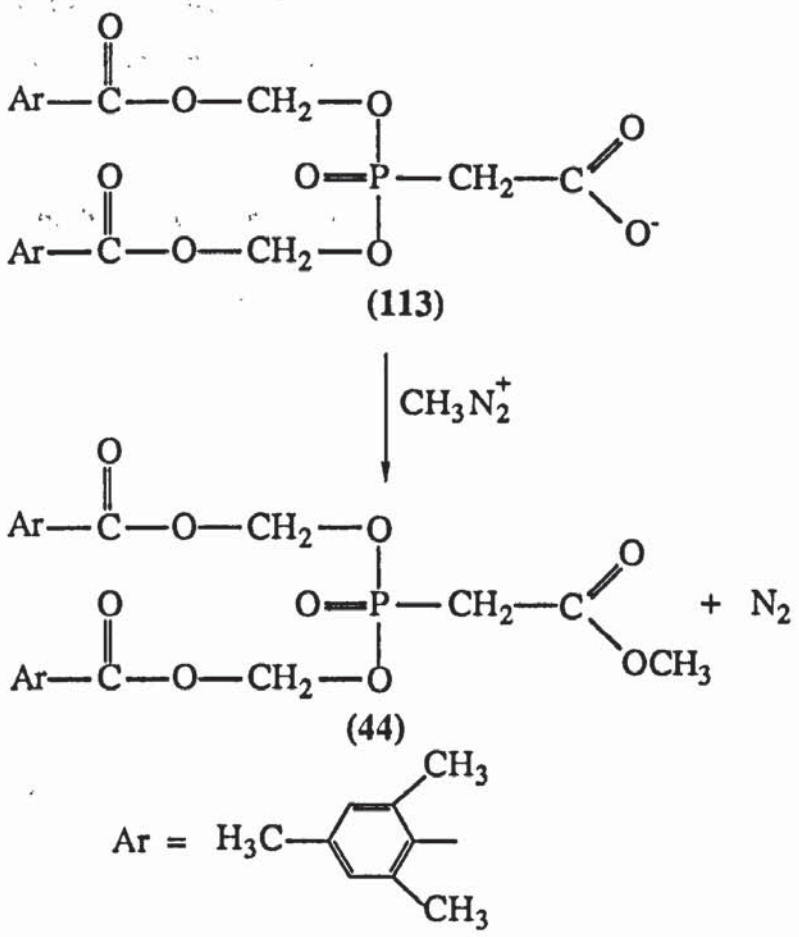

Figs 3.14 and **3.15** suggest that as methyl substitution on the phenyl ring is increased, carboxylesterase cleavage is directed away from the benzoyl ester towards the carboxymethyl ester. Therefore, the di(2,4,6-trimethylbenzoyloxymethyl) triester **(44, Ar=2,4,6-$(CH_3)_3C_6H_2$)** degraded almost exclusively to the corresponding di(2,4,6-trimethylbenzoyloxymethyl) diester **(113, Ar=2,4,6-$(CH_3)_3C_6H_2$)** on incubation with both porcine and rabbit liver carboxylesterase. This is presumably a result of the bulky nature of the trisubstituted phenyl ring restricting access to the active site of the enzyme and consequently favouring attack at the carboxymethyl function.

Incubation of the unsubstituted di(benzoyloxymethyl) triester (**44, Ar=C_6H_5**) with rabbit liver carboxylesterase resulted mainly in cleavage of the benzoyl ester, whereas incubation with porcine liver carboxylesterase resulted in cleavage of both the benzoyl and carboxymethyl esters. This suggests a different substrate specificity for esterases from pigs and rabbits and highlights the problems associated with the prediction of human response from animal data.

The detection of the benzoic acids in the esterase incubations is consistent with the formation of the benzoyloxymethyl diesters (**101**) *via* a cascade process. Enzymatic hydrolysis of the benzoyl ester is thought to yield the unstable hydroxymethyl intermediate (**45**), which spontaneously eliminates one molecule of formaldehyde to form the diester (**101**) (**Fig 3.17**)

Fig 3.17 - Enzymatic hydrolysis of di(benzoyloxymethyl) triesters of PAA (**44**)

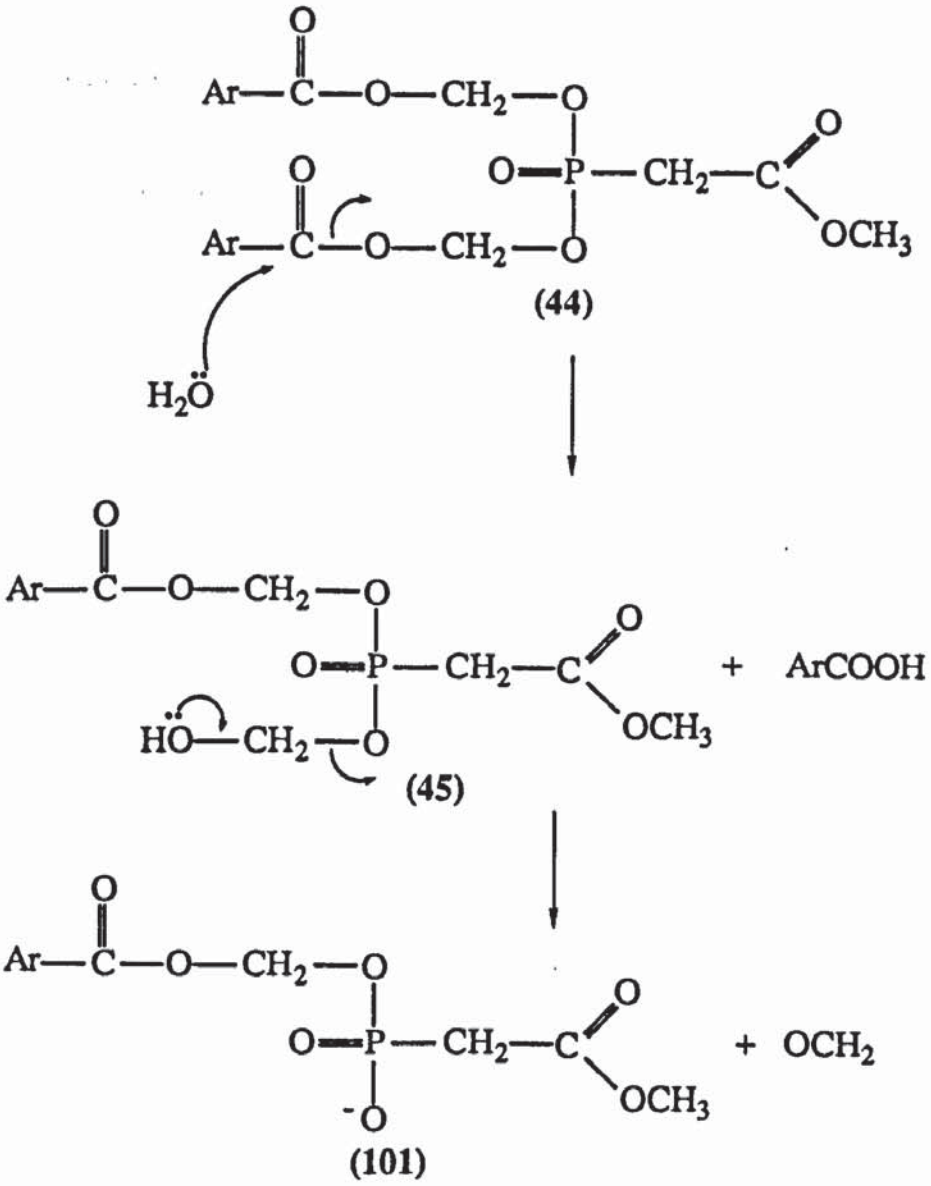

There was no evidence to suggest that any of the monoanionic benzoyloxymethyl diesters **(101)** degrade further to form either the monoester **(105)** or phosphonoacetate**(8)**. It is known that charged compounds are poor substrates for enzymes[179] and it is probably the close proximity of the anionic charge to the benzoyloxymethyl group on the diesters **(101)** that prevent them being substrates for the esterase. Indeed, Srivastva and Farquhar[112] also experienced difficulties in the removal of the second acyloxymethyl group during the enzymatic hydrolysis of di(alkanoyloxymethyl) phenyl phosphates **(108)**. In a separate study, Levy and Ocken[180] showed that the pig liver carboxylesterase hydrolysis of carboxylate diesters, such as diethyl malonate, was restricted to the loss of one ester group. They suggested that this was due to like-charge repulsion between the monoanionic ester and the esterase, predicting the presence of negatively charged groups at or near the active site of the enzyme.

3.7.2. Bioactivation of Triesters (44) with Plasma

Human plasma is derived from blood following removal of the red blood cells by centrifugation. It is a rich source of a wide variety of enzymes including lactate dehydrogenase, histaminase, amylase and esterases,[179, 181] therefore the probability of enzyme-induced modification of a molecule in plasma is quite high. Ideally a prodrug should be sufficiently stable in plasma to ensure that it reaches the site of action in high concentration.

The di(benzoyloxymethyl) triesters (44) were incubated with human plasma and the reactions analysed by ion-pair reversed-phase HPLC. As for the esterase studies, solubility problems coupled with the lack of standards meant that accurate rate data could not be obtained. However, it can be seen from **Fig 3.18** that the metabolic profiles in plasma show some similarities to those observed with carboxylesterase.

Fig 3.18 – Chromatograms obtained from the incubation of di(benzoyloxymethyl) triesters of phosphonoacetate with human plasma (t = 10 min)

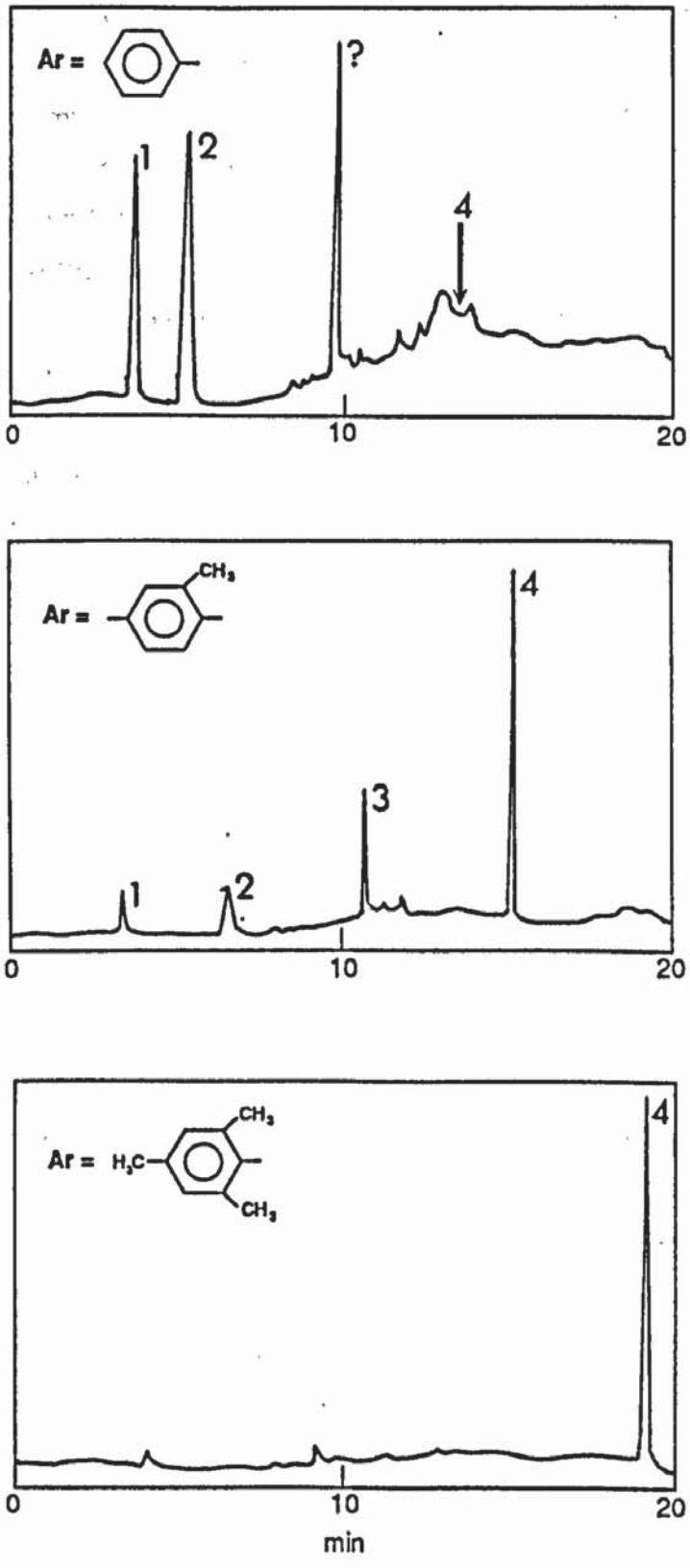

After 10 min, the unsubstituted di(benzoyloxymethyl) triester (**44**, **Ar=C_6H_5**) was almost completely metabolised to benzoic acid and benzoyloxymethyl (methoxycarbonylmethyl)phosphonate (**101**, **Ar=C_6H_5**). An unknown compound with a retention time of 9.7 min appeared in the same chromatogram. This could be the 4-hydroxymethyl intermediate (**45**), however later time points were not taken and as such this can not be confirmed. As methyl groups were introduced into the phenyl ring the triesters (**44**) exhibited a greater degree of stability in plasma. This was most clearly demonstrated by the di(2,4,6-trimethylbenzoyloxymethyl) triester (**44**, **Ar=2,4,6-$(CH_3)_3C_6H_2$**) which showed little reaction after 10 min incubation with human plasma. This effect must be due to the steric bulk of this triester, which presumably cannot gain access to the active site of the enzyme and therefore cannot form the 2,4,6-trimethylbenzoyloxy-enzyme complex. A similar steric effect was observed by Srivastva and Farquhar[112] when di(alkanoyloxymethyl) phenyl phosphates (**108**) were incubated with mouse plasma. Contrary to the results with pig and rabbit liver carboxylesterase, the methoxycarbonyl function of the bis(2,4,6-trimethylbenzoyloxymethyl) triester (**44**, **Ar=2,4,6-$(CH_3)_3C_6H_2$**) remained intact. This indicates that the carboxylesterases found in human plasma are distinct from those isolated from the livers of pigs and rabbits, and as such the triester (**44**, **Ar=2,4,6-$(CH_3)_3C_6H_2$**) is a poor substrate for human plasma carboxylesterase.

3.7.3. Summary

Triester (**44**) incubations with carboxylesterases and plasma revealed that the cascade effect can operate in biological systems. However, bioactivation was restricted to the removal of only one protecting group from phosphorus to form the benzoyloxymethyl diesters (**101**). The methoxycarbonyl group may also be removed if esterase attack can be directed away from the benzoyloxymethyl function via steric crowding. The enzymatic removal of the second protecting group from phosphorus was presumably prevented by the close proximity of the benzoyloxy ester function to the anionic charge on the diester. This suggested that removal of the second group may be possible by increasing the distance of the esterase sensitive moiety from the anion, therefore attention was turned to the di(4-alkanoyloxybenzyl) (methoxycarbonylmethyl)phosphonates (**93**).

3.8. Activation Studies of Di(4-Alkanoyloxybenzyl) (Methoxycarbonylmethyl)-phosphonates (93) and Lithium 4-Alkanoyloxybenzyl (Methoxycarbonylmethyl)-phosphonates (104)

In the preceeding section (section 3.7) bioactivation of the di(benzoyloxymethyl) triesters (44) was restricted to the removal of only one protecting group from phosphorus to give the benzoyloxymethyl diester (101). To promote the removal of the second phosphorus ester, it seems likely that the distance between the negative charge and the site of esterase attack in the diester (101) needs to be increased. Consequently, the activation of the 4-alkanoyloxybenzyl triesters (93) and diesters (104) were investigated. In this case the charge on the diester (104) is now nine bonds removed from the site of esterase attack, an increase of ~2.7Å, or the length of an aromatic ring, over the benzoyloxymethyl analogue (101).

3.8.1. Bioactivation of Triesters (93) with Carboxylesterase

The triesters (93, R=CH_3, CH_3CH_2, $CH_3(CH_2)_2$, $(CH_3)_2CH$, $CH_3(CH_2)_3$, $(CH_3)_3C$, $CH_3(CH_2)_4$, 1mM) were incubated with porcine liver carboxylesterase [0.5 units (R=CH_3), 0.05 units (all other triesters)] in a 0.1 M phosphate-buffered water - acetonitrile mixture (9:1, v/v, total volume 1 ml). The reactions were monitored by ion-pair reversed-phase HPLC, eluting with a gradient of acetonitrile-10 mM tetrabutylammonium hydroxide in water. As for the benzoyloxymethyl triesters (44), solubility problems were encountered with the triesters (93) and, since the reaction rates were determined from the disappearance of the triesters, the results must be treated with some caution. Table 3.7 gives the mobile phase compositions, retention times and calculated half-lives ($t_{1/2}$) for the alkanoyloxybenzyl triesters (93). From Table 3.7 the rate of enzymatic hydrolysis reaches an optimum when the R group contains 3 carbon atoms. The reasons for this will be examined later.

The products from the esterase hydrolysis of the triesters (93) eluted with the solvent front. In an attempt to determine the degradation mechanism, di(4-ethanoyloxybenzyl) (methoxycarbonylmethyl)phosphonate (93, R=CH_3), the most water soluble triester, was incubated with pig liver carboxylesterase (5 units) and the reaction studied by ^1H and ^{31}P NMR spectroscopy. The triester was observed to degrade to the 4-ethanoyloxybenzyl diester [(104, R=CH_3), δ_H 2.26 (s, CH_3), 3.58 (s, OCH_3), 4.86 (d, J_{PH} 7.3 Hz, CH_2OP), 7.08 (d, J_{HH} 8.4 Hz, Ar) and 7.40 ppm (d, J_{HH} 8.4 Hz, Ar); δ_P 15.34 ppm (s)] and 4-hydroxybenzyl alcohol [δ_H 4.45 (s, CH_2), 6.81 (d, J_{HH} 8.6 Hz, Ar) and 7.19 ppm (d, J_{HH} 8.4 Hz, Ar)]. 4-Ethanoyloxybenzyl alcohol was not detected, therefore, in

common with the proposed mechanism of chemical hydrolysis (Fig 3.8), this suggests that the triesters (93) react with esterase to give the 4-hydroxybenzyl intermediate (106), which spontaneously degrades to generate 4-hydroxybenzyl alcohol and the appropriate alkanoyloxybenzyl diester (103). The monoester (105) would probably have been observed if the reactions had been monitored for a sufficient length of time.

Table 3.7 - Mobile phase compositions, retention times (Rt) and half-lives ($t_{1/2}$) for alkanoyloxybenzyl triesters (93) incubated with pig liver carboxylesterase

R	% MeCN	% H_2O	Rt (min)	$t_{1/2}$ (min)[a]
CH_3	70	30	3.63	223[b]
CH_3CH_2	70	30	5.32	10.5
$CH_3(CH_2)_2$	70	30	8.78	5.9
$CH_3(CH_2)_3$	85	15	6.72	61.8
$CH_3(CH_2)_4$	90	10	7.15	72.8
$(CH_3)_2CH$	80	20	5.50	6.3
$(CH_3)_3C$	85	15	6.51	61.4

a) mean, n=2

b) extrapolated to account for 10 fold increase in esterase concentration compared to data for other triesters.

3.8.2 Bioactivation of Diesters (104) with Carboxylesterase

The diesters (104, R=CH_3, CH_3CH_2, $CH_3(CH_2)_2$, $(CH_3)_2CH$, $CH_3(CH_2)_3$, $(CH_3)_3C$, 5 mM) were incubated with porcine liver carboxylesterase (10 units) in a phosphate-buffered 0.1 M D_2O - acetonitrile mixture (9:1, v/v, total volume 1 ml) and the reactions were monitored by ^1H and ^{31}P NMR spectroscopy. No solubility problems were encountered with the diesters (104), therefore it was possible to obtain reliable rate data. The diesters were found to degrade in the presence of carboxylesterase to give 4-hydroxybenzyl alcohol [δ_H 4.45 (s, CH_2), 6.80 (d, J_{HH} ~8 Hz, Ar) and 7.20 ppm (d, J_{HH} ~8 Hz, Ar)] and the monoester [(105), δ_H 2.59 (d, J_{PH} 19.6 Hz, PCH_2) and 3.58 ppm (s, OCH_3); δ_P 11.70 ppm (s), (t, J_{PH} 18.5 Hz, ^1H coupled)] . In contrast to the chemical hydrolysis reactions, small quantities of the 4-hydroxybenzyl intermediate [(107), δ_H

2.75 (d, J_{PH} 20.5 Hz, PCH_2), 3.58 (s, OCH_3), 4.75 (d, J_{PH} 7.1 Hz, CH_2OP), 6.78 (d, J_{HH} ~8 Hz, Ar) and 7.23 ppm (d, J_{HH} ~8 Hz, Ar); δ_P 15.07 ppm (s)] were detected. This confirms the formation of the monoester (**105**) *via* the proposed cascade effect (**Fig 3.19**). Addition of phosphonoacetic acid [δ_H 2.52 ppm (d, J_{PH} 20.1 Hz, PCH_2); δ_P 17.41 ppm (s)] to the t=infinity sample of the diester (**104**, **R=$(CH_3)_3C$**) incubations confirmed that the reactions stop at the monoester (**105**).

Fig 3.19 - Carboxylesterase hydrolysis of alkanoyloxybenzyl diesters (**104**)

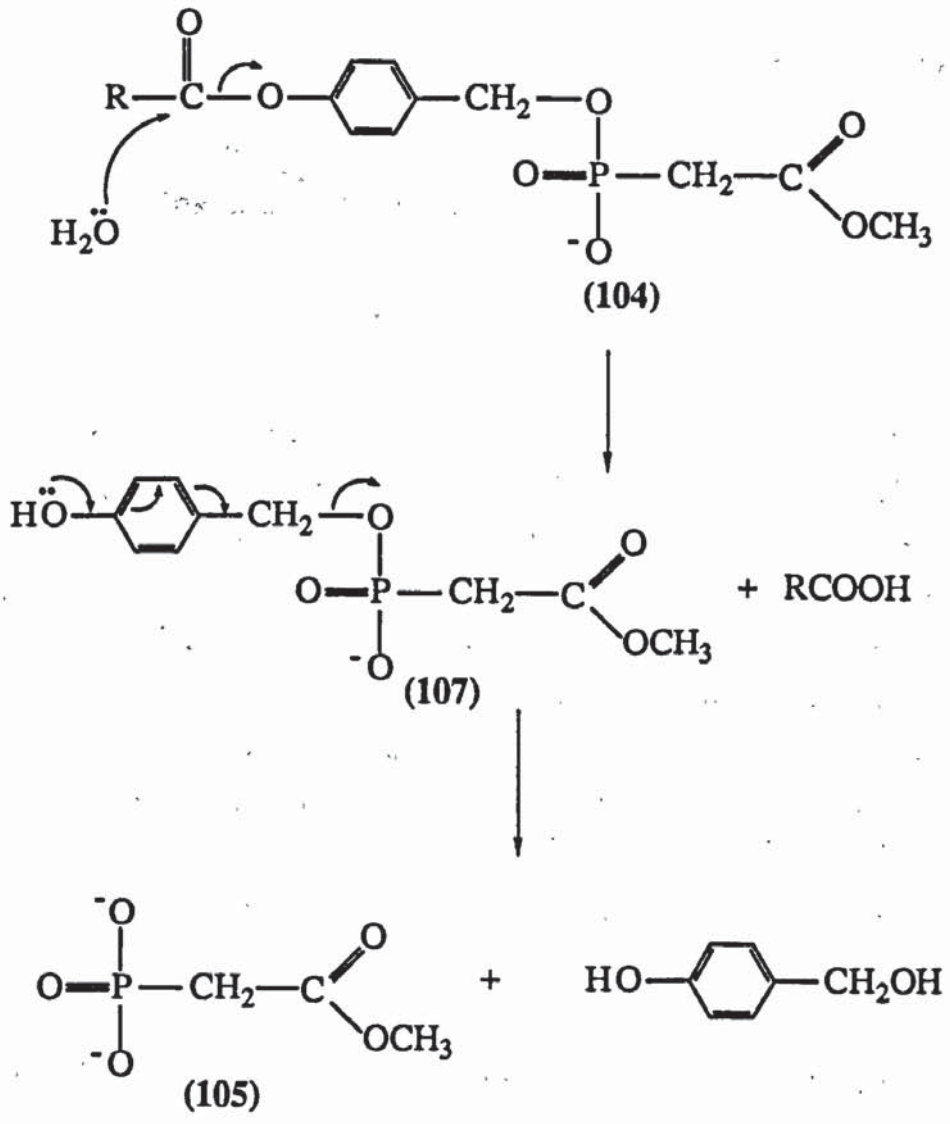

Fig 3.20 shows the reaction profile for the enzymatic hydrolysis of lithium (4-pivaloyloxybenzyl) (methoxycarbonylmethyl)phosphonate (**104**, **R=$(CH_3)_3$**) followed by ^{31}P NMR spectroscopy. This profile shows the disappearance of diester (**104**), the formation and subsequent degradation of the hydroxybenzyl diester (**107**) and the appearance of the monoester (**105**).

Fig 3.20 - Reaction profile for the carboxylesterase hydrolysis of lithium 4-pivaloyloxybenzyl (methoxycarbonylmethyl)phosphonate (**104**, R=$(CH_3)_3C$)

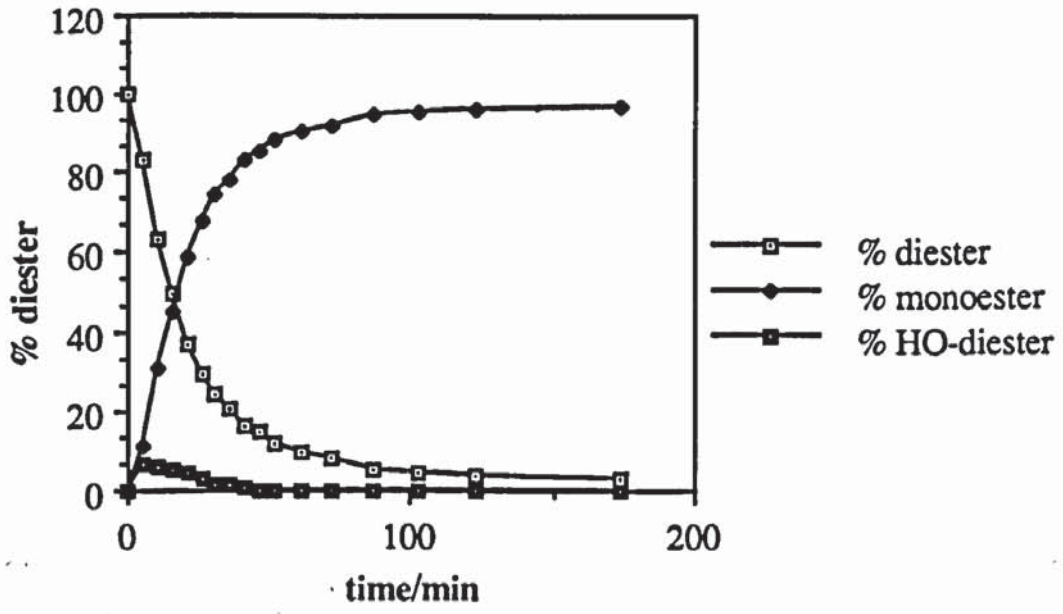

At early time points, 4-hydroxybenzyl alcohol accounted for less than half of the total number of carbonium ions presumably generated from the diesters (**104**).This may result from interaction of the highly reactive 4-hydroxybenzyl carbonium ion with a nucleophile other than water, such as products of hydrolysis, a serine on the enzyme or the buffer. In the solvolysis of diphenyl benzyl phosphate in phenol, Kenner and Mather[182] observed an electrophilic aromatic substitution reaction which trapped the generated benzyl carbonium ion as 2- and 4-benzyl phenol. An analogous reaction of the 4-hydroxybenzyl carbonium ion with 4-hydroxybenzyl alcohol in the enzymatic hydrolysis of the triesters (**93**) and diesters (**104**) would give 3'-(4-hydroxybenzyl)-4'-hydroxybenzyl alcohol, however this was not formed as the ^1H NMR spectra of the diester hydrolyses suggested only 1,4-disubstituted products. The reaction profile for the carboxylesterase hydrolysis of di(4-ethanoyloxybenzyl) methyl phosphonate (**114**)[183] was similar to that observed for the monoester, ethanoyloxybenzyl methylphosphonate (**115**). The two equivalents of the 4-hydroxybenzyl carbonium ion generated from the diester (**114**) did not lower catalytic efficiency when compared to the monoester (**115**), suggesting that there was no interaction between the active site of the enzyme and the carbonium ion.

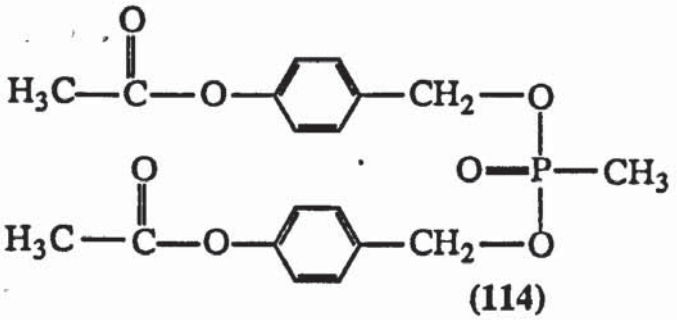

(114)

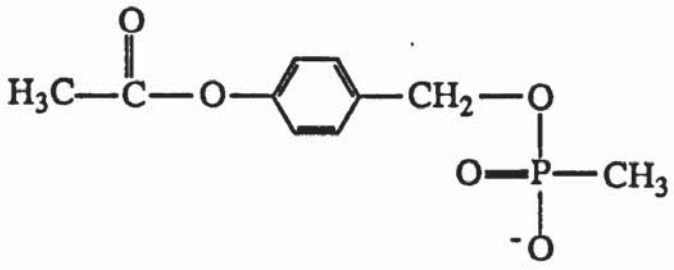

(115)

In an attempt to investigate the role of the phosphate buffer in the enzyme hydrolysis reactions, the carboxylesterase hydrolysis of the diester (**114**) was repeated, this time using a ten-fold dilution (0.01 M) of the original phosphate buffer. In contrast to the small amount of 4-hydroxybenzyl alcohol formed with 0.1 M buffer, here more than 90% of the carbonium ion was trapped as 4-hydroxybenzyl alcohol throughout the course of the reaction. This result suggests that in the carboxylesterase hydrolysis of the alkanoyloxybenzyl triesters (**93**) and diesters (**104**) the inorganic phosphate buffer competes with water to trap the 4-hydroxybenzyl carbonium ion. Indeed, unassigned peaks in the NMR spectra of the diester (**104**) reactions at δ_P 3.88 ppm and δ_H 4.64 (2 H, d, J_{PH} 6.0 Hz), 6.76 (2 H, d, J_{HH} ~8 Hz) and 7.20 ppm (2 H, d, J_{HH} ~8 Hz) are consistent with the formation of 4-hydroxybenzyl phosphate (**108**). The monoanion of benzyl phosphate is reported to hydrolyse *via* P-O cleavage with a half-life of 86 h at 75.6°C and pH 7.[184, 185] In the reaction mixture, the hydrolysis of 4-hydroxybenzyl phosphate to 4-hydroxybenzyl alcohol was found to have a half-life of ~1 h at 37°C, pH 7.4. The higher reactivity of this compound suggests a change in mechanism with the electron-donating hydroxy group promoting hydrolysis via C-O bond cleavage.

From the integration of the peaks in the ^{31}P NMR and ^{1}H NMR spectra for the 4-alkanoyloxybenzyl diester (**104**), 4-hydroxybenzyl diester (**107**) and monoester (**105**) the half-lives ($t_{1/2}$) for the hydrolysis of different alkanoyloxybenzyl diesters (**104**) by pig liver carboxylesterase were calculated and are given in **Table 3.8.**

Table 3.8 - Half-lives for the carboxylesterase hydrolysis of 4-alkanoyloxybenzyl diesters (104)

R	$t_{1/2}$ (min) ^{1}H NMR	$t_{1/2}$ (min) ^{31}P NMR	$t_{1/2}$ (min) mean
CH_3	71.4	86.1[a]	78.8
CH_3CH_2	9.1	9.6	9.4
$CH_3(CH_2)_2$	3.4	4.4	3.9
$CH_3(CH_2)_3$	6.2	6.5	6.3
$(CH_3)_2CH$	3.9	3.9	3.9
$(CH_3)_3C$	16.3	16.9	16.6

a) mean, n=3.

These data parallel the trend observed for the enzyme incubations of the di(4-alkanoyloxybenzyl) triesters (93) (**Table 3.7**), in which the rate of reaction rapidly increases as the length of the alkyl chain increases. The optimum number of carbon atoms in the alkyl group was three (R=$CH_3(CH_2)_2$, $(CH_3)_2CH$), and anymore than this caused the reaction rate to decrease. In an attempt to account for the observed trend, three parameters, steric, electronic and hydrophobic, will be considered for each alkyl group with respect to the alkanoyloxybenzyl diesters (104). Considering the steric influence, **Fig 3.21** shows a plot of the half-lives for the enzyme hydrolysis of the alkanoyloxybenzyl diesters (104) (**Table 3.8**) against their alkyl substituent taft steric parameters, Es (**Table 3.5**). Under conditions of chemical hydrolysis these compounds display a linear relationship between steric size and reaction rate. That is, the rate of hydrolysis decreases as the taft steric parameter decreases (ie. steric size increases) (**Fig 3.11**). However, in the carboxylesterase incubations the rate of hydrolysis of the diesters (104) increases as the value of Es decreases to -0.4, corresponding to a 3 carbon alkyl group. A reduction in Es below this optimum value causes the reaction rate to fall.

Fig 3.21 - Plot of the half-lives for the enzyme hydrolysis of alkanoyloxybenzyl diesters **(104) (Table 3.8)** against their alkyl substituent Es values **(Table 3.5)**

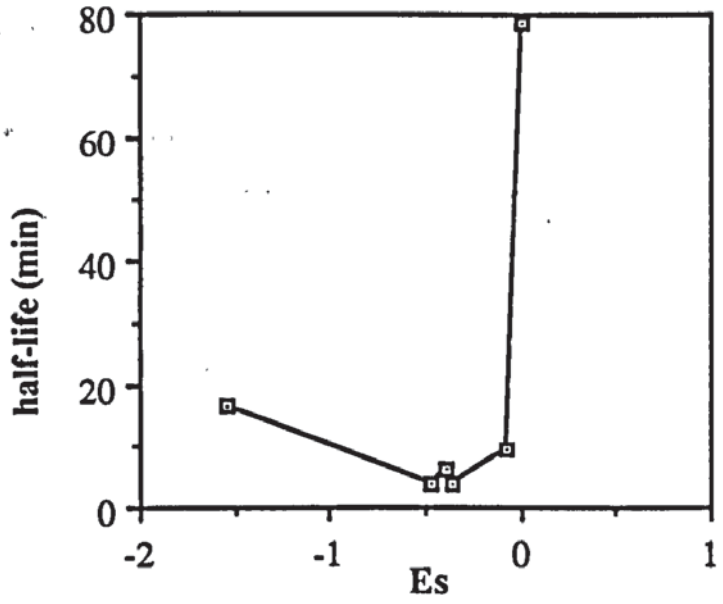

The electronic properties (σ) of a substituent can be derived from the Hammett equation[155, 186] **(Eqn. 2.9)** as previously described in **section 2.5.2.** The electronic nature of the alkyl group in the 4-alkanoyloxy substituent will have minimal effect on the σ_p value, therefore it is likely that the observed trend in enzyme hydrolysis rates is largely independent of intermolecular electronic variations.

The final parameter to be considered is the substituent partition, or hydrophobic, parameter (π).[187] Meyer[188] showed that the narcotic activity of many simple organic compounds paralleled their oil/water partition coefficients (P) and initiated the use of such measurements as a means of defining relative lipophilicity (hydrophobicity) of biologically active organic compounds. P is defined as the equilibrium concentration of the monomeric species of a compound in the non-aqueous phase (usually octanol), $[D]_n$, divided by that of the neutral form in the aqueous phase, $[D]_a$

$$P = [D]_n/[D]_a$$

Log P gives a measure of the hydrophobicity of the whole molecule, however knowing the relative lipophilicity of the various substituents (π_x) is sufficient for correlation analysis. π_X has been defined as

$$\pi_X = \log P_X - \log P_H$$

where P_X is the partition coefficient of a derivative and P_H that of the parent compound. A positive value for π_X means that, relative to the parent compound, the substituent X favours the octanol phase (lipophilic), whereas a negative π_X value favours the water phase (hydrophilic) relative to the parent compound. **Table 3.9** gives π_X values for different alkyl substituents (R).[187]

Table 3.9 - π_X values for alkyl groups

R	π_X
CH_3	0.56
CH_3CH_2	1.02
$CH_3(CH_2)_2$	1.55
$CH_3(CH_2)_3$	2.13
$(CH_3)_2CH$	1.53
$(CH_3)_3C$	1.98

Fig 3.22 - Plot of the half-lives for the enzyme hydrolysis of 4-alkanoyloxybenzyl diesters **(104)** (**Table 3.8**) against their alkyl substituent π values (**Table 3.9**)

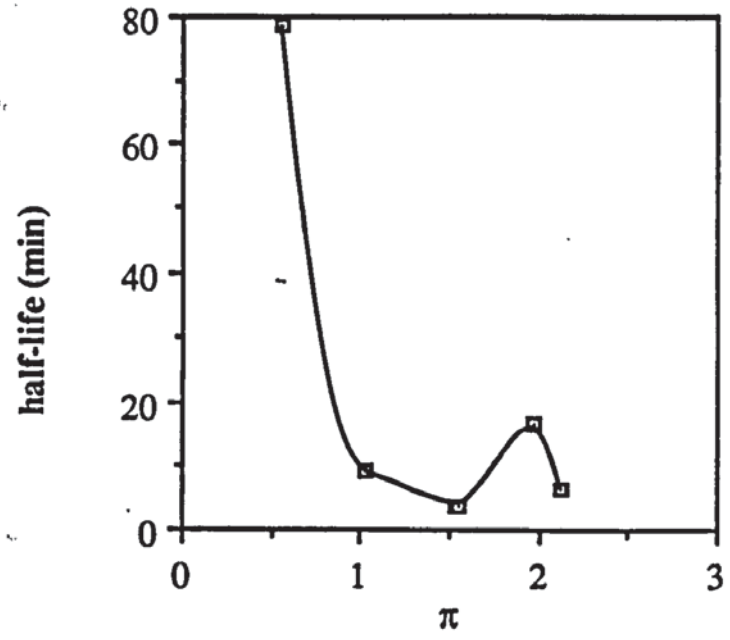

Fig 3.22 suggests that as the lipophilicity of the molecule is increased to an optimal π_x value of 1.5, corresponding to a 3 carbon alkyl group, the rate of enzymatic hydrolysis increases very rapidly. However, beyond this optimum value increasing the lipophilicity of the molecule decreases the rate of reaction.

From the above analysis it would appear that the main contributory factors determining the rate of carboxylesterase hydrolysis of alkanoyloxybenzyl triesters **(93)** and diesters **(104)** are the length and shape of the alkyl group attached to the ester link. The molecules are very similar in terms of electronic properties and as such this does not appear to influence the reaction rate. The observed trend probably arises from variations in the ease of binding of the alkyl chain of the acyl residue into the hydrophobic region at the active site of the enzyme. For pig liver carboxylesterase the acyl affinity site appears to optimally accommodate a three carbon alkyl group, hence the degree of enzyme-substrate binding, and therefore the rate of hydrolysis, is maximised for the n-butanoyl and iso-butanoyloxybenzyl triesters **(93, R=$CH_3(CH_2)_2$, $(CH_3)_2CH$)** and diesters **(104, R=$CH_3(CH_2)_2$, $(CH_3)_2CH$)**. Any deviation from this optimum size will reduce the binding of the substrate to the active site of the enzyme and hence reduce the reaction rate. The slower rate of hydrolysis observed for the pivaloyloxybenzyl esters **(93 and 104, R=$(CH_3)_3C$)** compared to the corresponding straight chain analogues **(93 and 104, R=$CH_3(CH_2)_3$)** presumably results from the bulky nature of the pivaloyl group reducing binding of the substrate to the enzyme active site. However, pig liver carboxylesterase is thought to contain more than one active site,[179, 180] therefore the rate of hydrolysis could increase again if the alkyl chain was of sufficient size such that the secondary acyl affinity site is also occupied.

Webb[176] observed a similar trend in the enzymatic hydrolysis of a wide range of aliphatic and aromatic esters, R_1COOR_2, incubated with horse liver carboxylesterase. The effects of change in the acyl (R_1) and alkyl (R_2) parts of the substrate molecule were largely independent. Considering the acyl group (R_1) first, the reactivity of the esters was found to increase up to a chain length of 4 to 5 carbon atoms; addition of a further 2 carbon atoms had little effect, but a further increase in chain length, up to 10 carbon atoms, caused a fall in reactivity. In the case of the alkyl group (R_2) there was a similar increase in reactivity to a maximium of 4 to 6 carbon atoms and any further increase in chain length produced a fall in the rate of reaction. Branching in the chains resulted in reduced reactivity with esterases.

Similar effects of chain length have been shown by other workers. Hofstee[189] found that the reactivity of straight chain fatty acid esters of 3-hydroxybenzoate increased with the

length of the alkyl chain up to 12 carbon atoms. With a purified carboxylesterase from goat intestinal mucosa, Malhotra and Philip[190] found an optimum of 4 carbon atoms in the alkyl group for the hydrolysis of 4-nitrophenyl alkanoates. Esters with a chain length of 12 or more carbon atoms were not hydrolysed. The extent of the hydrophobic region at the active centre of the enzyme has also been suggested to account for these observations.

3.8.3. Stability of Triesters (93) and Diesters (104) in Plasma

The alkanoyloxybenzyl triesters (93, R=CH_3, $CH_3(CH_2)_2$, $(CH_3)_3C$) and diesters (104, R=CH_3, $CH_3(CH_2)_2$, $(CH_3)_3C$) were incubated with human plasma under physiological conditions (pH 7.4, 37°C) and the reactions monitored by HPLC and ^{31}P NMR spectroscopy respectively. Solubility problems were again encountered with the triesters, however degradation to the diesters (104) was observed and approximate half-lives were calculated from the disappearance of the triester peak (Table 3.10). The alkanoyloxybenzyl diesters (104) were also observed to degrade in plasma to give (methoxycarbonylmethyl)phosphonate (105), the reaction proceeding through the 4-hydroxybenzyl intermediate (107) (Fig 3.19). Half-lives for this degradation were derived from the integrals of the diester (104) and monoester (105) peaks (Table 3.10).

Table 3.10 - Half-lives for alkanoyloxybenzyl triesters and diesters in human plasma

R	Triester $t_{1/2}$[a] (min)	Diester $t_{1/2}$[b] (h)
CH_3	5.9	9.2
$CH_3(CH_2)_2$	9.8	10.7
$(CH_3)_3C$	24 h	163.2

a) mean, n=2; min unless otherwise stated

b) one measurement.

Although the reaction rates are faster for the triesters (93) than the diesters (104) a comparable trend is observed. As for the much slower chemical hydrolyses (Tables 3.3 and 3.4) the rate of hydrolysis increases with increasing steric bulk of the alkyl group. These results are in contrast to those observed with pig liver carboxylesterase (Tables 3.7 and 3.8) in which the 4-ethanoyloxybenzyl diester (104, R=CH_3) was much more stable

than the propanoyloxy derivative (**104**, R=$CH_3(CH_2)_2$). This strongly suggests that human plasma carboxylesterases have different substrate specificities from those derived from pig liver. In common with the results obtained with pig liver carboxylesterase, the methoxycarbonyl group was unaffected by human plasma. This was confirmed by the observed stability of an authentic sample of disodium (methoxycarbonylmethyl)phosphonate incubated with plasma under identical reaction conditions to the diesters.

3.8.4. Stability of Diesters (104) with Porcine Brain

Like plasma, the brain is a rich source of a wide variety of enzymes. These include carboxylesterase, cholinesterase, monoamine oxidase, arylsulphatase and tyrosine hydroxylase,[179, 191] therefore bioactivation of alkanoyloxybenzyl phosphonates within the brain would be expected. To investigate this effect the diesters (**104**, R=CH_3, $CH_3(CH_2)_2$, $(CH_3)_3C$) were incubated with the S9 fraction of porcine brain and the reactions monitored by ^{31}P NMR spectroscopy. The S9 fraction was obtained as the supernatant following centrifugation of the total brain homogenate at 10,000 g for 20 min. This fraction contains all components of the brain with the exception of large pieces of cellular membrane and nuclei. The diesters (**104**) were found to degrade to (methoxycarbonylmethyl)phosphonate (**105**), presumably via the 4-hydroxybenzyl intermediate (**107**) (**Fig 3.19**). The half-lives for these reactions are given in **Table 3.11**.

Table 3.11 - Half-lives for alkanoyloxybenzyl diesters (**104**) incubated with porcine brain S9 fraction

R	$t_{1/2}$ (h)
CH_3	1.9
$CH_3(CH_2)_2$	4.1
$(CH_3)_3C$	50

It is apparent from **Tables 3.10** and **3.11** that the porcine brain-mediated bioactivation of the diesters follow a similar trend to that observed with human plasma. That is, the greater the steric bulk of the alkanoyl group (R) the slower the rate of reaction. In

common with the carboxylesterase and plasma studies, the diesters (**104**) degraded only as far as the monoester (**105**), the methoxycarbonyl function remaining unaffected.

3.8.5. Summary

In the presence of porcine liver carboxylesterase, human plasma and pig brain S9 fraction the reasonably hydrolytically stable di(alkanoyloxybenzyl) triesters (**93**) were degraded to the corresponding alkanoyloxybenzyl diesters (**104**), which were in turn degraded further to the monoester, (methoxycarbonylmethyl)phosphonate (**105**). The degradation of these compounds occurred through enzymatic hydrolysis of the alkanoyloxy group to form the 4-hydroxybenzyl derivatives (**106, 107**), which underwent rapid C-O bond fission to form the resonance-stabilised 4-hydroxybenzyl carbonium ion and the appropriate phosphonate esters (**Fig 3.8**).

The rate of enzymatic hydrolysis was dependent on the structural nature of the alkanoyl group. Incubations of the triesters (**93**) and diesters (**104**) in both human plasma and the S9 fraction of pig brain revealed a linear relationship between steric bulk of the alkanoyl group and rate of hydrolysis, with the ethanoyloxybenzyl substrate ($R=CH_3$) being the most reactive. However, when the same compounds were incubated with porcine liver carboxylesterase, hydrolysis was most rapid when a 3 carbon alkyl group ($R=CH_3(CH_2)_2$, $(CH_3)_2CH$) was attached to the carboxyl ester function. Presumably this results from differences in specificity of the carboxylesterases derived from different sources. Degradation did not proceed beyond the monoester (**105**) in any system and phosphonoacetate was not observed.

3.9. Conclusions

The high chemical stability observed for the phosphonoacetate triesters (**44, 93**) confirmed that the electron-withdrawing effect of the methoxycarbonyl group was responsible for the inherent instability of the phosphonoformate triesters (**38**) towards nucleophilic attack at phosphorus. The hydrolysis of (**38**) also includes some C-P bond cleavage with the formation of a phosphite. As a consequence, triesters of phosphonoformate are not suitable prodrug forms.

Previous studies on the enzymatic bioactivation of phosphate triester prodrugs[112] revealed difficulties in the removal of the second protecting group from phosphorus. The first alkanoyloxybenzyl group was removed readily by carboxylesterase to give a diester,

however the second alkanoyloxymethyl group on the diester was released much more slowly. This suggests that to achieve rapid bioactivation to the monoester (**105**), the phospho anion on the diester must be well separated from the site of esterase activity. This rationale led to the development of a di(4-alkanoyloxybenzyl) phosphonate prodrug system in which both phospho protecting groups can be removed in the presence of esterase *via* the intermediacy of the 4-hydroxybenzyl esters, which readily degrade to the phospho anion and a benzyl carbonium ion. The rate of enzymatic hydrolysis, and subsequent removal of the protecting group, can be influenced by the structural nature of the alkanoyl group. Consequently, it may now be possible to design a prodrug which has sufficient stability in plasma to reach the CNS in high concentration, wherein rapid metabolism by brain-associated enzymes occurs.

Complete bioactivation of triesters of phosphonoacetate to the parent drug has yet to be achieved and only the methyl ester (**105**) has been isolated. The methoxycarbonyl group exhibits a high degree of stability towards chemical and enzymatic hydrolysis, and as such further studies are required for the removal of this carboxylate ester. One possible solution is the replacement of the methoxy group with a better leaving group, such as phenoxy. Alternatively, a more controlled release of the free acid may be possible with the synthesis of a phosphonoacetate triester in which all three negative charges are masked by 4-alkanoyloxybenzyl groups (**116**).

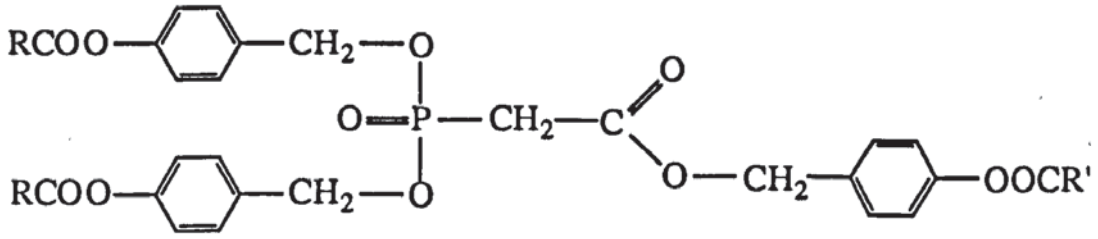

(116)

Similar to the enzymatic removal of the two protecting groups on phosphorus the rate of generation of the free carboxylate would almost certainly be dependent on the nature of the alkyl group (R'), therefore complete degradation to phosphonoacetate should be possible in a controlled manner. Similarly, the carboxyl function could be masked by a simple biodegradable acyloxymethyl group.

One of the major problems associated with the 4-alkanoyloxybenzyl prodrug approach is the release of the highly reactive 4-hydroxybenzyl carbonium ion which may interact with cellular nucleophiles (eg. DNA,glutathione) and cause toxicity.[96] Indeed, when tested for antiviral properties (**section 3.4**), the 4-ethanoyloxybenzyl- and 4-pivaloyloxybenzyl

triesters of PAA (**104**, R=CH_3, $(CH_3)_3C$) exhibited acute toxicity, possibly due to the generation of the carbonium ion. For this reason methods to trap this intermediate internally should be investigated. One possibility could be to introduce a nucleophilic group, such as a hydroxymethyl substituent, into the *ortho* position of the benzene ring (**117**). Theoretically, this could interact intramolecularly with the carbonium ion to give an overall neutral ether (**118**) and harmlessly trap the potentially toxic intermediate (**Fig 3.23**)

Fig 3.23 - Internal trapping of the 4-hydroxybenzyl carbonium ion

(117) **(118)**

At this stage in the development of a prodrug system it is important to determine the extent to which di(4-alkanoyloxybenzyl) triesters of PAA (**93**) are transported across the BBB into the brain. Information on the probability of success could be achieved by measurement of their octanol/water partition coefficients or Log P values.[192] Indeed, there is a linear relationship between the cerebrovascular permeability of a compound and its lipophilicity.[193, 194, 195] Hansch *et al*[196] have determined a log P of 2.0 (ie. partition of 100:1, octanol-water) for optimal brain uptake, lipophilicity in excess of this resulting in interaction of the molecule with plasma proteins and hence reduced transport into the brain. Further information on the extent of BBB permeation of these triesters (**93**) could be gained by the synthesis of a radiolabelled triester and subsequent monitoring of its transport across a model of the BBB. An appropriate model based on porcine brain endothelial cells[197, 198] is currently being developed within the Pharmaceutical Sciences Institute at Aston University. For the most promising triesters, brain uptake could be measured directly by HPLC analysis of homogenised rat brain following intravenous administration of the prodrug.

Providing that these studies are successful the 4-alkanoyloxybenzyl prodrug system can be developed as an effective means of delivering a wide range of antiviral agents, including the potent anti-HIV drugs, PMEA and AZT, to the brain.

EXPERIMENTAL

^1H NMR spectra were recorded on a Varian EM-360 60 MHz spectrometer with tetramethylsilane (Me_4Si) as the reference; high resolution ^1H (300 and 250.1 MHz), ^{31}P (121.5 and 101.3 MHz) and ^{13}C (75.5 and 62.9 MHz) NMR were recorded on Bruker AC spectrometers. ^{31}P and ^{13}C spectra were referenced to 85% H_3PO_4 and ethylbenzene respectively and all are ^1H decoupled (composite pulse decoupling) unless otherwise stated: positive chemical shifts are downfield from the reference. Mass spectra were recorded on a V.G. Micromass 12 instrument at 70ev and a source temperature of 300°C; accurate mass data were recorded by the SERC mass spectrometry service at Swansea University on a V.G. 7070E instrument under EI, CI, and positive ion FAB (thioglycerol or nitrobenzyl alcohol matrix) techniques. IR spectra were recorded on a Perkin-Elmer 1310 Spectrophotometer. UV scans were recorded on a Unicam SP 800 ultraviolet recording spectrophotometer. Melting points were measured on a Gallenkamp Electrothermal Digital apparatus and are not corrected. Flash column chromatography[133] was performed using Sorbsil C60 silica gel. TLC was performed using plastic-backed Kieselgel 60 silica gel plates containing a fluorescent indicator. Spots were visualised under 254 nm UV light or with the aid of iodine. Elemental analyses were performed by Butterworths Laboratories, Middlesex. The following solvents were dried by heating under reflux followed by distillation over the appropriate drying reagent: dichloromethane (P_2O_5), acetone (4Å molecular sieve), toluene (Na) and triethylamine (KOH). Chemicals were obtained from Aldrich Chemical Company and porcine and rabbit liver carboxylesterases were obatined from Sigma Chemical Company. The phosphate buffer (0.1 M, pH 7.4) was prepared by mixing aqueous solutions of disodium (or dipotassium) hydrogen phosphate (0.2 M, 40.5 ml) and sodium (or potassium) dihydrogen phosphate (0.2 M, 9.5 ml), and the volume was adjusted to 100 ml with water. The D_2O phosphate buffer (0.1 M, pD 8.0) was prepared by dissolving a mixture of KH_2PO_4 (0.0572 g) and K_2HPO_4 (0.2752g) in D_2O (20 ml). The pH was measured and the pD calculated from the following equation:[199]

$$pD = pH + (429/T) - 1.04$$

CHAPTER 4 - SYNTHESIS

4.1. Preparation of Benzyl Alcohols

4-Aminobenzyl alcohol.[130] **(51, X=NH_2)** 4-nitrobenzyl alcohol (10g, 0.07 mol), ethanol (10ml) and Adams platinum catalyst (1g) were shaken in hydrogen (5500cm^3) at atmospheric pressure. The solution was filtered through celite and the ethanol removed by evaporation to leave a brown oil which solidified on cooling to 0-4°C for 24 h to give **(51, X=NH_2)** as a yellow solid (7.38g, 0.06 mol, 86%); mp 58-61°C; Rf ($CHCl_3$:MeOH, 10:1) 0.25; υ (Nujol) 3620 (N-H), 3460 cm^{-1} (N-H); δ_H ($CDCl_3$, 60 MHz) 2 - 4 (3H, bs, NH_2, OH, exchanges with D_2O), 4.53 (2H, s, CH_2), 6.67 (2H, d, J_{HH} 8 Hz, Ar), 7.42 ppm (2H, d, J_{HH} 8 Hz, Ar).

4-Azidobenzyl alcohol.[130] **(51, X=N_3)** A solution of sodium nitrite (3.39 g, 0.049 mol) in 30 ml water was added dropwise to a solution of 4-aminobenzyl alcohol (5.50g, 0.045 mol) in 5M HCl (200ml) at 0-5°C and stirred for 30 min. The presence of excess nitrosonium ion, NO^+, was checked with starch-iodide paper. Sodium azide (11.70g, 0.18 mol) was added in portions over 30 min and stirring continued for a further 2 h. The mixture was added to iced water (100ml), neutralised with 10 M NaOH (90ml) and extracted with chloroform. The extracts were dried (Na_2SO_4) and the solvent evaporated to give **(51, X=N_3)** as an orange-brown solid (5.09g, 0.03 mol, 74%); mp 26-28°C; λ_{max} ($CHCl_3$) 251nm; Rf ($CHCl_3$:CH_3OH, 3:1) 0.70; υ (Nujol) 3305 (OH), 2100 cm^{-1} (N_3); δ_H ($CDCl_3$, 60 MHz) 4.6 (2H, s, CH_2), 6.8 (2H, d, J_{HH} 8 Hz, Ar), 7.15 (2H, d, J_{HH} 8 Hz, Ar); m/z (EI) 149 ($M^{+\cdot}$, 42%), 122 (100), 91 (52), 28 (77).

4-Ethanoyloxybenzyl alcohol.[131] **(51, X=CH_3COO)** Acetic anhydride (5.10g, 50 mmol) was added dropwise to a stirred solution of 4-hydroxybenzyl alcohol (6.2g, 50 mmol) in 2.5 M NaOH (20 ml) at -5 to -10°C. After 4 h the mixture was extracted with ether (2 x 30 ml), then washed with 5% $NaHCO_3$ (2 x 30ml). The combined extracts were dried (Na_2SO_4) and concentrated. Flash column chromatography[133] (EtOAc:Hexane, 60:40, Rf 0.70) gave **(51, X=CH_3COO)**as a colourless solid (5.5g, 0.03 mol, 66%); υ (Nujol) 3400 (OH), 1750 cm^{-1} (C=O); δ_H ($CDCl_3$, 60 MHz) 2.2 (3H, s, CH_3), 3.3 (1H, br s, OH, exchanges with D_2O), 7.1 (2H, d, J_{HH} 8 Hz, Ar), 7.4 ppm (2H, d, J_{HH} 8 Hz, Ar); m/z (EI) 166 ($M^{+\cdot}$, 73%), 123 (100), 106 (78), 95 (58), 77 (82).

The following compounds were prepared by the reaction between 4-hydroxybenzyl alcohol and the appropriate anhydride using a method similar to that described for **(51, X=CH_3COO)**.

4-Propanoyloxybenzyl alcohol.[131] **(51, X=CH_3CH_2COO).** Flash column chromatography (EtOAc : Hexane, 1:1, Rf 0.67) gave **(51, X=CH_3CH_2COO)** as a brown oil (42%); δ_H ($CDCl_3$, 250.1 MHz) 1.20 (3H, t, J_{HH} 7.5 Hz, CH_3), 2.53 (2H, q, J_{HH} 7.5 Hz, CH_2), 3.7 (1H, br s, OH, exchanges with D_2O), 4.45 (2H, s, CH_2OH), 6.97 (2H, d, J_{HH} 8.3 Hz, Ar), 7.22 ppm (2H, d, J_{HH} 8.3 Hz, Ar).

4-n-Butanoyloxybenzyl alcohol.[131] **(51, X=$CH_3(CH_2)_2COO$).** Flash column chromatography (Still) (EtOAc : Hexane, 1:1, Rf 0.60) gave **(51, X=$CH_3(CH_2)_2COO$)** as a brown oil (60%); δ_H ($CDCl_3$, 250.1 MHz) 0.99 (3H, t, J_{HH} 7.3 Hz, CH_3), 1.65 (2H, sextet, J_{HH} 7.4 Hz, CH_2), 2.44 (2H, t, J_{HH} 7.3 Hz, CH_2), 3.75 (1H, br s, OH, exchanges with D_2O), 4.43 (2H, s, CH_2), 6.93 (2H, d, J_{HH} 8.4 Hz), 7.19 ppm (2H, d, J_{HH} 8.3 Hz, Ar); δ_C (62.9 MHz) 13.20 (s, CH_3), 18.03 (s, CH_2), 36.10 (s, CH_2), 63.64 (s, CH_2OH), 121.06 (s, 2 x aromatic CH), 127.53 (s, 2 x aromatic CH), 138.40 (s, aromatic C), 149.47 (s, aromatic C), 172.01 ppm (s, C=O).

4-iso-Butanoyloxybenzyl alcohol.[131] **(51, X=$(CH_3)_2CHCOO$).** Flash column chromatography (EtOAc : Hexane, 1:1, Rf 0.55) gave **(51, X=$(CH_3)_2CHCOO$)** as a light brown semi-solid (80%); δ_H ($CDCl_3$, 250.1 MHz) 1.22 (6H, d, J_{HH} 6.9 Hz, $(CH_3)_2$), 2.71 (1H, sept, J_{HH} 6.9 Hz, CH), 4.30 (1H, br s, OH, exchanges with D_2O), 4.39 (2H, s, CH_2OH), 6.93 (2H, d, J_{HH} 8.4 Hz, Ar), 7.17 ppm (2H, d, J_{HH} 8.2 Hz, Ar); δ_C (62.9 MHz) 18.78 (s, $(CH_3)_2$), 34.02 (s, CH), 63.97 (s, CH_2OH), 121.28 (s, 2 x aromatic CH), 127.87 (s, 2 x aromatic CH), 138.52 (s, aromatic C), 149.86 (s, aromatic C), 175.90 ppm (s, C=O).

4-Hexanoyloxybenzyl alcohol.[131] **(51, X=$CH_3(CH_2)_4COO$).** Flash column chromatography (EtOAc : Hexane, 1:1, R_f 0.51) gave **(51, X=$CH_3(CH_2)_4COO$)** as a colourless oil (4%); δ_H ($CDCl_3$, 250.1 MHz) 0.92 (3H, t, J_{HH} 6.9 Hz, CH_3), 1.39 (4H, m, 2 x CH_2), 1.75 (2H, pen, J_{HH} 7.2 Hz, CH_2), 2.09 (1H, br s, OH, exchanges with D_2O), 2.54 (2H, t, J_{HH} 7.3 Hz, CH_2COO), 4.87 (2H, s, CH_2OH), 7.05 (2H, d, J_{HH} 8.5 Hz, Ar), 7.34 ppm (2H, d, J_{HH} 8.4 Hz, Ar).

4-Pivaloyloxybenzyl alcohol.[131] **(51, X=$(CH_3)_3CCOO$).** Method 1. This was prepared in the same way as **(51, X=CH_3COO)** except that trimethylacetyl chloride was used instead of acetic anhydride. Flash column chromatography (EtOAc:Hexane, 1:1, Rf 0.52) gave **(51, X=$(CH_3)_3CCOO$)** as a colourless semi-solid (17%); υ (Nujol) 3300 (OH), 1740 cm^{-1} (C=O); δ_H ($CDCl_3$, 250.1 MHz) 1.35 (9H, s, $(CH_3)_3$), 4.65 (2H, s, CH_2), 7.02 (2H, d, J_{HH} 8.3 Hz, Ar), 7.35 ppm (2H, d, J_{HH} 8.2 Hz, Ar).

4-Pivaloyloxybenzyl alcohol. Method 2. 4-hydroxybenzyl alcohol (10g, 0.081 mol) in 1M NaOH (75 ml) was poured into a solution of trimethylacetyl chloride (11.67g, 0.097 mol) and tetrabutylammonium chloride (11.1 g, 0.040 mol) in CH_2Cl_2 (75 ml) and left to stir at room temperature for 4 hours. The CH_2Cl_2 layer was washed with 5% $NaHCO_3$ (2 x 40 ml), dried (Na_2SO_4) and concentrated. Flash column chromatography (EtOAc : Hexane, 6:4, Rf 0.42) gave **(51, X=$(CH_3)_3CCOO$)** as a colourless semi-solid (6.36g, 0.031 mol, 38%). Data as for Method 1.

4.2. Preparation of 4-Nitrobenzyl Iodide

4-Nitrobenzyl iodide.[132] **(56, X=NO_2)** A mixture of 4-nitrobenzyl chloride (5g, 0.03 mol) and potassium iodide (4.98g, 0.03 mol) was refluxed in ethanol (300ml) for one hour. On cooling a white precipitate formed which was filtered-off and washed with water. Recrystallisation from ethanol gave **(56, X=NO_2)** as yellow needles (5.26g, 0.02 mol, 67%), mp 124-127°C; Rf (EtOAc) 0.68; δ_H ($CDCl_3$, 300 MHz) 4.41 (2H, s, CH_2), 7.95 (2H, d, J_{HH} 8.0 Hz, Ar), 8.10 (2H, d, J_{HH} 8.0 Hz, Ar).

4.3. Preparation of (Methoxycarbonyl)phosphonic Dichloride and Disilver (Methoxycarbonyl)phosphonate

Dimethyl (methoxycarbonyl)phosphonate[113] **(48).** Trimethyl phosphite **(46)** (50g, 0.40 mol) was heated to 120°C in a fume cupboard. Methyl chloroformate **(47)** (41.58g, 0.44 mol) was added dropwise over 30 mins. The mixture was heated at 120°C for a further 1.5 h. Vacuum distillation (86 - 90°C, 1 mmHg) gave **(48)** as a colourless liquid (55g, 0.32 mol, 80%); δ_H ($CDCl_3$, 300 MHz) 3.72 (6H, d, J_{PH} 11.0 Hz, 2 x $POCH_3$), 3.91 ppm (3H, s, $COCH_3$); δ_P (121.5 MHz) -3.04 ppm (s), (sept q, J_{PH} 9.1, 1.0 Hz, ^1H coupled).

Bis(trimethylsilyl) (methoxycarbonyl)phosphonate[129] **(49).** A mixture of dimethyl (methoxycarbonyl)phosphonate **(48)** (10g, 0.06 mol) and trimethylsilyl bromide (19.8ml, 0.15 mol) was stirred at room temperature under argon for 3 h. The excess trimethylsilyl bromide and methylbromide by-product were removed in vacuo (20 mmHg) to give **(49)** as a colourless liquid (9.81g, 0.035 mol, 58%); δ_H ($CDCl_3$, 60 MHz) 0.5 (18H, s, 2 x $OSi(CH_3)_3$, 3.9 ppm (3H, s, OCH_3); δ_P (121.5 MHz) 0.41 (s).

(Methoxycarbonyl)phosphonic dichloride[129] **(50)**. Bis(trimethylsilyl) (methoxycarbonyl)phosphonate **(49)** (10g, 0.035 mol) was added dropwise to a stirred suspension of PCl_5 (14.6g, 0.070 mol) in dichloromethane (20ml) at room temperature. The reaction proceeded exothermically and was complete within 30 mins. Distillation (105-109^{0}C, 20 mmHg) gave **(50)** as a colourless liquid (4.42g, 0.025 mol, 72%); δ_H ($CDCl_3$, 60 MHz) 4.05 ppm(3H, s, OCH_3); δ_P (121.5 MHz) -2.94 ppm (s).

Disodium (methoxycarbonyl)phosphonate[113] **(54)**. Dimethyl (methoxycarbonyl)phosphonate **(48)** (5g, 0.030 mol) and trimethylsilyl bromide (13.77g, 0.09 mol) were stirred at room temperature under argon for 3 h. Volatile components were evaporated in vacuo (1 mmHg) and the residue added to 30g of Amberlite IRC 50 (Na^+ form) in water (50 ml). After 1.5 h the cation exchange resin was filtered and washed with water (50 ml). The combined aqueous portions were washed with diethyl ether (2 x 50 ml), concentrated and the resulting residue triturated with ethanol (2 x 50 ml) to give **(54)** as a colourless solid (4.01g, 0.021 mol, 72%); mp >300^{0}C; λ_{max} (H_2O) 237 nm; δ_H (D_2O, 300 MHz) 3.72 ppm (3H, s, OCH_3); δ_P (121.5 MHz) -0.84 ppm (s).

Disilver (methoxycarbonyl)phosphonate[112] **(55)**. Silver nitrate (5.44g, 0.032 mol) was added to a stirred solution of disodium (methoxycarbonyl)phosphonate **(54)** (3g, 0.016 mol in 50 ml water) in the dark. A white precipitate of **(55)** formed immediately (5.26g, 0.014 mol, 91%); mp >300^{0}C; δ_H (D_2O, 300 MHz) 3.81 ppm (3H, s, OCH_3); δ_P (121.5 MHz) -0.84 ppm (s).

4.4. Preparation of Dibenzyl (Methoxycarbonyl)phosphonates

Dibenzyl (methoxycarbonyl)phosphonate **(38, X=H)**. A solution of (methoxycarbonyl)phosphonic dichloride **(50)** (2.00g, 11.2 mmol) in dichloromethane (10 ml) was added dropwise over 20 minutes to a stirred solution of benzyl alcohol **(51, X=H)** (2.43g, 22.5 mmol) and triethylamine (2.22g, 22.5 mmol) in dichloromethane (30 ml) at 0°C under argon. The mixture was stirred for 4 hours at room temperature. The triethylammonium hydrochloride was removed by washing with saturated $NaHCO_3$ (2 x 30 ml). The dichloromethane layer was dried (Na_2SO_4), concentrated and purified by flash column chromatography (EtOAc, Rf 0.59) to give **(38, X=H)** as a colourless oil (2.30 g, 7.2 mmol, 64%). (Found: C, 60.21; H, 5.53. $C_{16}H_{17}O_5P$ requires C, 60.00; H, 5.35); υ (thin film) 1710 (C=O), 1280 cm^{-1}(P=O); δ_H ($CDCl_3$, 250.1 MHz) 3.77(3 H, d, J_{PH} 1.1 Hz, OCH_3), 5.18 (4 H, d, J_{PH} 8.3 Hz, 2 x CH_2), 7.33 ppm (10 H, s, Ar); δ_P (121.5 MHz) -4.94 ppm (s), (pent q, J_{PH} 8.5, 1.0 Hz, ^{1}H coupled); δ_C (62.9 MHz) 52.53 (d,

J_{PC} 5.5 Hz, OCH_3), 69.66 (d, J_{PC} 6.3 Hz, 2 x CH_2), 128.20 (s, 4 x aromatic CH), 128.63 (s, 4 x aromatic CH), 128.80 (s, 2 x aromatic CH), 135.05 (d, J_{PC} 6.2 Hz, 2 x aromatic C), 166.88 ppm (d, J_{PC} 272.1 Hz, C=O); m/z (FAB, thioglycerol matrix) 321 ($M + H^+$, 57%), 229 (10), 214 (13), 181 (100), 141 (17), 91 (87). Observed accurate mass 321.0892 ($M + H^+$); $C_{16}H_{18}O_5P$ requires 321.0892.

The following triesters of phosphonoformate were prepared from (methoxycarbonyl)phosphonic dichloride (**50**) and the appropriate alcohol (2 equivalents) by methods similar to that described for (**38, X=H**).

Di(4-azidobenzyl) (methoxycarbonyl)phosphonate (**38, X=N_3**). This was isolated without flash column chromatogaphy as a brown solid (63%); m.p. 28-30 °C; (Found: C, 47.52; H, 3.88; N, 20.72. $C_{16}H_{15}N_6O_5P$ requires C, 47.77; H, 3.76; N, 20.89); λ_{max} ($CHCl_3$) 251, 212 nm; υ (Nujol) 2100 (N_3), 1700 (C=O), 1280 cm^{-1}(P=O); δ_H ($CDCl_3$, 300 MHz) 3.91 (3 H, s, OCH_3), 5.32 (4 H, d, J_{PH} 9.1 Hz, 2 x CH_2), 6.90 (4H, d, J_{HH} 8.3 Hz, Ar), 7.05 ppm (4H, d, J_{HH} 8.5 Hz, Ar); δ_P (121.5 MHz) -4.78 ppm (s), (pent, J_{PH} 8.6 Hz, ^1H coupled); δ_C (62.9 MHz) 52.56 (d, J_{PC} 5.4 Hz, OCH_3), 69.04 (d, J_{PC} 6.3 Hz, 2 x CH_2), 118.92 (s, 4 x aromatic CH), 129.89 (s, 4 x aromatic CH), 131.53 (d, J_{PC} 6.4 Hz, 2 x aromatic C), 140.64 (s, 2 x aromatic C), 166.60 ppm (d, J_{PC} 272.2 Hz, C=O); m/z (CI) 420 ($M + NH_4^+$, 13%), 375 (32), 149 (59), 132 (100). Observed accurate mass 420.1185 ($M + NH_4^+$); $C_{16}H_{15}N_6O_5P.NH_4^+$ requires 420.1187.

Di(4-chlorobenzyl) (methoxycarbonyl)phosphonate (**38, X=Cl**). Flash column chromatography (EtOAc:Hexane, 1:1, Rf 0.28) gave (**38, X=Cl**) as a colourless oil which solidified on standing at 4 °C (0.91g, 1 mmol, 33%); m.p. 30-33 °C; (Found: C, 49.66; H, 4.05. $C_{16}H_{15}O_5PCl_2$ requires C, 49.38; H, 3.89); υ (Nujol) 1720 (C=O), 1280 cm^{-1} (P=O); δ_H ($CDCl_3$, 300 MHz) 3.81 (3 H, s, OCH_3), 5.16 (4 H, d, J_{PH} 8.2 Hz, 2 x CH_2), 7.28 (4 H, d, J_{HH} 9.4 Hz, Ar), 7.33 ppm (4H, d, J_{HH} 9.3 Hz, Ar); δ_P (121.5 MHz) -4.80 ppm (s), (pent, J_{PH} 8.6 Hz, ^1H coupled); δ_C (75.5 MHz) 52.67 (d, J_{PC} ~6 Hz, OCH_3), 68.93 (d, J_{PC} 6.0 Hz, 2 x CH_2), 128.89 (s, 4 x aromatic CH), 129.57 (s, 4 x aromatic CH), 133.43 (d, J_{PC} ~6 Hz, 2 x aromatic C), 134.99 ppm (s, 2 x aromatic C), carbonyl not detected ; m/z (FAB, thioglycerol matrix) 389 ($M + H^+$, 91%), 249 (36), 212 (28), 125 (100). Observed accurate mass 389.011 ($M + H^+$); $C_{16}H_{16}O_5PCl_2$ requires 389.011. The mass spectrum showed peaks at 389, 391 and 393 in the ratio 1:0.6:0.1 as expected for a molecule containing two chlorine atoms.

Di(4-ethanoyloxybenzyl) (methoxycarbonyl)phosphonate (**38, X=CH_3COO**). Flash column chromatography (EtOAc : Hexane, 3:1, Rf 0.5) gave (**38, X=CH_3COO**) as a light brown oil (0.9g, 2 mmol, 35%); υ (Nujol) 1743 (C=O), 1275 cm^{-1} (P=O); δ_H($CDCl_3$, 300 MHz) 2.27 (6 H, s, 2 x CH_3), 3.77 (3H, s, OCH_3), 5.15 (4H, d, J_{PH} 8.8 Hz, 2 x CH_2), 7.05 (4H, d, J_{HH} 8.4 Hz, Ar), 7.36 (4 H, d, J_{HH} 8.7 Hz, Ar), 4.65 ppm (s, CH_2OH, 2-3% of ethanoyloxybenzyl alcohol present); δ_P (121.5 MHz) -4.92 ppm (s), (pent, J_{PH} 8.0 Hz, ^1H coupled); δ_C (75.5 MHz) 21.06 (s, CH_3), 52.57 (d, J_{PC} ~6 Hz, OCH_3), 69.00 (d, J_{PC} 6.0 Hz, 2 x CH_2), 121.58 (s, 4 x aromatic CH), 128.78 (s, 4 x aromatic CH), 132.56 (d, J_{PC} 6.0 Hz, 2 x aromatic C), 150.97 (s, 2 x aromatic C), 169.23 ppm (s, C=O), one carbonyl not observed; m/z (FAB, thioglycerol matrix) 437 ($M + H^+$, 34%), 395 (11), 287 (16), 255 (47), 149 (100), 121 (21), 107 (100). Observed accurate mass 437.1001 ($M + H^+$); $C_{20}H_{22}O_9P$ requires 437.1001.

Di(4-pivaloyloxybenzyl) (methoxycarbonyl)phosphonate (**38, X=$(CH_3)_3CCOO$**). Flash column chromatography (EtOAc : Hexane, 1:1; Rf 0.31) gave (**38, X=$(CH_3)_3CCOO$**) as a light pink solid (30%); m.p. 27-29 °C; (Found: C, 60.24; H, 6.48. $C_{26}H_{33}O_9P$ requires C, 60.00; H, 6.39); υ (Nujol) 1740 (C=O), 1720 (C=O), 1280 cm^{-1} (P=O); δ_H ($CDCl_3$, 300 MHz) 1.21 (18 H, s, 2 x $(CH_3)_3$), 3.76 (3H, s, OCH_3), 5.10 (4 H, d, J_{PH} 8.8 Hz, 2 x CH_2), 6.98 (4H, d, J_{HH} 8.2 Hz, Ar), 7.30 ppm (4H, d, J_{HH} 8.4 Hz, Ar); δ_P (121.5 MHz) -4.95 ppm (s); δ_C (75.5 MHz) 27.06 (s, $(CH_3)_3$), 39.04 (s, $(CH_3)_3\underline{C}$), 52.56 (d, J_{PC} ~6 Hz, OCH_3), 69.11 (d, J_{PC} 6.0 Hz, CH_2), 121.77 (s, 4 x aromatic CH), 129.45 (s, 4 x aromatic CH), 132.32 (d, J_{PC} 6.0 Hz, 2 x aromatic C), 151.96 ppm (s, 2 x aromatic C), 176.84 ppm (s, C=O), one carbonyl not obseved; m/z (FAB, thioglycerol matrix) 522 ($M + 2H^+$, 8%), 437 (6), 329 (9), 191 (100), 107 (100), 85 (100), 57 (100). Observed accurate mass 522.2019 ($M + 2H^+$); $C_{26}H_{35}O_9P$ requires 522.2019.

Di(4-trifluoromethylbenzyl) (methoxycarbonyl)phosphonate (**38, X=F_3C**). Concentration gave a colourless oil. Traces of trifluoromethylbenzyl alcohol were removed by Kugel distillation at 90°C, 1 mm Hg to give (**38, X=F_3C**) (54%); (Found: C, 47.28; H, 3.34. $C_{18}H_{15}O_5PF_6$ requires C, 47.39; H, 3.31); υ (Nujol) 1750 (C=O), 1340 cm^{-1} (P=O); δ_H ($CDCl_3$, 300 MHz) 3.81 (3 H, s, OCH_3), 5.25 (4 H, d, J_{PH} 8.4 Hz, 2 x CH_2), 7.45 (4 H, d, J_{HH} 8.3 Hz, Ar), 7.58 ppm (4 H, d, J_{HH} 8.3 Hz, Ar); δ_P (121.5 MHz) -4.65 ppm (s), (pent, J_{PH} 8.0 Hz, ^1H coupled); δ_C (75.5 MHz) 52.79 (d, J_{PC} ~6 Hz, OCH_3), 68.64 (d, J_{PC} 6.0 Hz, 2 x CH_2), 125.65 (s, 4 x aromatic CH), 128.32 (s, 4 x aromatic CH), 131.00 (q, J_{CF} 34.0 Hz, 2 x aromatic C), 138.76 (d, J_{PC} ~6 Hz, 2 x aromatic C), carbonyl not observed; m/z (FAB, thioglycerol matrix) 457 ($M + H^+$, 40%), 297(6), 159 (100), 140 (17), 109 (10), 91 (4). Observed accurate mass 457.064 ($M + H^+$); $C_{18}H_{16}O_5PF_6$ requires 457.064.

Di(4-methylbenzyl) (methoxycarbonyl)phosphonate (**38, X=CH_3**). Flash column chromatography (EtOAc : Hexane, 1:1, Rf 0.51) gave (**38, X=CH_3**) as a brown oil (30%); υ (thin film) 1720 (C=O), 1280 cm^{-1} (P=O); δ_H ($CDCl_3$, 300 MHz) 2.35 (6 H, s, 2 x CH_3), 3.78 (3 H, s, OCH_3), 5.15 (4 H, d, J_{PH} 8.2 Hz, 2 x CH_2), 7.15 (4 H, d, J_{HH} 8.2Hz, Ar), 7.24 ppm (4 H, d, J_{HH} 8.2Hz, Ar) (2-3% of 4-methylbenzyl alcohol is present); δ_P (121.5 MHz) -5.02 ppm (s), (pent, J_{PH} 8.0 Hz, ^1H coupled); δ_C (75.5 MHz) 21.23 (s, 2 x CH_3), 52.47 (d, J_{PC} 3.5 Hz, OCH_3), 69.71 (d, J_{PC} 6.0 Hz, 2 x CH_2), 128.25 (s, 4 x aromatic CH), 129.05 (s, 4 x aromatic CH), 132.09 (d, J_{PC} 6.0 Hz, 2 x aromatic C), 138.74 (s, 2 x aromatic C), 165.14 ppm (d, J_{PC} 270 Hz, C=O); m/z (FAB, thioglycerol matrix) 349 ($M + H^+$, 44%), 226 (10), 122 (85), 105 (60). Observed accurate mass 349.231 ($M + H^+$); $C_{18}H_{21}O_5P$ requires 349.231.

Di(4-nitrobenzyl) (methoxycarbonyl)phosphonate (**38, X=NO_2**). A solution of 4-nitrobenzyl iodide (**56, X=NO_2**) (0.38g, 1.44 mmol.) in toluene (25 ml) was added dropwise over 30 min to a suspension of disilver (methoxycarbonyl)phosphonate (**55**) (0.27g, 0.76 mmol) protected from light and under argon, and left to stir for 24 h. The silver iodide precipitate was removed by filtration and the filtrate washed with water (2 x 30 ml), dried (Na_2SO_4) and concentrated. The residue was purified by flash column chromatography (EtOAc : Hexane, 2:1, Rf 0.60). Recrystallisation from toluene/petroleum ether gave (**38, X=NO_2**) as a colourless solid (0.21g, 0.51 mmol, 67%); m.p. 58-62 °C; (Found: C, 47.05; H, 3.75; N, 6.75. $C_{16}H_{15}N_2O_9P$ requires C, 46.83; H, 3.69; N, 6.83); υ (Nujol) 1700 (C=O), 1520 (NO_2, asymmetrical), 1340 (NO_2, symmetrical), 1280 cm^{-1} (P=O); δ_H ($CDCl_3$, 300 MHz) 3.92 (3 H, s, OCH_3), 5.47 (4 H, d, J_{PH} 9.1 Hz, 2 x CH_2), 7.96 (4 H, d, J_{HH} 8.3 Hz, Ar), 8.13 ppm (4 H, d, J_{HH} 8.3 Hz, Ar); δ_P (101.3 MHz) -3.90 ppm (s), (pent q, J_{PH} 8.2, 1.0 Hz, ^1H coupled); δ_C (62.9 MHz) 52.95 (d, J_{PC} 5.5 Hz, OCH_3), 68.03 (d, J_{PC} 5.7 Hz, 2 x CH_2), 123.83 (s, 4 x aromatic CH), 128.17 (s, 4 x aromatic CH), 141.72 (d, J_{PC} 6.5 Hz, 2 x aromatic C), 147.98 ppm (s, 2 x aromatic C), carbonyl not detected; m/z (CI) 428 ($M + NH_4^+$, 100%), 411 (3), 274 (6), 166 (98), 136 (50).

Attempted synthesis of *di(4-methoxybenzyl) (methoxycarbonyl)phosphonate* (**38, X=CH_3O**). The synthesis of (**38, X=CH_3O**) was attempted in a similar way to (**38, X = H**) from 4-methoxybenzyl alcohol (**51, X=CH_3O**) and (methoxycarbonyl)phosphonic dichloride (**50**). The triester could not be isolated and the only characterised product was di(4-methoxybenzyl) ether (**57**) which was purified by flash column chromatography (EtOAc : Hexane, 1:1, Rf 0.70) as a colourless oil (42%); δ_H ($CDCl_3$, 300 MHz) 3.79 (6 H, s, 2 x OCH_3), 4.46 (4 H, s, CH_2), 6.88 (4 H, d, J_{HH}

8.0 Hz, Ar), 7.29 ppm (4 H, d, J_{HH} 8.0Hz, Ar); δ_C (75.5 MHz) 46.24 (s, 2 x CH_2), 55.23 (s, 2 x CH_3), 113.72 (s, 4 x aromatic CH) 130.00 ppm (s, 4 x aromatic CH), 4 aromatic C not detected; m/z (EI) 258 ($M^{+\cdot}$, 80%), 228 (100), 197 (57), 137 (60), 121 (33), 107 (49), 91 (46).

Ether formation was confirmed by comparison of the spectra with those from an authentic sample of di-(4-methoxybenzyl) ether synthesised by the reaction of 4-methoxybenzyl alcohol with 4-methoxybenzyl chloride.

The synthesis of **(38, X=CH_3O)** was also attempted in a similar way to **(38, X=NO_2)** from 4-methoxybenzyl iodide[200] **(56, X=CH_3O)** and disilver (methoxycarbonyl)phosphonate **(55)**. Analysis of the products revealed that **(38, X=CH_3O)** was not formed.

Di(3-methoxybenzyl) (methoxycarbonyl)phosphonate **(59)**. This was prepared in a similar way to **(38, X=H)** from 3-methoxybenzyl alcohol and (methoxycarbonyl)phosphonic dichloride **(50)**. Flash column chromatography (EtOAc:Hexane, 2:1, Rf 0.57) gave **(59)** as a colourless oil. (Found: C, 56.33; H, 5.65. $C_{18}H_{21}O_7P$ requires C, 56.84; H, 5.57); υ (thin film) 1720 (C=O), 1280 cm^{-1} (P=O); δ_H ($CDCl_3$, 300 MHz) 3.78 (6H, s, 2 x CH_3OAr), 3.80 (3H, d, J_{PH} 0.9 Hz, $COCH_3$), 5.19 (4H, d, J_{PH} 8.3 Hz, 2 x CH_2), 6.86 - 7.29 ppm (8H, m, Ar); δ_P (101.3 MHz) -6.36 ppm (s), (pent q, J_{PH} 8.2, 1.1 Hz, ^1H coupled); m/z (FAB, thioglycerol matrix) 380 (M + H^+, 9%), 241 (100), 121 (100), 91 (42). Observed accurate mass 380.103 (M + H^+); $C_{18}H_{22}O_7P$ requires 380.103.

Dibenzyl (benzyloxycarbonyl)phosphonate **(67)**. This was prepared in a similar way to **(38, X=H)** from benzyl alcohol and (benzyloxycarbonyl)phosphonic dichloride. Flash column chromatography gave **(67)** as a yellow oil (34%); (Found: C, 65.28; H, 5.35; $C_{22}H_{21}O_5P$ requires C, 66.66; H, 5.34); υ (thin film) 1720 (C=O), 1270 cm^{-1} (P=O); δ_H ($CDCl_3$, 300 MHz), 5.16 (4H, d, J_{PH} 7.9 Hz, 2 x CH_2OP), 5.21 (2H, s, $COCH_2$), 7.30 - 7.39 ppm (15H, m, Ar); δ_P (121.5 MHz) - 5.08 ppm (s), (pent, J_{PH} 8.0 Hz, ^1H coupled); δ_C (75.5 MHz) 67.65 (d, J_{PC} 4.1 Hz, $CO\underline{C}H_2$), 69.72 (d, J_{PC} 5.8 Hz, 2 x CH_2OP), 128.17 (s, aromatic CH), 128.60 (s, aromatic CH), 128.69 (s, 2 x aromatic CH), 128.75 (s, aromatic CH), 134.33 (s, aromatic C), 135.05 ppm (d, J_{PC} 6.8 Hz, 2 x aromatic C), 2 aromatic CH overlapping and carbonyl not detected; m/z (FAB, nitrobenzyl alcohol matrix) 397 (M + H^+, 23%), 181 (63), 107 (17), 91 (100), 77 (24). Observed accurate mass 397.1205 (M + H^+); $C_{22}H_{22}O_5P$ requires 397.1205.

4.5. Preparation of Sodium Benzyl (Methoxycarbonyl)phosphonates

Sodium benzyl (methoxycarbonyl)phosphonate **(61, X=H).** Using a method similar to that described for other phosphonoformate diesters[137] a solution of sodium iodide (1.03g, 6.88 mmol) in acetone (5 ml) was added to a solution of dibenzyl (methoxycarbonyl)phosphonate **(38, X=H)** (2.00g, 6.25 mmol) in acetone (10 ml). The reaction mixture was stirred and heated under reflux for one hour. The diester **(61, X=H)** was precipitated as a colourless powder. After filtration the sample was dissolved in water and re-precipitated by the addition of acetone (0.30g, 1.2 mmol, 17%); m.p. >210 °C; (Found: C, 42.52; H, 3.78. $C_9H_{10}O_5PNa$ requires C, 42.87; H, 4.00); υ (Nujol) 1690 (C=O), 1265 cm^{-1} (P=O); δ_H (D_2O, 300 MHz) 3.48 (3 H, s, OCH_3), 4.80 (2 H, d, J_{PH} 7.82 Hz, CH_2), 7.21 ppm (5 H, s, Ar); δ_P (121.5 MHz) -2.65 ppm (s), (t, J_{PH} 8.5 Hz, ^1H coupled); δ_C (75.5 MHz) 54.56 (d, J_{PC} ~5 Hz, OCH_3), 71.02 (d, J_{PC} 5.3 Hz, CH_2), 130.60 (s, 2 x aromatic CH), 131.12 (s, aromatic CH), 131.47 (s, 2 x aromatic CH), 139.42 ppm (d, J_{PC} 5.3 Hz, aromatic C), carbonyl not detected; m/z (FAB, thioglycerol matrix) 275 (M + Na^+, 100), 253 (M + H^+, 71), 185 (22), 177 (2), 115 (61), 91 (55). Observed accurate mass 253.0242 (M + H^+); $C_9H_{11}O_5PNa$ requires 253.0242.

The following compounds were prepared by the reaction of sodium iodide with the appropriate phosphonate triester using a method similar to that described above.

Sodium 4-azidobenzyl (methoxycarbonyl)phosphonate **(61, X=N_3)** was obtained as a colourless solid (58%); m.p. 154-156 °C; (Found: C, 36.73; H, 2.93; N, 14.39. $C_9H_9N_3O_5PNa$ requires C, 36.87; H, 3.09; N, 14.33); λ_{max} (water) 251, 207 (shoulder) nm; υ (Nujol) 2100 (N_3), 1700 (C=O), 1280 cm^{-1} (P=O); δ_H (D_2O, 300 MHz) 3.53 (3 H, s, OCH_3), 4.88 (2 H, d, J_{PH} 9.6 Hz, CH_2), 7.05 (2 H, d, J_{HH} 8.3 Hz, Ar), 7.39 ppm (2 H, d, J_{HH} 8.6 Hz, Ar); δ_P (121.5 MHz) -2.93 ppm (s), (t q, J_{PH} 8.0, 0.8 Hz, ^1H coupled); δ_C (75.5 MHz) 44.67 (d, J_{PC} ~6 Hz, OCH_3), 60.68 (d, J_{PC} ~6 Hz, CH_2), 111.89 (s, 2 x aromatic CH), 122.56 (s, 2 x aromatic CH), 126.25 (d, J_{PC} ~6 Hz, aromatic C), 132.74 (s, aromatic C), carbonyl not detected; m/z (FAB, thioglycerol matrix) 316 (M + Na^+, 100%), 294 (M + H^+, 43), 245 (86), 185 (55), 125 (76), 104 (26). Observed accurate mass 294.0229 (M + H^+); $C_9H_{10}N_3O_5PNa$ requires 294.0229.

Sodium 4-chlorobenzyl (methoxycarbonyl)phosphonate **(61, X=Cl).** A solid was precipitated after 2 h at room temperature. Purification gave **(61, X=Cl)** as a colourless powder (91%); m.p. 175-179 °C; (Found: C, 37.91; H, 3.15. $C_9H_9O_5PClNa$ requires C, 37.71; H, 3.17); υ (Nujol) 1710 (C=O), 1260 cm^{-1} (P=O); δ_H (D_2O, 300 MHz) 3.50

(3 H, s, OCH_3), 4.81 (2 H, d, J_{PH} 8.8 Hz, CH_2), 7.20 (2 H, d, J_{HH} 8.7 Hz, Ar), 7.24 ppm (2 H, d, J_{HH} 8.7 Hz, Ar); δ_P (121.5 MHz) -2.93 ppm (s), (t, J_{PH} 8.0 Hz, ^1H coupled); δ_C (75.5 MHz) 54.53 (d, J_{PC} ~6 Hz, OCH_3), 70.24 (d, J_{PC} 5.3 Hz, CH_2), 131.29 (s, 2 x aromatic CH), 132.26 (s, 2 x aromatic CH), 136.21 (s, aromatic C), 138.16 (d, J_{PC} ~6 Hz, aromatic C), carbonyl not detected; m/z (FAB, thioglycerol matrix) 595 (2M + Na^+, 21%), 309 (M + Na^+, 100), 287 (M + H^+, 22), 251 (3), 227 (9), 115 (71). Observed accurate mass 308.967 (M + Na^+); $C_9H_9O_5PClNa_2$ requires 308.967. The mass spectrum showed peaks at 287 and 289 in the ratio of 1:0.43 as expected for a molecule containing one chlorine atom.

Sodium 4-trifluoromethylbenzyl (methoxycarbonyl)phosphonate **(61, X=F3C).** The reaction mixture was stirred for 2 h at room temperature to give **(61, X=F3C)** as a colourless solid (56%); m.p. >225 °C; υ (Nujol) 1700 (C=O), 1270 cm^{-1} (P=O); δ_H (D_2O, 300 MHz) 3.48 (3 H, s, OCH_3), 4.88 (2 H, d, J_{PH} 8.31 Hz), 7.37 (2 H, d, J_{HH} 8.7 Hz, Ar), 7.53 ppm (2 H, d, J_{HH} 8.5 Hz, Ar); δ_P (121.5 MHz) -2.86 ppm (s), (t, J_{PH} 9.0 Hz, ^1H coupled).

Sodium 4-methylbenzyl (methoxycarbonyl)phosphonate **(61, X=CH_3)** was obtained as a colourless solid (89%); m.p. 155-157 °C; (Found: C, 44.74; H, 4.39. $C_{10}H_{12}O_5PNa$ requires C, 45.13; H, 4.54); υ (Nujol) 1710 (C=O), 1260 cm^{-1} (P=O); δ_H (D_2O, 300 MHz) 2.30 (3 H, s, CH_3), 3.66 (3 H, s, OCH_3), 4.96 (2 H, d, J_{PH} 8.6Hz, CH_2), 7.24 (2 H, d, J_{HH} 8.0Hz, Ar), 7.31 ppm (2 H, d, J_{HH} 8.1 Hz, Ar); δ_P (121.5 MHz) -2.91 ppm (s), (t, J_{PH} 8.2 Hz, ^1H coupled); δ_C (75.5 MHz) 22.92 (s, CH_3), 54.49 (d, J_{PC} ~6 Hz, OCH_3), 70.95 (d, J_{PC} 5.3 Hz, CH_2), 130.94 (s, 2 x aromatic CH), 131.94 (s, 2 x aromatic CH), 136.31 (d, J_{PC} 5.3 Hz, aromatic C), 141.51 ppm (s, aromatic C), carbonyl not detected; m/z (FAB, thioglycerol matrix) 1087 (4M + Na^+, 4%), 821 (3M + Na^+, 13), 555 (2M + Na^+, 25), 289 (M + Na^+, 100), 267 (M + H^+, 16), 185 (10), 105 (33), 91 (6). Observed accurate mass 289.022 (M + Na^+); $C_{10}H_{12}O_5PNa_2$ requires 289.022.

Sodium 4-nitrobenzyl (methoxycarbonyl)phosphonate **(61, X=NO_2)** was obtained as a colourless solid (73%); m.p. >300 °C; (Found: C, 36.71; H, 3.16; N, 4.48. $C_9H_9NO_7PNa$ requires C, 36.55; H, 3.05; N, 4.70); υ (Nujol) 1700 (C=O), 1260 cm^{-1} (P=O); δ_H (D_2O, 300 MHz) 3.62 (3 H, s, OCH_3), 5.01 (2 H, d, J_{PH} 9.8Hz, CH_2), 7.91 (2 H, d, J_{HH} 8.3 Hz, Ar), 8.07 ppm (2 H, d, J_{HH} 8.3 Hz, Ar); δ_P (121.5 MHz) -2.70 ppm (s), (t q, J_{PH} 8.7, 0.8 Hz, ^1H coupled); δ_C (75.5 MHz) 44.76 (s, OCH_3), 59.60 (d, J_{PC} ~6 Hz, CH_2), 116.45 (s, 2 x aromatic CH), 120.59 (s, 2 x aromatic CH), 137.67 (d, J_{PC} ~6 Hz, aromatic C), 140.08 ppm (s, aromatic C), carbonyl not detected; m/z (FAB,

thioglycerol matrix) 298 (M + H^+, 43%), 267 (4), 184 (84), 115 (100). Observed accurate mass 298.009 (M + H^+); $C_9H_{10}NO_7PNa$ requires 298.009.

Sodium benzyl (benzyloxycarbonyl)phosphonate (**65**). This was prepared in a similar way to (**61, X=H**) from dibenzyl (benzyloxycarbonyl)phosphonate (**67**) and NaI to give (**65**) as a colourless solid (64%); mp > 210°C; υ (Nujol) 1680 (C=O), 1260 cm^{-1} (P=O); δ_H ($CDCl_3$, 300 MHz), 4.70 (2H, d, J_{PH} 7.7 Hz, CH_2OP), 7.10 - 7.18 ppm (10H, m, Ar); δ_P (121.5 MHz) - 3.04 ppm (s), (t, J_{PH} 8.0 Hz, ^1H coupled); δ_C (75.5 MHz) 69.42 (d, J_{PC} 3.2 Hz, $CO\underline{C}H_2$), 70.95 (d, J_{PC} 5.2 Hz, CH_2OP), 130.54 (s, aromatic CH), 131.03 (s, aromatic CH), 131.25 (s, aromatic CH), 131.33 (s, aromatic CH), 131.44 (s, aromatic CH), 137.91 (s, aromatic C), 139.34 (d, J_{PC} 6.0 Hz, aromatic C), 175.45 ppm (d, J_{PC} 241.9 Hz, C=O), one aromatic CH overlapping; m/z (FAB, nitrobenzyl alcohol matrix) 351 (M + Na^+, 58%), 329 (M + H^+, 50), 176 (100), 91 (33), 77 (12). Observed accurate mass 351.0374 (M + Na^+); $C_{15}H_{14}O_5Na_2P$ requires 351.0374.

4.6. Preparation of Dibenzyl Methylphosphonate

Dibenzyl methylphosphonate[140] (**62**). This was prepared in the same way as (**38, X=H**) except that methyl phosphonic dichloride was used instead of (methoxycarbonyl)phosphonic dichloride (**50**). Flash column chromatography (EtOAc, Rf 0.33) gave (**62**) as a brown oil (40%); υ 1240 cm^{-1} (P=O); δ_H ($CDCl_3$, 250.1 MHz) 1.50 (3 H, d, J_{PH} 17.0 Hz, CH_3), 5.01 (4 H, d, J_{PH} 8.2 Hz, 2 x CH_2), 7.35 ppm (10 H, s, Ar); δ_P (101.3 MHz) 31.38 ppm (s); m/z (EI) 277 ($M^{+\cdot}$, 3%), 185 (100), 155 (13), 107 (48), 91 (53), 77 (32).

4.7. Preparation of Sodium Benzyl Phosphite

Monobenzyl phosphite (**64**). Dibenzyl phosphite (**63**) (4.5g, 0.017 mol) and sodium iodide (2.81g, 0.019 mol) were heated to reflux in acetone (50 ml) for 3 h. The title compound precipitated as a colourless solid (2.30g, 0.012 mol, 71%); υ (Nujol) 1210 cm^{-1} (P=O); δ_H (D_2O, 250.1 MHz) 4.86 (2H, d, J_{PH} 8.0 Hz, CH_2), 6.75 (1H, d, J_{PH} 632.0 Hz, PH), 7.37 ppm (5H, s, Ar); δ_P (101.3 MHz) 6.91 ppm (s).

4.8. Preparation of Di(benzoyloxymethyl) (Methoxycarbonylmethyl)phosphonates

Iodomethyl benzoate[169] **(98, Ar=C_6H_5)**. Chloromethyl benzoate (10g, 0.059 mol) and sodium iodide (10.7g, 0.071 mol) were stirred in dry acetone (75 ml) for 24 h. The acetone was evaporated and ether was added to the residue. The resulting suspension was filtered and the filtrate washed with sodium thiosulphate solution (3 x 40 ml) and water (2 x 30 ml). The ether layer was dried ($MgSO_4$) and the solvent evaporated. Flash column chromatography (EtOAc, Rf 0.71)gave **(98, Ar=C_6H_5)** as a brown semi-solid (11.3g, 0.043 mol, 73%); υ (thin film) 1730 cm^{-1} (C=O); δ_H ($CDCl_3$, 60 MHz) 6.1 (2 H, s, CH_2I), 7.2 - 8.2 ppm (5 H, m, Ar).

Iodomethyl 2-methylbenzoate[169] **(98, Ar=2-$CH_3C_6H_4$)**. This was prepared in a similar way to **(98, Ar=C_6H_5)** from chloromethyl 2-methylbenzoate and NaI. Vacuum distillation (88-91°C, 0.6 mm Hg) gave **(98, Ar=2-$CH_3C_6H_4$)** as a brown semi-solid (60%); υ (thin film) 1740 cm^{-1} (C=O); δ_H ($CDCl_3$, 60 MHz) 2.55 (3H, s, CH_3), 6.05 (2H, s, CH_2I), 7.10 - 7.90 ppm (4H, m, Ar).

Iodomethyl 2,4,6-trimethylbenzoate[169] **(98, Ar=2,4,6-$(CH_3)_3C_6H_2$)**. This was prepared in a similar manner to **(98, Ar=C_6H_5)** from chloromethyl 2,4,6-trimethylbenzoate and sodium iodide; δ_H ($CDCl_3$, 60 MHz) 2.35 (9 H, s, 3 x CH_3), 6.10 (2 H, s, CH_2I), 6.85 (2 H, s, Ar).

Di(benzoyloxymethyl) (methoxycarbonylmethyl)phosphonate **(44, Ar=C_6H_5)** was prepared using a similar method to that described for **(38, X=NO_2)** from iodomethyl benzoate **(98, Ar=C_6H_5)** and disilver (methoxycarbonylmethyl)phosphonate **(97)**, prepared by the action of $AgNO_3$ on disodium (methoxycarbonylmethyl)phosphonate **(96)**. Flash column chromatography (EtOAc, Rf 0.56) gave **(44, Ar=C_6H_5)** as a colourless oil (40%); (Elemental analysis not correct. Found: C, 52.28; H, 4.43. $C_{19}H_{19}O_9P$ requires C, 54.04; H, 4.53); υ (thin film) 1740 (C=O), 1270 cm^{-1} (P=O); δ_H ($CDCl_3$, 250.1 MHz) 3.05 (2 H, d, J_{PH} 24.2 Hz, PCH_2), 3.52 (3 H, s, OCH_3), 5.89 (2 H, d d, J_{gem} 8.9 Hz, J_{PH} 5.3 Hz, CH_AH_BO), 5.96 (2 H, d d, J_{gem} 8.8 Hz, J_{PH} 5.5 Hz, CH_AH_BO), 7.20 - 7.80 ppm (10 H, m, Ar); δ_P (101.3 MHz) 21.15 ppm (s), (m, ^1H coupled); δ_C (62.5 MHz) 34.35 (d, J_{PC} 138.3 Hz, PCH_2), 52.54 (s, OCH_3), 82.19 (d, J_{PC} 6.0 Hz, 2 x OCH_2O), 128.08 (s, 6 x aromatic CH), 129.82 (s, 4 x aromatic CH), 133.81 (s, 2 x aromatic C), 164.71 (s, 2 x C=O), 169.20 ppm (s, C=O) (High resolution spectra recorded after some decomposition had occurred); m/z (FAB, nitrobenzyl alcohol matrix) 423 ($M + H^+$, 10%), 393 (15), 363 (100), 137 (15), 105 (100), 77 (49). Observed accurate mass 423.326 ($M + H^+$); $C_{19}H_{20}O_9P$ requires 423.326.

Di(2-methylbenzoyloxymethyl) (methoxycarbonylmethyl)phosphonate (44, Ar=2-$CH_3C_6H_4$). This was prepared in a similar manner to (44, Ar=C_6H_5) from iodomethyl 2-methylbenzoate (98, Ar=2-$CH_3C_6H_4$) and disilver (methoxycarbonylmethyl)phosphonate (97). Flash column chromatography (EtOAc:Hexane, 1:1, Rf 0.09 then EtOAc, Rf 0.92) gave (44, Ar=2-$CH_3C_6H_4$) as a colourless oil (40%); (Found C, 55.71; H, 5.21. $C_{21}H_{23}O_9P$ requires C, 56.01; H, 5.15); υ (thin film) 1730 (C=O), 1240 cm^{-1} (P=O); δ_H ($CDCl_3$, 300 MHz) 2.59 (6 H, s, 2 x CH_3), 3.11 (2 H, d, J_{PH} 22.2 Hz, PCH_2), 3.61 (3 H, s, OCH_3), 5.89 (2 H, d d, J_{gem} 12.1 Hz, J_{PH} 5.94 Hz, CH_AH_BO), 5.96 (2 H, d d, J_{gem} 13.1 Hz, J_{PH} 5.2 Hz, CH_AH_BO), 7.60 ppm (8 H, m, Ar); δ_P (121.5 MHz) 20.05 ppm (s), (m, ^1H coupled); δ_C (75.5 MHz) 21.81 (s, 2 x CH_3), 34.62 (d, J_{PC} 149.2 Hz, PCH_2), 52.70 (s, OCH_3), 81.90 (d, J_{PC} 5.8 Hz, 2 x OCH_2O), 125.86 (s, 2 x aromatic CH), 127.51 (s, 2 x aromatic C), 131.07 (s, 2 x aromatic CH), 131.88 (s, 2 x aromatic CH), 132.96 (s, 2 x aromatic CH), 141.52 (s, 2 x aromatic C), 165.23 ppm (s, 2 x C=O), other carbonyl not observed; m/z (FAB, nitrobenzyl alcohol matrix) 451 (M + H^+, 6%), 421 (23), 391 (100), 137 (25), 119 (100). Observed accurate mass 451.1158 (M + H^+); $C_{21}H_{24}O_9P$ requires 451.1158.

Di(2,4,6-trimethylbenzoyloxymethyl) (methoxycarbonylmethyl)phosphonate (44, Ar=2,4,6-$(CH_3)_3C_6H_2$) was prepared in a similar manner to (44, Ar=C_6H_5) from iodomethyl 2,4,6-trimethylbenzoate (98, Ar=2,4,6-$(CH_3)_3C_6H_2$) and disilver (methoxycarbonylmethyl)phosphonate (97). Flash column chromatography (EtOAc:Hexane, 1:3, Rf 0.02 then EtOAc, Rf 0.9) gave (44, Ar=2,4,6-$(CH_3)_3C_6H_2$) as a colourless oil (44%); υ (thin film) 1740 (C=O), 1250 cm^{-1} (P=O); δ_H ($CDCl_3$, 300 MHz) 2.26 - 2.28 (18 H, m, 6 x $ArCH_3$), 3.15 (2 H, d, J_{PH} 21.73 Hz, CH_2), 3.76 (3 H, s, OCH_3), 5.88 (2 H, d d, J_{gem} 12.0 Hz, J_{PH} 5.4 Hz, CH_AH_BO), 5.93 (2 H, d d, J_{gem} 12.9 Hz, J_{PH} 5.1 Hz, CH_AH_BO), 6.82 - 6.85 (4 H, m, Ar); δ_P 19.83 (s), (m, ^1H coupled); δ_C (75.5 MHz) 19.88 (s, 2 x CH_3), 20.18(s, 2 x CH_3), 21.14 (s, 2 x CH_3), 34.44 (d, J_{PC} 140.6 Hz, PCH_2), 52.73 (s, OCH_3), 82.05 (d, J_{PC} 5.3 Hz, 2 x CH_2), 128.64 (s, 4 x aromatic CH), 135.94 (s, 2 x aromatic C), 139.77 (s, 4 x aromatic C), 140.21 (s, 2 x aromatic C), 165.17 (s, 2 x C=O), 168.20 ppm (s, C=O); m/z (FAB, nitrobenzyl alcohol matrix) 529 (M + Na^+, 79%), 447 (46), 147 (100). Observed accurate mass 529.1603 (M + Na^+). $C_{25}H_{31}O_9PNa$ requires 529.1603.

4.9. Preparation of Dibenzyl (Methoxycarbonylmethyl)phosphonates

(Methoxycarbonylmethyl)phosphonic dichloride[170] **(103).** Dimethyl (methoxycarbonylmethyl)phosphonate **(102)** (22.4 g, 0.12 mol) was heated to 60 - 70°C. Solid PCl_5 (51.30 g, 0.24 mol) was added at such a rate that the temperature of the mixture was kept in the range 60 - 70°C. After addition the mixture was stirred at this temperature for 2 h. High vacuum distillation (64 - 68°C, 0.05 mm Hg) gave **(103)** as a colourless liquid (18.2 g, 0.095 mol, 79%); δ_H ($CDCl_3$, 300 MHz) 3.73 (2H, d, J_{PH} 19.1 Hz, PCH_2), 3.81 (3H, s, OCH_3); δ_P (121.5 MHz) 23.03 ppm (s), (t, J_{PH} 19.1 Hz, ^1H coupled); δ_C (75.5 MHz) 48.33 (d, J_{PC} 100.4 Hz, PCH_2), 53.46 (s, OCH_3), 162.77 ppm (d, J_{PC} 6.2 Hz, C=O).

The following compounds were prepared from (methoxycarbonylmethyl)phosphonic dichloride **(103)** and the appropriate alcohol **(51)** by a method similar to that described for dibenzyl (methoxycarbonyl)phosphonate **(38, X=H).**

Dibenzyl (methoxycarbonylmethyl)phosphonate **(39, X=H).** Flash column chromatography (EtOAc : Hexane, 2:1, Rf 0.2) gave **(39, X=H)** as a yellow oil (34%); (Elemental analysis not correct. Found: C, 58.70; H, 5.71. $C_{17}H_{19}O_5P$ requires C, 61.08; H, 5.73); υ (thin film) 1740 (C=O), 1275 cm^{-1} (P=O); δ_H ($CDCl_3$, 300 MHz) 2.97 (2 H, d, J_{PH} 21.5 Hz, PCH_2), 3.66 (3 H, s, OCH_3), 5.03 (2 H, d d, J_{gem} 12 Hz, J_{PH} 8.4 Hz, CH_AH_BO), 5.10 (2 H, d d, J_{gem} 12 Hz, J_{PH} 9.4 Hz, CH_AH_BO), 7.33 ppm (10 H, s, Ar); δ_P (121.5 MHz) 20.36 ppm (s), (m, ^1H coupled); δ_C (75.5 MHz) 34.11 (d, J_{PC} 135.8 Hz, PCH_2), 52.25 (s, OCH_3), 67.76 (d, J_{PC} 6.0 Hz, CH_2), 127.66 (s, 2 x aromatic CH), 128.27 (s, 4 x aromatic CH), 128.21 (s, 4 x aromatic CH), 135.56 (d, J_{PC} 6.0 Hz, 2 x aromatic C), 165.69 ppm (d, J_{PC} 6.0 Hz, C=O); m/z (FAB, nitrobenzyl alcohol matrix) 669 ($2M + H^+$, 12.4%), 335 ($M + H^+$, 68), 181 (24), 91 (100). Observed accurate mass 335.111 ($M + H^+$); $C_{17}H_{20}O_5P$ requires 335.111.

Di(4-nitrobenzyl) (methoxycarbonylmethyl)phosphonate **(39, X=NO_2).** Flash column chromatography (EtOAc, Rf 0.29) gave **(39, X=NO_2)** as a colourless solid (11%); (Found: C, 48.53; H, 3.84; N, 5.96. $C_{17}H_{17}N_2O_9P$ requires C, 48.12; H, 4.04; N, 6.60); mp 76 - 78°C; δ_H ($CDCl_3$, 300 MHz) 3.12 (2 H, d, J_{PH} 21.4 Hz, CH_2), 3.74 (3 H, s, OCH_3), 5.18 (2 H, d d, J_{gem} 12.2 Hz, J_{PH} 8.9 Hz, CH_AH_BO), 5.23 (2 H, d d, J_{gem} 12.2 Hz, J_{PH} 8.9 Hz, CH_AH_BO), 8.20 (4 H, d, J_{HH} 4.1 Hz, Ar), 8.23 ppm (4 H, d, J_{HH} 4.2 Hz, Ar); δ_P (121.5 MHz) 21.52 ppm (s), (m, ^1H coupled); δ_C (75.5 MHz) 34.11 (d, J_{PC} 37.4 Hz, PCH_2), 52.80 (s, OCH_3), 66.60 (d, J_{PC} 6.7 Hz, 2 x CH_2), 123.80 (s,

4 x aromatic CH), 127.97 (s, 4 x aromatic CH), 142.60 (d, J_{PC} 6.6Hz, 2 x aromatic C), 147.86 (s, 2 x aromatic C), 165.53 (d, J_{PC} 5.7 Hz, C=O).

Attempted synthesis of *bis(4-methoxybenzyl) (methoxycarbonylmethyl)phosphonate* **(39, X=CH_3O).** The synthesis of **(39, X=CH_3O)** was attempted in a similar way to **(38, X=CH_3O)** from 4-methoxybenzyl alcohol and (methoxycarbonylmethyl)phosphonic dichloride. However, **(39, X=CH_3O)** could not be isolated and the reaction gave di(4-methoxybenzyl)ether **(57)** with data similar to that described for the attempted preparation of **(38, X=CH_3O).**

4.10. Preparation of Di(4-alkanoyloxybenzyl) (Methoxycarbonylmethyl)-phosphonates

The following compounds were prepared from (methoxycarbonylmethyl)phosphonic dichloride **(103)** and the appropriate alkanoyloxybenzyl alcohol **(51)** by a method similar to that described for dibenzyl (methoxycarbonyl)phosphonate **(38, X=H).**

Di(4-ethanoyloxybenzyl) (methoxycarbonylmethyl)phosphonate **(93, R=CH_3).** Flash column chromatography (EtOAc, Rf = 0.33) gave **(93, R=CH_3)** as a colourless oil (15%); (Elemental analysis not correct. Found: C, 54.15; H, 4.77. $C_{21}H_{23}O_9P$ requires C, 55.95; H, 5.15); υ (thin film) 1740 (C=O), 1200 cm^{-1} (P=O); δ_H ($CDCl_3$, 250.1 MHz) 2.29 (6 H, s, 2 x CH_3), 3.00 (2 H, d, J_{PH} 21.5 Hz, PCH_2), 3.69 (3 H, s, OCH_3), 5.02 (2 H, d d, J_{gem} 11.8, J_{PH} 9.6 Hz, CH_AH_BO), 5.09 (2 H, d d, J_{gem} 11.8, J_{PH} 9.6 Hz, CH_AH_BO), 7.08 (4 H, d, J_{HH} 9.2 Hz, Ar), 7.38 ppm (4 H, d, J_{HH} 9.2 Hz, Ar); δ_P (101.3 MHz) 21.22 ppm (s), (m, ^1H coupled); δ_C (62.9 MHz) 14.08 (s, 2 x CH_3), 27.38 (d, J_{PC} 136.4 Hz, PCH_2), 45.61 (s, OCH_3), 60.42 (d, J_{PC} 6.1 Hz, 2 x CH_2O), 114.79 (s, 4 x aromatic CH), 122.21 (s, 4 x aromatic CH), 126.38 (d, J_{PC} 6.2 Hz, 2 x aromatic C), 143.73 (s, 2 x aromatic C), 162.27 (s, C=O), 163.78 ppm (s, C=O); m/z (FAB, nitrobenzyl alcohol matrix) 451 ($M + H^+$, 22%), 345 (35), 303 (25), 149 (54), 136 (40), 107 (100). Observed accurate mass 451.1158 ($M + H^+$); $C_{21}H_{24}O_9P$ requires 451.1158.

Di(4-propanoyloxybenzyl)(methoxycarbonylmethyl)phosphonate **(93, R=CH_3CH_2).** Flash column chromatography (EtOAc : Hexane, 1:1, Rf 0.30) gave **(93, R=CH_3CH_2)** as a colourless oil (18%); (Found: C, 57.50; H, 5.75. $C_{23}H_{27}O_9P$ requires C, 57.75; H, 5.69); υ (thin film) 1773 (C=O), 1211 cm^{-1} (P=O); δ_H ($CDCl_3$, 250.1 MHz) 1.24 (6 H, t, J_{HH} 7.5 Hz, 2 x CH_3), 2.57 (4 H, q, J_{HH} 7.6 Hz, 2 x CH_2CO), 2.99 (2 H, d, J_{PH} 21.5

Hz, CH_2), 3.66 (3 H, s, OCH_3), 5.01 (2 H, d d, J_{gem} 11.8, J_{PH} 8.9 Hz, CH_AH_BO), 5.06 (2 H, d d, J_{gem} 11.8, J_{PH} 8.9 Hz, CH_AH_BO), 7.06 (4 H, d, J_{HH} 8.5 Hz, Ar), 7.34 ppm (4 H, d, J_{HH} 8.5 Hz, Ar); δ_P (101.3 MHz) 21.19 ppm (s), (m, ^1H coupled); δ_C (62.9 MHz) 8.91 (s, 2 x CH_3), 27.59 (s, 2 x CH_2), 34.31 (d, J_{PC} 136.2 Hz, PCH_2), 52.51 (s, OCH_3), 67.37 (d, J_{PC} 6.2 Hz, 2 x CH_2), 121.70 (s, 4 x aromatic CH), 129.11 (s, 4 x aromatic CH), 133.19 (d, J_{PC} 6.2 Hz, 2 x aromatic C), 150.78 (s, 2 x aromatic C), 165.82 (d, J_{PC} 5.7 Hz, C=O), 172.65 ppm (s, 2 x C=O); m/z (FAB, nitrobenzyl alcohol matrix) 479 ($M + H^+$, 26%), 317 (54), 163 (100), 135 (54). Observed accurate mass 479.1471 ($M + H^+$); $C_{23}H_{28}O_9P$ requires 479.1471.

Di(4-n-butanoyloxybenzyl) (methoxycarbonylmethyl)phosphonate (**93, R=$CH_3(CH_2)_2$**). Flash column chromatography (EtOAc : Hexane, 2:1, Rf 0.43) gave (**93, R=$CH_3(CH_2)_2$**) as a cream coloured solid (17%); (Found: C, 59.02; H, 5.97. $C_{25}H_{31}O_9P$ requires C, 59.30; H, 6.17); υ (Nujol) 1767 (C=O), 1298 cm^{-1} (P=O); δ_H ($CDCl_3$, 250.1 MHz) 0.98 (6 H, t, J_{HH} 7.4 Hz, 2 x CH_3), 1.70 (4 H, t q, J_{HH} 7.3 Hz, 2 x CH_2), 2.47 (4 H, t, J_{HH} 7.3 Hz, 2 x CH_2), 2.94 (2 H, d, J_{PH} 21.5 Hz, PCH_2), 3.61 (3 H, s, OCH_3), 4.95 (2 H, d d, J_{gem} 11.8 Hz, J_{PH} 8.5 Hz, CH_AH_BO), 5.03 (2 H, d d, J_{gem} 11.8 Hz, J_{PH} 8.2 Hz, CH_AH_BO), 7.02 (4 H, d, J_{HH} 8.5 Hz, Ar), 7.29 ppm (4 H, d, J_{HH} 8.5 Hz, Ar); δ_P (101.3 MHz) 21.20 ppm (s), (m, ^1H coupled); δ_C (62.9 MHz) 13.45 (s, 2 x CH_3), 18.22 (s, 2 x CH_2), 34.18 (d, J_{PC} 136.0 Hz, PCH_2), 35.95 (s, 2 x CH_2CO), 52.41 (s, OCH_3), 67.30 (d, J_{PC} 6.1 Hz, 2 x CH_2O), 121.68 (s, 4 x aromatic CH), 129.06 (s, 4 x aromatic CH), 133.19 (d, J_{PC} 6.1 Hz, 2 x aromatic C), 150.70 (s, 2 x aromatic C), 165.77 (d, J_{PC} 5.7 Hz, C=O), 171.71 ppm (s, 2 x C=O); m/z (FAB, nitrobenzyl alcohol matrix) 507 ($M + H^+$, 9%), 437 (2), 331 (35), 225 (96), 177 (100). Observed accurate mass 507.1784 ($M + H^+$); $C_{25}H_{32}O_9P$ requires 507.1784.

Di(4-iso-butanoyloxybenzyl) (methoxycarbonylmethyl)phosphonate (**93, R=$(CH_3)_2CH$**). Flash column chromatography (EtOAc : Hexane, 2:1, Rf=0.29) gave (**93, R=$(CH_3)_2CH$**) as a cream coloured solid (23%); (Found: C, 59.20; H, 6.15. $C_{25}H_{31}O_9P$ requires C, 59.30; H, 6.17); υ (Nujol) 1760 (C=O), 1729 (C=O), 1267 cm^{-1} (P=O); δ_H ($CDCl_3$, 250.1 MHz) 1.30 (12 H, d, J_{HH} 6.9 Hz, 2 x $(CH_3)_2$), 2.70 (2 H, septet, J_{HH} 7.0 Hz, 2 x CH), 2.99 (2 H, d, J_{PH} 21.5 Hz, PCH_2), 3.67 (3 H, s, OCH_3), 5.01 (2 H, d d, J_{gem} 11.8 Hz, J_{PH} 8.6 Hz, CH_AH_BO), 5.08 (2 H, d d, J_{gem} 11.8 Hz, J_{PH} 8.6 Hz, CH_AH_BO), 7.04 (4 H, d, J_{HH} 8.5 Hz, Ar), 7.34 ppm (4 H, d, J_{HH} 8.5 Hz, Ar); δ_P (101.3 MHz) 21.17 ppm (s), (m, ^1H coupled); δ_C (62.9 MHz) 18.78 (s, 2 x $(CH_3)_2$), 34.02 (s, 2 x CH), 34.32 (d, J_{PC} 136.2 Hz, PCH_2), 52.52 (s, OCH_3), 67.39 (d, J_{PC} 6.2 Hz, 2 x CH_2), 121.66 (s, 4 x aromatic CH), 129.11 (s, 4 x aromatic CH), 133.14 (d, J_{PC} 6.2 Hz, 2 x aromatic C), 150.90 (s, 2 x aromatic C), 165.83 (d, J_{PC} 5.7 Hz, C=O),

175.31 ppm (s, 2 x C=O); m/z (FAB, nitrobenzyl alcohol matrix) 507 (M + H^+, 11%), 435 (3), 329 (21), 225 (80), 177 (100), 149 (78). Observed accurate mass 507.1784 (M + H^+); $C_{25}H_{32}O_9P$ requires 507.1784.

Di(4-pivaloyloxybenzyl) (methoxycarbonylmethyl)phosphonate (**93, R=$(CH_3)_3C$**). Flash column chromatography (EtOAc : Hexane, 1:1, Rf 0.61) gave (**93, R=$(CH_3)_3C$** as a colourless solid which was recrystallised from toluene : hexane, 1:1 (19%); mp 91 - 92 °C; (Found: C, 60.94; H, 6.38. $C_{27}H_{35}O_9P$ requires C, 60.65; H, 6.60); υ (Nujol) 1754 (C=O), 1722 (C=O), 1248 cm^{-1} (P=O); δ_H ($CDCl_3$, 250.1 MHz) 1.36 (18 H, s, 2 x $(CH_3)_3$), 3.00 (2 H, d, J_{PH} 21.5 Hz, PCH_2), 3.69 (3 H, s, OCH_3), 5.03 (2 H, d d, J_{gem} 11.8 Hz, J_{PH} 8.3 Hz, CH_AH_BO), 5.11 (2 H, d d, J_{gem} 11.7 Hz, J_{PH} 8.4 Hz, CH_AH_BO), 7.05 (4 H, d, J_{HH} 8.5 Hz, Ar), 7.36 ppm (4 H, d, J_{HH} 8.5 Hz, Ar); δ_P (101.3 MHz) 21.18 ppm (s), (m, ^1H coupled); δ_C (62.9 Hz) 27.00 (s, 2 x $(CH_3)_3$), 34.36 (d, J_{PC} 136.2 Hz, PCH_2), 38.98 (s, 2 x $(CH_3)_3\underline{C}$), 52.55 (s, OCH_3), 67.45 (d, J_{PC} 6.2 Hz, 2 x CH_2), 121.66 (s, 4 x aromatic CH), 129.11 (s, 4 x aromatic CH), 133.07 (d, J_{PC} 6.2 Hz, 2 x aromatic C), 151.15 (s, 2 x aromatic C), 165.85 (d, J_{PC} 5.8 Hz, C=O), 176.84 ppm (s, 2 x C=O); m/z (FAB, nitrobenzyl alcohol matrix) 535 (M + H^+, 6%), 343 (9), 207 (4), 191 (85), 155 (23), 107 (100), 85 (38), 57 (100). Observed accurate mass 535.2100 (M + H^+); $C_{27}H_{36}O_9P$ requires 535.2100.

Di(4-pentanoyloxybenzyl) (methoxycarbonylmethyl)phosphonate (**93, R=$CH_3(CH_2)_3$**). Flash column chromatography (EtOAc, Rf 0.83) gave (**93, R=$CH_3(CH_2)_3$**) as a colourless oil (19%); (Found: C, 60.78; H, 6.43. $C_{27}H_{36}O_9P$ requires C, 60.65; H, 6.60); δ_H ($CDCl_3$, 250 MHz) 0.96 (6 H, t, J_{HH} 7.3 Hz, 2 x CH_3), 1.43 (4 H, t q, J_{HH} 7.6 Hz, 2 x CH_2), 1.73 (4 H, t t, J_{HH} 7.3 Hz, 2 x CH_2), 2.55 (4 H, t, J_{HH} 7.6 Hz, 2 x CH_2), 2.99 (2 H, d, J_{PC} 21.5 Hz, PCH_2), 3.67 (3 H, s, OCH_3), 4.98 (2 H, d d, J_{gem} 11.8 Hz, J_{PH} ~8 Hz, CH_AH_BO), 5.09 (2 H, d d, J_{gem} 11.8 Hz, J_{PH} ~8 Hz, CH_AH_BO), 7.06 (4 H, d, J_{HH} 8.5 Hz, Ar), 7.34 ppm (4 H, d, J_{HH} 8.5 Hz, Ar); δ_P (101.3 MHz) 21.19 ppm (s), (m, ^1H coupled); δ_C (62.9 MHz) 13.61 (s, 2 x CH_3), 22.11 (s, 2 x CH_2), 26.84 (s, 2 x CH_2), 33.96 (s, 2 x CH_2CO), 34.22 (d, J_{PC} 136.8 Hz, PCH_2), 52.58 (s, OCH_3), 67.59 (d, J_{PC} 6.2 Hz, 2 x CH_2O), 121.75 (s, 4 x aromatic CH), 128.94 (s, 4 x aromatic CH), 133.06 (d, J_{PC} 6.2 Hz, 2 x aromatic C), 150.80 (s, 2 x aromatic C), 165.76 (d, J_{PC} 5.7 Hz, C=O), 172.15 ppm (s, 2 x C=O); m/z (FAB, nitrobenzyl alcohol matrix) 535 (M + H^+, 18%), 451 (8), 345 (54), 239 (100); Observed accurate mass 535.2097 (M + H^+). $C_{27}H_{37}O_9P$ requires 535.2097.

Di(4-hexanoyloxybenzyl) (methoxycarbonylmethyl)phosphonate (**93, R=$CH_3(CH_2)_4$**). Flash column chromatography (EtOAc : Hexane, 1:1, Rf 0.46) gave (**93,**

R=$CH_3(CH_2)_4$) as a colourless oil (5%); (Insufficient sample for precise analysis. Found: C, 61.1; H, 6.5. $C_{29}H_{39}O_9P$ requires C, 61.92; H, 6.99); υ (thin film) 1735 (C=O), 1210 cm^{-1} (P=O); δ_H ($CDCl_3$, 250.1 MHz) 0.90 (6 H, t, J_{HH} 6.7 Hz, 2 x CH_3), 1.35 - 1.77 (12 H, m, 6 x CH_2), 2.54 (4 H, t, J_{HH} 7.4 Hz, 2 x CH_2), 2.98 (2 H, d, J_{PH} 21.5 Hz, PCH_2), 3.67 (3 H, s, OCH_3), 4.99 (2 H, d d, J_{gem} 11.7 Hz, J_{PH} ~8 Hz, CH_AH_BO), 5.10 (2 H, d d, J_{gem} 11.7 Hz, J_{PH} ~8 Hz, CH_AH_BO), 7.06 (4 H, d, J_{HH} 8.4 Hz, Ar), 7.35 ppm (4 H, d, J_{HH} 8.4 Hz, Ar); δ_P (101.3 MHz) 21.17 ppm (s), (m, ^1H coupled); δ_C (62.9 MHz) 13.81 (s, 2 x CH_3), 22.21 (s, 2 x CH_2), 24.48 (s, 2 x CH_2), 31.15 (s, 2 x CH_2), 34.24 (s, 2 x CH_2), 34.53 (d, J_{PC} 136.2 Hz, PCH_2), 52.56 (s, OCH_3), 67.41 (d, J_{PC} 6.2 Hz, 2 x CH_2O), 121.75 (s, 4 x aromatic CH), 129.14 (s, 4 x aromatic CH), 133.18 (d, J_{PC} 6.3 Hz, 2 x aromatic C), 150.78 (s, 2 x aromatic C), 172.07 ppm (s, 2 x C=O), other carbonyl not detected; m/z (FAB, nitrobenzyl alcohol matrix) 563 (M + H^+, 7%), 311 (9), 205 (60), 177 (28), 155 (67). Observed accurate mass 563.2410 (M + H^+); $C_{29}H_{40}O_9P$ requires 563.2410.

4.11. Preparation of Lithium 4-Alkanoyloxybenzyl (Methoxycarbonylmethyl)-phosphonates

Lithium 4-ethanoyloxybenzyl (methoxycarbonylmethyl)phosphonate (**104, R=CH_3**). Lithium iodide (0.054 g, 0.41 mmol) was added to a solution of di(4-ethanoyloxybenzyl) (methoxycarbonylmethyl)phosphonate (**93, R=CH_3**) (0.18 g, 0.41 mmol) in ether : acetone, 6:4 (2.0 ml) and the reaction mixture stirred for 72 hours at room temperature. The resulting solid was purified by dissolution in water and precipitation by the addition of ether to give (**104, R=CH_3**) as a colourless solid (0.10g, 0.33 mmol, 81%); mp 204 - 206 °C; (Elemental analysis not correct. Found: C, 45.28; H, 4.25. $C_{12}H_{14}O_7PLi$ requires C, 46.78; H, 4.58); υ (Nujol) 1754 (C=O), 1211 cm^{-1} (P=O); δ_H (D_2O, 250.1 MHz) 2.25 (3 H, s, CH_3), 2.79 (2 H, d, J_{PH} 20.4 Hz, PCH_2), 3.58 (3 H, s, OCH_3), 4.86 (2 H, d, J_{PH} 7.3 Hz, CH_2), 7.08 (2 H, d, J_{HH} 8.5 Hz, Ar), 7.40 ppm (2 H, d, J_{HH} 8.5 Hz, Ar); δ_P (101.3 MHz) 15.27 ppm (s), (t t, J_{PH} 20.3, 7.3 Hz, ^1H coupled); δ_C (62.9 MHz) 23.41 (s, CH_3), 38.12 (d, J_{PC} 120.8 Hz, PCH_2), 55.58 (s, OCH_3), 69.14 (d, J_{PC} 5.3 Hz, OCH_2), 124.74 (s, 2 x aromatic CH), 132.04 (s, 2 x aromatic CH), 138.65 (d, J_{PC} 6.7 Hz, aromatic C), 152.81 (s, aromatic C), 173.87 (d, J_{PC} 6.3 Hz, C=O), 176.50 ppm (s, C=O); m/z (FAB, nitrobenzyl alcohol matrix) 315 (M + Li^+, 100%), 259 (10), 167 (50), 136 (16). Observed accurate mass 309.0715 (M + H^+); $C_{12}H_{15}O_7PLi$ requires 309.07155.

The following compounds were prepared as colourless solids by the reaction of lithium iodide with the appropriate phosphonate triester using a method similar to that described above:

Lithium 4-propanoyloxybenzyl (methoxycarbonylmethyl)phosphonate (**104, R=CH_3CH_2**) (73%); mp 187 - 188 °C; (Elemental analysis not correct. Found: C, 44.94; H, 4.78; $C_{13}H_{16}O_7PLi$ requires C, 48.47; H, 5.01); υ (Nujol) 1760 (C=O), 1704 (C=O), 1205 cm^{-1} (P=O); δ_H (D_2O, 250.1 MHz) 1.19 (3H, t, J_{HH} 7.5 Hz, CH_3), 2.66 (2H, q, J_{HH} 7.5 Hz, CH_2), 2.88 (2H, d, J_{PH} 20.4 Hz, PCH_2), 3.66 (3H, s, OCH_3), 4.95 (2H, d, J_{PH} 7.5 Hz, CH_2), 7.15 (2H, d, J_{HH} 8.4 Hz, Ar), 7.48 ppm (2H, d, J_{HH} 8.4 Hz, Ar); δ_P (101.3 MHz) 15.58 ppm (s), (t t, J_{PH} 20.4, 7.4 Hz, ^1H coupled); δ_C (62.9 MHz) 11.17 (s, CH_3), 30.34 (s, CH_2), 38.12 (d, J_{PC} 120.8 Hz, PCH_2), 55.58 (s, OCH_3), 69.15 (d, J_{PC} 5.6 Hz, CH_2), 124.74 (s, 2 x aromatic CH), 132.04 (s, 2 x aromatic CH), 138.52 (s, aromatic C), 152.87 (s, aromatic C), 179.89 ppm (s, C=O), other carbonyl not detected; m/z (FAB, nitrobenzyl alcohol matrix) 329 (M + Li^+, 100%), 323 (M + H^+, 6), 259 (7), 167 (38), 136 (11). Observed accurate mass 323.0872 (M + H^+); $C_{13}H_{17}O_7PLi$ requires 323.0872.

Lithium 4-n-butanoyloxybenzyl (methoxycarbonylmethyl)phosphonate (**104, R=$CH_3(CH_2)_2$**) (68 %); mp 189 - 190°C; (Elemental analysis not correct. Found: C, 48.77; H, 5.33; $C_{14}H_{18}O_7PLi$ requires C, 50.02; H, 5.40); υ (Nujol) 1760 (C=O), 1697 (C=O), 1211 cm^{-1} (P=O); δ_H (D_2O, 250.1 MHz) 1.00 (3H, t. J_{HH} 7.4 Hz, CH_3), 1.74 (2H, t q, J_{HH} 7.3 Hz, CH_2), 2.63 (2H, t, J_{HH} 7.3 Hz, CH_2), 2.89 (2H, d, J_{PH} 20.4 Hz, PCH_2), 3.66 (3H, s, OCH_3), 4.95 (2H, d, J_{PH} 7.5 Hz, CH_2), 7.15 (2H, d, J_{HH} 8.4 Hz, Ar), 7.49 ppm (2H, d, J_{HH} 8.4 Hz, Ar); δ_P (101.3 MHz) 15.80 ppm (s), (t t, J_{PH} 20.4, 7.5 Hz, ^1H coupled); δ_C (62.9 MHz) 15.76 (s, CH_3), 20.90 (s, CH_2), 38.11 (d, J_{PC} 120.6 Hz, PCH_2), 38.66 (s, CH_2), 55.57 (s, OCH_3), 69.13 (d, J_{PC} 5.2 Hz, CH_2), 124.74 (s, 2 x aromatic CH), 132.04 (s, 2 x aromatic CH), 138.61 (d, J_{PC} 6.3 Hz, aromatic C), 152.80 (s, aromatic C), 179.08 ppm (s, C=O), other carbonyl not detected; m/z (FAB, nitrobenzyl alcohol matrix) 343 (M + Li^+, 100%), 337 (M + H^+, 2), 309 (9), 259 (8), 167 (44), 136 (7). Observed accurate mass 337.1028 (M + H^+); $C_{14}H_{19}O_7PLi$ requires 337.1028.

Lithium 4-iso-butanoyloxybenzyl (methoxycarbonylmethyl)phosphonate (**104, R=$(CH_3)_2CH$**). (35%); mp 202 - 204°C; (Elemental analysis not correct. Found: C, 45.05; H, 5.51. $C_{14}H_{18}O_7PLi$ requires C, 50.02; H, 5.40); δ_H (D_2O, 250.1 MHz) 1.28 (6 H, d, J_{HH} 7.0 Hz, $(CH_3)_2$), 2.88 (1 H, sept, J_{HH} 7.0 Hz, CH), 2.88 (2 H, d, J_{PH} 20.4 Hz, PCH_2), 3.66 (3 H, s, OCH_3), 4.95 (2 H, d, J_{PH} 7.5 Hz, CH_2O), 7.14 (2 H, d, J_{HH}

8.5 Hz, Ar), 7.48 ppm (2 H, d, J_{HH} 8.5 Hz, Ar); δ_P (101.3 MHz) 15.57 ppm (s), (t t, J_{PH} 20.5, 7.5 Hz, ^1H coupled); δ_C (62.9 MHz) 21.05 (s, $(CH_3)_2$), 36.89 (s, CH), 38.12 (d, J_{PC} 121.0 Hz, PCH_2), 55.57 (s, OCH_3), 69.14 (d, J_{PC} 5.3 Hz, CH_2O), 124.66 (s, 2 x aromatic CH), 132.05 (s, 2 x aromatic CH), 138.54 (s, aromatic C), 152.92 (s, aromatic C), 165.05 (s, C=O), 182.61 ppm (s, C=O); m/z (FAB, nitrobenzyl alcohol matrix) 343 (M + Li^+, 100%), 337 (M + H^+, 2), 259 (15), 167 (74). Observed accurate mass 337.1028 (M + H^+); $C_{14}H_{19}O_7PLi$ requires 337.1028.

Lithium 4-pivaloyloxybenzyl (methoxycarbonylmethyl)phosphonate (**104, R=$(CH_3)_3C$**). (85%); mp 221 - 222°C; (Elemental analysis not correct. Found: C, 50.70; H, 5.62. $C_{15}H_{20}O_7PLi$ requires C, 51.56; H, 5.77); υ (Nujol) 1747 (C=O), 1704 (C=O), 1186 cm^{-1} (P=O); δ_H (D_2O, 250.1 MHz) 1.27 (9 H, s, $(CH_3)_3$), 2.81 (2 H, d, J_{PH} 20.4 Hz, PCH_2), 3.58 (3 H, s, OCH_3), 4.87 (2 H, d, J_{PH} 7.5 Hz, CH_2O), 7.06 (2 H, d, J_{HH} 8.3 Hz, Ar), 7.41 ppm (2 H, d, J_{HH} 8.4 Hz, Ar); δ_P (101.3 MHz) 15.56 ppm (s), (t t, J_{PH} 20.3, 7.2 Hz, ^1H coupled); δ_C (62.9 MHz) 29.48 (s, $(CH_3)_3$), 38.13 (d, J_{PC} 120.8 Hz, PCH_2), 41.80 (s, $(CH_3)_3\underline{C}$), 55.59 (s, OCH_3), 69.15 (d, J_{PC} 5.3 Hz, CH_2), 124.64 (s, 2 x aromatic CH), 132.09 (s, 2 x aromatic CH), 138.55 (d, J_{PC} 6.9 Hz, aromatic C), 153.20 (s, aromatic C), 173.86 (d, J_{PC} 6.3 Hz, C=O), 184.08 ppm (s, C=O); m/z (FAB, nitrobenzyl alcohol matrix) 357 (M + Li^+, 100%), 337 (5), 309 (14), 209 (8), 149 (28). Observed accurate mass 357.1267 (M + Li^+); $C_{15}H_{20}O_7PLi_2$ requires 357.1267.

Lithium 4-pentanoyloxybenzyl (methoxycarbonylmethyl)phosphonate (**104, R=$CH_3(CH_2)_3$**). (46%); mp 177.0-179°C; δ_H (D_2O, 250.1 MHz) 0.92 (3 H, t, J_{HH} 7.2 Hz, CH_3), 1.39 (2 H, sextet, J_{HH} 7.4 Hz, CH_2), 1.70 (2 H, pent, J_{HH} 7.2 Hz, CH_2), 2.65 (2 H, t, J_{HH} 7.4 Hz, CH_2CO), 2.88 (2 H, d, J_{PH} 20.4 Hz, PCH_2), 3.66 (3 H, s, OCH_3), 4.95 (2 H, d, J_{PH} 7.5 Hz, CH_2O), 7.14 (2 H, d, J_{HH} 8.4 Hz, Ar), 7.48 ppm (2 H, d, J_{HH} 8.3 Hz, Ar); δ_P (101.3 MHz) 15.57 ppm (s), (t t, J_{PH} 20.5, 7.6 Hz, ^1H coupled); δ_C (62.9 MHz) 15.94 (s, CH_3), 24.55 (s, CH_2), 29.38 (s, CH_2), 36.54 (s, CH_2), 38.12 (d, J_{PC} 121.1 Hz, PCH_2), 55.58 (s, OCH_3), 69.15 (d, J_{PC} 5.4 Hz, CH_2), 124.75 (s, 2 x aromatic CH), 132.06 (s, 2 x aromatic CH), 138.62 (d, J_{PC} 6.7 Hz, aromatic C), 152.83 (s, aromatic C), 173.92 (s, C=O), 179.37 ppm (s, C=O); m/z (FAB, nitrobenzyl alcohol matrix) 357 (M + Li^+, 100%), 309 (44), 259 (43), 167 (100), 136 (29). Observed accurate mass 357.1332 (M + Li^+); $C_{15}H_{20}O_7PLi_2$ requires 357.1267.

4.12. Preparation of Disodium (Methoxycarbonylmethyl)phosphonate

Disodium (methoxycarbonylmethyl)phosphonate **(105)**. A solution of $NaHCO_3$ (3.02 g, 0.036 mol) in 75 ml H_2O was added dropwise to a solution of bis(trimethylsilyl) (methoxycarbonylmethyl)phosphonate (5.45 g, 0.018 mol) in acetone (75 ml) and left to stir at room temperature for 48 h. The mixture was concentrated to give a cream-coloured solid, which was re-dissolved in water and precipitated by the addition of diethyl ether to give **(105)** as a colourless solid (2.8 g, 0.014 mol, 79%); δ_H (CD_3CN : D_2O, 1:1, 250.1 MHz) 2.52 (2 H, d, J_{PH} 19.3 Hz, PCH_2), 3.53 ppm (3 H, s, OCH_3); δ_P (101.3 MHz) 11.35 ppm (s), (t, J_{PH} 19.3 Hz, ^1H coupled); δ_C (62.9 MHz) 40.78 (d, J_{PC} 108.6 Hz, PCH_2), 55.15 (s, OCH_3), 176.77 ppm (d, J_{PC} 6.1 Hz, C=O).

CHAPTER 5 - STABILITY AND ACTIVATION STUDIES

5.1. Hydrolysis of Triesters of Phosphonoformate (38) Monitored by HPLC

High pressure liquid chromatography (HPLC) was performed using a Waters 600E gradient solvent delivery system fitted with a Merck reversed-phase C-18 endcapped Lichrospher 100 column (particle size 5μm; 250 x 4 mm), Lichrocart reverse phase C-18 endcapped guard column and monitored by UV at λ_{max} 254 nm using a Waters 484 Tunable Absorbance Detector. Hydrolysis samples (20 μl) were injected directly via a Waters 700 Satellite WISP and eluted with a linear or convex (Waters pre-programmed gradient curves 4 and 5, as required) gradient of acetonitrile : 10 mM tetrabutylammonium chloride in water (flow rate 1 ml min^{-1}), initial conditions, 35 : 65 (v/v); final conditions, 90 : 10 (v/v); gradient time 20 min. Convex gradient type was selected to ensure elution of the triester within the 20 minute gradient time. Chromatograms were recorded on a Waters 745B integrator.

Hydrolyses were performed in glass screw-capped vials using a total volume of 1 ml and a final concentration of triester of 100 μg ml^{-1} or 400 μg ml^{-1}. A mixture of acetonitrile : 0.1 M phosphate buffer (pH 7.4) (1 : 1, v/v) was pre-incubated at 37°C for 10 min. Hydrolysis was initiated by the addition of an acetonitrile solution of triester (50 μl) to give the required final concentration and then incubated at 37°C in a shaking water bath. At the appropriate time the incubation was removed from the water bath and the solution was used directly for HPLC analysis. The HPLC analysis time (20 min) necessitated individual hydrolysis experiments for each time point. Hydrolyses were monitored for approximately 2-3 half-lives. Control experiments were performed in neat acetonitrile.

5.2. Hydrolysis of Dibenzyl (Methoxycarbonyl)phosphonate (38, X=H) Followed by ^{31}P NMR Spectroscopy

The triester (38, X=H) (6.0 mg, 18.75 μmol) was dissolved in CD_3CN (0.5 ml) and its ^{31}P NMR (101.3 MHz) spectrum recorded with the NMR probe at 36.4 °C [δ_P -3.75 ppm (s)]. Phosphate buffer (0.1 M, pH 7.4, 0.5 ml, pre-incubated at 37°C) was added to the triester solution. ^{31}P NMR (101.3 MHz) spectra were recorded every 4.25 min for the first 45 min, then at t=1, 1.25, 1.5, 2, 2.5, 3, 4, 5 and 6 h. The reaction mixture was left to stand in the NMR tube for 2 weeks at room temperature, after which time the decoupled and ^{1}H coupled spectra were recorded and the pH of the mixture measured to

be 7.2. This reduction in pH was confirmed by a change in the chemical shift of the inorganic phosphate buffer from 2.50 to 1.63 ppm.

To confirm the identity of the hydrolysis products, authentic samples of diester (**61, X=H**), dibenzyl phosphite (**63**), sodium monobenzyl phosphite (**64**), sodium dibenzyl diester (**65**) and dibenzyl phosphate (**66**) were added to the reaction mixture resulting in an increase in size of the appropriate peak. Each FID was transformed with a line broadening of 1 Hz and the area of each peak calculated from its width at half-height. To evaluate the ^{31}P NMR response of each component type known quantities (~ 10 μmol) of the hydrolytically stable diester (**61, X=H**), monobenzyl phosphite (**64**) and dibenzyl phosphate (**66**) were dissolved in CD_3CN - D_2O phosphate buffer (0.1 M, pH 7.4, pD 8.0) (1:1, v/v). The assumption was made that monobenzyl phosphite (**64**) and dibenzyl phosphite (**63**) have identical responses, as do the triester (**38, X=H**) and the diesters (**61, X=H, 65**). ^1H NMR (250.1 MHz) spectroscopy confirmed the ratios from the weights, however, under identical spectrometer conditions to the kinetics experiment, the ^{31}P NMR spectrum showed that monobenzyl phosphite (**64**) had an area response 1.55 times greater than the diester (**61, X=H**) and dibenzyl phosphate (**66**) had an area response 1.1 times greater than the diester (**61, X=H**). These factors were applied to the data and the percentage of the components present at each time point calculated.

The ^{31}P NMR (101.3 MHz) chemical shifts of the hydrolysis products were constant throughout the experiment: Triester (**38, X=H**) -3.70 ppm (s), (pent q, J_{PH} 8.5, 1.0 Hz, ^1H coupled); Diester (**61, X=H**) -4.71 ppm (s), (t q, J_{PH} 7.2, 0.9 Hz, ^1H coupled); Dibenzyl phosphite (**63**) 10.82 ppm (s), (d pent, J_{PH} 719, 9.6 Hz, ^1H coupled); Benzyl phosphite (**64**) 5.90 ppm (s), (d t, J_{PH} 625, 8.3 Hz, ^1H coupled); Diester (**65**) -4.97 ppm (s), (t, J_{PH} 6.7 Hz, ^1H coupled); Dibenzyl phosphate (**66**) 1.07 ppm (s), (pent, J_{PH} 6.7 Hz, ^1H coupled).

5.3. Control Reaction Between Benzyl Alcohol and the Triester (38, X=H)

Benzyl alcohol (1.35 mg, 12.5 μmol) was added to a sample vial containing MeCN - phosphate buffer (0.1 M, pH 7.4) (0.95 ml, 1:1, v/v, pre-incubated at 37°C). An acetonitrile solution (0.05 ml) of the triester (**38, X=H**) (0.4 mg, 1.25 μmol) was added to this mixture and the reaction monitored by HPLC every 30 min for 4 h.

5.4. Hydrolysis of Dibenzyl Phosphite (63)

Dibenzyl phosphite (**63**) (4.0 mg, 15.0 μmol) was added to a solution of CD_3CN - phosphate buffer (0.1 M, pH 7.4) (1.0 ml, 1:1, v/v) and the ^{31}P NMR (101.3 MHz) spectrum run, δ_P 10.95 ppm (s). The mixture was incubated at 37°C for 24 h, after which time the only product detected by ^{31}P NMR spectroscopy was monobenzyl phosphite (**64**), δ_P 6.08 ppm (s). Dibenzyl phosphate (**66**) was <u>not</u> detected.

5.5. Large Scale Hydrolysis of the Triester (38, X=H): Isolation of Dibenzyl Phosphite (63), Benzyl (Benzyloxycarbonyl)phosphonate (65) and Dibenzyl Phosphate (66)

A solution of the triester (**38, X=H**) (0.3g, 0.94 mmol) in MeCN (10 ml) was added dropwise to a mixture of MeCN - 0.1 M phosphate buffer (pH 7.4) (150 ml, 1:1, v/v, pre-incubated at 37°C). The mixture was monitored by HPLC and after complete hydrolysis of the triester, the volume was reduced to approximately 100 ml (contains ~ 30% MeCN). A sample of this (30 ml) was applied to an activated 1g C-18 Bond-Elut solid phase extraction column. The column was washed with water (3 x 3 ml) to elute the charged components of the mixture. Elution with MeCN (2 x 2 ml), gave dibenzyl phosphite, which was characterised by ^{31}P NMR spectroscopy, δ_P 11.15 ppm, (s), (d pent, J_{PH} 721, 9.6 Hz, ^1H coupled). By HPLC, this coeluted with peak 4 (retention time = 14.1 min).

All of the other components had eluted, either in the load or water eluates. These were pooled (35 ml) and diluted with water (105 ml) to lower the concentration of the MeCN to approximately 7%. This solution was applied to a new 1g C-18 Bond-Elut solid phase extraction column, which was then washed successively with water (3 x 3 ml), 15% MeCN in water (2 x 2 ml) and 25% MeCN in water (2 x 2 ml). Each wash was analysed by ^{31}P NMR (101.3 MHz) spectroscopy and HPLC. The second 15% MeCN wash contained dibenzyl phosphate (25%) [δ_P 1.06 ppm, (s), (pent, J_{PH} 7.2 Hz, ^1H coupled)] and benzyl (benzyloxycarbonyl)phosphonate (75%) [δ_P -4.68 ppm (s), (t, J_{PH} 7.8 Hz, ^1H coupled)]. Addition of authentic samples of these compounds enhanced the intensity of the appropriate peaks in ^{31}P NMR and the sample gave peaks coeluting with (**65**) and (**66**) by HPLC. The first 25% MeCN wash contained dibenzyl phosphate (**66**) (10%) and benzyl (benzyloxycarbonyl)phosphonate (**65**) (90%), The second 25% MeCN wash contained only the diester (**65**) [δ_P -4.79 ppm, (s), (t, J_{PH} 7.3 Hz, ^1H coupled)].

5.6. ^{18}O Hydrolysis Studies with the Triesters of Phosphonoformate (38, X=H, NO_2, N_3)

A solution of the triester (15 mg) in dry acetonitrile (1.0 ml) was added to 80% [^{18}O], 20% [^{16}O] water (1.0 ml) buffered with NaH_2PO_4/Na_2HPO_4 (0.00285 g/0.0138 g, 0.1 M, pH 7.4) and left to stand in the dark for 4 h. Following concentration to dryness the alcohol was extracted into dichloromethane (3 ml) and the diester salt into water (3 ml). The dichloromethane fraction was dried (Na_2SO_4) and the solvent removed by evaporation to leave the alcohol. This was analysed for ^{18}O incorporation by ^{13}C NMR (75.5 MHz) spectroscopy and FAB (thioglycerol matrix) mass spectrometry. The aqueous fraction was concentrated on the freeze-drier to leave the diester salt as a colourless solid. This was analysed by ^{31}P NMR spectroscopy and FAB (thioglycerol matrix) mass spectrometry.

The experiment was repeated for the triester (38, X=H). This time the total reaction mixture was analysed by ^{31}P NMR (101.3 MHz) spectroscopy using a sweep width of 1309 Hz, a data block size of 32K, an acquisition time of 12.5 s, 3720 scans and 12.5 data points per Hz. The FID was transformed with a line broadening of 0.1 Hz. The reaction mixture was also analysed by ^{13}C NMR (62.9 MHz) spectroscopy.

5.7. Hydrolysis of the Triesters of Phosphonoformate (38, X=NO_2, N_3, CF_3) Followed by ^{31}P NMR Spectroscopy

The triesters (~15 μmol) were dissolved in CD_3CN (0.5 ml) and their ^{31}P NMR (101.3 MHz) spectra recorded with the NMR probe at 36.4°C [38, X=NO_2, δ_P -3.54 ppm (s); 38, X=N_3, δ_P -3.71 ppm (s); 38, X=CF_3, δ_P -3.60 ppm (s)]. Phosphate buffer (0.1 M, pH 7.4, 0.5 ml, pre-incubated at 37°C) was added to the triester solution and ^{31}P NMR spectra were recorded at regular time intervals. A sweep width of 2702 Hz was used, together with a data block size of 32 K, an acquisition time of 3.03 s, 80 scans and 3.3 data points per Hz. Each FID was transformed with a line broadening of 1.0 Hz and the reaction rates, corrected for component type response (section 5.2.), determined from peak heights.

5.8. ^{31}P NMR Study of the Chemical Reduction of Sodium 4-Azidobenzyl (Methoxycarbonyl)phosphonate (61, X=N_3)

The diester (**61, X=N_3**) (4.56 mg, 15.5 μmol) was dissolved in phosphate buffer (0.1 M, pH 7.4) - CH_3CN (0.50 ml, 1:1, v/v, pre-incubated at 37°C). D_2O (0.2 ml) was added as a lock and the ^{31}P NMR (101.3 MHz) spectrum run, δ_P -4.56 ppm (s), with the probe at 36.4°C. Dithiothreitol (24.0 mg, 155 μmol) in phosphate buffer (0.1 M, pH 7.4) - CH_3CN (0.5 ml, 1:1, v/v, pre-incubated at 37°C) was added to the diester solution and the reaction monitored for 12 h by ^{31}P NMR (101.3 MHz) spectroscopy. A sweep width of 6172 Hz was used together with a data block size of 32K, an acquisition time of 2.7 s, 80 scans and 3.3 data points per Hz. The FID was transformed with a line broadening of 0.1 Hz.

5.9. Chemical Hydrolysis of Di(benzoyloxymethyl) Triesters of Phosphonoacetate (44) Followed by HPLC

These experiments were performed in an identical way to the hydrolysis of the dibenzyl (methoxycarbonyl)phosphonates (**38**) (**Section 5.1.**). The composition of the mobile phase changed from 35:65, MeCN - water (v/v) to 90:10, MeCN - water (v/v) over 20 min using Waters pre-programmed convex curve 5 resulting in retention times of 13.18, 15.07 and 19.17 min for the benzoyl (**44, Ar=C_6H_5**), 2-methylbenzoyl (**44, Ar=2-$CH_3C_6H_4$**) and 2,4,6-trimethylbenzoyl (**44, Ar=2,4,6-$(CH_3)_3C_6H_2$**) triesters respectively.

5.10. Incubation of Di(benzoyloxymethyl) Triesters of Phosphonoacetate (44) with Esterase Followed by HPLC

The HPLC conditions used were as in **section 5.1.** The incubations were performed in glass screw-capped vials at 37°C with a total volume of 2ml and a final concentration of triester of 200 μg ml^{-1}. Hydrolysis was initiated by the addition of an acetonitrile solution of the triester (20 μl, 400 μg) to a mixture of phosphate buffer (0.1 M, pH 7.4, 1.694 ml), MeCN (0.280 ml) and porcine liver carboxylesterase (suspension in 3.2 M $(NH_4)_2SO_4$ solution, pH 8, 11 mg protein ml^{-1}, 230 units protein mg^{-1}; 6 μl, 37 units), pre-incubated at 37°C. The reaction was analysed by direct injection of samples (20 μl) onto the column.

The incubations were repeated using rabbit liver carboxylesterase (crystalline suspension in 3.6 M $(NH_4)_2SO_4$, 0.01 M Tris, pH 8.5, 1.9 mg protein ml^{-1}, 95 units protein mg^{-1}). To initiate the reaction an MeCN solution of the triester (20 µl, 400 µg) was added to a mixture of 0.1 M phosphate buffer (pH 7.4, 1.780 ml) and rabbit liver carboxylesterase (200 µl, 37 units), pre-incubated at 37°C. Acetonitrile was not added as it resulted in precipitation of the enzyme.

5.11. Incubation of Di(2,4,6-Trimethylbenzoyloxymethyl) (Methoxycarbonylmethyl)phosphonate (44, Ar=2,4,6-$(CH_3)_3C_2H_6$) with Porcine Liver Carboxylesterase Followed by Reaction with Diazomethane

The HPLC conditions were as in **section 5.1.** The triester (**44, Ar=2,4,6-$(CH_3)_3C_2H_6$**) was incubated with esterase for several hours. The resulting single component (retention time 13.11 min on HPLC) was isolated on a C-18 Bond-Elut solid phase extraction column using 50% MeOH as the eluent. An ethereal solution of diazomethane was added to the eluate until a yellow colouration persisted. The excess diazomethane was removed by a stream of nitrogen to give a colourless solution. This was injected directly onto the column (20 µl) to give a peak co-eluting with the parent triester (**44, Ar=2,4,6-$(CH_3)_3C_2H_6$**) at 19.17 min.

5.12. Incubation of Di(benzoyloxymethyl) Triesters of Phosphonoacetate (44) with Human Plasma Followed by HPLC

The HPLC conditions used were as in **section 5.1.** The plasma was obtained as the supernatant fraction following the centrifugation of human blood at 750 g for 10 min. The incubations were performed in glass screw-capped vials at 37°C using a total volume of 1 ml and a final concentration of triester of 400 µg ml^{-1}. The reaction was initiated by the addition of an acetonitrile solution of the triester (**44**) (20 µl, 400 µg) to neat plasma (980 µl, pre-incubated at 37°C). Samples (300 µl) were taken at t=5 and 10 min and added to centrifuge tubes containing chilled MeCN (300 µl), thereby stopping the reaction. This was followed by centrifugation at 1500 g for 5 min and injection of the supernatant directly onto the column for HPLC analysis. Negative control experiments were performed whereby standard compounds were incubated with plasma.

5.13. Rates of Hydrolysis of Di(4-alkanoyloxybenzyl) Triesters of Phosphonoacetate (93)

A solution of the triester (93) in CD_3CN (0.10 ml, 1.0 μmol) was added to an NMR tube containing D_2O phosphate buffer (0.1 M, pD 8.0) (0.90 ml). The reaction mixtures were incubated at 37°C and monitored by ^1H NMR (250.1 MHz) spectroscopy over several weeks. A sweep width of 5000 Hz was used together with a data block size of 32 K, an acquisition time of 3.3 s, 160 scans and 3.3 data points per Hz. Rates of hydrolysis were calculated from the intensities of the CH_2OP peaks for the triester and the diester.

5.14. Rates of Hydrolysis of 4-Alkanoyloxybenzyl Diesters of Phosphonoacetate (104)

A solution of the diester (104) in D_2O phosphate buffer (0.1 M, pD 8.0) (0.10 ml, 5 μmol) was added to an NMR tube containing D_2O phosphate buffer (0.1 M, pD 8.0) - CD_3CN (0.9 ml, 8:1, v/v). The reaction mixture was incubated at 37°C and monitored by ^1H NMR (250.1 MHz) spectroscopy over several weeks. The spectrometer conditions were identical to those used for the triesters (93) apart from the number of scans which totalled 80. The rates of hydrolysis were calculated from the intensities of one of the diester peaks and the acid product peak.

5.15. Hydrolysis of Di(4-alkanoyloxybenzyl) Triesters of Phosphonoacetate (93) with Esterase Monitored by HPLC

HPLC conditions were similar to those reported in **section 5.1.** except that the samples were eluted isocratically with mixtures of 10 mM tetrabutylammonium hydroxide (TBA) in MeCN - 10 mM TBA in water. The composition of the mobile phase varied according to the nature of R (**Table 5.1**). Chromatograms were displayed and stored on an NEC Powermate SX Plus using Baseline control, collection and display software and printed on an NEC Pinwriter P5300.

Table 5.1 - Mobile phase compositions for di(alkanoyloxybenzyl) triesters

R	% MeCN	% water	Retention Time (min)
CH_3	70	30	3.63
CH_3CH_2	70	30	5.32
$CH_3(CH_2)_2$	70	30	8.78
$(CH_3)_2CH$	80	20	5.50
$CH_3(CH_2)_3$	85	15	6.72
$(CH_3)_3CC$	85	15	6.51
$CH_3(CH_2)_4$	90	10	7.15

Enzyme hydrolyses were performed in glass screw-capped vials incubated at 37°C in a shaking water bath, using a total volume of 1 ml and a final concentration of triester of 1 μmol ml^{-1}. Prior to hydrolysis a solution of porcine liver carboxyesterase (suspension in 3.2 M $(NH_4)_2SO_4$ solution, pH 8, 11 mg protein ml^{-1}, 230 units protein mg^{-1}) was prepared in phosphate buffer (0.1 M, pH 7.4) containing 50 units (**93, R=CH_3**) or 5 units enzyme ml^{-1} (all other triesters). A solution of the triester in acetonitrile (0.10 ml, 1μmol, pre-incubated at 37°C) was added to a vial containing phosphate buffer (0.89 ml, pre-incubated at 37°C) and a sample removed for HPLC analysis (t=0). Enzyme hydrolysis was initiated by addition of the esterase solution [0.01 ml, 0.5 units (**93, R=CH_3**), 0.05 units (all other triesters)] to the reaction vial at 37°C. At the appropriate time, samples were removed from the reaction vessel for HPLC analysis. Where enzyme hydrolysis was reasonably rapid (**93, R=CH_3CH_2, $CH_3(CH_2)_2$, $(CH_3)_2CH$**) a new experiment had to be performed for each time point due to the HPLC analysis time. Hydrolyses were performed in duplicate and control experiments were carried out in the absence of esterase.

5.16. Hydrolysis of 4-Alkanoyloxybenzyl Diesters of Phosphonoacetate (104) with Esterase Followed by ^1H and ^{31}P NMR Spectroscopy

Enzyme hydrolyses were performed in 5mm NMR tubes using a total volume of 1 ml and a final concentration of diester (**104**) of 5 μmol ml^{-1}. Immediately before incubation a solution of porcine liver carboxylesterase was prepared in D_2O phosphate buffer (0.1 M, pD 8.0) containing 500 units of enzyme ml^{-1}. A mixture of D_2O phosphate buffer (0.1

M, pD 8.0, 0.78 ml) and CD_3CN (0.10 ml) was incubated in an NMR tube at 37°C. A D_2O phosphate buffered solution of the diester (0.1 ml, 5 μmol) was added to the NMR tube and a ^1H NMR (250.1 MHz) spectrum recorded (t=0) using a sweep width of 5000 Hz, a data block size of 32 K, an acquisition time of 3.3 s, 91 scans and 3.3 data points per Hz. Each FID was transformed with a line broadening of 0.1 Hz and the temperature of the probe was 36.4 °C.

Enzyme hydrolysis was initiated by addition of the esterase solution (0.02 ml, 10 units) followed by gentle mixing. The NMR tube was placed back in the spectrometer and the reaction monitored by ^1H NMR spectroscopy every 5 - 10 min for several hours using the Bruker KINETICS programme. The rates of hydrolysis were determined from the intensities of the P-CH_2 peaks for the diester **(104)**, hydroxy-diester **(107)** and monoester **(105)** at each time point. The data for the 2 diesters was confirmed from the heights of the corresponding CH_2OP peaks.

The experiments were repeated and this time the hydrolysis was followed by ^{31}P NMR (101.3 MHz) spectroscopy using a sweep width of 4386 Hz, a data block size of 32K, an acquisition time of 3.7 s, 80 scans and 3.7 data points per Hz. Each FID was transformed with a line broadening of 1.0 Hz. The rates of hydrolysis were calculated using the integrals to determine the percentages of the 2 diesters and the monoester present at each time point. Controls were performed in the absence of esterase. To evaluate the ^{31}P and ^1H NMR response of each component type known weights (approx 5 μmol) of diester **(104, R=CH_3)** and monoester **(105)** were combined. Both ^1H (peak heights and integrals) and ^{31}P (integrals) NMR spectra confirmed the ratios from the weights.

5.17. Incubations of Di(4-alkanoyloxybenzyl) Triesters of Phosphonoacetate (93, R=CH_3, $CH_3(CH_2)_2$, $(CH_3)_3C$) with Human Plasma Followed by HPLC

HPLC conditions were similar to those reported in **section 5.15.** except that a Waters 510 gradient delivery system and a Shimadzu SPD-6A UV detector were used. Chromatograms were displayed and stored on an NEC APC IV and printed on an Amstrad DMP 3000. Human blood from two sources (30 ml) was centrifuged at 750 g for 10 min to give plasma as the supernatant fraction. Plasma incubations were performed in glass screw-capped vials, incubated at 37°C in a shaking water bath, using a total volume of 1 ml and a final concentration of triester of 1 μmol ml^{-1}.

To initiate the reaction, plasma (0.5 ml, pre-incubated at 37°C) was added to a mixture of 0.1 M phosphate buffer (pH 7.4, 0.4 ml) and an MeCN solution of the triester (**93**) (0.1 ml, 1 μmol), pre-incubated at 37°C. Samples (200 μl) were removed from the incubation vessel at different time points and immediately added to centrifuge tubes containing ice-cold MeCN (200 μl), whereupon plasma proteins were precipitated and the reaction stopped. The samples were centrifuged at 1000 g for 10 min and the supernatant analysed by HPLC. Duplicate experiments were performed with a different preparation and control experiments were carried out in the absence of plasma.

5.18. Incubation of 4-Alkanoyloxybenzyl Diesters of Phosphonoacetate (104, R=CH_3, $CH_3(CH_2)_2$, $(CH_3)_3C$) with Human Plasma Followed by ^{31}P NMR spectroscopy

Incubations were performed in a 5mm NMR tube at 36.4°C with a total volume of 1 ml and a final concentration of the diester (**104**) of 5 μmol ml^{-1}. To initiate the reaction plasma (0.5 ml, pre-incubated at 37°C) was added to a 0.1 M D_2O phosphate buffered solution of the diester (0.5 ml, 5 μmol, pre-incubated at 37°C) and the reaction monitored for several hours by ^{31}P NMR (101.3 MHz) spectroscopy using a sweep width of 4386 Hz, a data block size of 32K, an acquisition time of 3.7 s, 160 scans and 3.7 data points per Hz. Each FID was transformed with a line broadening of 1.0 Hz and the rates of hydrolysis calculated from integrals.

Negative control experiments were performed exactly as above on disodium (methoxycarbonylmethyl)phosphonate and phosphonoacetic acid. Other negative controls were performed in the absence of plasma.

5.19. Incubation of 4-Alkanoyloxybenzyl Diesters of Phosphonoacetate (104, R=CH_3, $CH_3(CH_2)_2$, $(CH_3)_3C$) with Porcine Brain - S9 Fraction

A section of porcine brain (5g) was washed thoroughly in phosphate buffer (0.1 M, pH 7.4). The brain was cut into small pieces and homogenised in 4 volumes of ice-cold buffer (20 ml). The homogenate was transferred to an ultra-centrifuge tube and spun at 10,000 g for 20 min at 4°C. The supernatant (S9 fraction) was removed, stored on ice and the pellet was discarded. A cofactors solution was prepared as follows:

1) 30.6 mg NADP
2) 169.2 mg Glucose 6-phosphate (G-6-P)
3) 101.6 mg $MgCl_2.6H_2O$
4) 80 IU G-6-P Dehydrogenase enzyme

Components 1, 2 and 3 were dissolved in phosphate buffer (0.1 M, pH 7.4, 10 ml) and stored on ice until required. Just prior to use, the G-6-P dehydrogenase enzyme was added with gentle mixing.

The incubations were performed in a 5 mm NMR tube at 36.4°C with a total volume of 1.2 ml and a final concentration of diester **(104)** of 4.2 μmol ml^{-1}. To initiate the incubation, the cofactors solution (0.2 ml), followed by the S9 fraction (0.50 ml) were added to an NMR tube containing a D_2O phosphate buffer (0.1 M, pD 8.0) solution of the diester (0.5 ml, 5 μmol, pre-incubated at 37°C). The reaction was monitored by ^{31}P NMR (101.3 MHz) spectroscopy over several hours using a sweep width of 4386 Hz, a data block size of 32 K, an acquisition time of 3.7 s, 160 scans and 3.7 data points per Hz. The FID was transformed with a line broadening of 1.0 Hz and the rate of hydrolysis calculated from the integrals. Negative control experiments were performed in the absence of diester and S9.

5.20. Antiviral Testing

The anti-HIV testing protocol applied to phosphonoformates **(38, X=N_3, NO_2, 61, X=N_3, 54 and 9)** and phosphonoacetates **(93, R=CH_3, $(CH_3)_3C$)** by the London and Cambridge testing centres was as follows:

a) 10 TCID50 / $2x10^5$ cells HIV were added to the total number of cells required (10^7 - 10^8) and absorbed to the cells for 90 min at 37°C.

b) Cells were washed three times in phosphate-buffered saline (PBS) to remove unabsorbed virus and re-suspended in the required volume of growth medium.

c) The infected cells were then cultured in 6 ml tubes with drugs at 2 concentrations (200 and 20 μM) for 72 h.

d) 200 μl of tissue culture supernatant from each sample was assayed for HIV antigen using a commercial Elisa.

e) Controls: infected cells without drug, and infected cells treated with AZT.

REFERENCES

1. Fenner, F., The Nature and Classification of Viruses in Man, in *Viral Chemotherapy*, Shugar, D., Ed., **1**, Pergamon Press, England, 1984, p1.

2. Bowman, W.C. and Rand, M.J., *Textbook of Pharmacology*, Blackwell Scientific Publications, England, 1980, section 33.1.

3. Lonberg-Holm J. and Philipson, L., Eds., *Virus Receptors, 2. Animal Viruses*, Chapman and Hall, London, 1981.

4. Gallo, R.C. and Montagnier, L., AIDS in 1988, *Scientific American*, **259**, 1988, 40.

5. McDougal, J.S., Kennedy, M.S., Sligh, J.M., Cort, S.P., Mawle, A. and Nicholson, J.K.A., Binding of HTLV-III/LAV to T4+ Cells by a Complex of the 110 K Viral Protein and the T4 Molecule, *Science*, **231**, 1986, 382.

6. Habeshaw, J.A. and Dalgleish, A.G., The Relevance of HIV env/CD4 Interactions to the Pathogenesis of Acquired Immune Deficiency Syndrome, *J. Acquired Immun. Defic. Syndrome*, **2**, 1989, 457.

7. Fisher, R.A., Bertonis, J.M., Meier, W., Johnson, V.A., Costopoulos, D.S., Lui, T., Tizard, R., Walker, B.D., Hirsch, M.S., Schooley, R.T. and Flavell, R.A., HIV Infection is Blocked *in vitro* by Recombinant Soluble CD4, *Nature*, **331**, 1988, 76.

8. Hussey, R.E., Richardson, N.E., Kowalski, M., Brown, N.R., Chang, H-C., Silicano, R.F., Dorfman, T., Walker, B., Sodroski, J. and Reinherz, E.L., A Soluble CD4 Protein Selectively Inhibits HIV Replication and Syncytium Formation, *Nature*, **331**, 1988, 78.

9. Deen, K.C., McDougal J.S., Inacker, R., Folena-Wasserman, G., Arthos, J., Rosenberg, J., Maddon, P.J., Axel, R. and Sucet, R.W., A Soluble Form of CD4 (T4) Protein Inhibits AIDS Virus Infection, *Nature*, **331**, 1988, 82.

10. Traunecker, A., Luke, W. and Karjalainen, K., Soluble CD4 Molecules Neutralise Human Immunodeficiency Virus Type 1, *Nature*, **331**, 1988, 84.

11. Smith, D.H., Byrn, R.A., Masters, S.A., Gregory, T., Groopman, J.E. and Capon, D.J., Blocking of HIV-1 Infectivity by a Soluble, Secreted Form of the CD4 Antigen, *Science*, **238**, 1987, 1704.

12. Palca, J., New AIDS Drugs Take Careful Aim, *Science*, **246**, 1989, 1559.

13. Berger, E.A., Clouse, K.A., Chaudhary, V.K., Chakrabarti, S., Fitzgerald, D.J., Pastan, I. and Moss, B., CD4-Pseudomonas Exotoxin Hybrid Protein Blocks the Spread of Human Immunodeficiency Virus Infection *in Vitro* and is Active Against Cells Expressing the Envelope Glycoproteins from Diverse Primate Immunodeficiency Retroviruses, *Proc. Natl. Acad. Sci. USA*, **86**, 1989, 9539.

14. Capon, D.J., Chamow, S.M., Mordenti, J., Marsters, S.A., Gregory, T., Mitsuya, H., Byrn, R.A., Lucas, C., Wurm, F.M. and Groopman, J.E., Designing CD4 Immunoadhesins for AIDS Therapy, *Nature*, **337**, 1989, 525.

15. Wilson, T.M.A., Nucleocapsid Disassembly and Early Gene Expression by Positive-Strand Viruses, *J. Gen. Virol.*, **66**, 1985, 1201.

16. Dimmock, N.J., Mechanism of Neutralisation of Animal Viruses, *J. Gen. Virol.*, **65**, 1984, 1015.

17. Choppin, P.W., Richardson, C.D. and Scheid, A., Analogues of Viral Polypeptides which Specifically Inhibit Viral Replications, in *Problems in Antiviral Therapy*, Stuart-Harris, C. and Oxford, J.S., Eds., Academic Press, London, 1983, p13.

18. Kato, N. and Eggers, H.J., Inhibition of Uncoating of Fowl Plague Virus by 1-Adamantanamine Hydrochloride, *Virology*, **37**, 1969, 632.

19. White, J., Matlin, K. and Helenius, A.V., Cell Fusion of Semliki Forest, Influenza and Vesicular Stomatitis Viruses, *J. Cell. Biol.*, **89**, 1981, 67.

20. Oxford, J.S., Amantadine - Problems with its Clinical Usage, in *Problems in Antiviral Therapy*, Stuart-Harris, C. and Oxford, J.S., Eds., Academic Press, London, 1983, p231.

21. Oberg, B., Inhibitors of Virus-Specific Enzymes, in *Problems in Antiviral Therapy*, Stuart-Harris, C. and Oxford, J.S., Eds., Academic Press, London, 1983, p35.

22. Nicholson, K.G., Antiviral Agents in Clinical Practice, (in 5 parts), *Lancet*, 1984, 2, 503, 562, 617, 677 and 736.

23. Varmus, H., Retroviruses, *Science*, **240**, 1988, 1427.

24. De Clercq, E., Potential Drugs for the Treatment of AIDS, *J. Antimicrob. Chemother.*, **23**, suppl A, 1989, 35.

25. Vrang, L. and Oberg, B., PPi Analogs as Inhibitors of Human T-Lymphotropic Virus Type III Reverse Transcriptase, *Antimicrob. Agents Chemother.*, **29**, 1986, 867.

26. Baglioni, C. and Nilsen, T.W., Mechanism of Antiviral Action of Interferon, *Interferon*, **5**, 1983, 23.

27. Luria, S.E., Darnell, J.E., Jr., Baltimore, D. and Campbell, A., Eds., *General Virology*, 3rd Edition, John Wiley and sons, New York, 1978.

28. Hanecak, R., Smeler, B.L., Anderson, C.W. and Wimmer, E., Proteolytic Processing of Poliovirus Polypeptides: Antibodies to Polypeptide P3-7C Inhibit Cleavage at Glutamine-Glycine Pairs, *Proc. Natl. Acad. Sci. USA*, **79**, 1982, 3973.

29. Pearl, L., Ed., *Retroviral Proteases. Control of Maturation and Morphogenesis*, Macmillan Press Ltd., England, 1990, p1 and references cited therein.

30. Corbridge, D.E.C., *Phosphorus. An Outline of its Chemistry, Biochemistry and Technology*, 4th Edition, Elsevier, UK, 1990, p952 and references cited therein.

31. Dixon, H.B.F. and Sparkes, M.J., Phosphonomethyl Analogues of Phosphonate Ester Glycolytic Intermediates, *Biochem. J.*, **141**, 1974, 715.

32. Boezi, J.A., The Antiherpesvirus Action of Phosphonoacetate, *Pharmac. Ther.*, **4**, 1979, 231.

33. Shipkowitz, N.L., Bower, R.R., Appell, R.N., Nordeen, C.W., Overby, L.R., Roderick, W.R., Schleicher, J.B. and Von Esch, A.M., Suppresion of Herpes Simplex Infection by Phosphonoacetic Acid, *Appl. Microbiol.*, **27**, 1973, 264.

34. Huang, E.S., Human Cytomegalovirus-IV. Specific Inhibition of Virus-Induced DNA Polymerase Activity and Viral DNA Replication by Phosphonoacetic Acid, *J. Virol.*, **16**, 1975,1560.

35. Hay, J., Brown, S.M., Jamieson, A.T., Rixon, F.J., Moss, H., Dargan, D.A. and Subak-Sharpe, J.H., The Effect of Phosphonoacetic Acid on Herpes Viruses, *J. Antimicrob. Chemother*, **3**, 1977, 63.

36. Shiraki, K., Okuno, T., Yamanishi, K. and Takahashi, H., Phosphonoacetic Acid Inhibits Replication of Human Herpesvirus-6, *Antiviral Research*, **12**, 1989, 311.

37. May, C.D., Miller, R.L., Rapp, F., The Effect of Phosphonoacetic Acid on the *in vitro* Replication of Varicella-Zoster Virus, *Intervirology*, **8**, 1977, 83.

38. Clark, L.L., Wart Treatment with Phosphonoacetic Acid or its Derivatives, US Patent 4, 016, 264, 1977.

39. Overby, L.R., Duff, R.G. and Mao, J.C.H., Antiviral Potential of Phosphonoacetic Acid, *Ann. N.Y. Acad. Sci. USA*, **73**, 1977, 310.

40. Bopp, B.A., Estep, C.B. and Andersson, D.J., Disposition of Disodium Phosphonoacetate ^{14}C in Rat, Rabbit, Dog and Monkey, *Fedn. Proc.*, **36**, 1977, 939.

41. Barahona, H., Daniel, M.D., Bekesi, J.G., Fraser, C.E.D., King, N.W., Hunt, R.D., Ingalls, J.K. and Jones, T.C., *In Vitro* Suppression of Herpesvirus Saimuri Replication by Phosphonoacetic Acid, *Proc. Soc. Exp. Biol. Med.*, **154**, 1977, 431.

42. Roboz, J., Suzuki, R., Bekesi, G. and Hunt, R., Preclinical Toxicological Study of Phosphonoacetic Acid: Determination in Blood by Selected Ion Monitoring, *Biochem. Mass Spectrometry*, **4**, 1977, 291.

43. Meyer, R.F., Varnell, E.D. and Kaufman, H.E., Phosphonoacetic Acid in the Treatment of Experimental Ocular Herpes Simplex Infections, *Antimicrob. Agents Chemother.*, **9**, 1976, 308.

44. Alenius, S., Dinter, Z. and Oberg, B., Therapeutic Effect of Phosphonoformate in Cutaneous Herpesvirus Infection in Guinea Pigs, *Antimicrob. Agents Chemother.*, **14**, 1978, 408.

45. Palmer, A.E., London, W.T., and Sever, J.L., Disodium Phosphonoacetate in Cream Base as Possible Topical Treatment for Skin Lesions of Herpes Simplex Virus in Cebus Monkeys, *Antimicrob. Agents Chemother.*, **12**, 1977, 510.

46. Newton, A., Inhibition of the Replication of Herpes Virus by Phosphonoacetate and Related Compounds, *Advan. Ophthal.*, **38**, 1979, 267.

47. Overby, L.R., Robishaw, E.E., Schleicher, J.B., Rueter, A., Shipkowitz, N.L. and Mao, J.C.H., Phosphonoacetic Acid: Inhibitor of Herpes Simplex Virus, *Antimicrob. Agents Chemother.*, **6**, 1974, 360.

48. Honess, R.W. and Watson, D.H., Herpes Simplex Virus Resistance and Sensitivity to Phosphonoacetic Acid, *J. Virol.*, **21**, 1977, 584.

49. Leinbach, S.S., Reno, J.M., Lee, L.F., Isbell, A.F. and Boezi, J.A., Mechanism of Phosphonoacetate Inhibition of Herpesvirus-Induced DNA Polymerase, *Biochemistry*, **15**, 1976, 426.

50. Hutchinson, D.W., Naylor, M. and Semple, G., Inhibition of Viral Nucleic Acid Synthesis by Analogues of Inorganic Pyrophosphate, *Chemica Scripta*, **26**, 1986, 91.

51. Mao, J. C-H., Otis, E.R., Von Esch, A.M., Herrin, T.R., Fairgrieve, J.S., Shipkowitz, N.L. and Duff, R.G., Structure-Activity Studies on Phosphonoacetate, *Antimicrob. Agents Chemother.*, **27**, 1985, 197.

52. Helgestrand, E.B., Flodh, H., Lernestaedt, J-O., Lundstrom, J. and Oberg, B., Trisodium Phosphonoformate: Antiviral Activities, Safety Evaluation and Preliminary Clinical Results, in *Developments in Antiviral Therapy*, Collier, E.H. and Oxford, J.S., Eds., Academic Press, London, 1980, p63.

53. Helgestrand, E.B., Eriksson, N.G., Johannson, B., Lannero, A., Larsson, A., Missiorny, J.O., Noren, B., Sjoberg, K., Stenberg, G., Stridh, S., Oberg, B., Alenius, S. and Philipson, L., Trisodium Phosphonoformate, a New Antiviral Compound, *Science*, **201**, 1978, 819.

54. Reno, J.M., Lee, L.F. and Boezi, J.A., Inhibition of Herpesvirus Replication and Herpesvirus-Induced Deoxyribonucleic Acid by Phosphonoformate Acid Polymerase, *Antimicrob. Agents Chemother.*, **13**, 1978, 188.

55. Perrin, D.D. and Stunzi, H., Antiviral Actions of Metal Ions and Metal-Chelating Agents, *Viral Chemotherapy*, Vol. 1, Shugar, D., Ed., Pergamon Press Ltd., U.K., 1984, p281.

56. Chanda, P.K. and Bannerjee, A.K., Inhibition of Vesicular Stomatitis Virus Transcriptase *in vitro* by Phosphonoformate and Ara-ATP, *Virology*, **107**, 1980, 962.

57. Stridh, S. Helgestrand, E., Lannero, B., Missiorny, A., Stenning, G. and Oberg, B., Effects of Pyrophosphate Analogues on Influenza Virus RNA Polymerase and Influenza Virus Multiplication, *Arch. Virol.*, **61**, 1979, 245.

58. Goodrich, J.M., Lee, K.W. and Hinze, H.L., *In Vitro* Inhibition of Herpesvirus Sylvilagus by Phosphonoacetic Acid and Phosphonoformate, *Arch Virol.*, **66**, 1980, 261.

59. Alenius, S., Inhibition of Herpesvirus Multiplication in Guinea Pig Skin by Antiviral Compounds, *Arch. Virol.*, **65**, 1980, 149.

60. Wallin, J., Lennestedt, J.O. and Lycke, E., Therapeutic Efficacy of Trisodium Phosphonoformate in Treatment of Recurrent Herpes Labialis, *Proc. Int. Conf. on Human Herpes Viruses*, Atlanta, Georgia, March, 1980.

61. Sandstrom, E.G., Byington, R.E., Kaplan, J.C. and Hirsch, M.S., Inhibition of Human T-Cell Lymphotropic Virus Type III *in vitro* by phosphonoformate, *Lancet*, 1985, 1480.

62. Sarin, P.S., Taguchi, Y., Sun, D., Thornton, A., Gallo, R. and Oberg, B., Inhibition of HTLV-III/LAV Replication by Foscarnet, *Biochem. Pharmac.*, **34**, 1985, 4075.

63. Connolly, G.M., Gazzard, B.G. and Hawkins, D.A., Fixed Drug Eruption due to Foscarnet, *Genitourin. Med.*, **66**, 1990, 97.

64. Oberg, B. Antiviral Effects of Phosphonoformate, *Pharmac. Ther.*, **40**, 1989, 213.

65. Wondrak, E.M., Lower, J. and Kurth, R., Inhibition of HIV-1 RNA-dependent DNA Polymerase and Cellular DNA Polymerases α, β and γ by Phosphonoformic Acid and Other Drugs, *J. Antimicrob. Chemother.*, **21**, 1988, 151.

66. Jacobson, M.A., Crowe, S., Levy, J., Aweeka, F., Gambertoglio, J., McManus, N. and Mills, J., Efect of Foscarnet Therapy on Infection with Human Immunodeficiency Virus in Patients with AIDS, *J. Infect. Dis.*, **158**, 1988, 862.

67. Sjovall, J., Karlsson, A., Ogenstad, S., Sandstrom, E., Saarimaki, E., Pharmacokinetics and Absorption of Foscarnet After Intravenous and Oral Administration to Patients with Human Immunodeficiency Virus, *Clinical Pharmacology and Therapeutics*, **44**, 1988, 65.

68. Bergadahl, S., Sonnerborg, A., Larsson, A. and Strannegard, O., Declining Levels of HIV p24 Antigen in Serum During Treatment with Foscarnet, *Lancet*, 1988, 1052.

69. Gaub, J., Pedersen, C., Poulsen, A.G., Mathiesen, L.R., Ulrich, K., Lundhardt, B.O., Faber, V., Gerstoft, J., Hofmann, B., Lernestadt, J-O., Nielsen, C.H., Nielsen, J.O. and Platz, P., The Effect of Foscarnet on HIV Isolation, T Cell Subsets and Lymphocyte Function in AIDS Patients, *AIDS Res. Human Retroviruses*, **1**, 1987, 27.

70. Kern, E.R., Glasgow, L.A. , Overall, J.C., Reno, J.M. and Boezi, J.A., Treatment of Experimental Herpesvirus Infections with Phosphonoformate and Some Comparisons with Phosphonoacetate, *Antimicrob. Agents Chemother.*, **14**, 1978, 817.

71. Cload, P.A. and Hutchinson, D.W., The Inhibition of the RNA Polymerase Activity of Influenza Virus A by Pyrophosphate Analogues, *Nucleic Acids Res.*, **11**, 1983, 5621.

72. De Clerq, E., Targets and Strategies for the Antiviral Chemotherapy of AIDS, *TIPS*, **11**, 1990, 198.

73. Merta, A., Votruba, I., Rosenberg, I., Otmar, M., Hrebabecky, H., Bernaerts, R. and Holy, A., Inhibition of Herpes Simplex Virus DNA Polymerase by Diphosphates of Acyclic Phosphonylmethoxyalkyl Nucleotide Analogues, *Antiviral Res.*, **13**, 1990, 209.

74. Cerny, J., Votruba, I., Vonka, V., Rosenberg, I., Otmar, M. and Holy, A., Phosphonylmethyl Ethers of Acyclic Nucleoside Analogues: Inhibitors of HSV-1 Induced Ribonucleotide Reductase, *Antiviral Res.*, **13**, 1990, 253

75. Holy, A., De Clercq, E. and Votruba, I., in *Nucleotide Analogues as Antiviral Agents*, Martin, J.C. (Ed.), ACS Symposium Series 401, The American Chemical Society, Ch. 4, 1989.

76. Gangemi, J.D., Cozens, R.M., De Clercq, E., Balzarini, J. and Hochkeppet, H-K., 9-(2-Phosphonylmethoxyethyl) Adenine in the Treatment of Murine Acquired Immunodeficiency Disease and Opportunistic Herpes Simplex Infections, *Antimicrob. Agents Chemother.*, **33**, 1989, 1864.

77. Tsuji, A. and Tamai, I., Na^+ and pH Dependent Transport of Foscarnet via the Phosphate Carrier System Across Intestinal Brush - Border Membrane, *Biochemical Pharmacology*, **38**, 1989, 1019.

78. Pardridge, W.M., Frank, H.J.L., Cornford, W.M., Braun, L.D., Crane, P.D. and Oldendorf, W.H., in *Neurosecretion and Brain Peptides*, Martin, J.B., Reichlin, S. and Bick, K.L., Eds., Raven Press, New York, 1981, p321.

79. Brightman, M.W., Morphology of Blood-Brain Interfaces, *Exp. Eye Res.*, **25**, 1977, 1.

80. Oldendorf, W.H., Blood-Brain Barrier Permeability to Drugs, *Ann. Rev. Pharmacol.*, **14**, 1974, 239.

81. Pardridge, W.M., Brain Metabolism: A Perspective from the Blood Brain Barrier, *Physiol. Rev.*, **63**, 1983, p1481.

82. Pardridge, W.M., Stategies for Delivery of Drugs Through the Blood-Brain Barrier, *Annual Reports in Medicinal Chemistry*, **20**, Academic Press Inc., USA, 1985, 305.

83. Fenner, F., The Pathogenesis and Frequency of Viral Infections in Man, in *Viral Chemotherapy*, Shuger, D., Ed., International Encyclopedia of Pharmacology and Therapeutics. Section III, **1**, Pergamon Press, England, p27.

84. Griffin, D.E., Viral Infections of the Central Nervous System, in *Antiviral Agents and Viral Diseases of Man*, 3rd Edition, Galasso, G.J., Whitley, R.J. and Merigan, T.C., Eds., Raven Press Ltd., New York, 1990, p461 and references cited therein.

85. Longson, M., The Treatment of Herpes Encephalitis, in *Chemotherapy of Herpes Simplex Virus Infections*, Oxford, J.S., Draser, F.A. and Williams, J.D., Eds., Academic Press, London, 1977, p115.

86. Poland, S.D., Costello, P., Dekaban, G.A. and Rice, G.P.A., Cytomegalovirus in the Brain: *In Vitro* Infection of Human Brain-Derived Cells, *J. Infect. Diseases*, **162**, 1990, 1252.

87. Navia, B.A., Jordan, B.D. and Price, R.W., The AIDS Dementia Complex: 1. Clinical Features, *Ann. Neurol.*, **19**, 1986, 517.

88. Price, R.W., Brew, B., Sidetis, J., Rosenblum, M., Scheck, A.C. and Cleary, P., The Brain in AIDS: Central Nervous System HIV-1 Infection and AIDS Dementia Complex, *Science*, **239**, 1988, 586.

89. Gurney, M.E., Mechanisms of Brain Damage by HIV-1, *Psychopharmacology Bulletin*, **24**, 1988, 311.

90. Yarchoan, R., and Broder, S., Development of Antiretroviral Therapy for the Acquired Immunodeficiency Syndrome and Related Disorders, *N. Engl. J. Med.*, **316**, 1987, 557.

91. Fauci, A.S., The Human Immunodeficiency Virus: Infectivity and Mechanisms of Pathogenesis, *Science*, **239**, 1988, 617.

92. Bundgaard, H., Ed., *Design of Prodrugs*, Elsevier, Amsterdam, 1985.

93. Higuchi, T., Stella, V., *Prodrugs as Novel Drug Delivery Systems*, American Chemical Society Symposium Series 14, American Chemical Society, Washington DC, 1975.

94. Stella, V., The Control of Drug Delivery via Bioreversible Modification, *Drug Delivery Systems, Characteristics and Biomedical Applications*, Juliano, R., Ed., Oxford University Press, New York, 1980, p112.

95. Notari, E., Prodrug Design, *Pharmacology Ther.*, **14**, 1981, 25.

96. Carl, P.L., Chakravarty, P.K. and Katzenellenbogen, J.A., A Novel Connector Linkage Applicable in Prodrug Design, *J. Med. Chem.*, **24**, 1981, 479.

97. Dixon, M. and Webb, E., *Enzymes*, 3rd Edition, Academic Press, New York, 1979.

98. Instrussi, C.E., Mitchell, B.M., Foley, K.M., Schultz, M., Shin, S-U. and Houde, R.W., The Pharmacokinetics of Heroin in Patients with Chronic Pain, *N. Engl. J. Med.*, **310**, 1984, 1213.

99. Holysz, R.P. and Stavely, H.E., Carboxy Derivatives of Benzyl Penicillin, *J. Am. Chem. Soc.*, **72**, 1950, 4760.

100. Jansen, A. and Russel, T., Some Novel Penicillin Derivatives, *J. Chem. Soc.*, 1965, 2127.

101. Daehne, W., Fredrikson, E., Gundersen, E., Lund, F., Yorch, P., Petersen, H.J., Roholt, K., Tybring, L. and Godtfredsen, W.O., Acyloxymethyl Esters of Ampicillin, *J. Med. Chem.*, **13**, 1970, 607.

102. Clayton, J., Cole, M., Elson, S., Lund, F., March, P., Petersen, H.J., Roholt, K., Tybring, L. and Godtfredsen, W.O., Preparation, Hydrolysis and Oral Absorption of Lactonyl Esters of Penicillins, *J. Med. Chem.*, **19**, 1976, 1385.

103. Bodin, M., Ekstrom, B., Forsgren, U., Jalar, L.P., Magni, L., Ramsay, C-H. and Sjoberg, B., Bacampicillin: A New Orally Well-Absorbed Derivative of Ampicillin, *Antimicrob. Agents Chemother.*, **8**, 1975, 518.

104. Rosowsky, A., Forsch, R., Yu, C., Lazarus, H. and Beardsley, G.P., Methotrexate Analogues. 21. Divirgent Influence of Alkyl Chain Length on the Dihydrofolate Reductase Affinity and Cytotoxicity of Methotrexate Monoesters, *J. Med. Chem.*, **27**, 1984, 605.

105. Frey, H. and Loscher, W., Cetyl GABA: Effect on Convulsant Thresholds in Mice and Acute Toxicity, *Neuropharmacology*, **19**, 1980, 217.

106. Galzigna, L., Garbin, L., Binachi, M. and Marzotto, A., Properties of 2 Derivatives of GABA Capable of Abolishing Cardiazol and Bicuculline-Induced Convulsions in the Rat, *Arch. Int. Pharmacodyn.*, **235**, 1978, 73.

107. Bodor, N. and Brewster, M., Problems of Drug Delivery to the Brain, *Pharmacology Ther.*, **19**, 1982, 337.

108. Bodor, N., Poller, R. and Selk, S., Elimination of a Quaternary Pyridinium Salt Delivered as its Dihydropyridine Derivative from the Brain of Mice, *J. Pharmacol. Sci.*, **67**, 1978, 685.

109. Bodor, N., Shelk, E. and Higuchi, T., Delivery of a Quaternary Pyridinium Salt Across the Blood-Brain Barrier as its Dihydropyridine Derivative, *Science*, **190**, 1975, 155.

110. Palomino, E., Kessel, D. and Horwitz, J.P., A Dihydropyridine Carrier System for Sustained Delivery of 2', 3' Dideoxynucleosides to the Brain, *J. Med. Chem.*, **32**, 1989, 622.

111. Farquhar, D., Srivastva, D.N., Kuttesch, N.J. and Saunders, P.P., Biologically Reversible Phosphate-Protective Groups, *J. Pharm. Sci.*, **72**, 1983, 324.

112. Srivastva, D.N. and Farquhar, D., Bioreversible Phosphate Protective Groups: Synthesis and Stability of Model Acyloxymethyl Phosphates, *Bioorg. Chem.*, **12**, 1984, 118.

113. Noren, J.O., Helgstrand, E., Johansson, N.G., Misiorny, A. and Stening, G., Synthesis of Esters of Phosphonoformic Acid and Their Antiherpes Activity, *J. Med. Chem.*, **26**, 1983, 264.

114. Vaghefi, M.M., McKernan, P.A. and Robins, R.K., Synthesis and Antiviral Activity of Certain Nucleoside 5'-Phosphonoformate Derivatives, *J. Med. Chem.*,**29**, 1986, 1389.

115. Robins, R.K., The Potential of Nucleotide Analogs as Inhibitors of Retroviruses and Tumors, *Pharm. Res.*, 1984, 11.

116. Griengl, H., Hayden, W., Penn, G., De Clerq, E. and Rosenwirth, B., Phosphonoformate and Phosphonoacetate Derivatives of 5-substituted 2'-Deoxyuridines: Synthesis and Antiviral Activity, *J. Med. Chem.*, **31**, 1988, 1831.

117. Janz, C., Wigand, R., Combined Interaction of Antiherpes Substances and Interferon β on the Multiplication of Herpes Simplex Virus, *Arch. Virol.*, **73**, 1982, 135.

118. Burkhardt, U. and Wigand, R., Combined Chemotherapy of Cutaneous Herpes Simplex Infection of the Guinea Pig, *J. Med. Virol.*, **12**, 1983, 137.

119. Lambert, R.W., Martin, J.A., Thomas, G.J., Duncan, I.B., Hall, M.J. and Heimer, E.P., Synthesis and Antiviral Activity of Phosphonoacetic and Phosphonoformic Acid Esters of 5-Bromo-2'-Deoxyuridine and Related Pyrimidine Nucleosides and Acyclonucleosides, *J. Med. Chem.*, **32**, 1989, 367.

120. Rosowsky, R.A., Saha, J., Fazely, F., Koch, J. and Ruprecht, R.M., Inhibition of Human Immunodeficiency Virus Type 1 Replication by Phosphonoformate Esters of 3'-Azido-3'-Deoxythymidine, *Biochem. Biophys. Res. Comm.*, **172**, 1990, 288.

121. Eriksson, B.F.H. and Schinazi, R.F., Combinations of 3'-Azido-3'-Deoxythymidine (Zidovudine) and Phosphonoformate (Foscarnet) against Human Immunodeficiency Virus Type 1 and Cytomegalovirus Replication *In Vitro*, *Antimicrob. Agents Chemother.*, **33**, 1989, 663.

122. Morton, A.R. and Howell, A., Bisphosphonates and Bone Metastases, *Br. J. Cancer*, **58**, 1988, 556.

123. Kirby, A.J. and Warren, S.G., *The Organic Chemistry of Phosphorus*, Elsevier Publishers, Amsterdam, 1967, p37.

124. Arbuzov, A.E. and Dunin, A.A., Action of Halogen-substituted Esters of Aliphatic Acids on Esters of Phosphorus Acids. I., *J. Russ. Phys. Chem. Soc.*, 1914, **46**, 295.

125. Issleib, K., Koetz, J., Balszuweit, A., Lettau, H., Thust, U. and Pallas, M., Verfahren Zur Herstellung Von Phosphonoformaten, 1983, East German Patent 215 085.

126. Reetz, T., Chadwick, D., Hardy, E., Kaufman, S., Carbamoylphosphonates, *J. Am. Chem. Soc.*, **77**, 1955, 3818.

127. McKenna, C.E., Higa, M.T., Cheung, N.H. and McKenna, M-C, The Facile Dealkylation of Phosphonic Acid Dialkyl Esters by Bromotrimethylsilane, *Tetrahedron Letts.*, **2**, 1977, 155.

128. Rabinowitz, R., The Reactions of Phosphonic Acid Esters with Acid Chlorides. A Very Mild Hydrolytic Route, *J. Org. Chem.*, **28**, 1963, 2975.

129. Morita, T., Okamoto, Y. and Sakurai, H., A Mild and Facile Synthesis of Alkyl- and Arylphosphonyl Dichlorides Under Neutral Conditions. Reaction of Bis(trimethylsilyl) Phosphonates with PCl_5, *Chem. Letts.*, 1980, 435.

130. Robinson, A-M., Evers, E.L., Griffin, R.J. and Irwin, W.J., Azidobenzyl Carbamates as Potential Prodrugs for Amines: Synthesis and Kinetic Evaluation, *J. Pharm. Pharmacol.*, **40**, 1988, 61P.

131. Grice, R. and Owen, L.N., Cytotoxic Compounds. Part IV. Substituted Benzyl Halides, *J. Chem. Soc.*, 1963, 1947.

132. Kumpf, G., Uber Nitrirte Phenylbenzylather and Nitrirte Benzyl-Chloride, *Justus Liebigs Ann. Chem.*, **224**, 1984, 96.

133. Still, W.C., Khan, M. and Mitra, A., A Rapid Chromatographic Technique for Preparative Separations with Moderate Resolution, *J. Org. Chem.*, **43**, 1978, 2923.

134. Amyes, T.L. and Richard, J.P., Concurrent *Stepwise* and Concerted Substitution Reactions of 4-Methoxybenzyl Derivatives and the Lifetime of the 4-Methoxybenzyl Carbocation, *J. Am. Chem. Soc.*, **112**, 1990, 9507.

135. Higuchi, T. and Schroeter, L.C., Reactivity of Bisulphite with a Number of Pharmaceuticals, *J. Am. Pharm. Assoc. Sci. Ed.*, **48**, 1959, 535.

136. Bogardus, J.B. and Higuchi, T., Kinetics and Mechanism of Hydrolysis of Labile Quaternary Ammonium Derivatives of Tertiary Amines, *J. Pharm. Sci.*, **71**, 1982, 729.

137. Zervas, L. and Dilaris, I., Dealkylation and Debenzylation of Triesters of Phosphoric Acid. Phosphorylation of Hydroxy and Amino Compounds, *J. Org. Chem.*, **77**, 1955, 5354.

138. Cremlyn, R.J.W., Kenner, G.W., Mather, J. and Todd, A., Sir, Studies on Phosphorylation. Part XVI. Iodides as Debenzylating and Dealkylating Agents, *J. Chem. Soc.*, 1958, 528.

139. Bel'skii, V., Kinetics of the Hydrolysis of Phosphate Esters, *Russ. Chem. Rev.*, **46**, 1977, 1578.

140. Hudson, R.F. and Harper, D.C., The Reactivity of Esters of Quinquevalent Phosphorus Anions, *J. Chem. Soc.*, 1958, 1356.

141. Iyer, R.P., Phillips, L.R., Biddle, J.A., Thakker, D.R. and Egan, W., Synthesis of Acyloxyalkyl Acylphosphonates as Potential Prodrugs of the Antiviral, Trisodium Phosphonoformate, *Tetrahedron Letts.*, **30**, 1989, 7141.

142. Krol, E.S., Davis, J.M. and Thatcher, G.R.J., Hydrolysis of Phosphonoformate Esters: Product Distribution and Reactivity Patterns, *J. Chem. Soc., Chem. Commun.*, 1991, 118.

143. Warren, S. and Williams, M.R., The Acid-Catalysed Decarboxylation of Phosphonoformic Acid, *J. Chem. Soc. B*, 1971, 618.

144. Irwin, W.J. *Kinetics of Drug Decomposition: BASIC Computer Solutions*, Elsevier, Amsterdam, 1990, p82, 175.

145. Dudek, G.O. and Westheimer, F.H., Solvolysis of Tetrabenzyl pyrophosphate, *J. Am. Chem. Soc.*, **81**, 1959, 2641.

146. Lowe, G., Potter, B.V.L., Sproat, B.S. and Hull, W.E., The Effect of ^{17}O and the Magnitude of the ^{18}O-Isotope Shift in 31P Nuclear Magnetic Spectroscopy, *J. Chem. Soc. Chem. Commun.*, 1979, 733.

147. Mega, T.L. and Van Etten, R.L., The ^{18}O Isotope Shift in ^{13}C Nuclear Magnetic Resonance Spectroscopy. 12. Position of Bond Cleavage in the Acid-catalysed Hydrolysis of Sucrose, *J. Am. Chem. Soc.*, **110**, 1988, 6372.

148. Kluger, R., Pike, D.C. and Chin, J., Kinetics and Mechanism of the Reaction of Dimethylacetylphosphonate With Water. Expulsion of a Phosphonate Ester from a Carbonyl Hydrate, *Can. J. Chem.*, **56**, 1978, 1792.

149. Martin, D.J. and Griffin, C.E., The Determination of Polar Substituent Constants for the Dialkoxy- and Diarylphosphono and Trialkyl- and Triarylphosphonium Groups, *J. Org. Chem.*, **30**, 1965, 4034.

150. Davidson, R.S., Sheldon, R.A. and Trippet, S., The Reactions of Tetraphenyldiphosphine with Aliphatic Carboxylic Acids and with Aldehydes, *J. Chem. Soc.*, 1968, 1700.

151. Hine, J. and Koser, G.F., The Mechanism of the Reaction of Phenylpropargylaldehyde with Aqueous Sodium Hydroxide to Give Phenylacetylene and Sodium Formate, *J. Org. Chem.*, **36**, 1971, 1348.

152. Narayanan, K.S. and Berlin, K.D., Hydrolysis of Diethyl Benzoylphosphonate in Aqueous and Hydrochloric Acid Solutions. Postulation of a Stable Pentavalent Phosphorus-Containing Intermediate, *J. Am. Chem. Soc.*, **101**, 1979, 109.

153. Warren, S. and Williams, M.R., Electrophilic Substitution at Phosphorus: Dealkylation and Decarboxylation of Phosphinylformate Esters, *J. Chem. Soc. Chem. Commun.*, 1969, 180.

154. Westheimer, F.H., Huang, S. and Covitz, F., Rates and Mechanisms of Hydrolysis of Esters of Phosphorus Acid, *J. Am. Chem. Soc.*, **110**, 1988, 181.

155. Hammett, L.P., *Physical Organic Chemistry*, McGraw-Hill, New York, 1940.

156. Hansch, C., Leo, A. and Taft, R.W., A Survey of Hammet Substituent Constants and Resonance and Field Parameters, *Chem. Rev.*, **91**, 1991, 165.

157. Hoz, S. and Wolk, J.L., Stabilisation of Carbenium Ions by an α-Azido Group, *Tetrahedron Letts.*, **31**, 1990, 4085.

158. Kennard, O., Watson, D.G., Allen, F.H., Motherwell, W.D.S., Town, W.G., Rodgers, J., Crystal Clear Data, *Chemistry in Britain*, **11**, 1975, 313.

159. Chem X, Developed and Distributed by Chemical Design Ltd., Oxford, England.

160. Clark, T., *A Handbook of Computational Chemistry. A Practical Guide to Chemical Structure and Energy Calculations*, John Wiley and Sons Inc., USA, 1985.

161. Stewart, J.J.P., MOPAC: A Semiempirical Molecular Orbital Program, *Journal of Computer-Aided Molecular Design*, **4**, 1990, 1.

162. Ingold, C.K., *Structure and Mechanism in Organic Chemistry*, Bell, London, Chap 16, 1969.

163. Bliss, E.A., Brown, T.B., Stevens, M.F.G. and Wong, C.K., The Biological and Chemical Properties of 4-Azidobenzenesulphonamide, *J. Pharm. Pharmacol.*, **315**, 1979, 66P.

164. Staros, J.V., Standring, D.N. and Knowles, J.R., Reduction of Aryl Azides by Thiols: Implications for the Use of Photoaffinity Reagents, *Biochem. Biophys. Res. Comm.*, **80**, 1978, 568.

165. Baker, N.D., Griffin, R.J. and Irwin, W.J., Azidoaminopyrimidines as Potential Topical Antipsoriatic Agents: a Reduction Model for Biological Inactivation , *J. Pharm. Pharmacol.*, **40**, 1988, 60P.

166. Moldeus, P. and Quanguan, J., Importance of the Glutathione Cycle in Drug Metabolism, *Pharmac. Ther.*, **33**, 1987, 37.

167. Cartwright, I.L., Hutchinson, D.W. and Armstrong, V.W., The Reaction Between Thiols and 8-Azidoadenosine Derivatives, *Nucleic Acids Research*, **3**, 1976, 2331.

168. Ulich, L.H.and Adams, R., The Reaction Between Acid Halides and Aldehydes, *J. Am. Chem. Soc.*, **43**, 1921, 660.

169. Bodor, N., Sloan, K.B., Kaminski, J.J., Shih, C., Pogany, S., A Convenient Synthesis of (Acyloxy)-alkyl α-Ethers of Phenols, *J. Org. Chem.*, **48**, 1983, 5280.

170. Bodnarchuk, N.D., Malovik, V.V., Derbach, G.I., Derivatives of Phosphono Carboxylic Acids, *Russ. J. Gen. Chem.*, **40**, 1970, 1210.

171. Malevannaya, R.A., Tsetkov, E.N., Kabachnik, M.I., Dialkoxyphosphinylacetic Acids and Some of their Analogues, *Russ. J. Gen. Chem.*, **41**, 1971, 1426.

172. Taft, R.W., *Steric Effects in Organic Chemistry*, Newman, S., Ed., John Wiley, New York, 1956, 556.

173. Taft, R.W., Polar and Steric Substituent Constants for Aliphatic and o-Benzoate Groups from Rates of Esterification and Hydrolysis of Esters, *J. Am. Chem. Soc.*, **74**, 1952, 3120.

174. Charton, M., The Nature of the Ortho Effect. II. Composition of the Taft Steric Parameters, *J. Am. Chem. Soc.*, **91**, 1969, 615.

175. Kulter, E. and Hansch, C., Steric Parameters in Drug Design: Monoamine Oxidase Inhibitors and Antihistamines, *J. Med. Chem.*, **12**, 1969, 647.

176. Dixon, M. and Webb, E.C., *Enzymes*, 3rd Ed., Academic Press, New York, p303 and references cited therein.

177. Aldridge, W.N., Serum Esterases, I. Two Types of Esterase (A and B) Hydrolysing p-Nitrophenyl Acetate, Propionate and Butyrate, and a method for their determination, *Biochem. J.*, **53**, 1953, 110.

178. Benohr, H.C., Franz, W. and Krisch, K., Carboxylesterasen der Mikrosomenfraktion, *Arch. Exp. Pathol. Pharmakol.*, **255**, 1966, 163.

179. Krisch, K., *The Enzymes*, Boyer, P.D., Ed., 3rd Edition, Academic Press, New York, p57 and references cited therein.

180. Levy, M. and Ocken, P.R., Purification and Properties of Pig Liver Esterase, *Arch. Biochem. Biophys.*, **135**, 1969, 259.

181. Altman, P.L., *Blood and Other Body Fluids*, Diitmer, D., Ed., *Fed. Am. Soc. Exp. Biol.*, 1961, 101.

182. Kenner, G.W. and Mather, J.J., Studies on Phosphorylation.Part XIV. The Solvolysis by Phenols of Benzyl Phosphates, *J. Chem. Soc.*, 1956, 3524.

183. Freeman, S., Irwin, W.J., Mitchell, A.G., Nicholls, D. and Thomson, W., Bioreversible Protection for the Phospho Group: Chemical Stability and Bioactivation of Di(4-acetoxybenzyl) Methylphosphonate with Carboxylesterase, *J. Chem. Soc. Commun.*, 1991, 875.

184. Parente, J.E., Risley, J.M. and Van Etten, R.L., ^{18}O Isotope Effect in ^{13}C Nuclear Magnetic Resonance Spectroscopy. 9. Hydrolysis of Benzyl Phosphate by Phosphatase Enzymes in Acidic Aqueous Solutions, *J. Am. Chem. Soc.*, **106**, 1984, 8156.

185. Kumamoto, J. and Westheimer, F.H., Hydrolysis of Mono- and Dibenzyl Phosphates, *J. Am. Chem. Soc.*, **77**, 1955, 2515.

186. Hammett, L.P., Some Relations Between Reaction Rates and Equilibrium Constants, *Chem. Rev.*, **17**, 1935, 125.

187. Hansch, C. and Leo, A.J., *Substituent Constants for Correlation Analysis in Chemistry and Biology*, Wiley Interscience, 1979, p13 and references cited therein.

188. Meyer, H., Zur Theorie der Alkolnarkose I. Welche Eigenschaft der Anaesthetica bedingtihre narkotische Wirkung?, *Arch. Exp. Pathol. Pharmakol.*, **42**, 1899, p110.

189. Hofstee, B.H.J., Specificity of Esterases. IV. Behaviour of Horse Liver Esterase Towards an Homologous Series of n-Fatty Acid Esters, *J. Biol. Chem.*, **207**, 1954, 219.

190. Malhotra, P. and Philip, G., Purification and Physical Properties of a Goat Intestinal Esterase, *Indian J. Biochem.*, **3**, 1966, 7.

191. Kumar, S., Ed., *Biochemistry of Brain*, Pergamon Press Ltd., UK, 1980. p5, 176, 326, 473 and 563.

192. Leo, A., Hansch, C. and Elkins, D., Partition Coefficients and Their Uses, *Chem. Rev.*, **71**, 1971, 525.

193. Levin, V., Relationship of Octanol/Water Partition Coefficient and Molecular Weight to Rat Brain Capillary Permeability, *J. Med. Chem.*, **23**, 1980, 682.

194. Rapport, S., *Blood-Brain Barrier in Physiology and Medicine*, Raven, New York, 1976.

195. Rapport, S. and Levitan, H., Neurotoxicity of X-ray Contrast Media. Relation to Lipid Solubility and BBB Permeability, *American Journal of Roentgenology*, **122**, 1974, 186.

196. Hansch, C., Steward, A. and Anderson, S., The Parabolic Dependence of Drug Action Upon Lipophilic Character as Revealed by a Study of Hypnotics, *J. Med. Chem.*, **11**, 1968, 1.

197. Audus, K.L. and Borchardt, R.T., Characterisation of an *in vivo* BBB Model System for Studying Drug Transport and Metabolism, *Pharm. Res.*, **3**, 1986, 81.

198. Audus, K.L., Bartel, R.L., Hidalgo, I.J. and Borchardt, R.T., The Use of Epithelial Cultures and Endothelial Cells for Drug Transport and Metabolism Studies, *Pharm. Res.*, **7**, 1990, 435.

199. T.H. Fife and T.C. Bruice, The Temperature Dependence of the ΔpD Correction for the Use of the Glass Electrode, *J. Phys. Chem.*, 1961, **65**, 1079.

200. Gardner, I.J. and Noyes, R.M., Effects of Substituents on the Radical Exchange Reaction Between Benzyl Iodide and Iodine, *J. Am. Chem. Soc.*, **83**, 1961, 2409.